Durham E-Theses

Methods of interpreting magnetic anomalies with application to the Minch dyke and magnetic anomalies over the lower and middle Benue trough of Nigeria

Ofoegbu, Charles Ononuju

How to cite:

Ofoegbu, Charles Ononuju (1981) *Methods of interpreting magnetic anomalies with application to the Minch dyke and magnetic anomalies over the lower and middle Benue trough of Nigeria*, Durham theses, Durham University. Available at Durham E-Theses Online: http://etheses.dur.ac.uk/7512/

METHODS OF INTERPRETING MAGNETIC ANOMALIES WITH APPLICATION TO

THE MINCH DYKE AND MAGNETIC ANOMALIES OVER THE LOWER AND MIDDLE

BENUE TROUGH OF NIGERIA

BY

CHARLES ONONUJU OFOEGBU

A thesis submitted for the degree of Doctor of Philosophy in the
University of Durham

Graduate Society   June 1982

ABSTRACT

A method of combined least squares and non-linear optimisation
for the interpretation of magnetic anomalies over dykes is here
presented. The method seeks to minimise a non-linear objective
function by iteratively varying the non-linear parameters of the dyke
while obtaining optimum values of the linear parameters by least squares
analysis until an acceptable fit is obtained between the observed and
computed anomalies. A study of the effects of demagnetization in
arbitrarily shaped bodies and methods for evaluating the demagnetization
effects of such bodies are also presented.

Sixteen profiles have been taken across a linear magnetic feature
which intersects the North Minch on the North Scottish Shelf. These have
been interpreted in terms of a dyke about 1 km wide using the non-linear
optimization techniques developed. The dyke is reversely magnetized in
a direction consistent with its Tertiary origin.

An aeromagnetic study of the Lower and Middle Benue Trough of
Nigeria has been carried out. Regions of high and low magnetic
anomalies have been correlated in an effort to find trends. Two
dimensional interpretation of several aeromagnetic profiles across
the trough has been carried out. Interpretation of the observed anoma-
lies in terms of topographic variations of the basement led to rather
unreasonable models. The anomalies were best interpreted in terms
of basic intrusive bodies which could occur either predominantly within
the Cretaceous sediments or within the metamorphic basement. The model
intrusives have variable thicknesses and directions of magnetization,
suggesting that although derived from the same basic mantle material,
the intrusions were emplaced at different polarity epochs. An attempt
is also made to explain the tectonic evolution of the trough in terms
of the models obtained.

ACKNOWLEDGEMENTS

TABLE OF CONTENTS

CHAPTER I   METHODS FOR THE INTERPRETATION OF
              MAGNETIC ANOMALIES   1

     1.1   Introduction   1

     1.2   Interpretation of Magnetic Anomalies
            by Non-Linear Optimization Techniques   2

     1.2.1 The Objective Function   2

     1.2.2 Use of Constraints and Scaling of the
            Problem   4

     1.2.3 Classification of Optimization Techniques   5

     1.2.4 Newton's and Quasi-Newton's Techniques   6

     1.2.5 The Simplex Method   11

     1.2.6 Accuracy of Optimum Parameters and
            Confidence Intervals for Solutions   12

     1.2.7 Programmed Versions for Bodies of Polygonal
            Cross-section   15

     1.3   Interpretation of Magnetic Anomalies due to
            Dykes by Non-Linear Optimization Techniques   18

     1.3.1 Mathematical Formulation of the Present
            Method   19

     1.3.2 Computer Programming of the Dyke
            Interpretation Method   22

     1.3.3 Advantages of the Present Method   25

     1.3.4 Non-Uniqueness in Dyke Interpretation   27

     1.4   Linear Inverse Method and Joint Analysis of
            Magnetic and Gravity Anomalies   31

     1.4.1 Use of Matrix Method in Computation of
            Pseudogravimetric Anomalies   32

CHAPTER I

METHODS FOR THE INTERPRETATION OF MAGNETIC ANOMALIES

1.1 Introduction

The final results of any form of magnetic survey is usually a set of data, profiles or a magnetic contour map from which the interpreter is expected to resolve the latent features of the area under investigation. These features influence the characteristics of the anomaly produced and include the size, shape and depth of the body as well as magnitude and orientation of the polarization vector associated with it.

Methods of interpreting magnetic anomalies fall into two main categories; the direct and the indirect methods. The indirect methods seek a solution by starting from a guessed likely source of the anomaly and successively adjust the parameters of the source body until an acceptable agreement is reached between the observed and computed anomalies. The direct methods on the other hand include methods for which a solution is sought direct from the observed profile.

This chapter gives a review of the methods of magnetic interpretation used in the present work. Particular emphasis has been placed on the methods developed in the course of this work. The interpretation of magnetic anomalies by non-linear optimization techniques is discussed. Application of these techniques to the interpretation of magnetic anomalies due to dykes is also presented. A brief consideration is given to the problem of ambiguity inherent in magnetic interpretation in general and dyke interpretation in particular.

The linear inverse method of magnetic interpretation as well as its use in the joint interpretation of magnetic and gravity data is discussed. Programing details of all the methods used in this work are also given. All interpretation methods used in the present work are based on two-dimensional approximation and all programmed versions have been written for use on the NUMAC IBM 370/168 computer.

1.2 Interpretation of Magnetic Anomalies by Non-linear Optimization Techniques

Non-linear optimization techniques are numerical techniques which seek to minimise or maximise a non-linear objective function by an iterative adjustment of its variable parameters with or without constraints (Box et al., 1969; Box 1965, 1966; Al-Chalabi, 1970, 1971; Powell, 1964, 1965; Westbrook, 1980).

1.2.1 The Objective Function

In geophysical interpretation, the problem of non-linear optimization reduces to that of minimization of an objective function F of n variables $(x_1, \ldots, x_n)$ which at each iteration represents a measure of agreement between an observed anomaly Fo and a computed anomaly Fc due to a model defined by both linear and non-linear parameters $(x_1, \ldots, x_n)$.

The objective function F maybe represented by one of the following relationships:

$$F = \sum_{i=1}^{KTOT} |Foi - Fci|^{\frac{1}{2}} \qquad \text{1.1a}$$

$$F = \sum_{i=1}^{KTOT} |Foi - Fci| \qquad \text{1.1b}$$

$$F = \sum_{i=1}^{KTOT} (Foi - Fci)^2 \qquad \text{1.1c}$$

where KTOT = number of station points

Foi = value of observed anomaly at the ith station point.

Fci = value of computed anomaly at the ith station point.

Better results are obtained using the relationships 1.1b and 1.1c in terms of approximating the original model and in producing minimum residuals (Al-Chalabi, 1970). In the present work, the equation 1.1c has been chosen partly because of the advantages it has in common with equation 1.1b already stated above, as well as its usefulness in the statistical analysis of the results of the optimization procedure. The last point will become more apparent when the problem of confidence limits and test of solution is discussed.

The behaviour of the objective function can be represented either mathematically or geometrically. Mathematically, the local behaviour of the objective function is represented by an m-dimensional Taylor series expansion:

$$F(x+d) = F(x) + \sum_{j=1}^{m} \frac{\partial F}{\partial x_j} d_j + \frac{1}{2} \sum_{j=1}^{m} \sum_{k=1}^{m} \frac{\partial^2 F}{\partial x_j \partial x_k} d_j d_k + \cdots \quad 1.2$$

where d_1, d_2, ... dm are the components of parameter changes along each of the m- mutually orthogonal axes, x_1, ... x_m. In the vicinity of the optimum, F can be adequately represented by the truncated Taylor series expansion :

$$F(x+d) = F(x) + \sum_{j=1}^{m} \frac{\partial F}{\partial x_j} d_j + \frac{1}{2} \sum_{j=1}^{m} \sum_{k=1}^{m} \frac{\partial^2 F}{\partial x_j \partial x_k} d_j d_k \quad 1.3$$

and this forms the basis of most optimization routines. Geometrically, the objective function maybe represented in an m-dimensional space obtained by constructing an Euclidean hyperspace in which each of the m- mutually orthogonal axes represents one variable parameter.

The objective function is then fully represented by contours of equal values. These contours maybe viewed in the same way as topographical contours and the behaviour of the objective function can then be qualitatively studied. In practice, however, only sections through the contours are used for the qualitative analysis of the objective function. This has also proved a useful tool in the demonstration of the problem of ambiguity in gravity and magnetic interpretation (Al-Chalabi, 1971).

1.2.2 Use of Constraints and Scaling of the Problem

The minimization of the objective function is usually subject to some constraints which in magnetic interpretation are determined by the geological feasibility of the model. These constraints may take the form of equality contraints given by

$$e_j \ (x_1, \ \ldots. \ x_n) \ = \ 0$$

or inequality constraints given by

$$Ci(x_1, \ \ldots. \ x_n) \ \geq \ 0$$

Models that satisfy all the constraints imposed are said to be feasible and all such models lie within a feasible region while all other models form the non-feasible region. Ideally an optimum solution is that for which the optimum parameters define a system which is an exact solution to the problem. Such a condition is, however, hardly realised in practice and the problem reduces to one of searching for the minimum of the objective function $F(x)$ in the x hyperspace. In addition to the overall minimum called the global minimum, there may exist several other possible minima called the local minima.

It is usually useful to scale the problem whose solution is desired by non-linear optimization as this often has a significant influence on the performance of optimization methods.

A well scaled problem is one in which the contours of the objective
function are approximately hyper-spherical or elongated parallel
to most search directions. Good scaling enables most optimization
routines to converge more rapidly and accurately to a solution.
Unusual or unbalanced scaling may, on the other hand, cause
difficulties for some optimization algorithms. Several effective
scaling methods exist and could be used. One such method
involves the transformation of the variables from their physical
nature to variables having certain desirable properties in terms
of optimization. An effective transformation should usually
ensure that in the neighbourhood of the minimum, all variables
are of similar magnitude as well as that a fixed change in any
of the variables results in similar changes in the objective
function F(x). In the present work only linear transformations
of the type

$$x_{new} = D \; x_{old}$$

have been used although non-linear transformations may also be used.

It is generally preferable for the objective function F(x)
to be of the order of unity in the region of the minimum and
the objective function is therefore accordingly scaled. The
solution to a given problem is not altered if the objective
function F(x) is multiplied by a positive constant nor is it
altered by the addition or subtraction of a constant value to the
objective function F(x).

1.2.3 Classification of Optimization Techniques

All optimization techniques fall into one of two main
classes. These are the Direct search methods or the Gradient
methods. The Direct search methods are those methods which do
not require the evaluation of any partial derivatives of the

objective function but rely solely on values of the objective function and its previous history. The Direct Search methods are further sub-divided into three classes; the Tabulation methods, e.g. Random search method, the Sequential methods, e.g. Simplex method and the Linear search methods, e.g. Alternating variable search method.

The Gradient methods on the other hand, choose the search direction using values of the partial derivatives of the objective function with respect to the independent variables as well as the objective function and its previous history. Examples of these methods include the methods of Steepest descent, Newton's method, and the Quasi-Newton's method. Of all these methods mentioned, the Simplex and the Quasi-Newton techniques have been used in the course of this work and these are briefly summarised in the next sections (1.2.4 and 1.2.5). All numerical optimization routines except the Tabulation Methods are iterative. These require an initial point Xo from which they proceed by the generation of a sequence of points Xi which represent improved approximations to the solution. Thus

$$F(Xi + 1) \leq F(Xi) \qquad\qquad 1.4$$

1.2.4 Newton's and Quasi-Newton's Technique

The method of steepest descent whose development and use is closely related to the classical Gauss method has remained the most widely used of all Gradient methods in magnetic interpretation. The underlying rationale of this method is that the best direction of search is that in which the objective function F decreases most rapidly (Box et al., 1969). The direction of steepest descent on which this method depends does not in most cases coincide with the direction to the minimum and convergence may

consequently be slow. The Newton's and Quasi-Newton's methods

therefore arose out of attempts to overcome this difficulty. The

methods have been described in detail by earlier authors (Box

et al., 1969; Davidon, 1968; Gill and Murray, 1974; Gill and

Murray, 1977; Al-Chalabi, 1970 and others). To fully understand

the Newton's and consequently the Quasi-Newton's technique,

requires us to reconsider the equation 1.3 which is a Taylor

series expansion of the objective function about the minimum

(Xmin);

$$F(X_{min}+d) = F(X_{min}) + \sum_{j=1}^{m} \left(\frac{\partial F}{\partial x_j}\right)_{x_{min}} dj + \frac{1}{2}\sum_{j=1}^{m}\sum_{k=1}^{m} \left(\frac{\partial^2 F}{\partial x_j \partial x_k}\right)_{x_{min}} d_j d_k \qquad 1.5$$

Evaluating the derivatives of equation 1.5 at the position of

the minimum gives

$$\frac{\partial F}{\partial x_1} = \left(\frac{\partial F}{\partial x_1}\right)_{x_{min}} + \sum_{j=1}^{m} \left(\frac{\partial^2 F}{\partial x_j \partial x_1}\right)_{x_{min}} d_j \qquad 1.6$$

In getting equation 1.6 terms higher than the second order

term have been neglected. At the minimum, this expression

reduces to an expression for the gradient vector $\underline{g}$ whose ith

component in the vicinity of the minimum is given as

$$\underline{g} = \frac{\partial F}{\partial x_1} = \sum_{j=1}^{m} \left(\frac{\partial^2 F}{\partial x_j \partial x_1}\right)_{x_{min}} d_j; \quad 1 = 1,2,\ldots\ldots,m \qquad 1.7$$

since at the minimum $\left(\frac{\partial F}{\partial x_1}\right)_{x_{min}} = 0$

In matrix notation, equation 1.7 can be written as follows

$$g = Gd \qquad 1.8a$$

The matrix G is the matrix of the second partial derivatives of

equation 1.7 and is called the Hessian matrix while the matrix of

the first partial derivatives g is called the gradient vector.

The step d towards the minimum is derived from equation 1.8a as

$$d = G^{-1}g \qquad\qquad 1.8b$$

and the position of the minimum x_{min} is therefore

$$x_{min} = x - G^{-1}g \qquad\qquad 1.8c$$

The class of gradient methods for which the direction d of the next iteration is given by equation 1.8b are called the Variable Metric Methods. This is because d is the direction in which the directional derivative of the function F is a minimum: i.e. the direction in which

$$d^T g \equiv d^T (\nabla F)$$

is a minimum subject to a constant length of d which is usually expressed in terms of the Hessian Matrix G. When the matrix G varies from point to point, the metric is variable, hence the name of these gradient methods. The general iterative rule then is

$$x_{i+1} = x_i - G^{-1}g \qquad\qquad 1.8d$$

where the directional gradient vector g is evaluated at the point x_i (Greenstadt, 1967, 1970).

The above iterative scheme (equations 1.8a, 1.8b, 1.8c and 1.8d) presupposes that the matrix of the second derivatives G can be readily evaluated at the minimum x_{min} which may not be the case since the position of the minimum is not known. In the case of a quadratic objective function, G is constant and its value at the minimum x_{min} is known. If however, the current search point x_i is not close to the minimum, and the function F is not quadratic, G is evaluated at the current point x_i. The use of the matrix G evaluated at each current search point in the iterative scheme discussed above forms the basis of the Newton method for finding the root of $\nabla F = 0$. The Newton's method ensures movement towards the minimum only if the matrix G is positive

definite. This is so because the method assumes the matrix

$$-G \equiv \left[\frac{\partial^2 F}{\partial x_k \partial x_j} \right]$$

as being negative definite.

The principal disadvantage of the Newton's method however,
lies in the need to evaluate and invert the Jacobian matrix G at
each stage of the iteration. The computation of the matrix G
and its inverse G^{-1} represent time consuming operations. To
overcome this drawback, Box et al. (1969) have suggested that
the matrix G and its inverse G^{-1} should not be recalculated after
each iteration, but instead only after every n iterations, say.
This modified procedure would usually necessitate many more
iterations and this may therefore defeat its purpose. Several
methods (Barnes, 1965; Broyden, 1965; Fletcher and Powell, 1963;
Fletcher, 1970) have therefore arisen in which the inverse
matrix G^{-1} is replaced by an approximation which is modified in
some simple manner at each iteration. These methods which usually
combine the initial advantages of the method of steepest descent
and the effectiveness of the Newton's method near the minimum
have been called the Quasi-Newton methods and best known of these
is the method developed by Davidon (1959) and modified and made
more efficient by Fletcher and Powell (1963). In particular,
when the function to be zeroed are the first partial derivatives
of another function or have first partial derivatives easily
computable, then it is possible if the function F is quadratic
to modify the approximating matrix H in such a way that the
function F is minimized in a finite number of steps. The theory
and application of the Quasi-Newton methods have been considered
by several authors (Fletcher, 1970; Broyden, 1967; Broyden, 1970;
Fletcher, 1965; Greenstadt, 1967; Greenstadt, 1970 and others).
The methods are closely similar differing only in their choice

of the approximating matrix H and only the application of the
most widely used of them (Davidon, 1959; Fletcher and Powell,
1963) is now presented. This Quasi-Newton method is here called
the Davidon-Fletcher-Powell method (DFP Method) (Greenstadt,
1970).

In the Davidon-Fletcher-Powell method, a sequence of
progressive estimates H_i is made of the inverse Hessian matrix
G^{-1} based only on the first partial derivatives of the function
F. In the absence of the gradient vector g_i, a finite-difference
approximation to the gradient vector is used. The sequence of
steps used in the method are as in the following cycle. From the
calculated gradient vector g_i at the search point x_i, the method
computes the next step direction using the current estimate of
G^{-1}, so that Eqn. 1.8b is now

$$d_i = -H_i g_i$$

The minimum of the objective function F is now found along the
direction d_i. If the total step to this point D_i is α_i multiple
of the step d, then

$$D_i = \alpha_i d_i$$

and

$$x_{i+1} = X_i + D_i$$

The usual correction of the estimate H_i to form the next estimate
H_{i+1} has been given by the same authors as follows :

$$H_{i+1} = H_i + \frac{D_i D_i^T}{(D_i^T Y_i)} - \frac{H_i Y_i Yi^T H_i}{(Y_i^T H_i Y_i)}$$

where

$$Y_i = g_{i+1} - g_i$$

upper

and the s~~s~~ script T represents the transpose of the vector in
question. Using the new value of H calculated from the equation
above, the cycle is repeated until convergence is attained.

Suggested convergence criteria are that either (a) the lengths, or (b) every component of the vectors $- H_i g_i$ and $- d_i H_i g_i$, which are respectively the full Newton step and the actual step taken, be less than some specified value.

1.2.5 The Simplex Method

The Simplex Method was first developed by Spendley et al., (1962), in modified form by Campey and Nickols (1961) and made more flexible by Nelder and Mead (1965). The best description of this method remains that of Box et al. (1969) and this is summarised here. This method involves the evaluation of the objective function at m + 1 mutually equidistant points in a space of m independent variables with these points forming the vertex of a regular simplex which in two-dimensions consists of an equilateral triangle.

The first step in the use of the simplex method involves the setting up of a regular simplex and the evaluation of the objective function at each vertex of the simplex. The vertex at which the objective function has its largest value is now reflected in the centroid of the m remaining vertices to give a new simplex and the objective function is re-evaluated. If however, the vertex selected for reflection at any stage is the most recently introduced vertex, the vertex with the next largest function value is reflected instead and should any vertex remain unchanged for more than a given number of consecutive iterations K, the size of the simplex is reduced by halving the distances of the remaining vertices from this vertex and the search procedure recommenced. The value of K depends on the number of independent variables and the following relationship has been suggested by Spendley et al. (1962).

$$K = 1.65m + 0.05m^2 \qquad\qquad 1.9$$

The method terminates the search and assumes convergence
when the size of the simplex has been reduced to an acceptable
minimum. In their modified form of the Simplex method,
Campey and Nickols (1961) saw no real need for maintaining a
regular simplex which they argue, to be scale dependent. This
method has been further modified to achieve flexibility (Nelder
and Mead, 1965). This modified simplex method involves reflection,
expansion and contraction of the simplex and gives criteria for
carrying out each of these operations.

1.2.6 Accuracy of Optimum Parameters and Confidence Intervals for Solutions

On convergence at the minimum by an optimization routine, it
is often desirable to obtain an estimate of the accuracy of the
variable parameters defining the optimum solution. The
computation of an estimate of parameter accuracy in terms of
observational errors and the residuals is a difficult task which
often involves a lot of statistical analysis. To simplify the
problem it is often useful to assume that the observational
errors are wholly accounted for by the residuals which are
randomly distributed in the region of the minimum and that the
system being optimized is fully defined by the parameters. Both
assumptions may however, be untrue and estimates of parameter
accuracy are sometimes of limited significance. The accuracy of
the parameters defining a solution can be determined by a
comparison of the variance at the minimum with the variance
elsewhere in the objective function hyperspace using the
variance-ratio, or F distribution (Westbrook, 1980). Detailed
analysis of the problem of errors can be found in several texts
on statistics (Scheffe, 1963; Silvey, 1975; Mood et al., 1963;
Topping, 1978; Barford, 1967 and many others). Only a practical

description of applications of the theory of errors to non-linear optimization techniques is given here. In practice the accuracy of parameters obtained from optimization is often expressed in terms of confidence intervals. Westbrook (1980) has given a practical method of deriving confidence limits on parameters using the values of the objective function corresponding to the solutions.

Following the nomenclature of Westbrook (1980), the value of the 100 $(1-\alpha)$ per cent confidence contour F_c is calculated as follows :

$$F_c = F_{min} \left[1 + \frac{n}{m-n-1} f_n, \ m-n-1(1-\alpha) \right] \qquad 1.10$$

where n   = number of variables

      m   = number of observation points

      F_{min} = minimum function value

      100 $(1-\alpha)\%$ = confidence limit

The term n is essentially the number of degrees of freedom of the model and m-n-1 represents the number of degrees of freedom of the solution. The values of f_n, m-n-1 which is a fractile of the variable – ratio or F distribution can readily be found in statistical tables.

A practical method of obtaining the region within which acceptable solutions for any one parameter x_i (say) will lie is to plot a graph of the objective function F against the parameter x_i with all other parameters fixed at their minimum values (Figure 1.1). A line defining F_c, the value of the objective function at the confidence limit (equation 1.10) is constructed. The intersections of this line with the graph are produced to the axes of the parameter in question to obtain the limiting values of the parameter defining the area within which possible acceptable solutions may lie for any desired degree of confidence. This
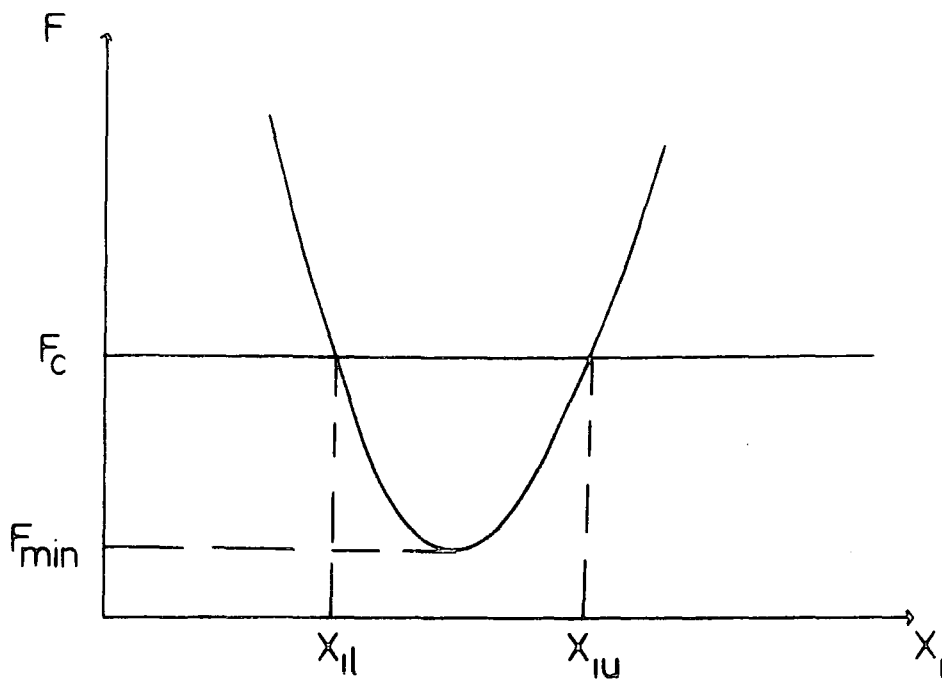
Fig 1·1 Graph of objective function against parameter X_1, all other parameters fixed at their minimum values

After Westbrook(1980)
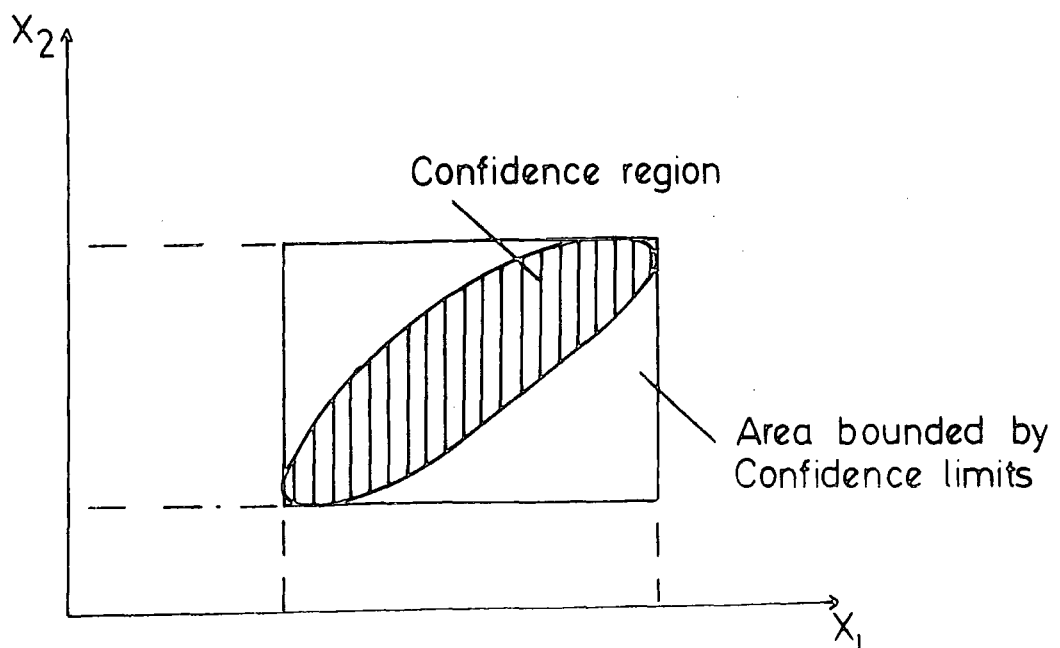
Fig 1·2 Hyperspatial section through the objective function showing the confidence region

After Westbrook(1980)

operation may be carried out for as many parameters as one is interested in. These estimates of the limits (x_{il} and x_{iu} for example) assume that all other parameters are fixed and these may therefore be under-estimates of the possible values they can take. To find the true errors, all other parameters are relaxed to find the minimum values of the objective function F for the range of x_i containing the confidence region. Acceptable solutions do not necessary have to exist everywhere in the region defined by the limits of the parameters but certainly they do not exist outside these limits (Figure 1.2).

In the case of an objective function which is of a least-squares type, a direct approach to obtaining the errors in the parameters may be adopted provided the function is quadratic with respect to the parameters in the neighbourhood of the minimum. The Hessian matrix G (section 1.2.4) is the same as the information matrix of the linear least squares inversion and the inverse Hessian G^{-1} is proportional to the covariance matrix. An unbiased estimate of the variance of the ith parameter x_i is in this case given as

$$\text{Var } x_i = \frac{2F}{m-n} G_{ii} \qquad \text{1.11a}$$

and the unbiased estimate of the covariance of x_i and x_j is given as

$$\text{covar } (x_i, x_j) = \frac{2F}{m-n} G_{ij} \qquad \text{1.11b}$$

(NAG Manual, 1977)

If x_{min} is the true solution, then the $100(1-\alpha)$ percent confidence interval on the parameter x_i is

$$x_i - \sqrt{\text{Var } x_i} \; t_{\alpha/2, \; m-n} \; <x_{min} <x_i + \sqrt{\text{Var} x_i} \cdot t_{\alpha/2, \; m-n}$$

where the term $t_{\alpha/2}$, m-n is the 100 $\alpha/2$ percentage point of the **t**- distribution with m-n degrees of freedom. This can be obtained from statistical tables.

Following Eadie et al. (1971), Westbrook (1980) has outlined an alternative but similar approach to the one outlined above. Al-Chalabi (1970) has also presented a similar set of equations for the least-squares type objective function. It is clear from this section that the choice of objective function made in section 1.2.1 above greatly enhances the ease with which the variances and consequently statistical analysis of the optimum parameters obtained in the course of optimization can be carried out.

1.2.7 Programmed versions for Bodies of Polygonal Cross-section

A useful method for computing magnetic anomalies caused by two-dimensional bodies of polygonal cross-section has been presented by Talwani and Heirtzler (1964). Following their nomenclature, the anomaly due to a body of polygonal section A-B-C-D-E-F (Fig. 1.3) can be evaluated by adding the effects of semi-infinite prisms for all sides of the body with due regard as to sign.

Proceeding in a clockwise direction around the body, the vertical and horizontal field strengths at a field point situated at the origin are given by the following equation _

$$V = 2(J_x Q - J_z P) \qquad\qquad 1.13$$

$$H = 2(J_x P + J_z Q)$$

where

$$Q = \frac{\mu_0}{4\pi} \sum_{i=1}^{N-1} \Big[((Z_{i+1}-Z_i)(x_i-x_{i+1})/((Z_{i+1}-Z_i)^2+(x_i-x_{i+1})^2))(\theta_i-\theta_{i+1})$$

$$-((Z_{i+1}-Z_i)^2/((Z_{i+1}-Z_i)^2+(x_i-x_{i+1})^2))\log \left(\frac{R2}{R1}\right) \Big]$$
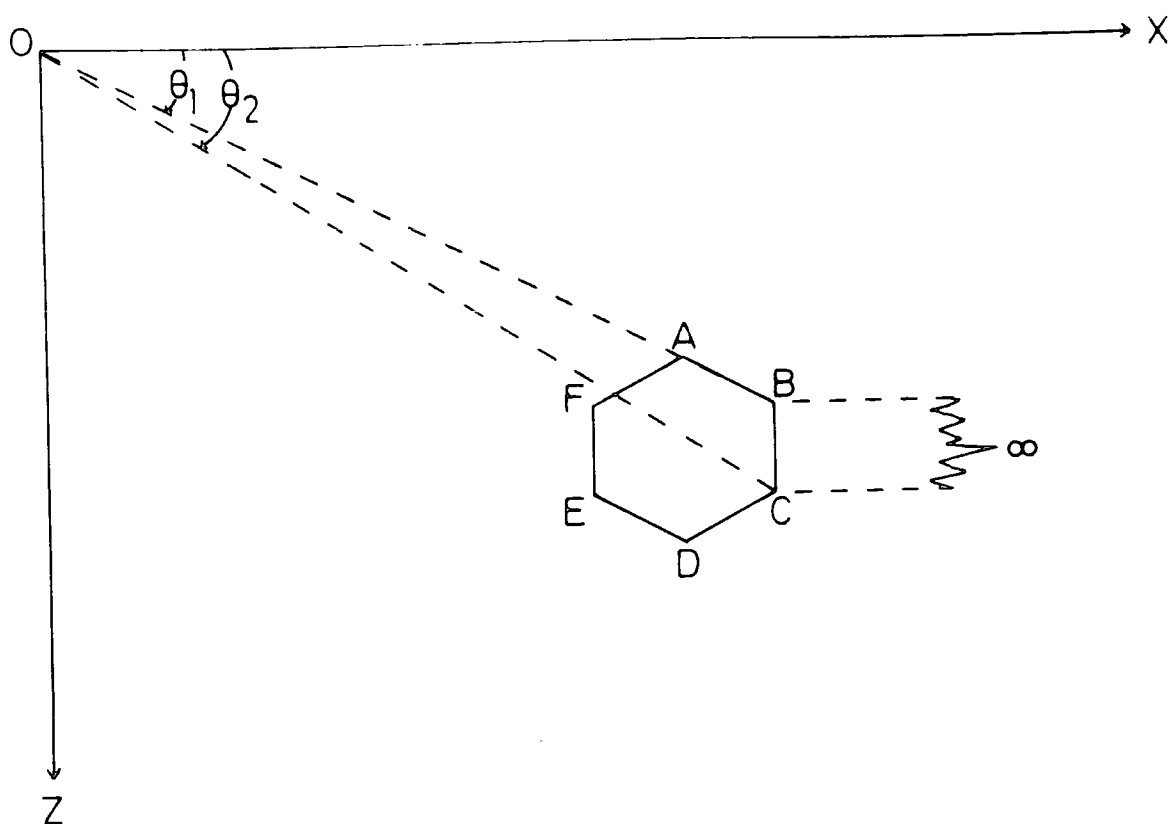
Fig 1·3 Model two dimensional body of arbitrary
cross section

$$P = \frac{\mu o}{4\pi} \sum_{i=1}^{N-1} \left[\left((z_{i+1} - z_i)^2 /((z_{i+1} - z_i)^2 + (x_i - x_{i+1})^2) \right) \right.$$

$$(\theta_i - \theta_{i+1}) + ((z_{i+1} - z_i)(x_i - x_{i+1})/((z_{i+1} - z_i)^2$$

$$\left. + (x_i - x_{i+1})^2) \right) \log \left(\frac{R_2}{R_1} \right) \right]$$

$$R_2 = (x_{i+1}^2 + z_{i+1}^2)^{\frac{1}{2}} \; ; \; R_1 = (x_i^2 + z_i^2)^{\frac{1}{2}}$$

$J_x = J \cos Im \cos\alpha m$

$J_z = J \sin Im$

J = Intensity of magnetization

Im = inclination of magnetization vector

αm = aximuth of magnetization vector

N = number of body points with the first point counted twice.

The x and z axes are horizontal and vertical respectively (Fig. 1.3).
The total field intensity T is given as :

$\quad$ T = Vsin Ie + H cosIe cosαe $\hspace{4cm}$ 1.14

where

$\quad$ Ie = inclination of Earth's field

$\quad$ αe = aximuth of Earth's field

Based on similar equations to those expressed above Al-Chalabi
(1970) has developed methods of interpretation of magnetic
anomalies due to arbitrarily shaped two-dimensional bodies by
non-linear optimization techniques. Using equation 1.14, a fortran
program MAGAT has been developed by Tantrigoda (personal communication)
for the calculation of magnetic anomalies due to bodies of rectangular
cross-section. The program MANOM is a modified version of the
program MAGAT which allows for the computation of magnetic anomalies

due to two-dimensional bodies of arbitrary cross.section. Both

programs have been tested against the program MAGN (Bott, 1969)

which exists on the Durham University Geophysics program Library

and found to give satisfactory restuls.

A fortran program OPMAG has been developed based on the

non-linear optimization techniques discussed in the preceding

sections, using the relationships developed above. The program

seeks to minimize an objective function F given by

$$F = \sum (F_{oi} - F_i - A_o - A_1 x_i)^2 \qquad\qquad 1.15$$

where

F_{oi} and F_i have their usual meaning given in section 1.2.1.

$A_o + A_1 x_i$ represent the zeroth and first order regional fields at

the ith field point. The term F_i represents the magnetic anomaly

due to one or more bodies at the ith field point and is given by

the equation 1.14. The program uses the Quasi-Newton optimization

technique discussed in section 1.2.4 above. To accomplish

optimization, a call to the NAG Library routine E04JAF is made

(NAG Reference Manual, 1977). There is no limit as to the number

of bodies making up the model provided the sum total of their body

points does not exceed forty (40). This program was only sparingly

used in the course of the present work as experience showed that

considerable amount of time is needed to obtain convergence when the

number of parameters to be optimised becomes exceedingly large which

was the case for most of the profiles interpreted over the Benue

Trough.

The use of the program was therefore limited to cases for which

the number of bodies expected to define the anomaly did not exceed

three (3) and the total number of body points does not exceed thirty

(30). A further reduction in time may be achieved if the magnet-

ization vector and its direction, as well as the regional field are

sufficiently known to be fixed.

1.3 Interpretation of Magnetic Anomalies due to Dykes by Non-linear Optimization Techniques

A number of automated approaches for the interpretation of magnetic anomalies due to two-dimensional bodies have been reported in the literature (Moo, 1965; Hall, 1968; Corbato, 1965; McGrath and Hood, 1970; Johnson, 1969; Won, 1981; Rao et al., 1973; Al-Chalabi, 1970; Westbrook, 1977; Khurana et al., 1981; Rao et al., 1981). Some of these have been specifically developed for the interpretation of anomalies due to dyke-like bodies (Won, 1981; Rao et al., 1981; Khurana et al., 1981). Won (1981) has evaluated the parameters of a dyke using the classical Gauss's method of solving non-linear equations. Convergence here depends on the closeness of the initial estimates of the parameters to the final solution and the number of equations to be solved may become exceedingly large when higher order regional fields are considered.

A combination of the methods of Gauss and steepest descent was presented by Marquardt (1963) and this has been applied in the space domain by Johnson (1969) and more recently in the frequency domain by Khurana et al., (1981). While good convergence was obtained in both cases, the rate of this convergence becomes exceedingly slow when all points on the profile are used in the scheme. The so called complex gradient method recently presented by Rao et al. (1981), requires the use of a few characteristic points on the amplitude and phase plots of the complex gradient to solve for the parameters of the dyke. This method involves a considerable amount of computation and might be time consuming. Most of these methods of dyke interpretation require the variation of excessively large number of parameters and consequently are time consuming. To overcome this some of these require some

parameters such as the magnetization and the regional field to be fixed.

A method of combined least-squares and non-linear optimization is here presented. The method seeks to minimise a non-linear objective function which represents the difference between the observed and computed anomalies due to a dyke by iteratively varying the non-linear parameters of the dyke, while obtaining optimum values of the linear parameters by least squares analysis until an acceptable fit is obtained between the observed and computed anomalies. The method has been tested on field data collected over the Minch and Hett dykes and is shown to be quicker and less expensive that most other approaches to dyke interpretation. This method was first suggested by Bott (personal communication) and initially developed by Butler (1968) in an M.Sc. dissertation at Durham. The approach of combining optimization methods with linear least squares inversion was adopted for more general two-dimensional magnetic inversion by Al-Chalabi (1970).

1.3.1 Mathematic Formulation of the Present Method

The total field anomaly due to a simple dyke model (Figure 1.4) is given as

$$T = 2JKf_1f_2 \sin d \ (\theta\sin\beta + \log (\frac{R2}{R1}) \cos\beta) \qquad 1.16$$

where

T = total field anomaly

J = intensity of magnetization of the dyke

$K = \mu o/4\pi$

$\beta = Ie' + Im' - d$

$Ie' = \tan^{-1}(\tan Ie/\cos \alpha e); \quad Im' = \tan^{-1} (\tan Im/\cos \alpha m)$

$f_1 = (1 - \cos^2 Ie \sin^2 \alpha e)^{\frac{1}{2}}; \quad f_2 = (1 - \cos^2 Im \sin^2 \alpha m)^{\frac{1}{2}}$

Ie = inclination of the Earth's field
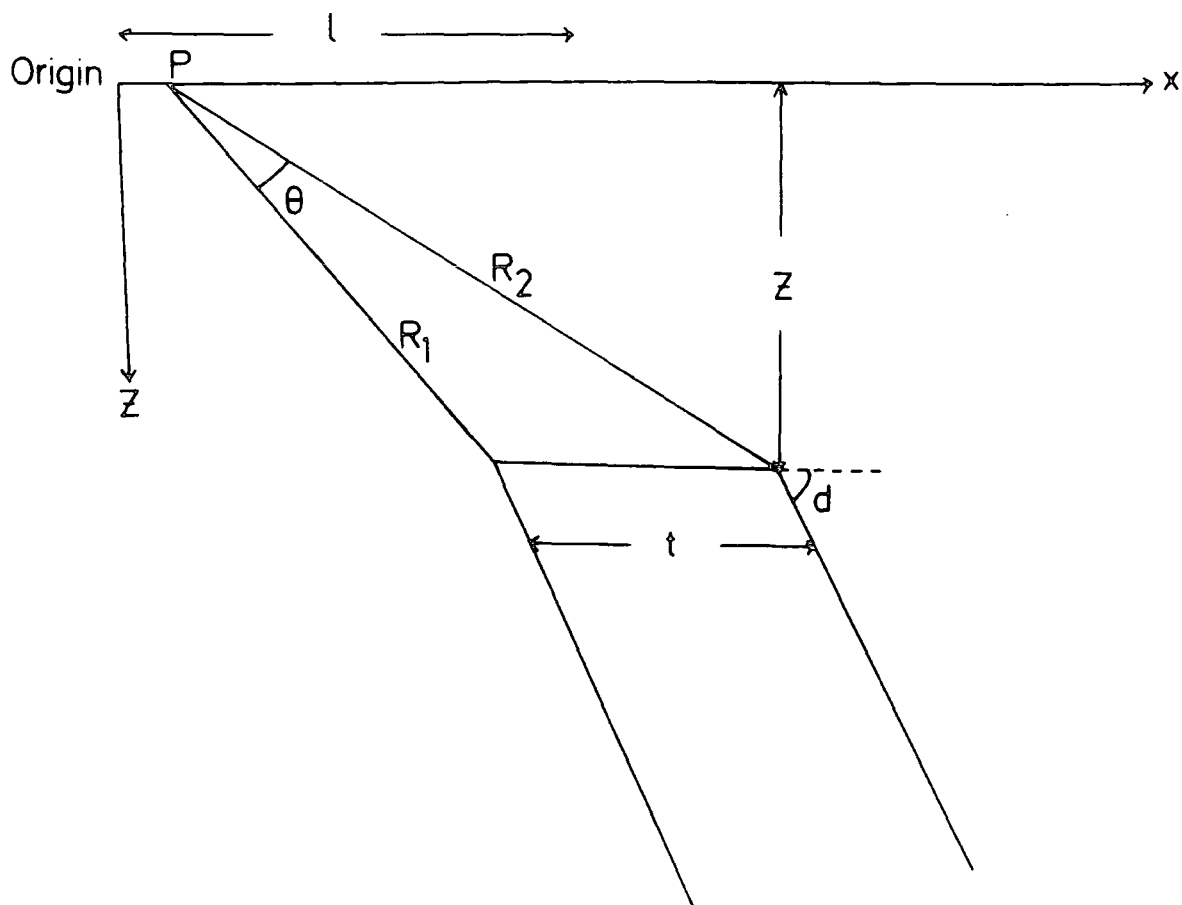
Fig. 1·4   Dyke Model giving notations

Im = inclination of direction of magnetization

αe = angle between the positve x and direction of magnetic north

αm = angle between positive x and horizontal projection of direction

of magnetization.

The above equation makes the following assumption:

(a) the dyke is uniformly magnetized

(b) the dyke has infinite strike length

(c) the dyke extends to infinite depth

(d) the dyke has parallel sides and horizontal top

(e) demagnetization effects are absent or negligible

The objective function to be minimized is

$$F = \sum_{i=1}^{N} (Ti-Ti'-Ao-A_1 x_i-A_2 x^2_i)^2 \qquad\qquad 1.17$$

where

T_i' is given by the equation for the magnetic anomaly due to a two-

dimensional, parallel sided, flat-topped and uniformly magnetized

dyke (Equation 1.16).

T_i is the observed anomaly at the ith field point.

$Ao + A_1 x_i + A_2 x_i^2$ is a quadratic regional field at the ith field point.

Combining equations 1.16 and 1.17, the objective function F is given as:

$$F = \sum_{i=1}^{N} (T_i - J_1 P(x_i) - J_2 Q(x_i) - A_o - A_1 x_i - A_2 x_i^2)^2 \qquad 1.18$$

where

$$J_1 = Jf_1 f_2 \sin d \sin \beta$$

$$J_2 = Jf_1 f_2 \sin d \cos \beta$$

$$P(x_i) = 2K\theta$$

$$Q(x_i) = 2 K \log (\frac{R_2}{R_1}) \qquad\qquad 1.19$$

and T_i, A_o, A_1 and A_2 all retain their usual meanings.

The angle θ and radial distances R_1 and R_2 can be expressed in

terms of the dyke parameters 1, t and z (Fig. 1.4).

$$P(x_i) = 2 K \tan^{-1} \left[tz/\ell^2 + (1 + \frac{t}{2} - x_i)(1 - \frac{t}{2} - x_i)) \right] \qquad 1.20$$

$$Q(x_i) = 2 K \log \left[(z^2 + (1 + \frac{t}{2} - x_i)^2)/(z^2 + (1 - \frac{t}{2} - x_i)^2) \right]$$

From equations 1.18, 1.19, 1.20, the parameters to be optimized are

1, t, z, J_1, J_2, A_o, A_1, and A_2. The parameters J_1, J_2, A_o, A_1 and

A_2 are linear parameters. The parameters defining the shape of the

dyke 1, t and z are the non-linear parameters and these in the

present scheme are evaluated by non-linear optimization routine.

A condition for a minimum of the objective function with respect

to J_1, J_2, A_o, A_1, and A_2 is that the partial derivatives of the

objective function F with respect to each of them is equal to zero.

$$\frac{\partial F}{\partial J_1} = o \quad ; \quad \frac{\partial F}{\partial J_2} = o$$

$$1.21$$

$$\frac{\partial F}{\partial A_o} = o \quad ; \quad \frac{\partial F}{\partial A_1} = o \quad ; \quad \frac{\partial F}{\partial A_2} = o$$

Carrying out these differentiations gives a set of five simultaneous

equations which, on solution, give optimal values of J_1, J_2, A_o,

A_1, and A_2 for any given values of 1, t and z; the parameters

defining the shape of the dyke. Only the parameters 1, t and z are

varied during the course of the optimization routine with J_1, J_2,

A_o, A_1 and A_2 obtained as described above for any values of 1, t and

z.

From the set of equations 1.19, it is possible to compute the

angle β, thus

$$\beta = \tan^{-1} (J_1/J_2) \qquad 1.22$$

and with slight re-arrangement of equation 1.19, a new term J' could

be derived.

$$J' = (J_1{}^2 + J_2{}^2)^{\frac{1}{2}} = Jf_1f_2 \sin d \qquad\qquad 1.23$$

The quantity J' given by equation 1.23 above in the case of a vertical dyke represents the intensity of magnetization in the xz-plane, otherwise it represents the intensity of magnetization multiplied by the sine of the angle d. If further external control exists for the angular terms αm and d, then it will be possible to compute the angle Im' which is the dip of the projection of the magnetization in the x-z plane and consequently the angle Im can be computed. With knowledge of the angular terms Im and αm the magnetization of the dyke can be computed from the following equation

$$J = J'(\cos^2 Im \sin^2 \alpha m + \sin^2 Im)^{\frac{1}{2}} \qquad\qquad 1.24$$

The true magnetization J cannot of course, be obtained unless its direction is known since the component of magnetization parallel to the strike of the dyke has no influence on the magnetic anomaly profile.

1.3.2 <u>Computer Programming of the Dyke Interpretation Method</u>

Several Fortran programs have been written for the interpretation of magnetic anomalies due to dykes using the optimization theory outlined in the last section. These programs are all straight forward in principle, easy to use and their use involves the following steps:

(a) Initial estimates of the parameters 1, t and z of the model dyke are made. These estimates are readily obtained from the observed anomaly profile using traditional characteristic methods such as one of those described by Åm (1972), Peters (1949) and Gay (1963). Due care should be taken when these estimates are made as their position to an extent determines the minimum to which most searches will converge.

(b)   Based on the initial estimates obtained above, various constraints are imposed to limit the search for a minimum to the geologically feasible region only.   These constraints in the case of a dyke are achieved by placing lower and upper bounds on permissible values of the parameters to be optimized.   The time taken to obtain optimal values of l, t, z, A_o, A_1, and A_2 is considerably reduced if good initial estimates of l, t and z as well as their lower and upper bounds are supplied.

(c)   Suitable scaling factors of the parameters are now provided. The scaling of the problems to be solved has already been discussed in detail in section 1.2.2 above.   The optimization process described in the last section is now used to obtain optimal values of the dyke parameters.   The optimization sub-routines carry out repeated evaluation of the objective function F by calls to an inner user-written subroutine which evaluates the equation 1.17 for specified values of l, t and z by the use of equation 1.18 followed by a linear least squares analysis to determine J_1, J_2, A_o, A_1 and A_2.

The program OPDYE2 is based on the scheme developed in the last section.   It seeks to obtain optimal values of l, t, z, A_o, A_1, A_2, J_1 and J_2 by iteratively varying l, t and z while at the same time obtaining the optimal values of J_1, J_2, A_o, A_1 and A_2 by least squares analysis.   An estimate of the angle β is also obtained using equation 1.22.   The program uses the Quasi-Newton optimization technique discussed in section 1.2.4 above.   To accomplish the optimization process, the program makes a call to the subroutine EO4JAF which is an easy to use Quasi-Newton algorithm which exists in the NAG subroutine library.

The program OPDYE4 is similar to the program OPDYE2 but uses the Simplex method discussed in section 1.2.5 instead of the Quasi-Newton technique.   To accomplish optimization, the program makes a

call to the NAG Library subroutine E04CCF instead of the sub-

routine E04JAF. The programs OPDYE5 and OPDYE6 are based on the

principles of the programs OPDYE2 and OPDYE4 respectively. They,

however, consider only the zeroth order regional field (A_o). The

program OPDYE7 though based on the same principle as the program

OPDYE2 already described above, it seeks to obtain optimal dyke

parameters by iteratively varying the parameters 1, t, z and β while

at the same time obtaining optimal values for the parameters A_o, A_1

and J', the magnetization in the plane of the profile by least

squares analysis. In addition to these is the program OPDYE8 which

uses the Quasi-Newton technique but assumes the observed anomaly to

have already been corrected for the regional field. The improvement

in speed of convergence obtained was not to any major extent. These

programs can readily be modified to allow the weighting of the field

points. Implementation schemes of these and other programs used in

this work as well as a listing of them are given in Appendix B to

this thesis.

The Simplex method which is used by the programs OPDYE4 and OPDYE6

tends to be very slow in converging to a minimum. The method is

however, usually robust and definitely assures convergence and is very

useful for functions that may be subject to inaccuracies. In

comparison with the Simplex method, the Quasi-Newton method used in

the programs OPDYE2, OPDYE5, OPDYE7 and OPDYE8 is generally faster

and can handle many more variables. However the method like other

Gradient methods is quite sensitive to curvatures and local gradients

thus the search could terminate by local convergence when the

particular function happens to have many ill-defined local minima.

Moreover, the approximation of the behaviour of the objective

function by a truncated Taylor's series may be very unrepresentative,

especially in regions far away from the solution. Combined with the

problem of providing analytical derivatives, these disadvantages of
the Quasi-Newton method might reduce the extent to which it may be
recommended for use in geophysical interpretation. These problems
did not affect the effectiveness of the method as used in the
present method of dyke interpretation. This was to a great extent
due to the greatly reduced number of parameters to be optimised and
the ability of the scheme to constrain the search as close as
possible to the geologically feasible regions only. The use of any
of these programs on the NUMAC computer requires about 0.20-0.80 cpu
seconds depending on the length of the profile and its complexities.
The final results of the use of any of these programs is a graphical
output giving a plot of the observed and computed anomalies as well as
the optimal model dyke - assumed to be vertical - required to explain
the observed anomaly.

1.3.3 Advantages of the Present Method

The method presented here has certain advantages over some of
the other methods of dyke interpretation. These are (a) all points
of a profile are used to obtain a solution; (b) guaranteed convergence
to an absolute minimum, (c) the speed at which a solution is obtained,
(d) geological feasibility of the solution can be taken into account
and (e) reduction in the number of parameters for which initial
estimates are required.

The method presented here assures convergence to an absolute
minimum and this can be readily illustrated by a study of the behaviour
of the objective function F described by the equation 1.13. Figure
1.5 shows a plot of the objective functions F as a function of the
thickness (t) and depth to the top (z) of a model dyke of thickness
2.0 km and depth to the top 1.0 km. That the present scheme
converges to an absolute minimum is clearly manifested in Figure 1.5

Figure 1.5   Plot of the Objective function (F) as a function of
thickness (t) and depth to the top (z) of a model
dyke of thickness 2 km and depth 1 km.

where the position of the minimum is at the point, t = 2.0 km and

z = 1.0 km. For dykes which are narrower than their depth, however,

it is only possible to determine the product tJ' (J' given in

equation 1.23) with high degree of confidence. The behaviour of

the objective function F for model dykes of varying thickness to

depth ratios have been investigated and the results of this study

are presented in the next section (Section 1.3.4). The behaviour

of the obective function in the case of a field dyke has also been

studied. It was found that the complexities of ambiguity associated

with the magnetization contrast of the dyke inherent in most other

methods (e.g. Khurana et al., 1981) is greatly reduced. Although

the contours were complicated, the position of the absolute minimum

was still clearly marked out. This can be attributed to the linearity

of the method with respect to the magnetization J.

Perhaps the greatest advantage of the present method lies in

the speed with which solutions are obtained. This is partly due to

the reduced number of parameters to be optimized and the ability of

the model to be constrained as well as the ease with which convergence

takes place. In general, the time taken to obtain a solution depends

on the number of variables, the behaviour of the objective function and

distance of the starting model from the absolute solution as well as

the length of the profile to be interpreted. Tests showed however,

that using the present scheme, the time taken to obtain a solution

for a modest profile of one hundred (100) field points in the presence

of fairly reasonable constraints will hardly exceed 1.40 cpu seconds.

The method has been tested on the interpretation of magnetic

anomalies across the Hett dyke. The Hett dyke is a quartz-dolerite

dyke of ENE trend which outcrops a few kilometers south of Durham,

north-east England. It cuts the Middle Coal Measures, but is overlain

by sediments of Upper Permian age, so that it is probably of late
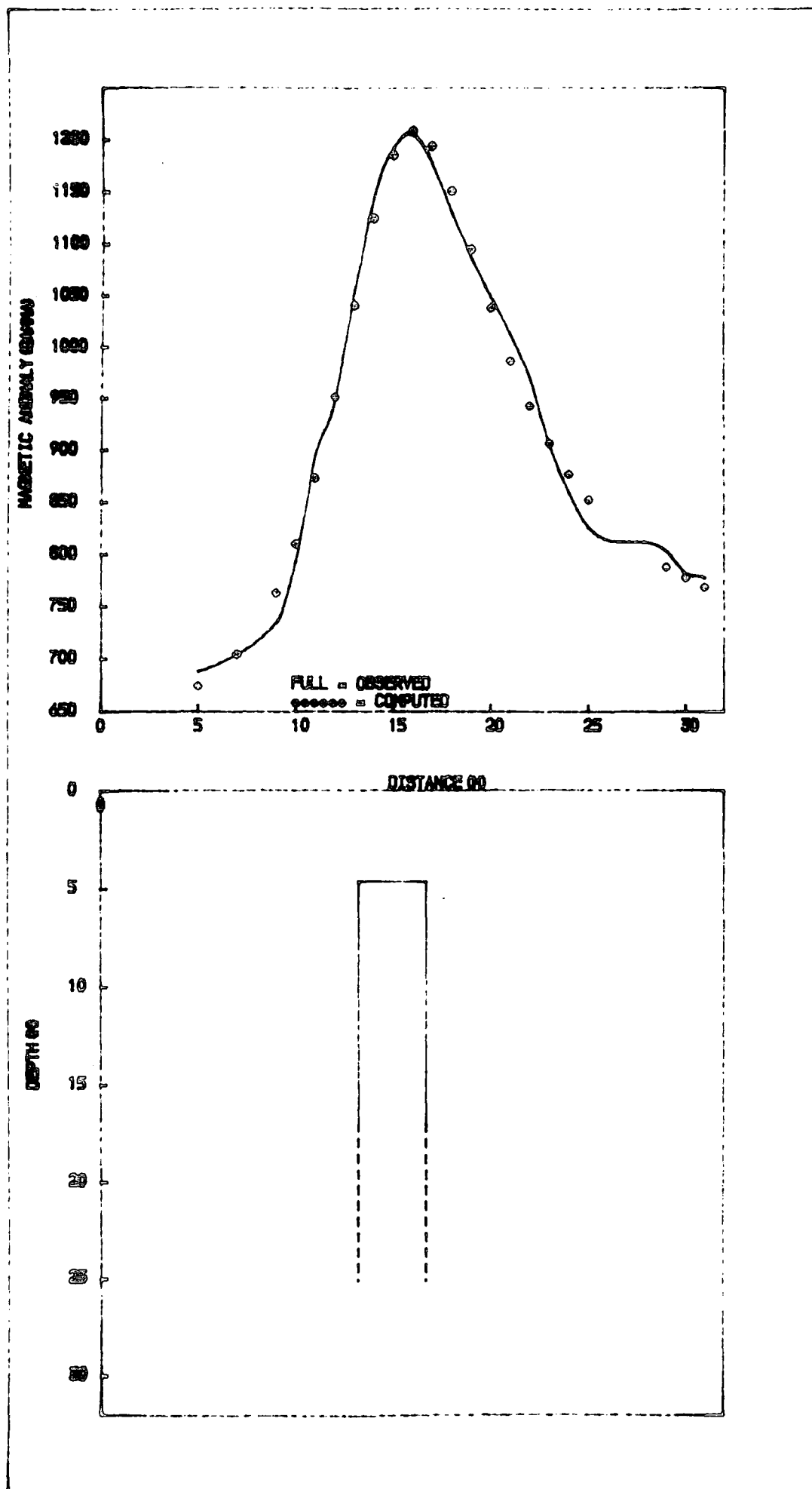
Figure 1.6 Optimum model dyke required to account for the anomaly
observed over the Hett dyke.

Carboniferous or early Permian age. A profile across the dyke near Crook, which is about 10 km west of Durham, has been interpreted using the scheme presented above. Here the dyke is covered by a thin layer of drift deposits. The model (Figure 1.6) suggests a thickness of 3.55 m, a depth to the top of 4.66 m and an angle β of 118.2°. This is approximately consistent with induced magnetization in the present direction of the Earth's field. The model took 0.71 cpu seconds to obtain using the NUMAC IMB 370 computer. The method has also been applied to a detailed study of the Minch dyke and the results of this study form Chapter Three of this thesis.

1.3.4 Non-uniqueness in Dyke Interpretation

It is well know that a given gravity or magnetic anomaly cannot be uniquely interpreted in terms of the depth, shape, density or magnetization of the causative body. For any observed gravity anomaly, it is possible to obtain a whole family of configurations, any one of which can satisfactorily account for the observed anomaly; the shallowest possible configuration is that whose highest point coincides with the surface of the ground. The problem is even more complicated for magnetic anomalies because of the additional uncertainty over the direction of magnetization of the body.

The problem of ambiguity is essentially a direct consequence of potential field theory but it is added to by other factors resulting directly from the practical limitations of the observations. These are incomplete knowledge of the actual length of the anomaly, limited number of observations and errors involved in their measurements, reduction and interpretation. Interpretations obtained by using such methods as non-linear optimization may also converge to a local minimum (section 1.2.2). Attempts have been

made by several authors at defining conditions under which a solution from the interpretation of a given gravity or magnetic data could be regarded as being unique (Skeels, 1947, 1963; Roy, 1962; Smith, 1978; Al-Chalabi, 1970).

A study of the ambiguity encountered in the interpretation of magnetic anomalies due to dykes is here given. This study is based on the behaviour of the objective function presented geometrically (section 1.2.1), by plotting the values of the objective function for any two chosen parameters of a model dyke for varying thickness-depth ratios. A similar study has been carried out by Al-Chalabi (1970, 1971), for the more general case of an arbitrarily shaped two-dimensional body of polygonal cross-section.

In theory the thickness (t), depth (z) and angle β of a model dyke required to explain a given magnetic anomaly can be uniquely determined from an interpretation of the observed anomaly. This is not however, the case in practice as some degree of ambiguity is introduced by the practical limitations of the observation caused by errors involved in the measurement, reduction and interpretation of the observation. The exact minimum to which convergence should take place cannot therefore be uniquely determined. The degree to which any solution departs from the expected unique solution is usually determined by the value of the objective function corresponding to the solution and this in turn, depends on the magnitude of the errors present. The estimation of confidence limits and lower and upper bounds on acceptable solution have been discussed in section 1.2.6 above. The additional ambiguity arising from errors in the observation depends to a great extent on the thickness-depth ratio of the model dyke; increasing as the thickness-depth ratio decreases.
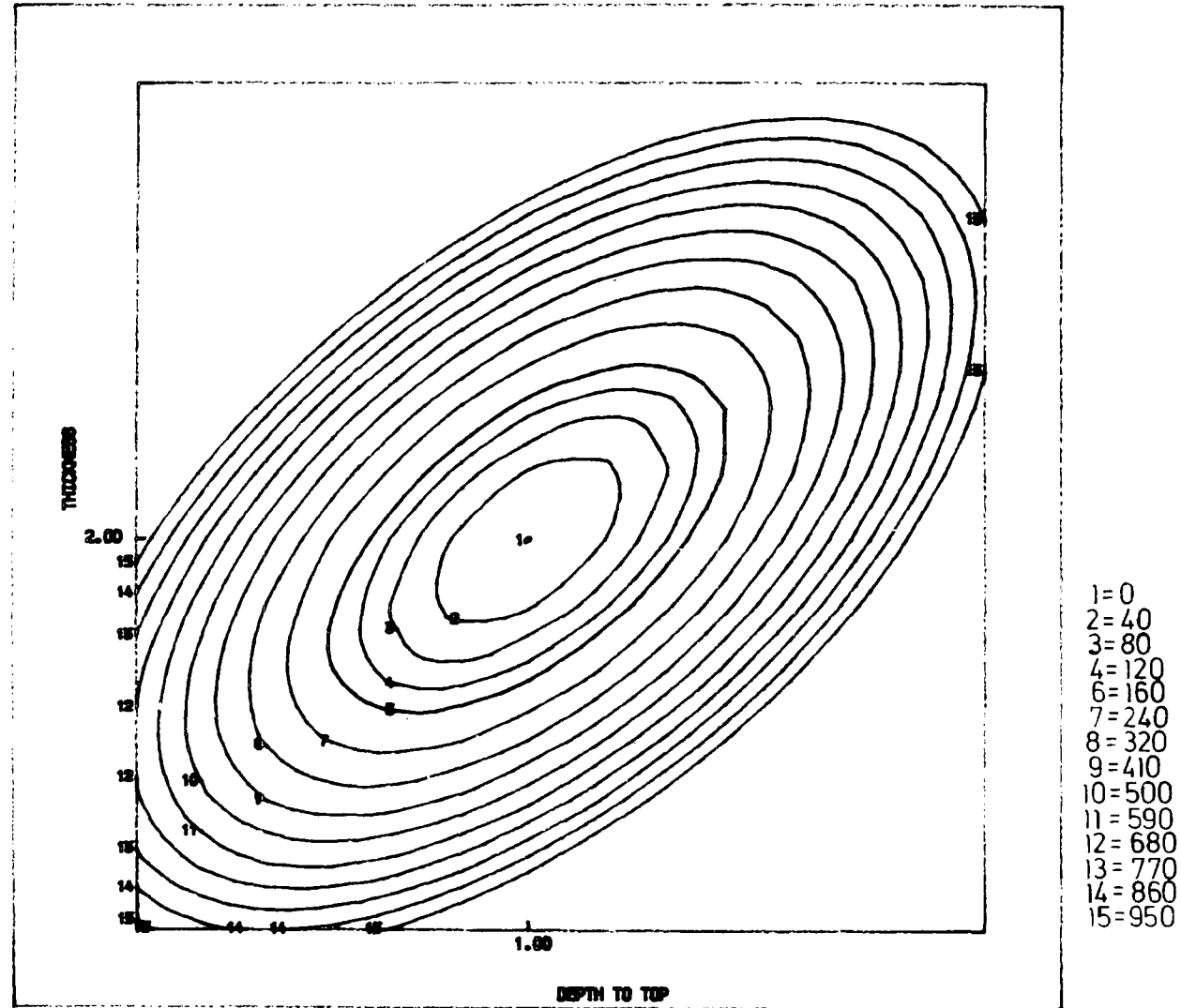
Figures 1.7a, 1.7b, 1.8a and 1.8b are plots of the objective function F as a function of the thickness (t) and depth to the top (z) of a model dyke of thickness-depth ratio equal to 2.0, 1.0, 0.50 and 0.25 respectively. The position of the minimum is most clearly defined for the model of thickness-depth ratio equal to two (Figure 1.7a). The progressive extension of the zero valued contour (labelled No. 1) in Figures 1.7b, 1.8a and 1.8b is an expression of the problem of ambiguity of the solution converged to. It is evident from these diagrams that the position of the minimum becomes less well defined as the thickness-depth ratio decreases. It is therefore, not possible to obtain a unique value for the thickness of a dyke if t << z (Figures 1.8a and 1.8b). A study of the behaviour of the objective function as a function of the magnetization in the plane of the profile (J') and the depth to the top of a dyke model has been carried out for thickness-depth ratios of 1.0, 0.50 and 0.25 (Figures 1.9a, 1.9b and 1.9c). Results similar to those for F(t,z) were obtained as only the depth to the top of the dyke can be obtained uniquely as the thickness-depth ratio reduces (Figures 1.9b and 1.9c). This case however is not as important as the case of a study of the behaviour of the objective function with respect to the thickness and magnetiz- ation in the plane of the profile presented next.

Figures 1.10a, 1.10b, 1.11a, 1.11b, 1.12a and 1.12b show plots of the objective function as a function of the thickness and magnetization (J') for model dykes of thickness-depth ratio of 8.0, 6.0, 4.0, 2.0, 1.0 and 0.50 respectively. As can be seem from these plots even for thickness-depth ratio as high as 8.0, the problem of ambiguity of solution still persists and solutions for the thickness and magnetization (J') are hardly unique. The elongation of the contours for the case of thickness-depth ratio equal to 0.50 is a clear manifestation of the degree of ambiguity encountered and the product of

a

b

Figure 1.7   Plot of the objective function (F) as a function of
             thickness (t) and depth (z) for thickness – depth
             ratios of (a) 2.0 and (b) 1.0.
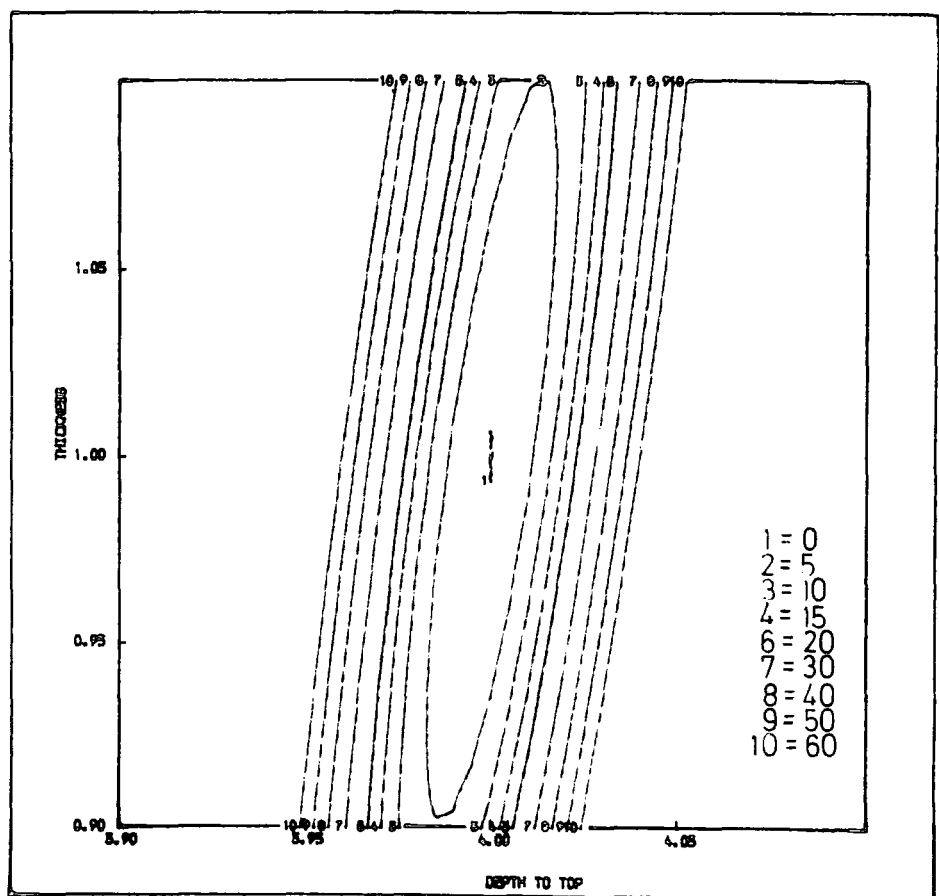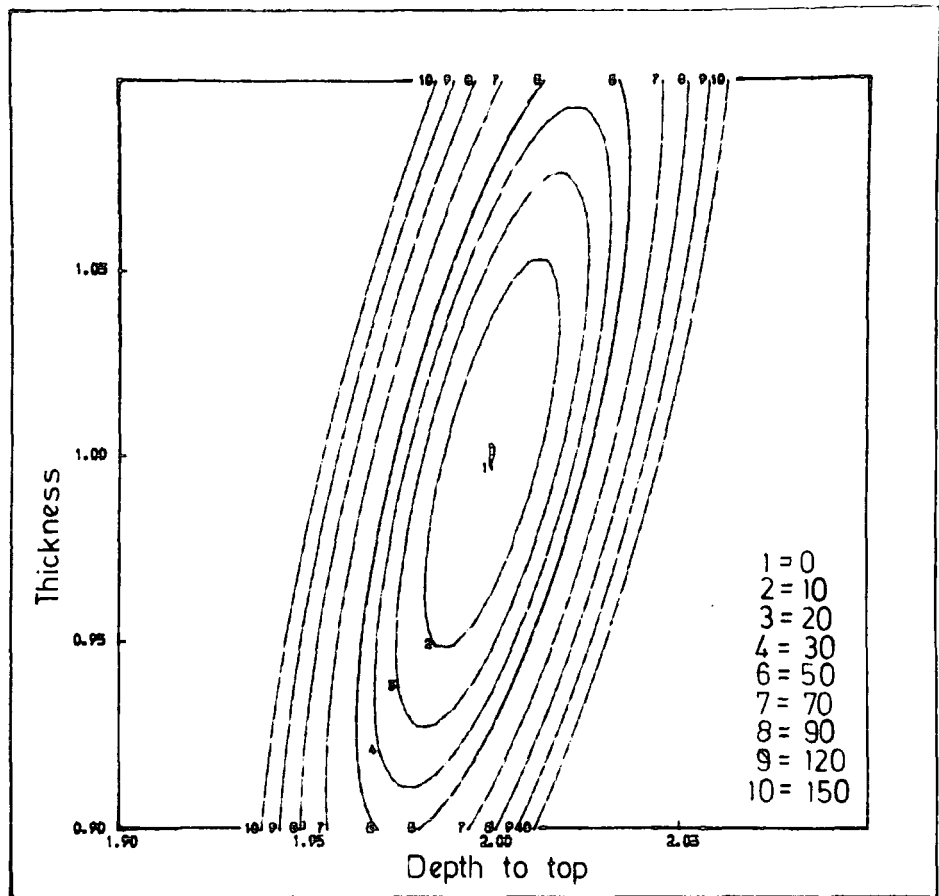
Figure 1.8 Plot of the objective function (F) as a function of
            thickness (t) and depth (z) for thickness – depth
            ratios of (a) 0.5 and 0.25.
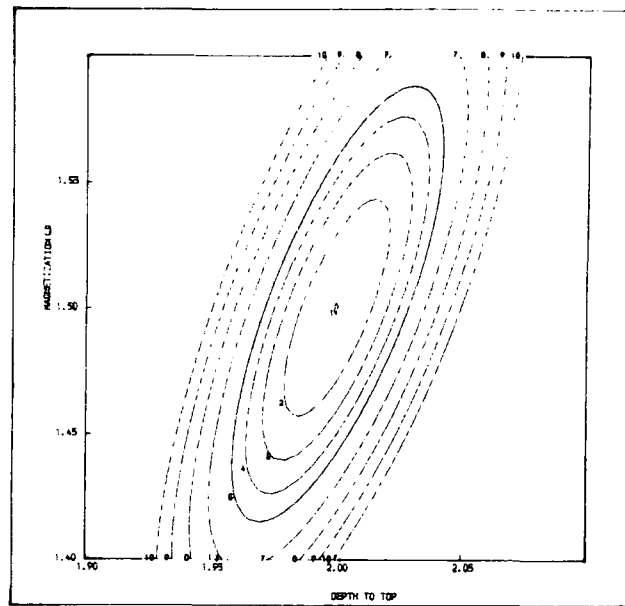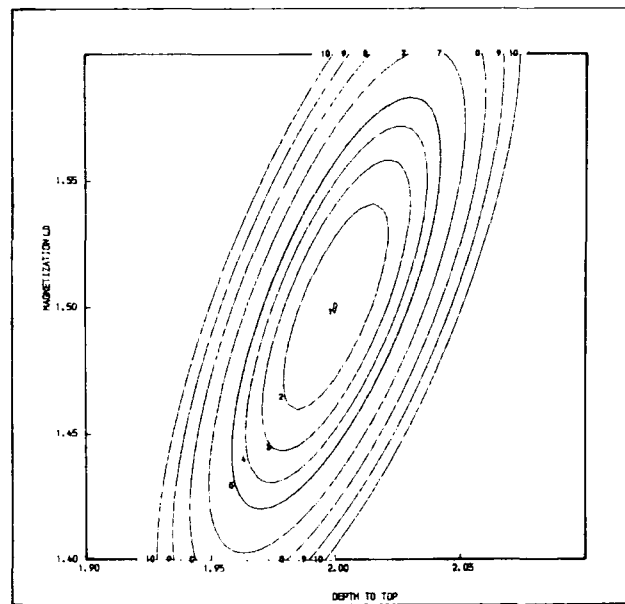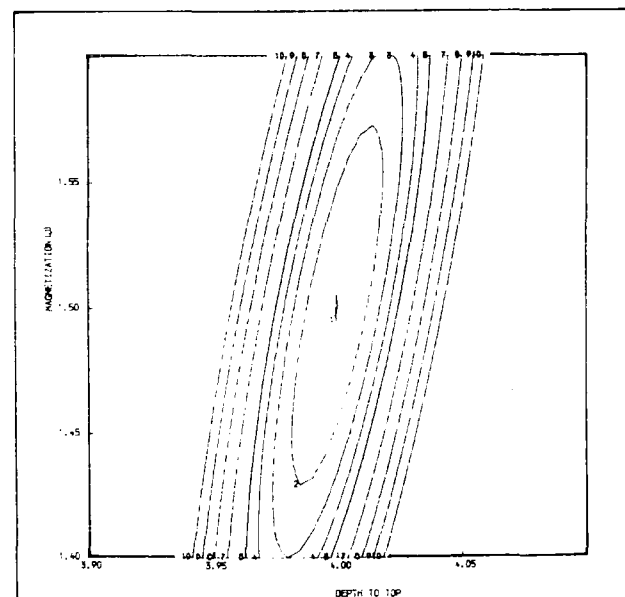
1=0
2=50
3=100
4=150
6=200
7=300
8=400
9=500
10=600

Figure 1.9   Plot of the objective function (F) as a function of
magnetization (J') and depth (z) for thickness – depth
ratios of (a) 1.0, (b) 0.5 and (c) 0.25.

Figure 1.10 Plot of the objective function (F) as a function of
thickness (t) and magnetization (J') for thickness –
depth ratios of (a) 8.0 and (b) 6.0.
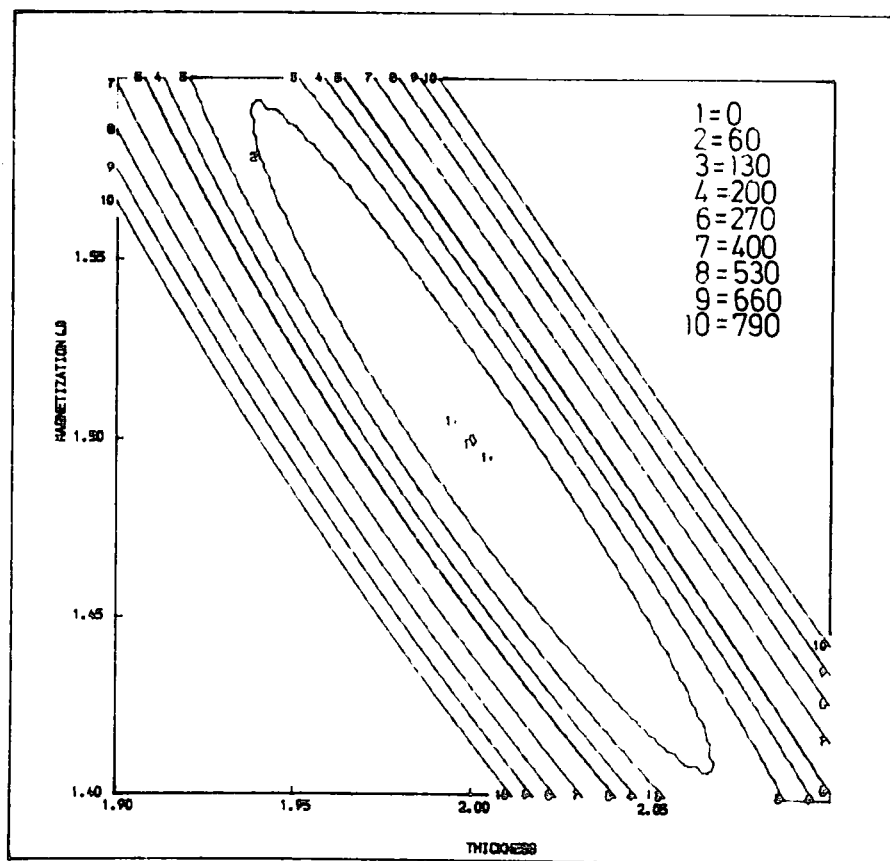
Figure 1.11   Plot of the objective function (F) as a function of
              thickness (t) and magnetization (J') for thickness -
              depth ratios of (a) 4.0 and (b) 2.0.
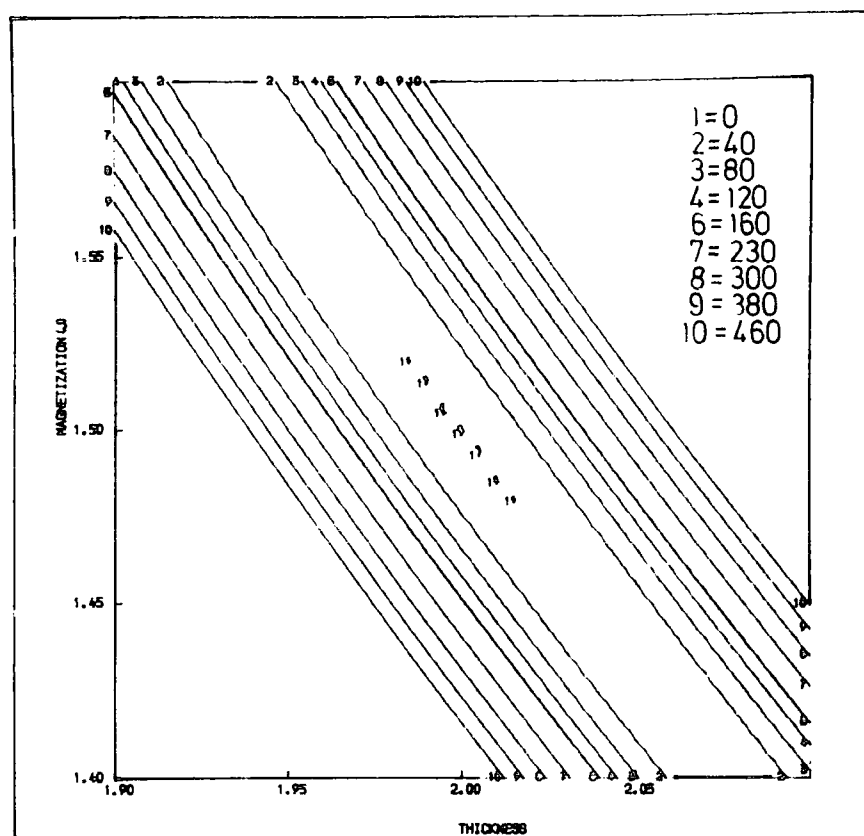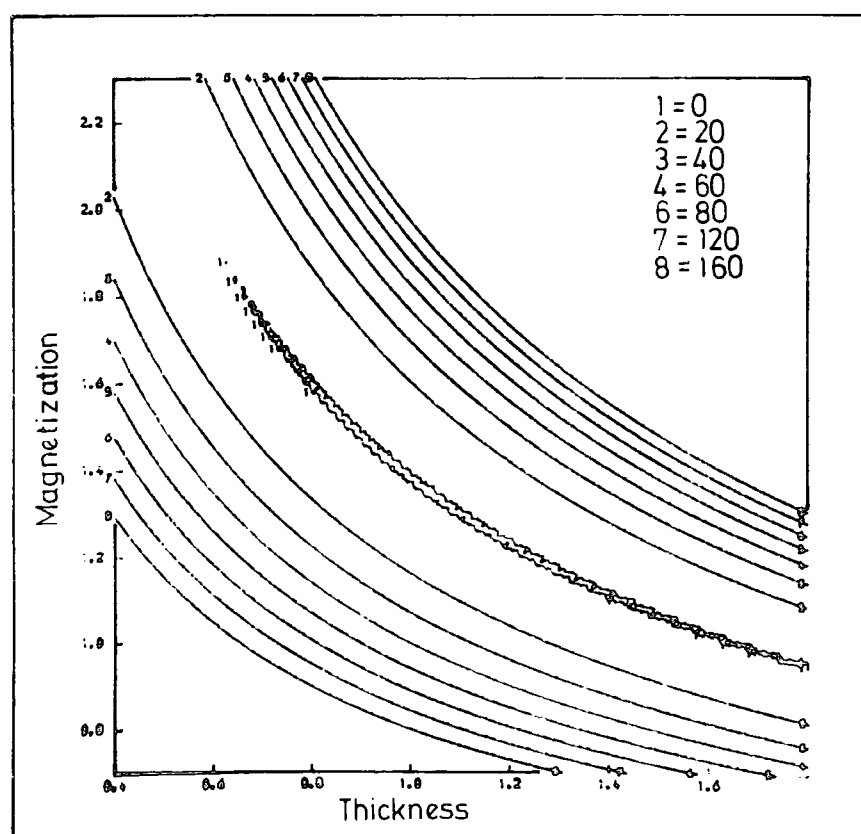
Figure 1.12   Plot of the objective function (F) as a function of
              thickness (t) and magnetization (J') for thickness –
              depth ratios of (a) 1.0 and (b) 0.50.

the thickness and the magnetization only varies very slightly along

the entire contour (Figure 1.12b). Even at a thickness-depth ratio

of 1.00, the position of the absolute minimum is still not clearly

marked out but the ambiguity in the solution is reduced (Figure 1.12a).

The elongation of the contours progressively reduces as the thickness-

depth ratio increases and this is an indication of the gradual

reduction in the degree of ambiguity as the thickness of the model

dyke becomes greater than the depth. At ratios of 4.0, 6.0 and 8.0

the position of the minimum becomes well defined although the

elongation of the zeroth value contours in the magnetization (J') axis

(Figures 1.10a, 1.10b and 1.11a) suggests that there exists more

uniqueness in the determination of the thickness than in the

determination of the magnetization.

The behaviour of the objective function, as a function of the

angle β and thickness of a dyke has been studied for model dykes of

varying thickness-depth ratio. Figures 1.13a, 1.13b, 1.14a, 1.14b,

1.15a and 1.15b, show plots of the objective function F in terms of

the thickness and the angle β for model dykes of thickness-depth ratio

of 0.25, 0.50, 1.00, 2.00, 4.00, and 8.00 respectively. Although

the position of the absolute minimum appears well defined for all

the ratios, the geometry of the contours progressively changes in an

interesting manner. For a thickness-depth ratio of 0.25, the contours

of the objective function appear slightly elongated parallel to

the thickness axis (Figure 1.13a). As the thickness to depth ratio

increases, there is a gradual decrease in the elongation of the

contours parallel to the thickness axis and an increase in the

elongation in the direction of the angle β (Figures 1.13b, 1.14a,

1.14b, 1.15a and 1.15b). A similar set of plots for the objective

function (F) in terms of the angle β and the magnetization in the

plane of the profile (J') are shown in Figures 1.16a, 1.16b, 1.17a,
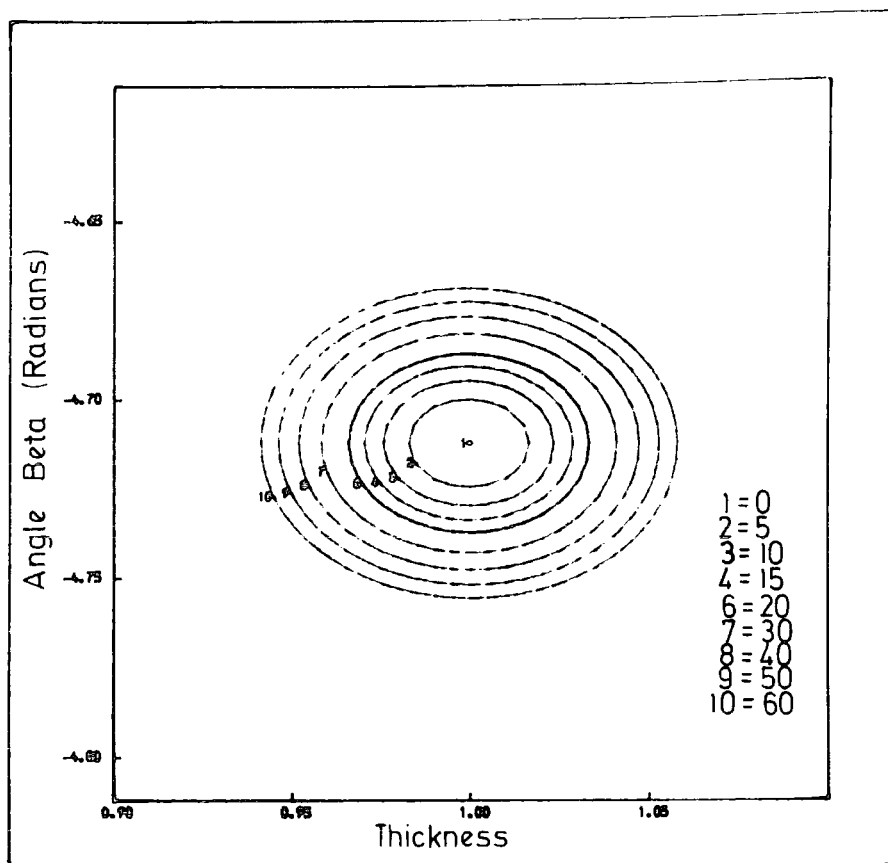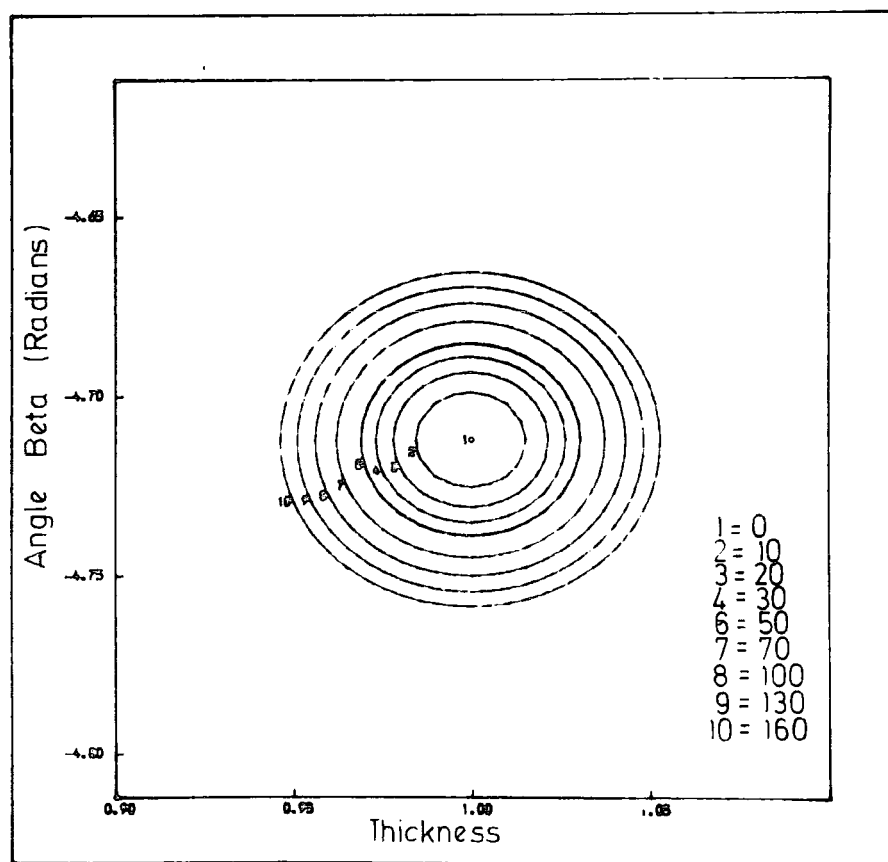
Figure 1.13 Plot of the objective function (F) as a function of the angle β and thickness (t) for thickness - depth ratios of (a) 0.25 and (b) 0.50.
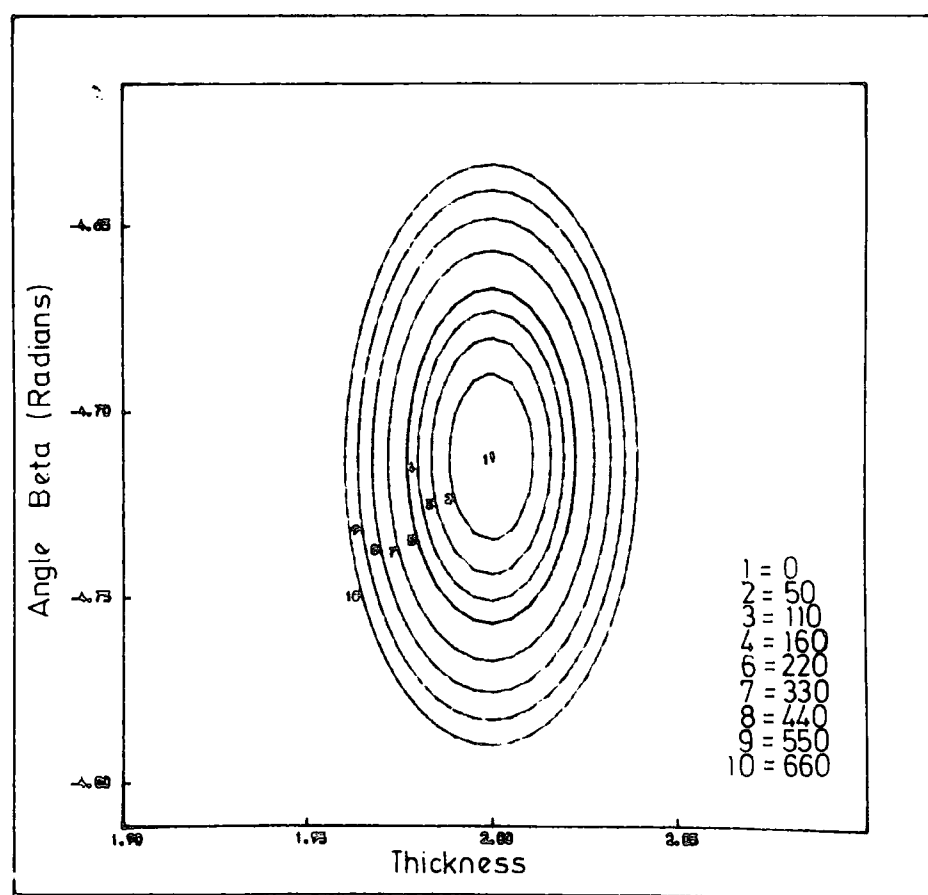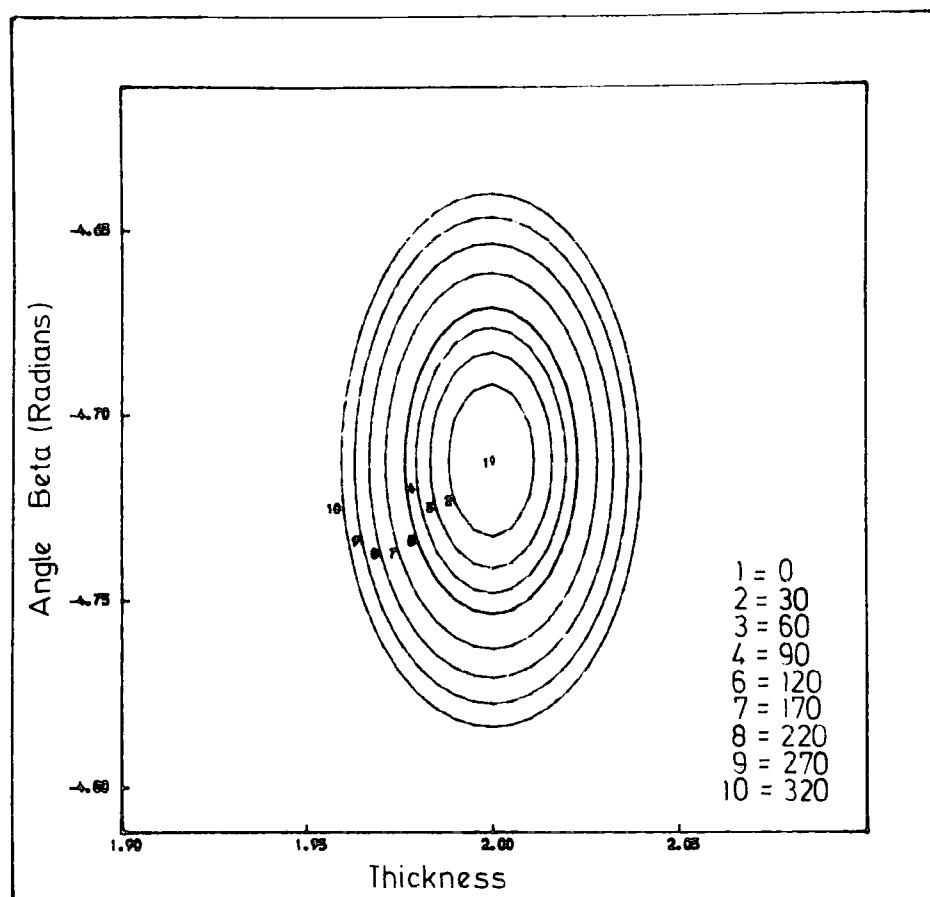
Figure 1.14   Plot of the objection function (F) as a function of
              the angle β and thickness (t) for thickness – depth
              ratios of (a) 1.0 and (b) 2.0.
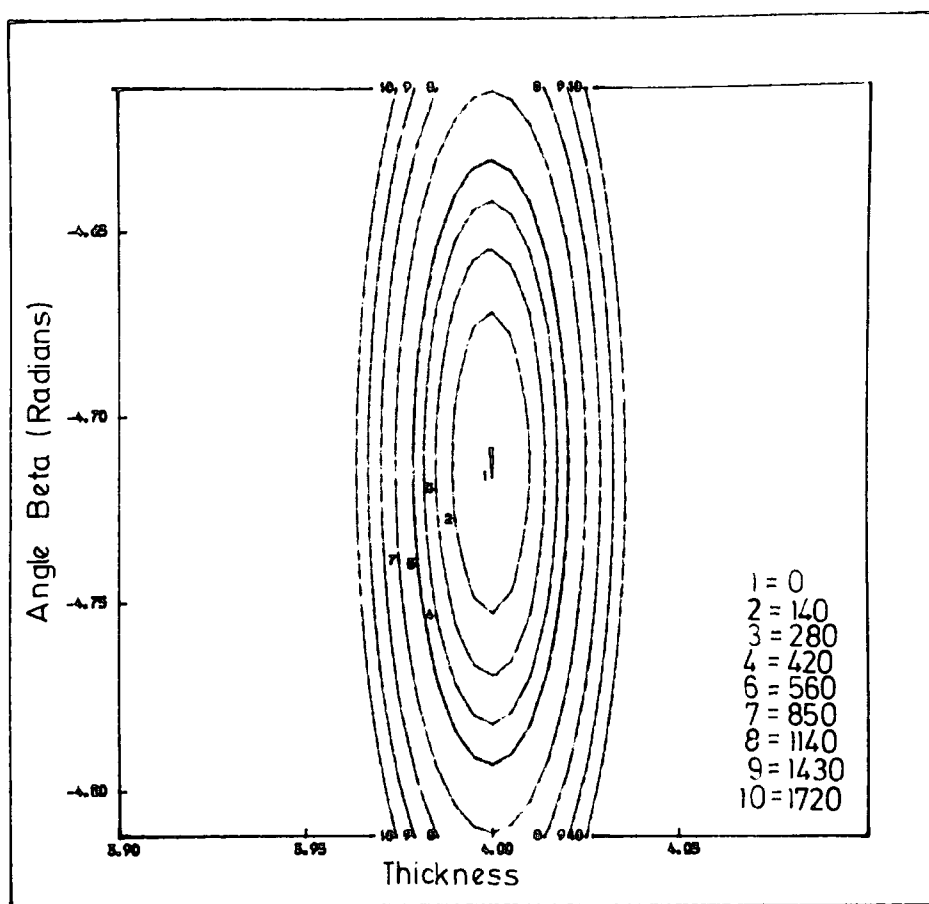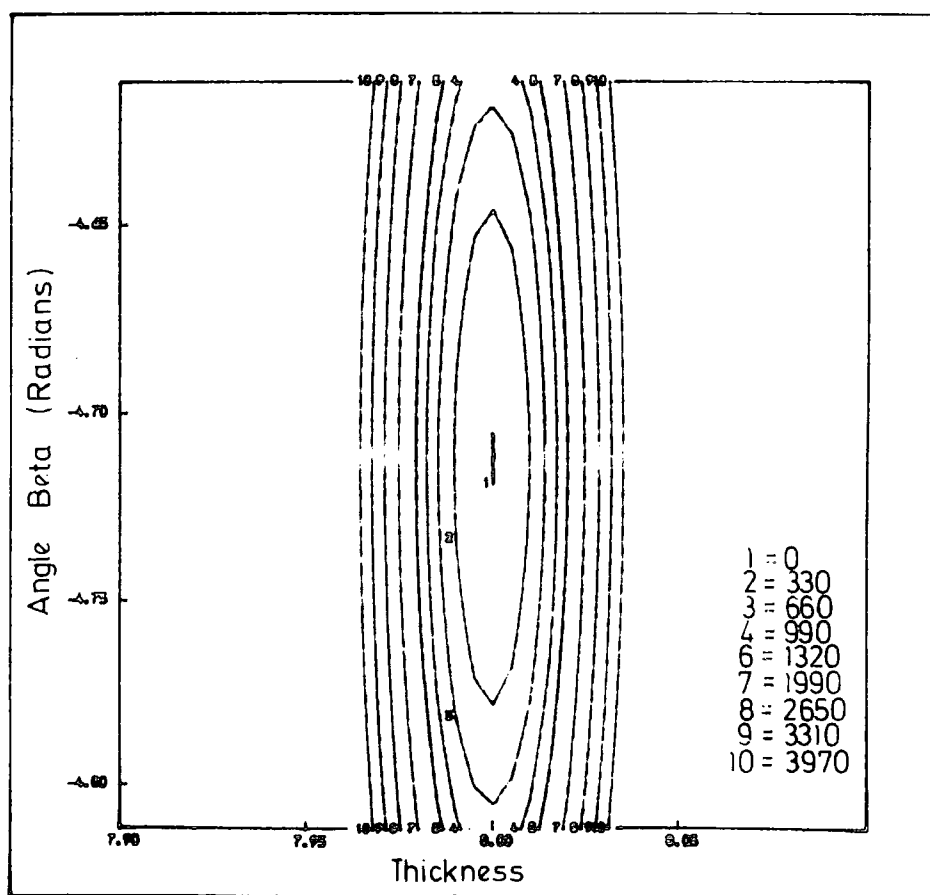
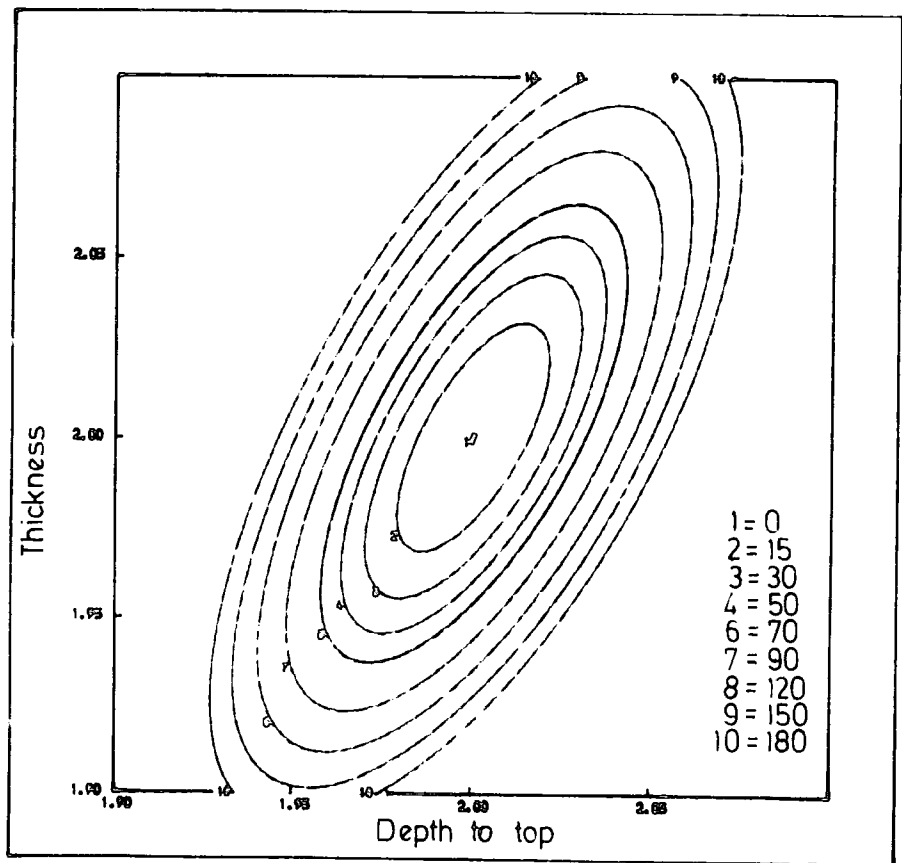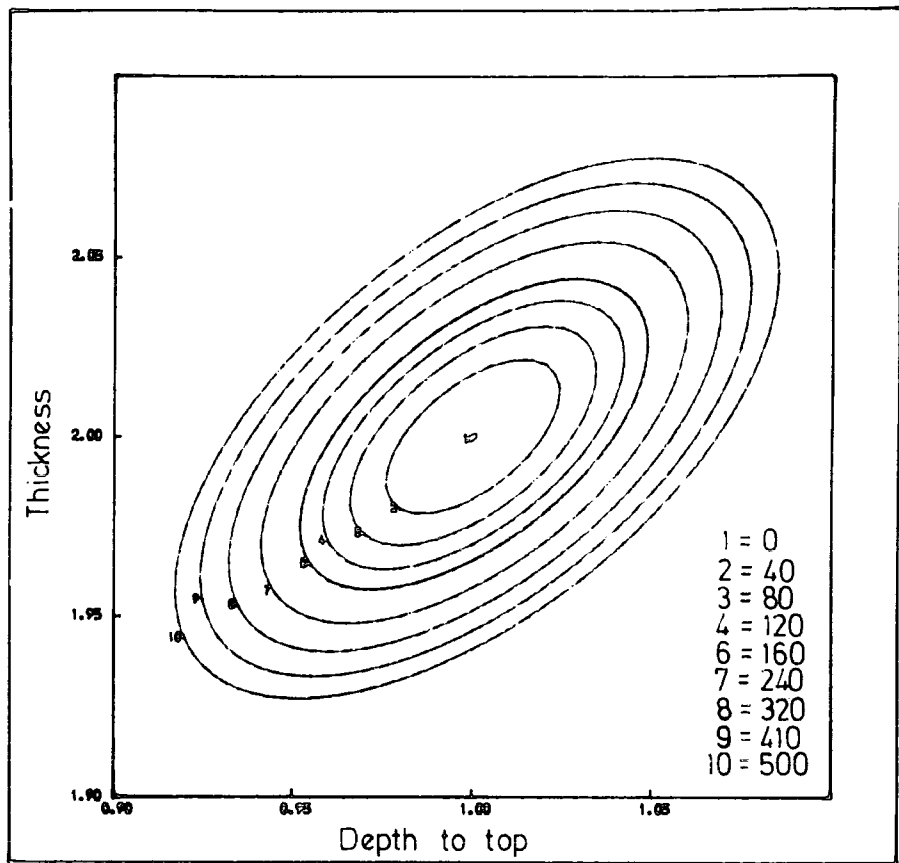Figure 1.15   Plot of the objective function (F) as a function of
              the angle β and thickness (t) for thickness – depth
              ratios of (a) 4.0 and (b) 8.0.
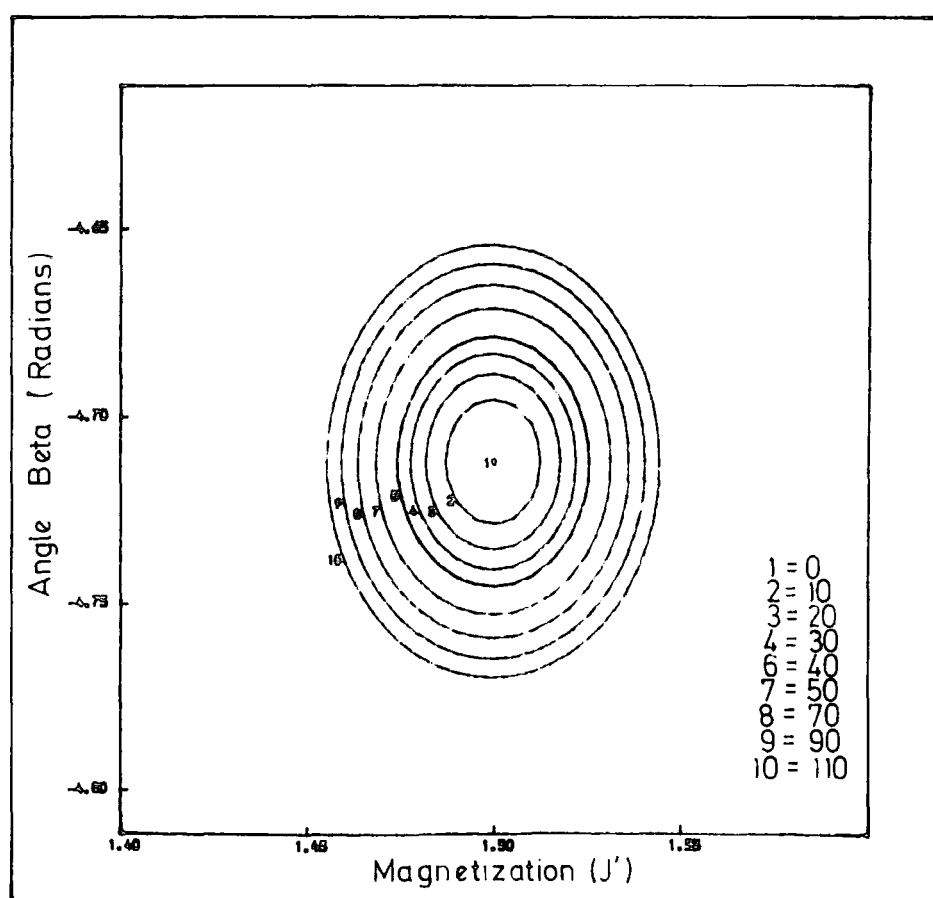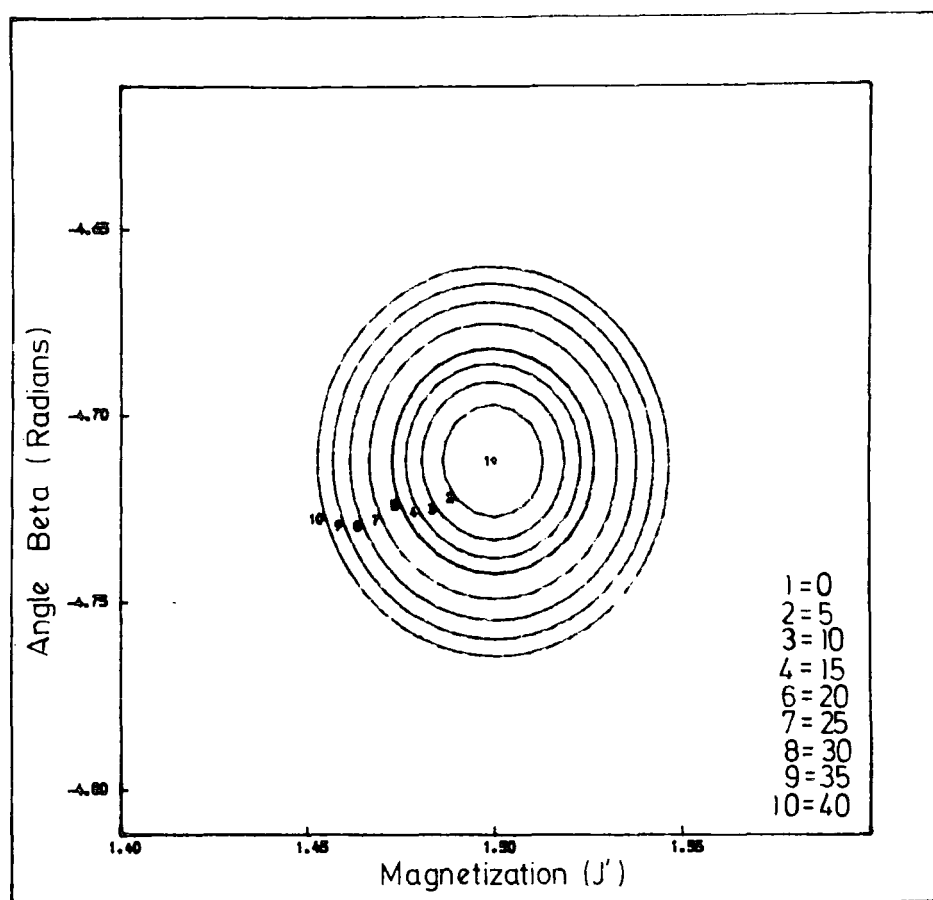
Figure 1.16   Plot of the objective function (F) as a function of
the angle β and the magnetization (J') for thickness –
depth ratios of (a) 0.25 and (b) 0.50.

1.17b, 1.18a and 1.18b. As in the previous case, the position of the absolute minimum can be precisely located. The elongation of the contours in the direction of the angle β as the thickness to depth ratio increases is not however as pronounced in this case as in the case of F(t,β).

1.4 Linear Inverse Method and Joint Analysis of Magnetic and Gravity Anomalies

Usually the linear inverse problem in magnetic interpretation reduces to the computation of the lateral variation of magnetization within a specified layer which gives rise to a given magnetic anomaly. To achieve this the layer is split up into a series of two-dimensional blocks each having uniform magnetization (Figure 1.19) and the observed anomaly at each field point on the surface expressed as the sum of contributions from the individual blocks :

$$Ai = \sum_{j=1}^{M} K_{ij} J_j \qquad (i=1 \dots, n; \; j=1 \dots, m) \qquad 1.26$$

where Ai is the observed anomaly at the ith field point

J_j is the intensity of magnetization of the jth block

Ki_j is the magnetic anomaly caused by the jth block at the ith field point for a unit intensity of magnetization.

The set of equations giving equation 1.26 can be solved directly for J_j provided m=n and K is non singular. If m<n however, the over determined set of equations can be solved by least squares or by some other means of minimization (Bott, 1967). In the fully determined case when m=n, in matrix notation, the solution is given as

$$J = K^{-1} A \qquad\qquad 1.27$$
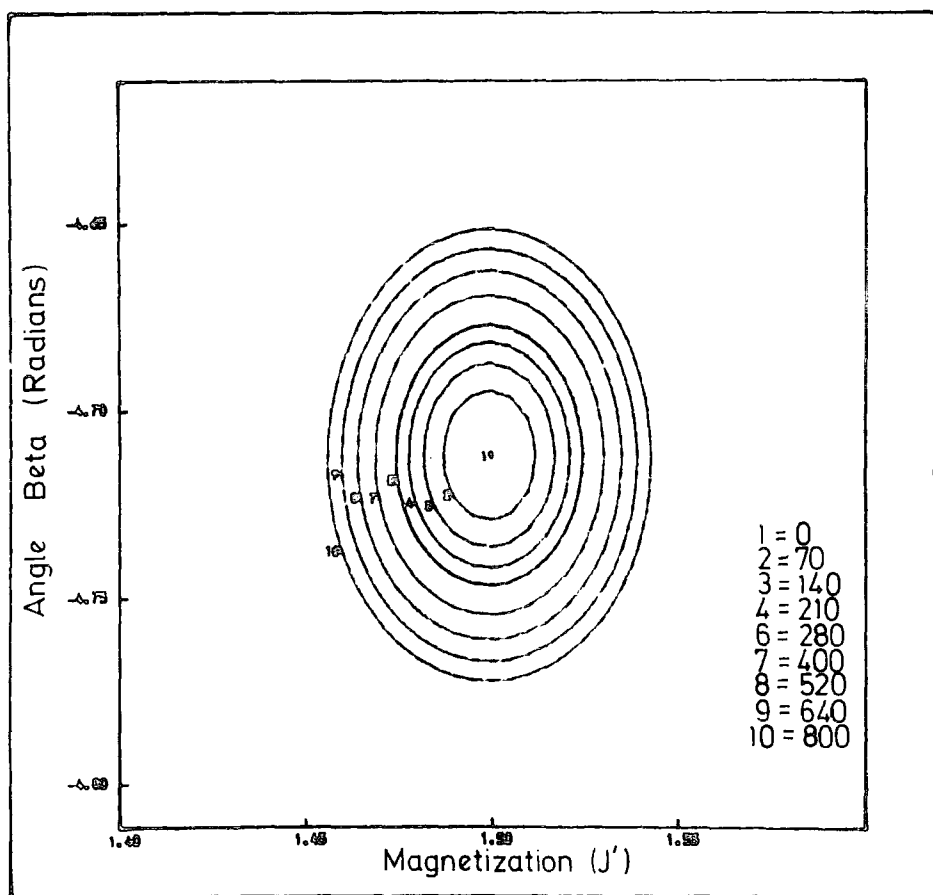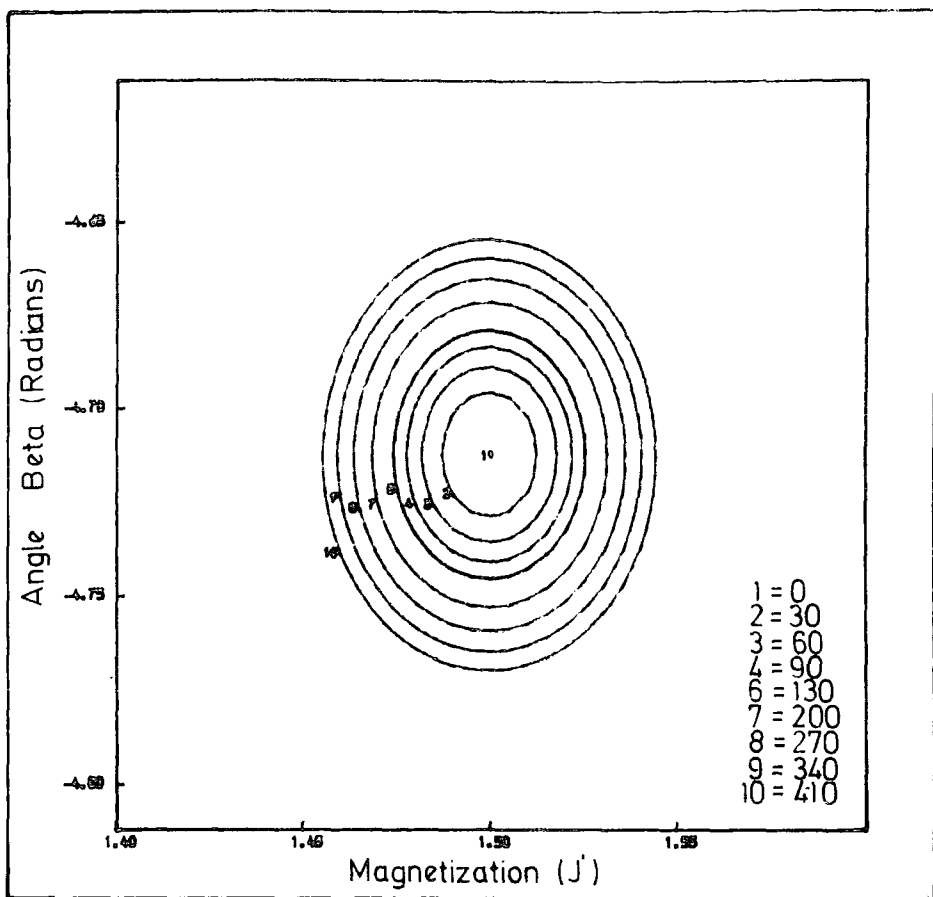
Figure 1.17 Plot of the objective function (F) as a function of the angle β and the magnetization (J') for thickness – depth ratios of (a) 1.0 and (b) 2.0.
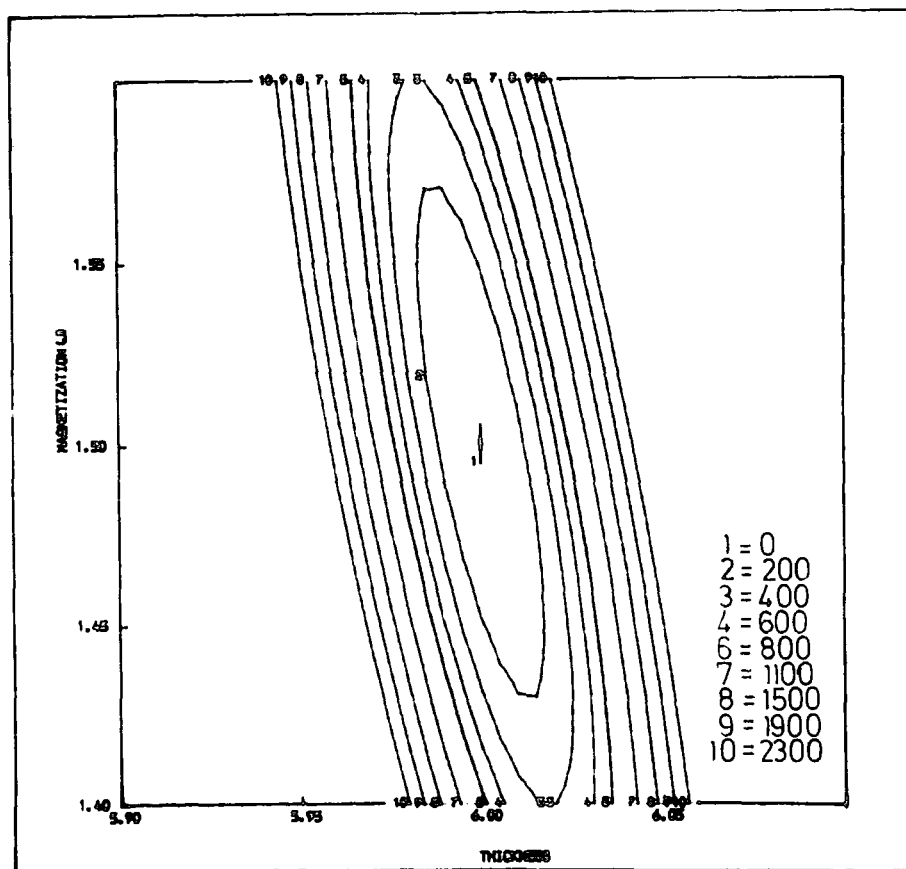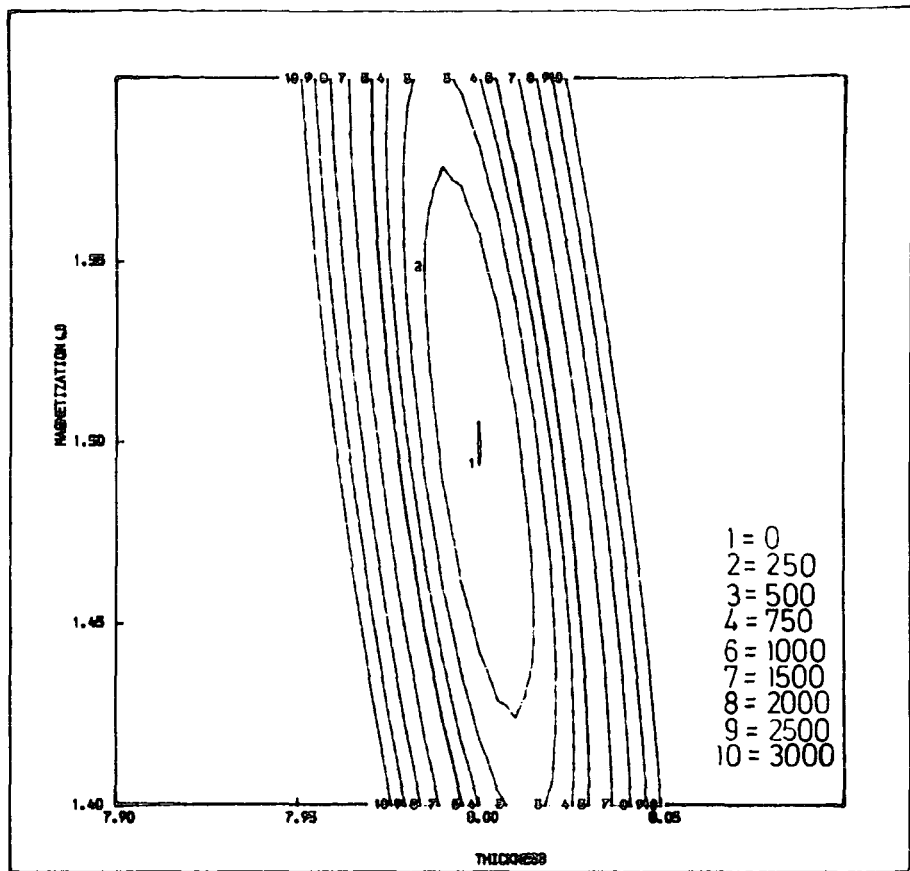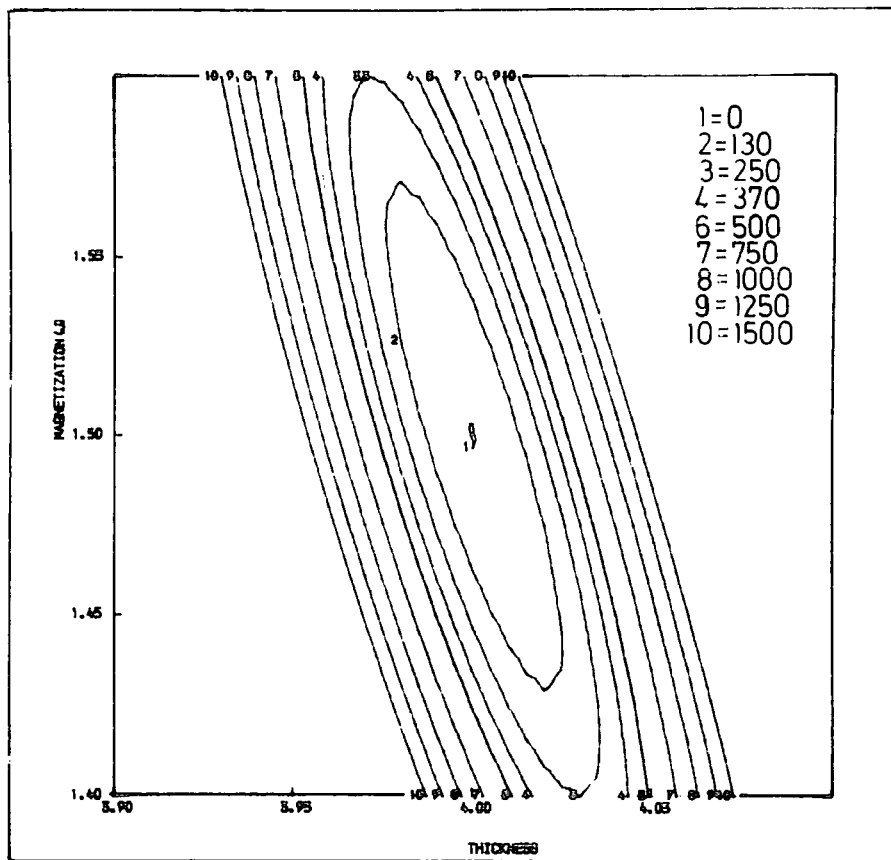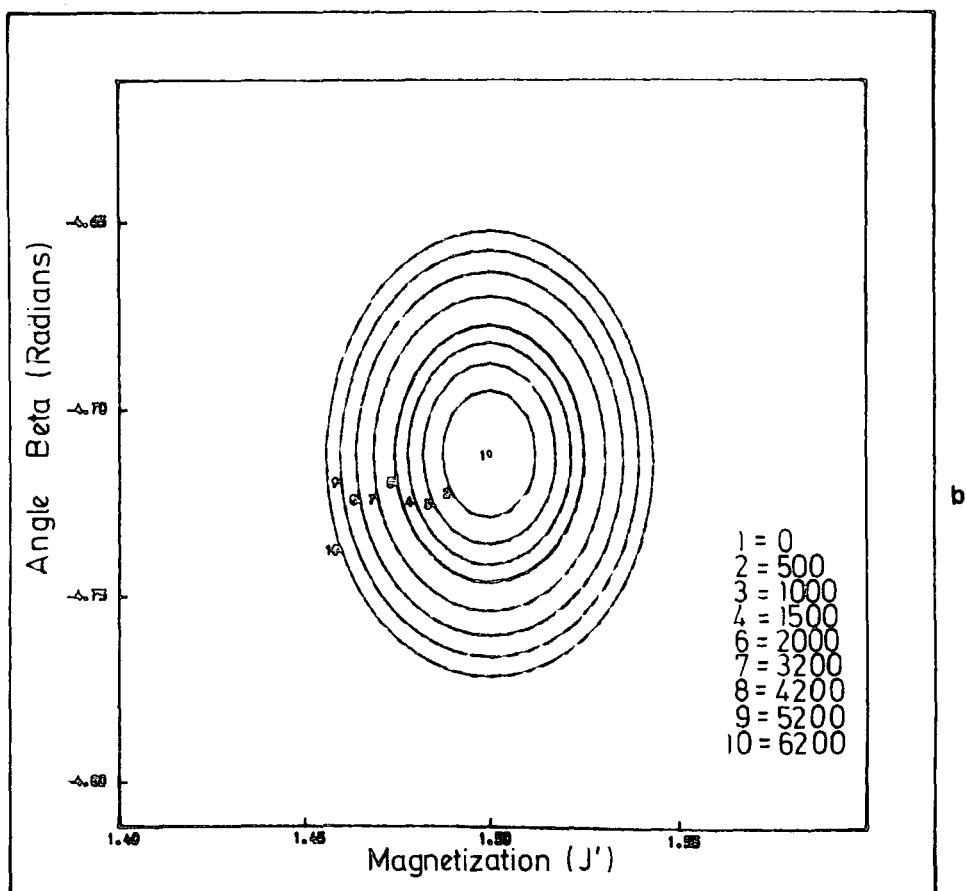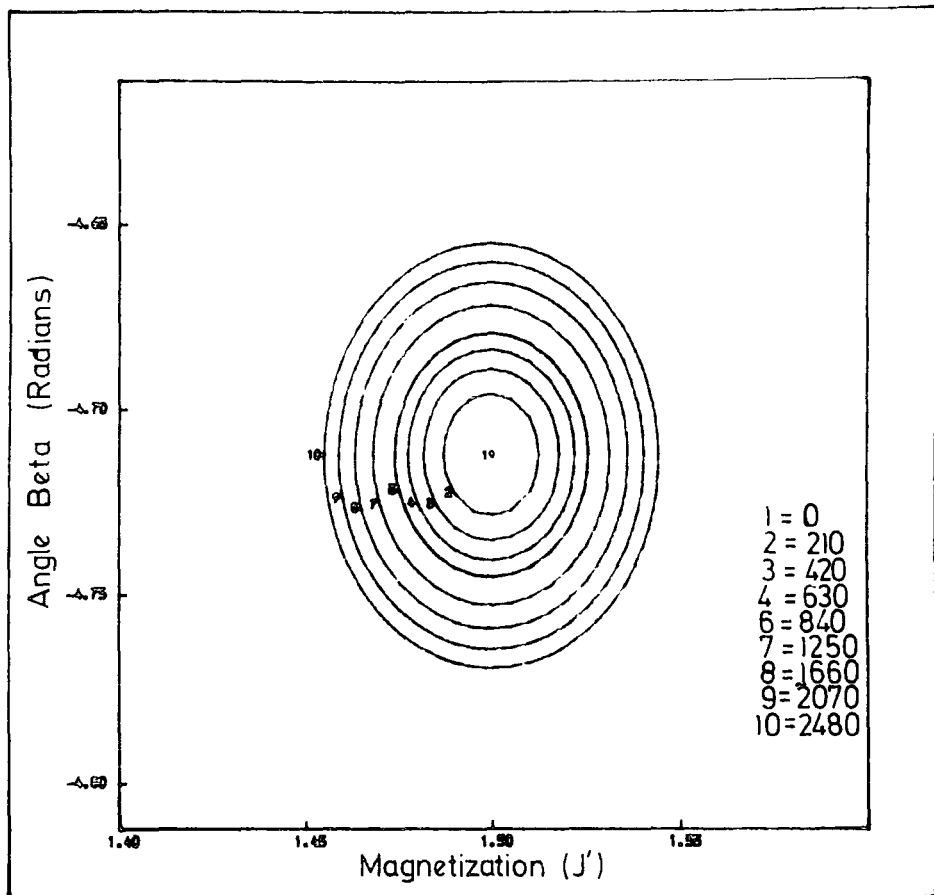
Figure 1.18 Plot of the objective function (F) as a function of the angle β and the magnetization (J') for thickness – depth ratios (a) 4.0 and (b) 8.0.
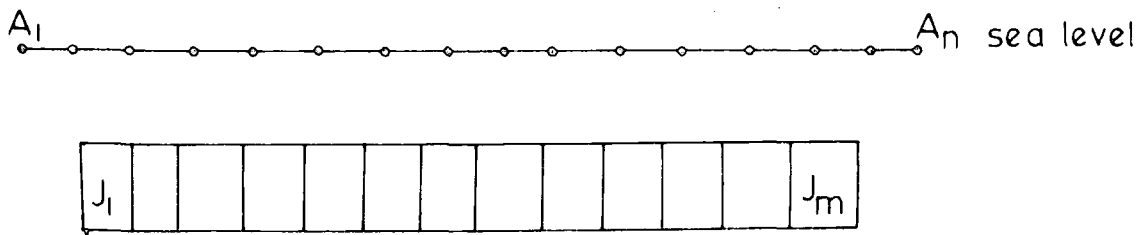
Fig 1·19 Model layer of Blocks
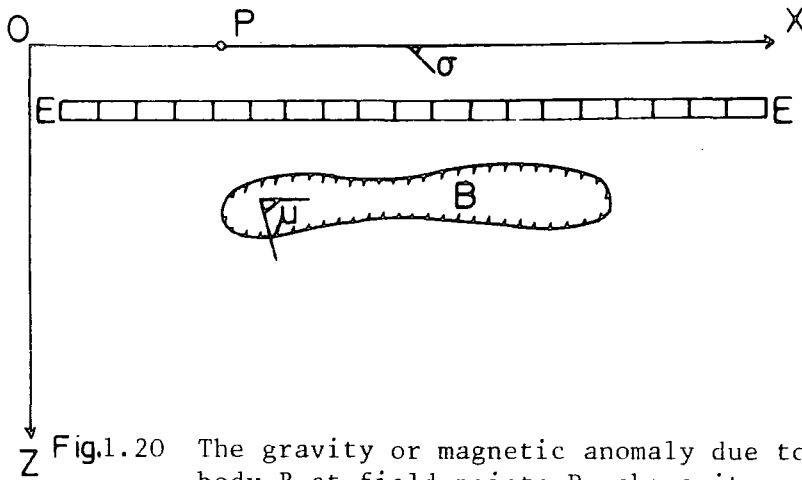
Fig.1.20 The gravity or magnetic anomaly due to a two-dimensional body B at field points P_c above it can be simulated to any desired degree of accuracy by a two-dimensional equivalent layer EE divided into retangular blocks each having uniform density or magnetization, provided the block size is chosen to be sufficiently small and the extent of the layer is sufficiently wide. (After Ingles, 1971).
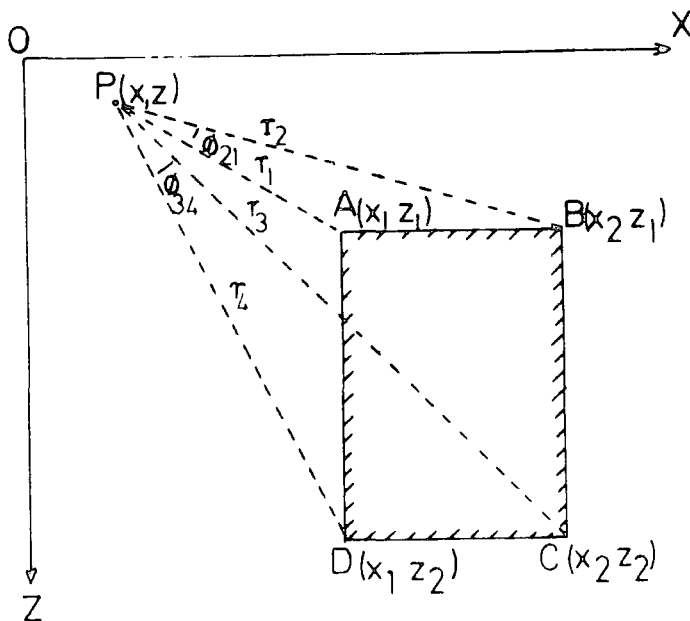
Figure 1.21 Geometry of the basic two-dimensional rectangular block used to form the equivalent layers in relation to a field point P. (After Ingles, 1971).

In the overdetermined case when m<n, the solution in matrix notation is given from a solution of the normal equation

$$K^T A = K^T KJ \qquad\qquad 1.28$$

whose theoretical solution is given as

$$J = (K^T K)^{-1} K^T A \qquad\qquad 1.29$$

The theory of the linear inverse method has been discussed by several authors (Bott, 1967; Tanner,1967; Emilia and Bodvarsson, 1969; Bott and Hutton, 1970; Bott and Ingles, 1972; Bott, 1973a). Applications of the method to the study of oceanic magnetic anomalies have been also discussed by most of these authors as well as its use in the joint interpretation of gravity and magnetic anomalies (Bott and Ingles, 1972; Bott, 1973a). An iterative adaptation of the theory has been used for theinterpretation of magnetic anomalies due to two dimensional bodies by Kunaratnam (1972). Following the approach of Bott and Ingles (1972) and Bott (1973a), the method is here applied to the conversion of magnetic anomalies over the Lower and Middle Benue Trough to pseudogravimetric anomalies. In all its application in the present work, attempts were made to make m equal to n hence constraining the programming to only the fully determined case (equation 1.27).

1.4.1 Use of Matrix Method in Computation of Pseudogravimetric Anomalies

To apply the matrix method discussed above to the joint interpretation of magnetic and gravity anomalies, no assumptions need to be made about the shape of the causative body though both the gravity and magnetic anomalies must be related to each other through the use of a common fictitious equivalent layer (Figure 1.20).

The magnetic anomaly due to any body may be uniquely interpreted
in terms of an equivalent magnetic layer as long as the directions
of magnetization and of the observed field strength are specified.
The corresponding gravity anomaly can likewise be uniquely inter-
preted in terms of a similar equivalent gravity layer.

The chosen fictitious layer is usually divided into a series
of blocks, each possessing uniform magnetization and density but
possibly of variable dimensions. In the present work rectangular
blocks of uniform dimensions have been used (Figure 1.21). The
gravity anomaly values G_i observed at the surface are related to
the density value d_j of the individual blocks by

$$G_i = \sum_{j=i}^{m} K_{ij} J_j \qquad\qquad 1.31$$

where

$$C_{ij} = 2G \left[(x_2 - x)\log(\frac{r3}{r2}) - (x_1 - x)\log(\frac{r4}{r1}) + \right.$$

$$\left. (z_2 - z)\phi_{34} - (z_1 - z)\phi_{21} \right]$$

$$K_{ij} = \frac{\mu oF}{4\pi G} \left[\frac{\partial Ci_j}{\partial x} \sin\beta - \frac{\partial Ci_j}{\partial z} \cos\beta \right]$$

$$F = (\sin^2 Im + \cos^2 Im \cos^2 \alpha m)^{\frac{1}{2}} (\sin^2 Ie + \cos^2 Ie \cos^2 \alpha e)^{\frac{1}{2}}$$

$\beta = \mu + \sigma$

$\mu = \tan^{-1} (\tan Im / \cos \alpha m)$

$\sigma = \tan^{-1} (\tan Ie / \cos \alpha e)$

Ie = dip of the Earth's field

Im = dip of the magnetization

αe = azimuth of the Earth's field direction

αm = azimuth of the magnetization direction and the terms

r_1, r_2, r_3, r_4, x_1, x, z_1, z, x_2, z_2, ϕ_{34}, ϕ_{21} follow from

Figure 1.21.

The terms C_{ij} and K_{ij} are readily evaluated by programs similar to GRAVN and MAGN (Bott, 1969) provided the co-ordinates of the blocks and field points as well as the angle β are specified. To compute the pseudogravimetric anomaly, the observed magnetic anomaly is inverted to give the magnetization values of the individual blocks forming the equivalent layer. The corresponding values of density for each of these blocks are computed by assuming a constant ratio between the magnetization J_j and the density d_j according to the Poisson relationship. In the exactly determined case (m=n) which has been considered in the present work the pseudogravimentric anomaly Gp is given as

$$Gp = fCK^{-1}A \qquad\qquad 1.32$$

where f is the constant of proportionality between the magnetization values J_j and the density values d_j. Thus to obtain the pseudo-gravity anomaly, the density values obtained using f are used in equation 1.29. A Fortran program MGRAV has been developed to compute pseudogravity anomalies from the observed magnetic anomalies using the method outlined above. The application of this program to magnetic anomalies over the Benue Trough will be discussed in a later chapter. The program has been written specifically for pseudo-gravity transformation but may be readily adapted for pseudo-magnetic transformation which is the inverse of pseudogravity transformation.

CHAPTER II

EVALUATION OF DEMAGNETIZATION EFFECTS OF ARBITRARILY SHAPED BODIES

2.1 Introduction

The effective field at any point inside a body is given by the vector sum of the original inducing field and an inner field called the demagnetization field. The demagnetization field arises from the local magnetic field produced at a point within the body by the body itself and depends to a great extent on the shape of the body. This field, as the name suggests, tends to diminish the original inducing field and hence demagnetize the body, but it may also locally increase it. The effective field is given as

$$\underline{F}e = \underline{F}o + \underline{F}_D \qquad\qquad 2.1$$

where

Fe is the effective or total field

Fo is the original field

F_D is the demagnetization field

The demagnetization field F_D can be expressed as a product of the magnetization vector (J) and the gradient of a potential given as

$$\phi(r) = \int \frac{\alpha(r')(r' - r)}{|r' - r|^3} \, d^3r' \qquad\qquad 2.2$$

where $\alpha(r')$ is a unit vector in the direction of the magnetization at the point r' assuming uniform magnetization. Combination of the equation 2.1 and 2.2 leads to an integral equation whose solution can be expressed as a power series in J/F_o, the first term of the series giving the demagnetization field at very large applied field or uniform magnetization. For sufficiently long bodies, the demagnetization field near each endface is substantially independent of the surface divergence of the magnetization at the other endface. The effect of

demagnetization will generally be insignificant for values of
susceptibility (K) less than 0.01 (CGS) or $4\pi \times 10^{-2}$ (MKS) and the
knowledge of the exact value of demagnetization is not generally
important when the susceptibility becomes less than 0.05 (cgs) or
0.62 (MKS). The problem of demagnetization was first considered in
Expermental Physics where it is often a great disadvantage in research
into magnetic materials since such studies usually involved investi-
gation of the relation between the magnetization J and the magnetizing
force.

The effects of demagnetization in ellipsoidal and non-ellipsoidal
bodies are discussed in this chapter. Most often it is advantageous
to consider bodies that have non-ellipsoidal shapes which are non-
uniformly magnetized to which geological structures conform. Three
methods for studying the demagnetization effects of arbtrarily shaped
bodies have been considered. The first involves the setting up a set
of simultaneous equations which, on solution by matrix inversion,
gives the values of effective magnetization vectors which are then
used to compute the effective magnetic anomaly associated with the
body at points on the surface. This method, which was originally due
to Sharma (1966), is here called the "Method of matrix inversion".
The second method is an iterative procedure for solving the same
problem and has the advantage of being speedy as it is much faster
than matrix inversion where the number of equations is large. This
method, originally suggested by Vogel (1963), is however, most
suitable for bodiesof low susceptibility and is here called the "Method
of successive iterations". A third method has been suggested by Lee
(1980) and is based principally on the evaluation of a set of surface
integrals using boundary value techniques. This method, here called
the "Method of surface integrals", is similar to the method of matrix
inversion, the only difference being that the latter makes use of

volume integrals.

All three methods depend on the fact that the demagnetizing field can be expressed by the usual equations used for the computation of magnetic fields due to a body at field points outside the body. Emphasis has been placed on the use of the first two methods.

2.2 Evaluation of Demagnetization Factors

The demagnetization field produced by an element of the body is proportional to the magnetization, the constant of proportionality being called the demagnetization factor (N). In ellipsoidal bodies which are usually uniformly magnetized, the demagnetization field is also uniform and it is convenient to express the demagnetization field in terms of a tensor demagnetization factor N_{ij} by means of the relation

$$F_{Di} = -\sum N_{ij} J_j \qquad\qquad 2.3$$

where F_{Di} is the ith component of the demagnetization field

J_j is the jth component of the magnetization vector

N_{ij} is the ith component of the demagnetization factor due to the magnetization J_j.

The demagnetization factor N_{ij} here transforms as a tensor due to the linearity of the relation in equation 2.3 (Joseph and Schlomann, 1965). General expressions for the demagnetization factor N_{ij} for ellipsoidal bodies have been given by several authors. Maxwell (1904) has shown how Poisson's equation can be adapted to the calculation of the demagnetization factors of a uniformly magnetized general ellipsoid. Kellog (1929) and Stratton (1941) have also given equations similar to those of Maxwell. Osborn (1945) has given tables and charts of demagnetization factors of a general ellipsoid for several axial ratios.

In the case of non-ellipsoidal bodies, the relationship between the demagnetization field and the magnetization is in general, non-uniform due to higher order correction terms in the series expansion of the field and the demagnetizing field cannot therefore be expressed simply in terms of a tensorial demagnetization factor. When, however, the applied field is very large, the demagnetizing field can be expressed in terms of a demagnetization factor which is a function of position within the body (Brown, 1962; Joseph, 1966, 1967).

$$F_{Di}(r) = -\sum N_{ij}(r) J_j \qquad\qquad 2.4$$

The computation of this demagnetization factor for non-ellipsoidal bodies has been attempted by different authors (Joseph and Schlomann, 1965; Joseph, 1966; Zeitz and Henderson, 1956; Åm and Stemland, 1975).

Joseph and Schlomann (1965) have derived expressions for the spatially varying tensorial demagnetization factor $N_{ij}(r)$ for rectangular prisms, the value for the zth diagonal tensor component $N_{zz}(r)$ being

$$
\begin{aligned}
N_{zz}(r) = \frac{1}{4\pi} \Big[&\cot^{-1}f(x,y,z) + \cot^{-1}f(-x,y,z) + \cot^{-1}f(x,-y,z) \\
&+ \cot^{-1}f(x,y,-z) + \cot^{-1}f(-x,-y,z) + \cot^{-1}f(x,-y,-z) \\
&+ \cot^{-1}f(-x,y,-z) + \cot^{-1}f(-x,-y,-z) \Big]
\end{aligned}
$$

$$2.5$$

where

$$f(x,y,z) = \frac{\left[(a-x)^2 + (b-y)^2 + (c-z)^2\right]^{\frac{1}{2}} (c-z)}{(a-x)(b-y)}$$

and a, b, c, x, y, and z are as expressed in figure 2.1a.

The other two diagonal tensor components $N_{xx}(r)$, $N_{yy}(r)$ can be inferred from the expression for $N_{zz}(r)$ by an interchange of x,y,z and a,b and c. Joseph and Schlomann (1965) also derived similar expressions for the off diagonal tensorial demagnetization factors $N_{xz}(r)$, $N_{yz}(r)$, $N_{xy}(r)$ for a rectangular prism. They presented
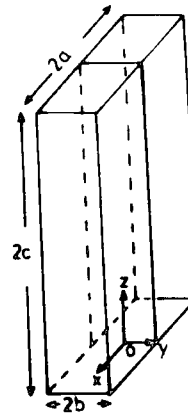
Figure 2·1a Model semi - infinite rectangular prism and
coordinate system used in calculation.

After Joseph & Schlomann(1965)
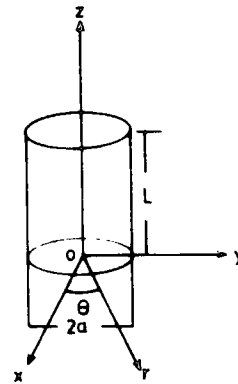
Figure 2·1b Model cylinder and coordinate system used
in calculation. After Joseph & Schlomann(1965)

equations for the spatially varying tensorial demagnetization factors for circular cylinders (Figure 2.1**b**) and have also suggested ways of computing the second order demagnetization factors for semi-infinite thin slabs and semi-infinite cylinders.

2.2.1 Evaluation of Average Demagnetization factors

The demagnetization factors of non-ellipsoidal bodies are not just functions of position within the body, but are also functions of the applied field and its distribution and the magnetization or suscept-ibility of the body. Circumstances often arise where interest is not in the local variations of the demagnetization factor but in how the body responds to an applied field in some average sense. This leads to the concept of an average demagnetization factor which is of two types. In the first type, a spatially varying demagnet-ization factor is averaged over the entire volume of the body to yield what is called the magnetometric demagnetization factor (Nm) while in the second kind, the average is taken in a plane perpendicular to the direction of the applied field and midway between the endfaces of the body to give what is known as the ballistic demagnetization factor (Nb) (Joseph, 1976).

Several authors have developed methods for evaluating average demagnetization factors of uniformly magnetized bodies of different shapes. Brown (1962) has computed both the ballistic and magnetometric demagnetization factors of a uniformly magnetized infinitely long rectangular bar which is transversely magnetized. Joseph (1966, 1976) has derived exact expressions for the ballistic and magnetometric demagnetization factors for uniformly magnetized cylinders (Figure 2.2a) and approximate expressions for both very short and very long cylinders. The following expressions were derived for Nb and Nm :
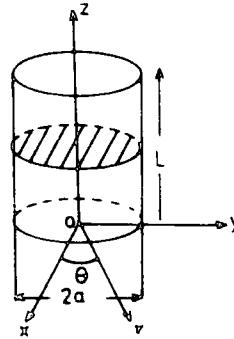
Figure 2.2a Cylinder and coordinate system used in calculation Hatched cross section is the median section over which the ballistic demagnetization factor is computed. After Joseph(1966)
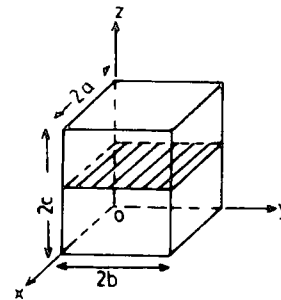
Figure 2.2b. Rectangular prism and coordinate system used in calculation. Hatched cross section is the section over which the ballistic demagnetization factor is computed.
After Joseph(1966)

$$Nb = 1 - (\frac{2}{\pi}) (\frac{P}{K_1}) \left[E_1(K_1) - E_2(K_1) \right] \qquad 2.6$$

$$Nm = 1 - (\frac{4}{3\pi P}) \{ (1+P^2)^{\frac{1}{2}} \left[P^2 E_1(K_2) + (1-P^2) E_2(K_2) \right] -1 \} \quad 2.7$$

where

$$K_1^2 = (1 + \tfrac{1}{4}P^2)^{-1} \; ; \; K_2 = (1 + P^2)^{-1}$$

P = L/2a (see Figure 2.2a)

$E_1(K)$ and $E_2(K)$ are the complete elliptic integrals of the first
and second kinds respectively.

The equations 2.6 and 2.7 reduce to the following set of equations

for very short (P<<1) and very long (P>>1) cylinders using the

appropriate elliptic integrals :

$$Nb \simeq 1 - (2P/\pi) \left[\mathbf{Log}(8/P) - 1 \right] \qquad P<<1$$

$$Nm \simeq 1 - (2P/\pi) \left[\mathbf{Log}(4/P) - \tfrac{1}{2} \right] \qquad 2.8$$

$$Nb \simeq (\tfrac{1}{2}P^2) \left[1 - (3/2P^2) + (25/8p4) \right]$$

$$P>>1$$

$$Nm \simeq (4/3\pi P) - (\tfrac{1}{8}P^2) \qquad 2.9$$

Complete derivations of equations 2.6 and 2.7 are given in Appendix

A. A fortran program FACT1 has been written to compute both the

ballistic and magnetometric demagnetization factors for a cylinder and

results from this program for varying dimensional ratios (P) are given

in Table 2.1. It will be seen from Table 2.1 that the ballistic

demagnetization factor decreases faster than the magnetometric

demagnetization factor with increasing dimensional ratio (P). This

is so because for large dimensional ratios, the demagnetization

factor N (r,z) becomes quite small in the interior of the body while

at the endfaces of the body, it approaches the value 0.50. Since Nm

includes contributions from the endfaces of the body while Nb is

determined solely by the behaviour of N(r,z) at the centre of the

body, Nb decreases faster than Nm for increasing dimensional
ratio (P).

Joseph (1967) has also provided comparable results for the
ballistic and magnetometric demagnetization factors for uniformly
magnetized rectangular prisms (Figure 2.2b) which reduces for very
large P(P = a/c) to the following :

$$Nb = \tfrac{1}{2}\pi\left[4\tan^{-1} 2q - (1/q) \log (1 + 4q^2)\right] \qquad 2.10$$

$$Nm = \tfrac{1}{2}\pi\left[4\tan^{-1}q - 2q \log q + (1/q)(q^2-1)\log(1 + q^2)\right] \qquad 2.11$$

where

$$q = b/c \text{ and } P = a/c \qquad \text{(see Figure 2.2b)}$$

Sharma (1966, 1968) has developed a method of calculating the
average demagnetization factor in any given direction for a
uniformly magnetized body of arbitrary shape. The method involves
the division of the body into several volume elements or cells of
rectangular cross-section and Sharma (1966, 1968) gives the value
of the average demagnetization factor as :

$$Ni = \overline{T}ii/4\Pi \qquad (i = x,y,z) \qquad 2.12$$

where

$$\overline{T}ii = \frac{1}{V} \int_V Tii \ (P) \ dP \qquad 2.13$$

and

$$Tii(P) = \frac{\partial^2}{\partial x_i \partial x_i} \int_V \frac{1}{r} \ dQ \qquad 2.14$$

where dP and dQ are volume elements separated by a distance r within
the body of volume V.

The results so far obtained for average demagnetization factors
have been based on the assumption of uniformly magnetized bodies or
samples that are of low susceptibility and these may not in practice,
be of much interest. This is so because the demagnetization effect

TABLE 2.1

VALUES OF COMPUTED DEMAGNETIZATION FACTORS FOR DIFFERENT

DIMENSIONAL RATIOS

Ratio	Ballistic	Magnetometric
0.10	0.784694	0.796990
0.20	0.657641	0.682234
0.30	0.563900	0.600788
0.40	0.491791	0.540976
0.50	0.435767	0.497248
0.60	0.392563	0.466340
0.70	0.360018	0.446091
0.80	0.336599	0.434968
0.90	0.321159	0.431824
1.00	0.312806	0.435767
2.00	0.102539	0.180957
3.00	0.048440	0.127582
4.00	0.028702	0.098291
5.00	0.018900	0.079883
6.00	0.013344	0.067263
7.00	0.009905	0.058079
8.00	0.007635	0.051099
9.00	0.006061	0.045614
10.00	0.004927	0.041191
12.00	0.003437	0.034500
14.00	0.002532	0.029677
16.00	0.001942	0.026038
18.00	0.001536	0.023193
20.00	0.001245	0.020908
30.00	0.000555	0.014008
40.00	0.000312	0.010532
50.00	0.000200	0.008438

will be negligible for low magnetizations and for higher magnet-
izations where it really matters, the magnetization becomes non-
uniform and hence the evaluation of demagnetization factors become
increasingly difficult. Alternative approaches to the problem
of demagnetization for arbitrarily shaped, not necessarily uniformly
magnetized bodies have been suggested (Sharma, 1966; Vogel, 1963;
Lee, 1980) and the application of these methods are presented in the
subsequent sections of this chapter.

2.3 Evaluation of Demagnetization Effects of Arbitrarily Shaped Bodies

The evaluation of the demagnetization effect of arbitrarily
shaped, non-uniformly magnetized bodies is a difficult problem. So
far three methods have been suggested. These are the method of
matrix inversion (Sharma, 1966), the method of successive iteration
due to Vogel (1963) and the use of surface integrals due to Lee
(1980). The approach in all three methods is to divide the body into
many volume elements or cells. Each cell is then assumed to be of
uniform magnetization, an assumption whose reliability depends on
the number and size of the volume elements. The methods were
originally developed for three dimensional bodies and are all based
on the assumption that the demagnetization field inside a body can be
represented by the integral formula used for the calculation of
magnetic fields outside a body, when the magnetization and geometrical
dimensions of the body are known. An unfortunate shortcoming of these
methods is the assumption that magnetization is in the direction of
the Earth's field. This is, however, often not true as quite often
the main magnetization may depend on the remanent component as has
been shown by a number of authors (Books, 1962; and others). The
effects of remanence may also affect dip estimates.

In the present study the body whose demagnetization effect is being studied is divided into blocks of rectangular cross-section and the direction of magnetization need not be in the direction of the Earth's field. While three-dimensional cases have been considered, emphasis has been laid on the evaluation of demagnetization effects of arbitrarily shaped two-dimensional bodies, magnetized in an arbitrary direction. A suitable starting point is the presentation of equations for the magnetic fields due to two and three dimensional bodies of rectangular cross-section.

2.3.1.1 Field Equations for Three Dimensional Prisms

In general the different components of magnetic anomaly are given by the following set of relations in three dimensions

$$\Delta X = J_x\ T_{xx} + J_y\ T_{xy} + J_z\ T_{xz}$$

$$\Delta Y = J_x\ T_{yx} + J_y\ T_{yy} + J_z\ T_{yz} \qquad 2.15$$

$$\Delta Z = J_x\ T_{zx} + J_y\ T_{zy} + J_z\ T_{zz}$$

$$\Delta T = \Delta X\ \cos \alpha e\ \cos Ie + \Delta Y\ \sin \alpha e\ \cos Ie + \Delta Z\ \sin Ie$$

where

ΔX, ΔY, ΔZ, ΔT are the x, y, z and total field components of the magnetic anomaly.

J_x, J_y and J_z are the x, y and z components of magnetization.

ΔT is assumed smaller than the total field T.

Expressions for the coefficient T_{xx}, T_{xy}, T_{xz}, T_{yy}, T_{yx}, T_{yz}, T_{zz}, T_{zx} and T_{zy} are given by the following integrals assuming the field point to be at the origin, (Figure 2.3a).
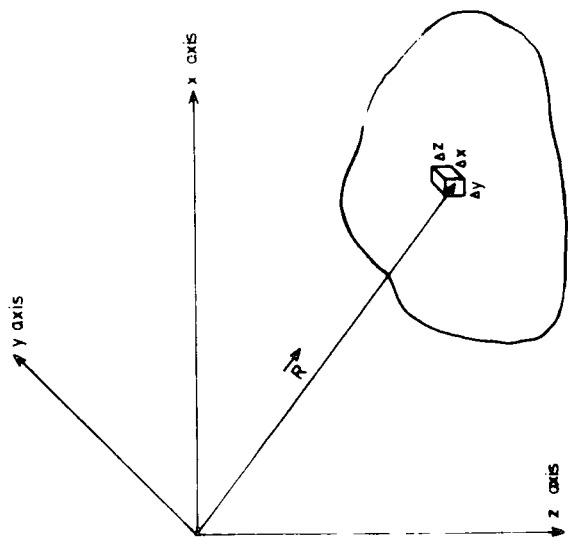
Fig 23a. Coordinate system and volume element $\Delta x \Delta y \Delta z$
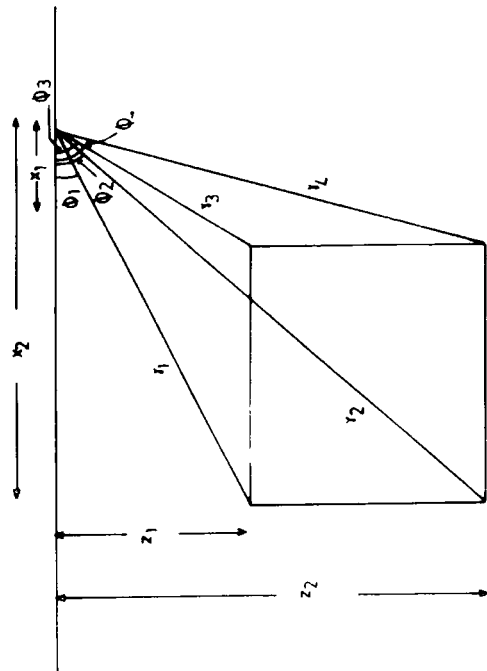
Fig 23b. Coordinate system and 2D block model.

$$T_{xx} = \frac{\mu_0}{4\pi} \int_V \frac{3x^2 - r^2}{r^5} \, dv$$

$$T_{xy} = \frac{\mu_0}{4\pi} \int_V \frac{3xy}{r^5} \, dv$$

$$T_{xz} = \frac{\mu_0}{4\pi} \int_V \frac{3xz}{r^5} \, dv$$

$$T_{yx} = T_{xy}$$

$$T_{yy} = \frac{\mu_0}{4\pi} \int_V \frac{3y^2 - r^2}{r^5} \, dv$$

2.16

$$T_{yz} = \frac{\mu_0}{4\pi} \int_V \frac{3yz}{r^5} \, dv$$

$$T_{zx} = T_{xz}$$

$$T_{zy} = T_{yz}$$

$$T_{zz} = \frac{\mu_0}{4\pi} \int_V \frac{3z^2 - r^2}{r^5} \, dv$$

These co-efficients reduce to the following expressions obtained by integration for rectangular prisms :

$$T_{xx} = \frac{\mu_0}{4\pi} \left\{ \tan^{-1}\left(\frac{Y_1 Z_1}{X_2 R_1}\right) - \tan^{-1}\left(\frac{Y_2 Z_1}{X_2 R_2}\right) \right.$$

$$+ \tan^{-1}\left(\frac{Y_2 Z_2}{X_2 R_3}\right) - \tan^{-1}\left(\frac{Y_1 Z_2}{X_2 R_4}\right)$$

$$+ \tan^{-1}\left(\frac{Y_2 Z_1}{X_1 R_5}\right) - \tan^{-1}\left(\frac{Y_1 Z_1}{X_1 R_6}\right)$$

$$+ \tan^{-1}\left(\frac{Y_1 Z_2}{X_1 R_7}\right) - \left. \tan^{-1}\left(\frac{Y_2 Z_2}{X_1 R_8}\right) \right\}$$

$$Txy = \frac{\mu o}{4\pi} \left\{ \log\left(\frac{Z_1+R_2}{Z_2+R_3}\right) - \log\left(\frac{Z_1+R_1}{Z_2+R_4}\right) \right.$$

$$\left. + \log\left(\frac{Z_1+R_6}{Z_2+R_7}\right) - \log\left(\frac{Z_1+R_5}{Z_2+R_8}\right) \right\}$$

$$Txz = \frac{\mu o}{4\pi} \left\{ \log\left(\frac{Y_1+R_4}{Y_2+R_3}\right) - \log\left(\frac{Y_1+R_1}{Y_2+R_4}\right) \right.$$

2.17

$$\left. + \log\left(\frac{Y_1+R_6}{Y_2+R_5}\right) - \log\left(\frac{Y_1+R_7}{Y_2+R_8}\right) \right\}$$

$$Tyy = \frac{\mu o}{4\pi} \left\{ \tan^{-1}\left(\frac{X_1 Z_1}{Y_2 R_5}\right) - \tan^{-1}\left(\frac{X_1 Z_2}{Y_2 R_8}\right) \right.$$

$$+ \tan^{-1}\left(\frac{X_2 Z_2}{Y_2 R_3}\right) - \tan^{-1}\left(\frac{X_2 Z_1}{Y_2 R_2}\right)$$

$$+ \tan^{-1}\left(\frac{X_1 Z_2}{Y_1 R_7}\right) - \tan^{-1}\left(\frac{X_1 Z_1}{Y_1 R_6}\right)$$

$$\left. + \tan^{-1}\left(\frac{X_2 Z_1}{Y_1 R_1}\right) - \tan^{-1}\left(\frac{X_2 Z_2}{Y_1 R_4}\right) \right\}$$

$$Tyz = \frac{\mu o}{4\pi} \left\{ \log\left(\frac{X_1+R_8}{X_2+R_3}\right) - \log\left(\frac{X_1+R_5}{X_2+R_2}\right) \right.$$

$$\left. + \log\left(\frac{X_1+R_6}{X_2+R_1}\right) - \log\left(\frac{X_1+R_7}{X_2+R_4}\right) \right\}$$

$$T_{zz} = \frac{\mu o}{4\pi} \left\{ \tan^{-1}\left(\frac{Y_1 X_1}{Z_2 R_7}\right) - \tan^{-1}\left(\frac{Y_1 X_2}{Z_2 R_4}\right) \right.$$

$$+ \tan^{-1}\left(\frac{X_2 Y_2}{Z_2 R_3}\right) - \tan^{-1}\left(\frac{X_1 Y_2}{Z_2 R_8}\right)$$

$$+ \tan^{-1}\left(\frac{X_2 Y_1}{Z_1 R_1}\right) - \tan^{-1}\left(\frac{X_1 Y_1}{Z_1 R_6}\right)$$

$$+ \tan^{-1}\left(\frac{X_1 Y_2}{Z_1 R_5}\right) - \left. \tan^{-1}\left(\frac{X_2 Y_2}{Z_1 R_2}\right) \right\}$$

where

$$R_1 = (X_2{}^2 + Y_1{}^2 + Z_1{}^2)^{\frac{1}{2}} \; ; \quad R_2 = (X_2{}^2 + Y_2{}^2 + Z_1{}^2)^{\frac{1}{2}}$$

$$R_3 = (X_2{}^2 + Y_2{}^2 + Z_2{}^2)^{\frac{1}{2}} \; ; \quad R_4 = (X_2{}^2 + Y_1{}^2 + Z_2{}^2)^{\frac{1}{2}} \quad 2.18$$

$$R_5 = (X_1{}^2 + Y_2{}^2 + Z_1{}^2)^{\frac{1}{2}} \; ; \quad R_6 = (X_1{}^2 + Y_1{}^2 + Z_1{}^2)^{\frac{1}{2}}$$

$$R7 = (X_1{}^2 + Y_1{}^2 + Z_2{}^2)^{\frac{1}{2}} \; ; \quad R_8 = (X_1{}^2 + Y_2{}^2 + Z_2{}^2)^{\frac{1}{2}}$$

and X_1, X_2; Y_1, Y_2; Z_1, Z_2; are the differences between the centres
of our rectangular blocks and the extensions of the sides of the
surroundoung prisms along the x, y, z axis respectively with the
sides of the prism assumed to be lying parallel to the co-ordinate
system and are obtained by subtracting the sides of the prisms from
the centres of the rectangular blocks.

2.3.1.2 Field Equations for Two-Dimensional Blocks

The corresponding equations to 2.17 above for a two-dimensional
body of square cross-section are obtained from the following
integrals:

$$T_{xx} = \frac{\mu o}{4\pi} \; 2 \int_{x_1}^{x_2} \int_{z_1}^{z_2} \frac{X^2 - Z^2}{(X^2 + Z^2)^2} \; dx \; dz$$

$$T_{xz} = \frac{\mu o}{4\pi} \; 4 \int_{x_1}^{x_2} \int_{z_1}^{z_2} \frac{XZ}{(X^2 + Z^2)^2} \; dx \; dz \qquad\qquad 2.19$$

$$T_{zz} = \frac{\mu o}{4\pi} \; 2 \int_{x_1}^{x_2} \int_{z_1}^{z_2} \frac{Z^2 - X^2}{(X^2 + Z^2)^2} \; dx \; dz$$

which on solution reduce to the following equations :

$$T_{xx} = \frac{\mu o}{4\pi} \; (\phi_1 - \phi_2 - \phi_3 + \phi_4)$$

$$T_{zz} = \frac{-\mu o}{4\pi} \; (\phi_1 - \phi_2 - \phi_3 + \phi_4) \qquad\qquad 2.20$$

$$T_{xz} = T_{zx} = \frac{\mu o}{4\pi} \; \log\left(\frac{r_2 r_3}{r_1 r_4}\right)$$

where r_2, r_3, r_4, ϕ_1, ϕ_2, ϕ_3, and ϕ_4 are as shown in Figure 2.3b. In arriving at the above equations the terms in y have been *ignored* as they make no contribution.

2.3.1.3 Expressions for the Total Field

Quite often interest is in the value of the total magnetic field ΔT rather than in its components. The total field magnetic anomaly due to a three dimensional prism of rectangular cross-section, is given as follows :

$$\Delta T = J \left[(\cos Im \cos \alpha m \ Txx + \sin \alpha m \cos Im \ Txy + \sin Im \ Txz) \right.$$

$$\cos \alpha e \ \cos Ie$$

$$+ \ (\cos Im \cos \alpha m \ Tyx + \sin \alpha m \cos Im \ Tyy + \sin Im \ Tyz)$$

$$\cos Ie \ \sin \alpha e$$

$$+ \ (\cos Im \cos \alpha m \ Tzx + \sin \alpha m \cos Im \ Tzy + \sin Im \ Tzz) \sin Ie \left. \right]$$

2.21

where the co-efficients Txx, Txy, Txz, Tyx, Tyy, Tyz, Tzx, Tzy and

Tzz are as given in equation 2.17. The equivalent equation to 2.21

above for a two-dimensional block of rectangular cross-section

(Figure 2.3b is as follows:

$$\Delta T = 2K \ J\frac{\mu o}{4\pi} \left[\sin \beta \ \log \frac{r_2 r_3}{r_1 r_4} \ + \ \cos \beta \ (\phi_2 \ - \ \phi_1 \ + \ \phi_3 \ - \ \phi_4) \right]$$

2.22

where

J = total magnetization

$K = (\sin^2 Im + \cos^2 Im \cos^2 \alpha m)^{\frac{1}{2}} (\sin^2 Ie + \cos^2 Ie \cos^2 \alpha e)^{\frac{1}{2}}$

$\beta = \tan^{-1}(\tan Im/\cos \alpha m) + \tan^{-1}(\tan Ie/\cos \alpha e)$

Im = Dip of magnetization

Ie = Dip of the Earth's field

αm = aximuth of magnetization

αe = aximuth of the Earth's field.

2.3.2 The Method of Matrix Inversion

In this method the body under consideration is divided into

a number of prisms or cells; the field at the centre of each cell

is then evaluated as a function of the magnetization of the

surrounding cells. The method was originally developed by Sharma (1966)

and the   description given here follows that of Sharma (1966).

The inner demagnetization field which is a function of

position in the body is given by

$$F_{Dj}{}^q = \frac{\mu o}{4\pi} \sum_i^{x,y,z} \sum_{P=1}^n J_i{}^P \left[\frac{\partial^2}{\partial K_i \partial_{ij}} \left(\frac{\theta}{r_{qp}} \ dv \right) \right] \qquad 2.23$$

where θ is an angle term expressing the magnetization direction whose value depends of the value of i and j.

$F_{Dj}{}^q$ = jth component of the demagnetization at the centre of the qth cell due to the magnetization in the ith direction of the pth cell.

r_{qp} = the radial distance between the qth and the pth cells

j and i take values x, y or z.

The effective field at the centre of the qth cell following equation 2.1 is therefore given by

$$F_{ej}{}^q = F_{oj}{}^q + \sum_{i,j}^{x,y,z} \sum_{P=1}^n J_i{}^P \ F_{ji}{}^{qp} \qquad 2.24$$

where n = number of cells making up the body

F_{oj} = the jth component of the original field for the qth cell

and the primed summation sign means except for the case p=q which is not included. $F_{ji}{}^{qp}$ represents the terms within the bracket in equation 2.23 which are obtained from the integrals of equation 2.16 where solutions are given in equation 2.17 as follows :

Fxx	= cosIm cosαm Txx	;	Fxy	= cosIm sinαm Txy
Fxz	= sinIm Txz	;	Fyx	= cosIm cosαm Tyx
Fyy	= cosIm sinαm Tyy	;	Fyz	= sinIm Tyz
Fzx	= cosIm cosαm Tzx	;	Fzy	= cosIm sinαm Tzy
Fzz	= sinIm Tzz			

2.25

The equation 2.24 on expansion leads to the following set of equations in which the original fields $F_{oj}{}^q$, the susceptibility and the co-efficients $F_{ji}{}^{pq}$ are the known and components of the effective magnetization vectors are the unknown.

$$Jex^1 = K\ Fox^1 + K\ \left[Jex^1\ Fxx^{11} + Jex^2\ Fxx^{12} + Jex^3\ Fxx^{13} + \ldots\ldots + \right.$$
$$Jex^n\ Fxx^{1n}$$
$$+ Jey^1\ Fxy^{11} + Jey^2\ Fxy^{12} + Jey^3\ Fxy^{13} + \ldots\ldots + Jey^n\ Fxy^{1n}$$
$$\left. + Jez^1\ Fxz^{11} + Jez^2\ Fxz^{12} + Jez^3\ Fxz^{13} + \ldots\ldots + Jez^n\ Fxz^{1n} \right]$$

$$Jex^2 = K\ Fox^2 + K\ \left[Jex^1\ Fxx^{21} + Jex^2\ Fxx^{22} + Fex^3\ Fxx^{23} + \ldots\ldots + \right.$$
$$Jex^n\ Fxx^{2n}$$
$$+ Jey^1\ Fxy^{21} + Jey^2\ Fxy^{22} + Jey^3\ Fxy^{23} + \ldots\ldots + Jey^n\ Fxy^{2n}$$
$$\left. + Jex^1\ Fxz^{21} + Jez^2\ Fxz^{22} + Jez^3\ Fxz^{23} + \ldots\ldots + Jez^n\ Fxz^{2n} \right]$$

2.26

$$Jex^n = K\ Fox^n + K\ \left[Jex^1\ Fxx^{n1} + Jex^2\ Fxx^{n2} + Jex^3\ Fxx^{n3} + \ldots\ldots + \right.$$
$$Jex^n\ Fxx^{nn}$$
$$+ Jey^1\ Fxy^{n1} + Jey^2\ Fxy^{n2} + Jey^3\ Fxy^{n3} + \ldots\ldots + Jey^n\ Fxy^{nn}$$
$$\left. + Jez^1\ Fxz^{n1} + Jez^2\ Fxz^{n2} + Jez^3\ Fxz^{n3} + \ldots\ldots + Jez^n\ Fxz^{nn} \right]$$

where the Je terms represent the effective magnetization vectors which is the sum of KFo and the inner magnetization vector. Jex^1 for example is the effective magnetization of the cell numbered "1" in the direction x and K is the susceptibility of the body. Fox^1 is the original field for the cell "1" in the x direction and the terms under the square bracket represent the inner field components. A similar set of equation to those of equation 2.26 above exist for the y and z components of the effective field and inner demagnetization field.

From the set of equations 2.26 and the equation 2.24, there is a set of 3n linear equations in 3n unknowns (the components of effective mangetization) which on solution, gives the different components of the effective magnetization for the different cells. The equation 2.24 can therefore be written as a simple summation thus:

$$Foj^q = \sum \sum J_i^p\ F_{ji}^{qp} \qquad\qquad 2.27$$

which can be expressed in a matrix notation as follows —

$$
\begin{bmatrix}
Fox^1 \\
\vdots \\
Fox^n \\
Foy^1 \\
\vdots \\
Foy^n \\
Foz^1 \\
\vdots \\
\vdots \\
Foz^1
\end{bmatrix}
\begin{bmatrix}
Fxx^{11} \cdots Fxx^{1n} & Fxy^{11} \cdots Fxy^{1n} & Fxz^{11} \cdots Fxz^{1n} \\
 & & \\
Fxx^{n1} \cdots Fxx^{nn} & Fxy^{n1} \cdots Fxy^{nn} & Fxz^{n1} \cdots Fxz^{nn} \\
Fyx^{11} \cdots Fyx^{1n} & Fyy^{11} \cdots Fyy^{1n} & Fyz \cdots Fyz^{1n} \\
 & & \\
Fyx^{n1} \cdots Fyx^{nn} & Fyy^{n1} \cdots Fyy^{nn} & Fyz^{n1} \cdots Fyx^{nn} \\
Fzx^{11} \cdots Fzx^{1n} & Fzy^{1n} \cdots Fzy^{1n} & Fzz^{11} \cdots Fzz^{1n} \\
 & & \\
Fzx^{n1} \cdots Fzx^{nn} & Fzy^{n1} \cdots Fzy^{nn} & Fzz^{n1} \cdots Fzz^{nn}
\end{bmatrix}
\begin{bmatrix}
Jex^1 \\
\vdots \\
Jex^n \\
Jey^1 \\
\vdots \\
Jey^n \\
Jez^1 \\
\vdots \\
\vdots \\
Jez^n
\end{bmatrix}
$$

$$2.28$$

The matrix on inversion gives the values of the components of the effective magnetization for all the cells. This forms the basis of the matrix inversion method.

So far a general three-dimensional treatment has been considered. The two-dimensional treatment follows directly on simplication. The equation 2.24 is replaced by the following equation :

$$
F_{ej}{}^q = Fo_j{}^q + \sum_{ij}^{x,z'} \sum_{P=1}^{n} J_i{}^P \, F_{ji}{}^{qp}
\qquad 2.29
$$

where $Fe_j{}^q$, $Fo_j{}^q$ and $J_i{}^P$ take their usual meanings, and $F_{ji}{}^{qp}$ are obtained from the set of equations 2.20 and the terms in y neglected. Thus

$$Fxx = cosIm \; cos\alpha m \; Txx \quad ; \quad Fxz = sinIm \; Txz$$
$$Fzx = cosIm \; cos\alpha m \; Tzx \quad : \quad Fzz = sinIm \; Tzz$$

$$2.30$$

The set of linear equations given in equation 2.26 is replaced by its two-dimensional equivalent given, thus :

$$Jex^1 = KFox^1 + K\left[Jex^1Fxx^{11} + Jex^2Fxx^{12} + Jex^3Fxx^{13} + \ldots\ldots\ldots + \right.$$

$$Jex^nFxx^{1n} + Jez^1Fxz^{11} + Jez^2Fxz^{12} + Jez^3Fxz^{13} + \ldots\ldots + $$

$$\left. Jez^nFxz^{1n}\right]$$

$$Jex^2 = KFox^2 + K\left[Jex^1Fxx^{21} + Jex^2Fxx^{22} + Jex^3Fxx^{23} + \ldots\ldots\ldots + \right.$$

$$Jex^n\ Fxx^{2n}$$

$$\left. + Jez^1Fxz^{21} + Jez^2Fxz^{22} + Jez^3Fxz^{23} + \ldots\ldots + Jez^nFxz^{2n}\right]$$

$$Jex^n = KFox^n + K\left[Jex^1Fxx^{n1} + Jex^2Fxx^{n2} + Jex^3Fxx^{n3} + \ldots\ldots + Jex^nFxx^{nn}\right.$$

$$\left. + Jez^1Fxz^{n1} + Jez^2Fxzn2 + Jez^3Fxz^{n3} + \ldots\ldots\ldots + Fez^nFxz^{nn}\right]$$

2.31

A similar set of equation to 2.31 above exists in terms of the z components of the effective magnetization. The three-dimensional matrix of equation 2.28 is replaced by the following matrix in two dimensions which, when inverted, gives the effective magnetization components Je_i^p:

$$
\begin{bmatrix} Fox^1 \\ \\ Fox^n \\ Foz^1 \\ \\ Foz^n \end{bmatrix}
\begin{bmatrix} Fxx^{11} - - - - - Fxx^{1n}Fxz^{11} - - - - - Fxz^{1n} \\ \\ Fxx^{n1} \qquad Fxx^{nn}Fxz^{n1} \qquad Fxz^{nn} \\ Fzx^{11} - - - - - - Fzx^{1n}Fzz^{11} - - - - - - - Fzz^{1n} \\ \\ Fzx^{n1} - - - - - - Fzx^{nn}Fzz^{n1} - - - - - - Fzz^{nn} \end{bmatrix}
\begin{bmatrix} Jex^1 \\ \\ Jex^n \\ Jez^1 \\ \\ Jez^n \end{bmatrix}
$$

2.32

A two dimensional treatment is preferred to the three-dimensional treatement because this reduces the number of equations to be solved from 3n to 2n and consequently reduces computing time. It is evident from the arguments given so far that most of the work involved in the

use of the method entails the evaluation of the co-efficients T_{ji}.

Once these are evaluated, the revised co-efficients $F_{ji}{}^{qp}$ are

easily obtained using equations 2.25 or 2.30, the computation of the

effective magnetization components only involves an inversion of the

matrices given in equation 2.28 (for 3-D case) or equation 2.32 (for

2-D case). To test the accuracy of the expressions in equations 2.17

and 2.20, fortran programs have been written for magnetic anomalies

due to two and three dimensional bodies divided into rectangular prisms.

The two-dimensional program ANOM2 has been extensively tested against

the program MAGN (Bott, 1969) while the three-dimensional program

ANOM3 has been extensively tested and used by Smith (1980) who

recognised the advantage of the ease with which the size of the

composing prisms can be changed and the ability of the program to

consider blocks of non-uniform magnetization.

Fortran programs DMAGFIELD2 and DMAGFIELD3 have been developed

for the computation of the components of effective magnetization in

both two and three dimensions respectively. The programs first

evaluate the co-efficients $F_{ji}{}^{qp}$ with which the matrices given in

equation 2.28 (for 3-D case) and equation 2.32 (for 2-D case) are

formed. The programs then make a call to the NAG Library routine

FO4JAF which inverts the matrices to obtain values of the different

components of the effective magnetization. Considerable time is

required by these programs in carrying out the matrix inversion,

especially when the number of blocks (n) exceeds twenty (20), as a

result of the number of equations to be solved. A major reduction

in the time can be achieved if instead of computing the different

components of the effective magnetization, the total effective

magnetization is computed. This would reduce the number of equations

solved in the program DMAGFIELD3 from 3n to n and the number of

equations solved by the program DMAGFIELD2 from 2n to n. The

equations 2.24 and 2.29 now reduce to :

$$Fe^q = Fo^q \sum_{P=1}^{n} Je^P F^{qP} / \quad q = 1, \ldots, n \qquad 2.33$$

and the matrices of equations 2.28 and 2.32 reduce to the following

matrix :

$$
\begin{bmatrix} Fo^1 \\ Fo^2 \\ \vdots \\ \\ \\ \\ \\ \\ \\ \\ Fo^n \end{bmatrix}
\begin{bmatrix} F^{11} & F^{12} & ----------F^{1n} \\ F^{21} & F^{22} & ----------F^{2n} \\ \vdots & \vdots & \vdots \\ & & \\ & & \\ & & \\ & & \\ & & \\ & & \\ & & \\ F^{n1} & F^{n2} & ----------F^{nn} \end{bmatrix}
\begin{bmatrix} Je^1 \\ Je^2 \\ \vdots \\ \\ \\ \\ \\ \\ \\ \\ Je^n \end{bmatrix}
$$

<div align="right">2.34</div>

which on inversion yields the values of the total effective

magnetization for the different volume elements. The co-efficients

F^{qP} have been derived in sections 2.3.1.1 and 2.3.1.2 above for

the three and two-dimensional cases respectively. In two dimensions

and considering a body divided into rectangular or square blocks, the

co-efficients F^{qP} is given by the following equation :

$$F^{qP} = 2 K \frac{\mu o}{4\pi} \left[\sin \beta \, \log\left(\frac{r_2 r_3}{r_1 r_4}\right) + \cos \beta (\phi_2 - \phi_1 + \phi_3 - \phi_4) \right]$$

<div align="right">2.35</div>

where the terms K, β, r_1, r_2, r_3, r_4, ϕ_1, ϕ_2, ϕ_3, and ϕ_4 have

meanings as given in section 2.3.1.2.

The Fortran program DMAGN using the NAG Library routine F04JAF

computes the values of the total effective magnetization for a two

dimensional body divided into squares based on equations 2.33, 2.34

and 2.35 given above. The effective magnetization vectors obtained

are used to compute the effective magnetic anomaly values at observation points on the surface which are then plotted out for comparison with the magnetic anomaly with the effects of demagnetization neglected. Application of this program to the study of demagnetization effects in two dimensional bodies is given in Section 2.3.5 below.

2.3.3 Method of Successive Iterations

An alternative approach to the matrix inversion technique is the method of successive iterations. The method was originally developed by Vogel (1963) and applied to the computation of average effective magnetization vectors in x, y and z direction assuming the body to be magnetized in the direction of the Earth's field. The method like the previous method is based on the assumption that the inner demagnetization field can be given by the integral

$$\frac{\mu o}{4\pi} \int_V J \ g \ \text{rad}^2 \ \frac{1}{r} \ dx \ dy \ dz \qquad\qquad 2.36$$

which is the familiar integral used for the evaluation of fields at points external to a body and is equivalent to the expression in equation 2.23. This equation holds good for both points within and outside the body. In the present study, the above equation is used to compute the field due to a body at points within the body given its magnetization properties. The method proceeds as follows.

A body subject to an original inducing field F_0 and having a susceptibility K has an original magnetization J_0 whose direction need not be in the direction of the Earth's field. Using the integral of equation 2.36, the magnetic field F_1^q associated with this magnetization J_0 is computed at points within the body and associated with this field F_1^q is the magnetization J_1^q. The

field $F_2{}^q$ due to this magnetization $J_1{}^q$, is again computed at points within the body using the equation 2.36 and associated with this field is the magnetization $J_2{}^q$ which is used to find the field $F_3{}^q$ and consequently $J_3{}^q$. This process is continued until the field at different points within the body changes by less than some assumed value at which point convergence is said to have taken place. The effective field at each of the points within the body is the vectoral sum of all the fields computed and is given thus :

$$Fe^q = F_0 + F_1{}^q + F_2{}^q + F_3{}^q + \ldots\ldots + F_n{}^q \qquad 2.37$$

where n is the number of iterations carried out. The effective magnetization values within the body are given by the following equation :

$$Je^q = K \left[F_0 + F_1{}^q + F_2{}^q + F_3{}^q + \ldots\ldots F_n{}^q \right] \qquad 2.38$$

where the susceptibility K need not remain constant throughout the body.

In the present study, the body under consideration is divided into several cells of rectangular cross-section and the iterative procedure outlined above is used to compute the effective magnet-ization value at the centre of each cell. The original inducing field F_0 need not be the same for the different cells. A fortran program DMAGN2 has been written for the evaluation of the effective magnetization of two-dimensional bodies using the procedure outlined above. The program evaluates the integral of equation 2.36 using the equation 2.22 and successively evaluates the magnetizations $J_1{}^q$, $J_2{}^q$ $\ldots\ldots$, $J_n{}^q$ and using the equation

2.38 the effective magnetization values for all the cells are
computed. The effective magnetization values so computed are used
to calculate the effective magnetic anomaly at points on the surface
external to the body which is then plotted out as in the previous
section. The application of this method, its relative merits and
disadvantages as well as a comparison between it and the method of
matrix inversion is discussed in Section 2.3.5 below.

2.3.4 Method of Surface Integrals

Two method of evaluating the demagnetization effects of arbitrarily
shaped, non uniformly magnetized bodies have already been introduced
in Sections 2.3.2 and 2.3.3 above. These were the methods of Matrix
Inversion and Successive Iterations. A third approach to the problem
of demagnetization is now presented. The method originally developed
by Lee (1980) is similar to the method of matrix inversion (Sharma,
1966) but makes use of surface integrals obtained using Maxwell's
equation rather than the volume integrals used by the method of
matrix inversion. The development of the method assumes the body of
permeability μ to be in a medium of permeability μ', with the potential
functions ϕ and ϕ' associated with the body and medium respectively
(Figure 2.4). The potential functions ϕ and ϕ' are related through a
surface integral equation derivable from Maxwell's equation which on
solution by matrix inversion, leads to an evaluation of the effective
field at points external to the body.

The following well known relations exist for the magnetic field
intensity, the magnetic induction, the current density, the permeability
and the displacement current vector :
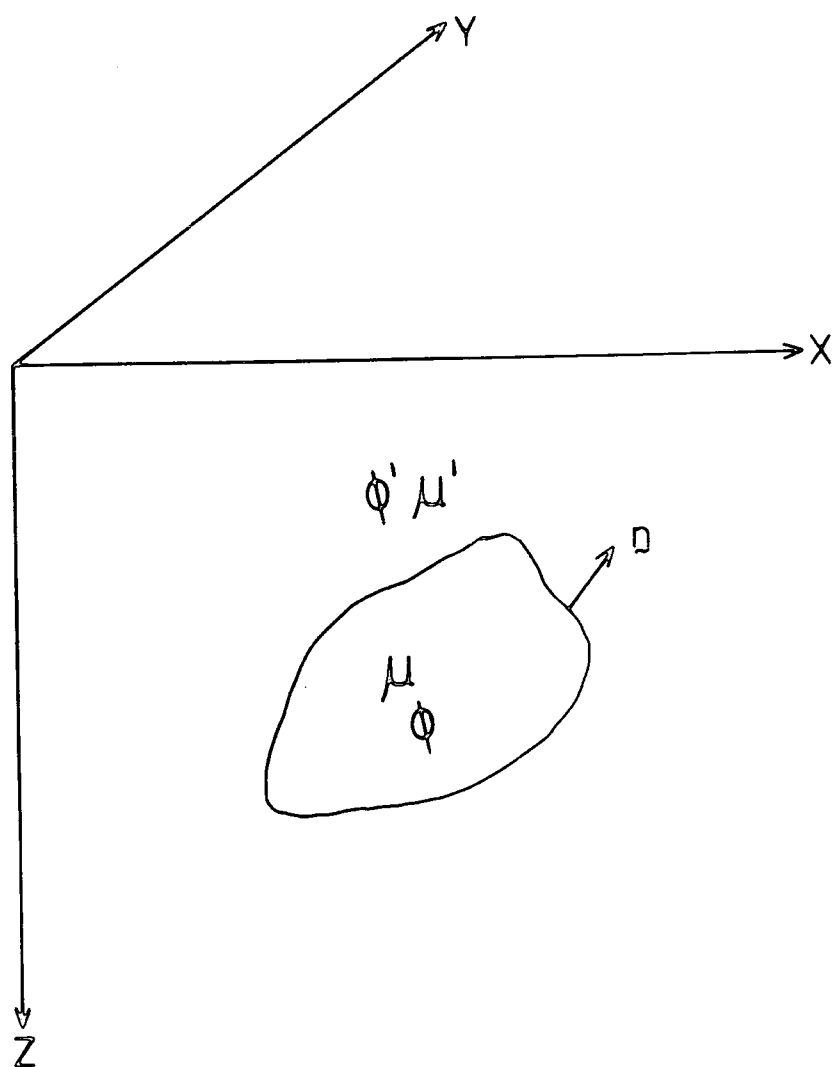
Figure 2·4.   Coordinate system used in calculations.
After Lee(1980)

$$\nabla \times H = J + \frac{\partial D}{\partial t} \qquad\qquad 2.39$$

$$\nabla \cdot B = 0$$

$$B = \mu \, \mu_0 H$$

where

H = magnetic field intensity

B = magnetic induction

J = current density

$\frac{\partial D}{\partial t}$ = Displacement current density

μ = permeability; μ_0 = Permeability of free space

Based on the set of equations 2.39, Lee (1975, 1980) has obtained the following surface integral equation relating the potential functions ϕ and φ' whose solution forms the basis of the present method :

$$\phi = \phi' + 2K \int_{s} \frac{\partial \phi}{\partial n} G \, ds \qquad\qquad 2.40$$

where

s = the surface of the inhomogeneity or body in question

K = $(\mu' - \mu)/(\mu' + \mu)$

n = outward normal of the surface s with respect to which the partial derivative is taken (Figure 2.4).

G = $\frac{1}{4}\pi R$

R = $\left[(x - x')^2 + (y - y')^2 + (z - z')^2 \right]^{\frac{1}{2}}$

The potential function ϕ' is related to the original inducing field encountered in the previous methods. An equation similar to that of equation 2.40 has been derived by Ramsey (1952). A numerical solution to the equation 2.40 has been presented by Lee (1980) following the elegant approach of Barnett (1972). Equation 2.40 can be reduced to the following form:

$$\phi = \phi' + \frac{K}{2\pi} \int_{s} \frac{\partial}{\partial n} \phi \frac{1}{R} \, ds \qquad\qquad 2.41$$

To obtain a general solution of the equation 2.41, the surface of the body under consideration is divided up into a number of surface cells or facets, over each of which the quantity $\mu(\frac{\partial \phi}{\partial n})$ is constant, (Barnet, 1972). The equation 2.41 then can be written for the ith surface cell as

$$\phi_i = \phi_i' + \frac{K}{2\pi} \sum_{j=1}^{N'} \int_{s_j} \frac{1}{R_{ij}} \frac{\partial \phi_i}{\partial n_j} ds_j + $$

$$\int_{si} \frac{\partial \phi_i}{\partial n_i} \frac{1}{R_{ii}} ds_i \qquad\qquad 2.42$$

where the summation does not include the ith cell and R_{ij} is the radial distance between the ith and jth surface cells. The above is an expression of equation 2.41 for the ith cell as a function of the surrounding cells and holds good at either side of the boundary. A suitable boundary condition therefore is :

$$\mu' \frac{\partial \phi_i}{\partial n'} = \mu \frac{\partial \phi_i}{\partial n} \qquad\qquad 2.43$$

where the prime denote term outside the boundary. Equation 2.42 then reduces to a set of linear equations expressed as

$$\frac{\partial \phi_i}{\partial n_i} + \frac{K}{2\pi} \sum_{j=1}^{N'} \frac{\partial \phi_i}{\partial n_j} \frac{\partial}{\partial n_i} \int_{s} \frac{1}{R_{ij}} ds = \frac{\partial \phi_i'}{\partial n_i} \qquad 2.44$$

The above equation is analogous to the equation 2.24 of Section 2.3.2 and defines a system of linear simultaneous equation in which $\frac{\partial \phi_i'}{\partial n_i}$ are the knowns and $\frac{\partial \phi_i}{\partial n_j}$ are the unknowns. and N is the number of surface cells making up the surface of the body. The integral

$$\frac{K}{2\pi} \frac{\partial}{\partial n_i} \int_{s} \frac{1}{R_{ij}} ds \qquad\qquad 2.45$$

represent co-efficients T_{ij} to be evaluated for each cell (i) with respect to every other cell (j), and once evaluated the system of equations in 2.44 can be solved to determine the unknowns $\frac{\partial \phi_i}{\partial n_j}$. The above integral equation (Equation 2.45) can be re-casted to the following form :

$$T_{ij} = \frac{K}{2\pi} \int_S \frac{\partial}{\partial n_i} \frac{1}{R_{ij}} \, ds \qquad 2.46$$

if the differentiation is carried out before the integration and the above equation has a value depending on the shape of the surface cells into which the body under consideration is divided.

Lee (1980) has made use of triangular facets following the mathematical formulation of Barnet (1972). All through the present work however, the body is assumed to be made up of rectangular/ square cells. The coefficients once evaluated, the equation 2.44 can be expanded thus:

$$\frac{\partial \phi_1'}{\partial n_1} = \frac{\partial \phi}{\partial n_1} T_{11} + \frac{\partial \phi}{\partial n_2} T_{12} + \ldots\ldots + \frac{\partial \phi}{\partial n_n} T_{1n} \qquad 2.47$$

$$\frac{\partial \phi_2'}{\partial n_2} = \frac{\partial \phi}{\partial n_1} T_{21} + \frac{\partial \phi}{\partial n_2} T_{22} + \ldots\ldots + \frac{\partial \phi}{\partial n_n} T_{2n}$$

.
.
.

$$\frac{\partial \phi_n'}{\partial n_n} = \frac{\partial \phi}{\partial n_1} T_{n1} + \frac{\partial \phi}{\partial n_2} T_{n2} + \ldots\ldots + \frac{\partial \phi}{\partial n_n} T_{nn}$$

The above is a set of n equations in n unknowns which, on solution by matrix inversion yields values for the unknown parameters $\frac{\partial \phi}{\partial n_j}$ and once these are determined the effective magnetic field is easily obtained from the following equation :

$$Hm = - \nabla \phi'm - \frac{K}{2\pi} \sum_{j=1}^{n} \frac{\partial \phi}{\partial n_j} \int_S \nabla \frac{1}{R} \cdot m \, ds \qquad 2.48$$

which follows directly from the usual equations for the magnetic
field in the direction of unit vector m due to an arbitrarily
shaped body. It is then clear that the method outlined here has a
close similarity to the method of matrix inversion outline earlier.

2.3.5 Study of Demagnetization Effects of Arbitrarily Shaped Bodies

The techniques discussed in the preceding Sections 2.3.2,
2.3.3 and 2.3.4 are here applied to the study of demagnetization effects
in arbitrarily shaped two-dimensional bodies. The approach has been
to divide the body under consideration into cells of retangular or
square cross-sections. The effective magnetization of each cell is
then computed using the methods already disccused. To study the
effects of demagnetization and its magnitude, the total field magnetic
anomaly due to the body whose magnetization is non-uniform is computed
and compared graphically with the equivalent magnetic anomaly with
demagnetization neglected. A great part of this study was carried out
using the program based on the method of matrix inversion. Results
obtained using the alternative approaches have, however, been compared
with those from the method of matrix inversion and the result of this
comparison is given in the appropriate section.

2.3.5.1 Effect of Susceptibility on Degree of Demagnetization and
         Inhomogeneity of Magnetization.

The effect of the susceptibility value on the degree to which a
body is demagnetized as well as the degree of inhomogeneity of the
magnetization of non-ellipsoidal bodies has been investigated. For
the purposes of this investigation, the body was divided into twenty
(20) cells and assumed to be subject to a homogeneous original
inducing field of 48,000 gammas. The effective magnetization values
for the cells and subsequently the effective total field magnetic

anomalies were calculated for susceptibility values of 1.00 (CGS) or

4π (MKS), 0.50 (CGS) or 2π (MKS), 0.10 (CGS) or 0.4π (MKS), 0.01 (CGS)

or 0.04π (MKS) and 0.001 (CGS) or 0.004π (MKS) using the program

DMAGN.

Figures 2.5, 2.6, 2.7, 2.8 and 2.9 show the original and effective

magnetic anomalies due to the body whose cell distribution is also

shown, for susceptibility equal to 4π MKS, 2π MKS, 0.4π MKS, 0.04π MKS,

and 0.004π MKS respectively. It is evident from these plots that the

effect of demagnetization is greatest when the susceptibility is 4π MKS

and decreases with decreasing susceptibility value. The effect of

demagnetization is virtually non existent when the susceptibility

value was 4π x 10^{-2} and 4π x 10^{-3} (Figures 2.8 and 2.9). It was

also found that the values of effective magnetization computed when

the susceptibility was 4π x 10^{-2} MKS and 4π x 10^{-3} MKS were

virtually uniform with the degree of inhomogeneity increasing as the

susceptibility value was increased. Therefore at rather low

susceptibility values, a non-ellipsoidal body could be described in

terms of an average magnetization.

2.3.5.2 Effect of Cell Size and Number on Degree of Demagnetization

The methods presented in this study are all based on the

assumption that the volume or surface cells into which the body is

divided can be considered to be of uniform magnetization. The

degree to which the number of cells determined the accuracy of

results was investigated by dividing the body used in the last section

into 10, 20, 40, 80, 160 and 320 cells. The effective magnetization

and anomaly were then recomputed. It was found that the effective

anomaly showed a slight decrease as block numbers increased from 10 to

80. The number of cells was, however, found not to make any

noticeable effect of the results for cell numbers of 160 and above.
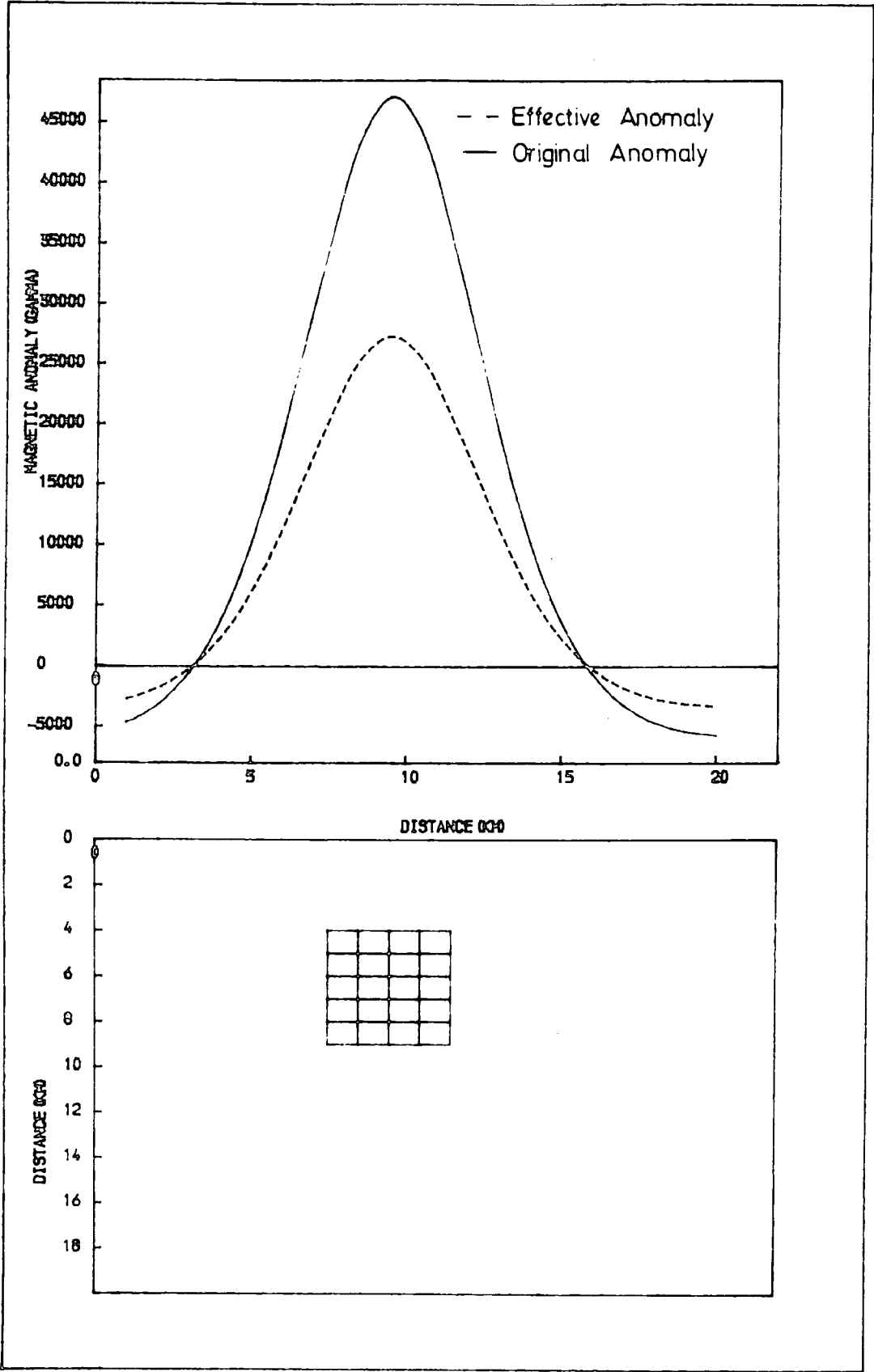
Figure 2.5 Plot of original and effective magnetic anomalies for a susceptibility of 4π(MKS).
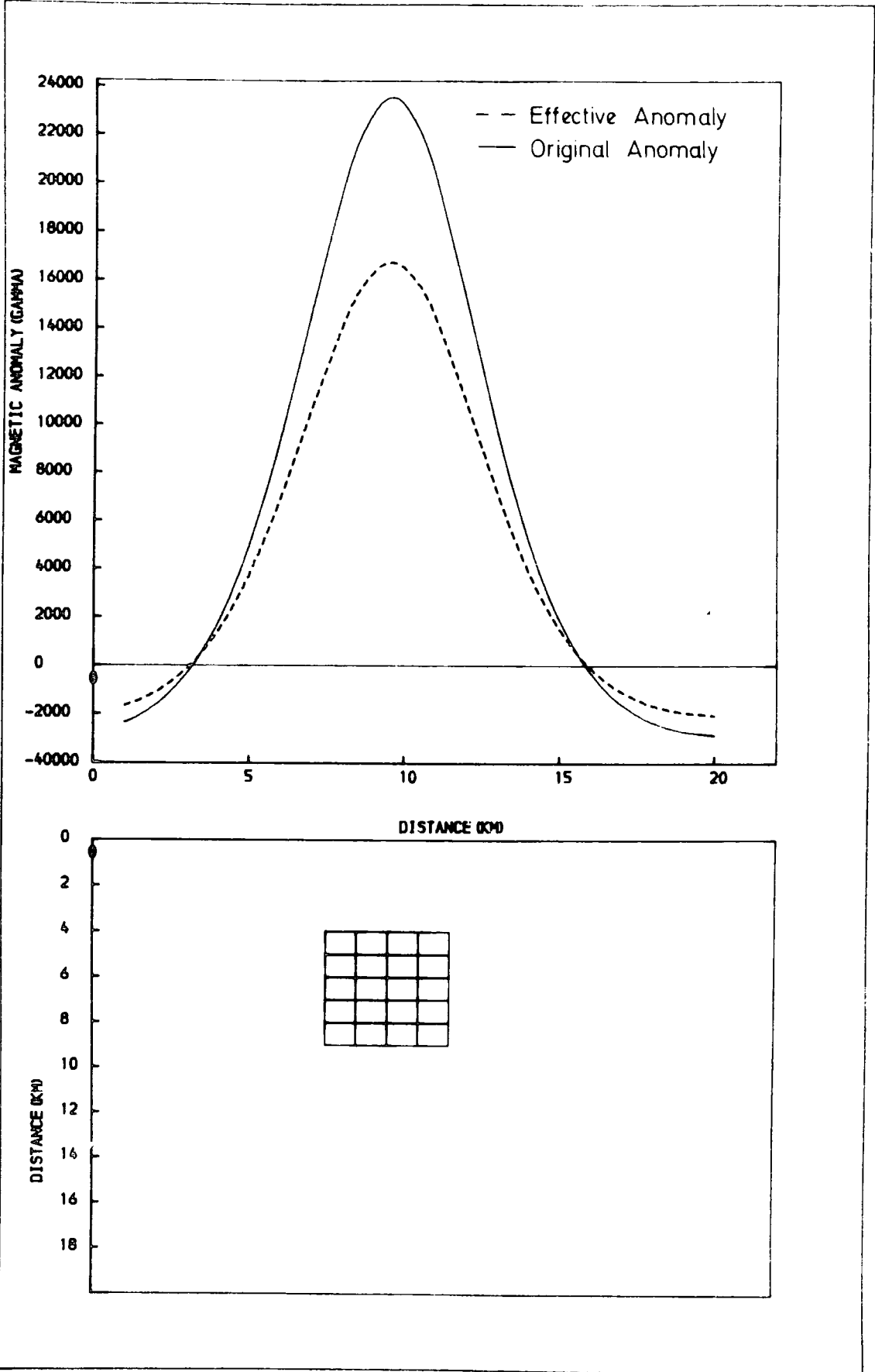
Figure 2.6 Plot of original and effective magnetic anomalies for a
susceptibility of 2π(MKS).
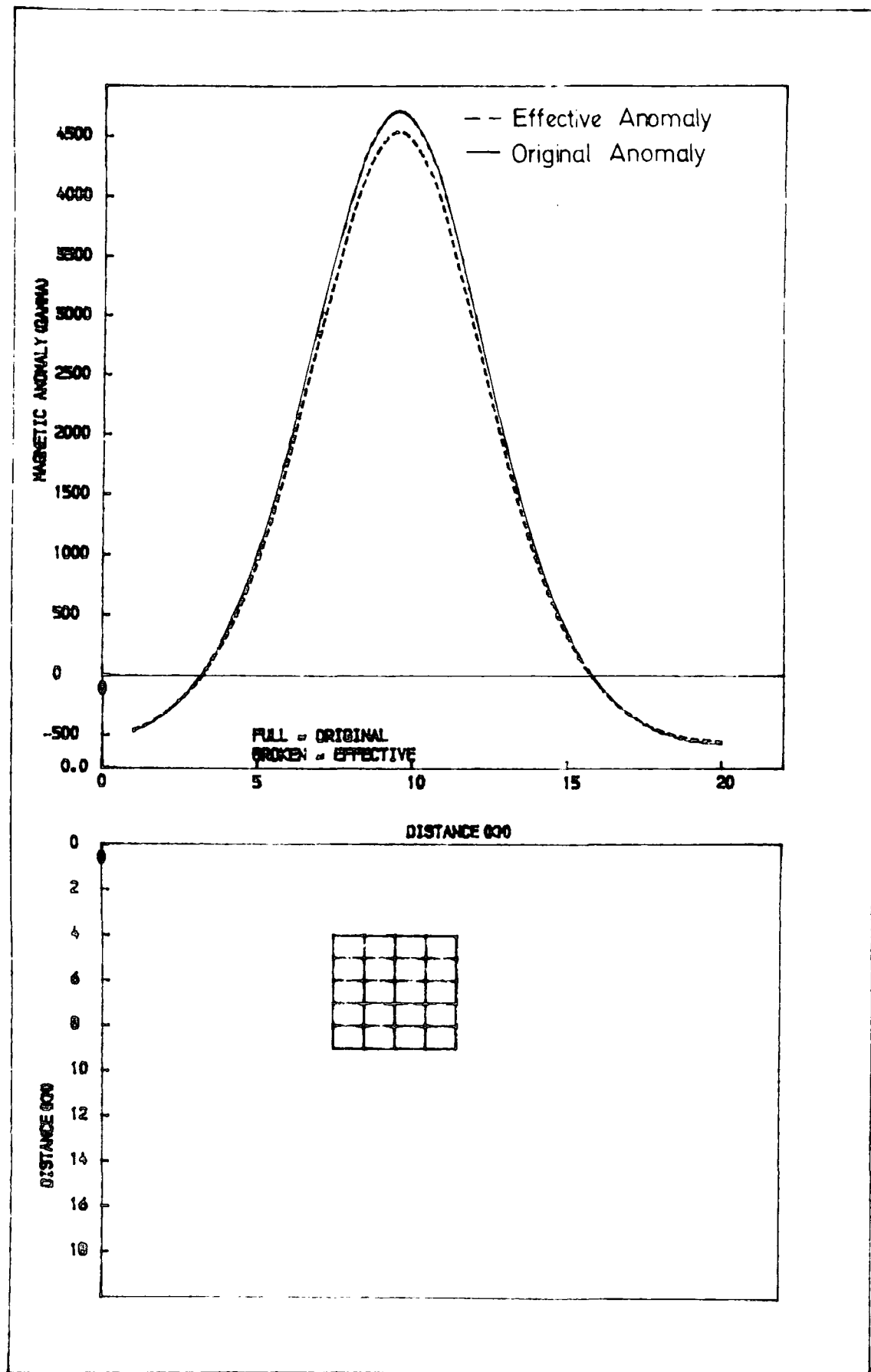
Figure 2.7   Plot of original and effective magnetic anomalies for
a susceptibility of $4\pi \times 10^{-1}$(MKS).
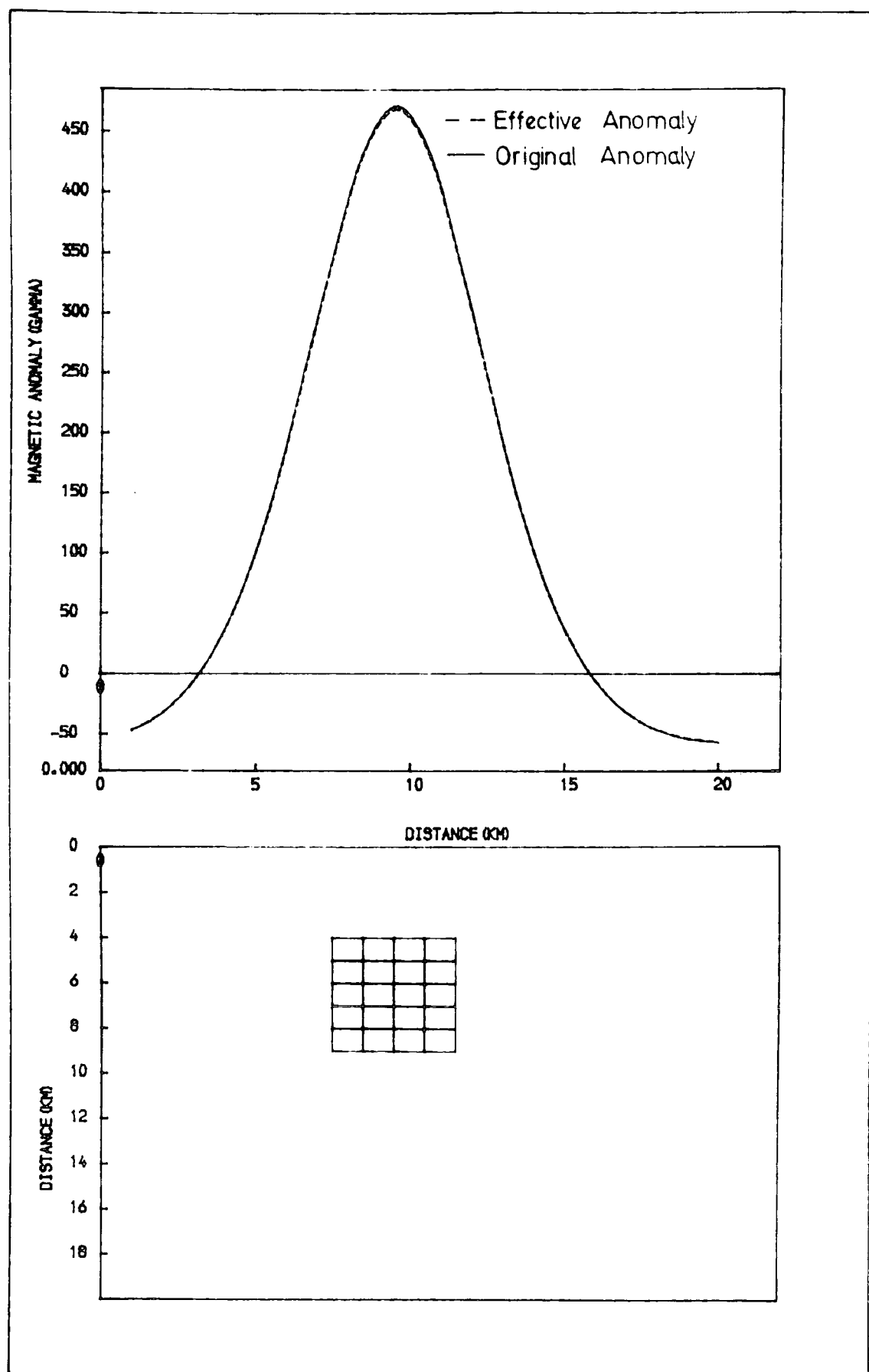
Figure 2.8 Plot of original and effective magnetic anomalies for a
susceptibility of $4\pi \times 10^{-2}$(MKS).
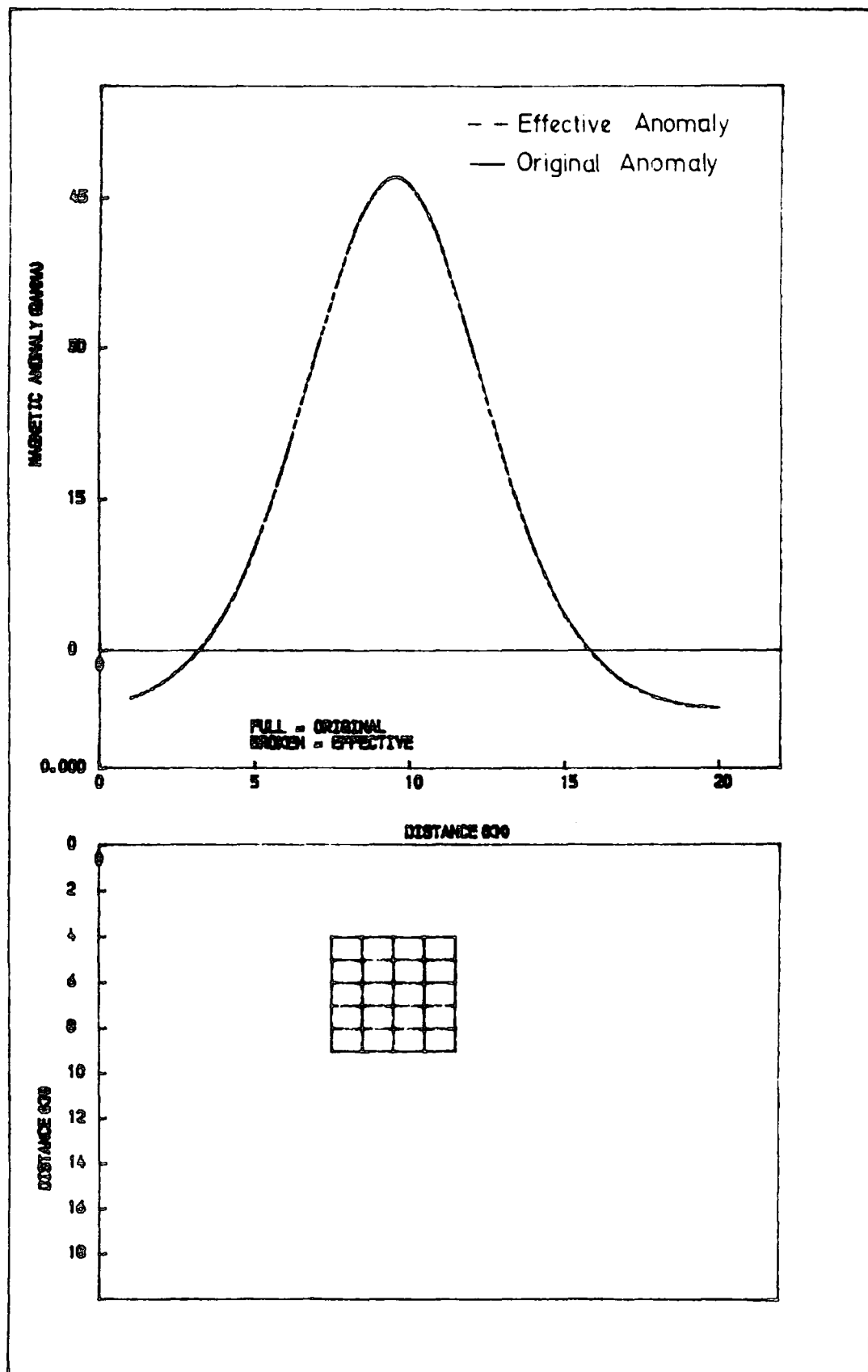
Figure 2.9 Plot of original and effective magnetic anomalies for a susceptibility of $4\pi \times 10^{-3}$ (MKS).

The resutls of Figures 2.5, 2.6, 2.7, 2.8 and 2.9 have been repeated using 80 cells and these are presented in Figures 2.10, 2.11, 2.12, 2.13 and 2.14. It is evident from a comparison of both sets that the variation of the magnitude of the effective field is not very significant. It was found that the relative gain in accuracy by using large numbers of cells is completely outweighed by the reduction in speed and hence increase in computation cost arising from the use of large numbers of cells and a modest number of 80 was therefore adopted in the present study.

2.3.5.3 Applicability to Cases of Arbitrary Magnetization Directions

The above techniques for evaluating the demagnetization effects of arbitrarily shaped bodies as presented here makes no assumption as to the direction of magnetization. The magnetization vector need not be oriented in the direction of the Earth's field. Figures 2.15a, 2.15b, 2.15c and 2.15d show the results obtained with an inducing field inclined at 72° and having an aximuth of 20° while the magnetization vector dips at 62° with an aximuth of 30° for susceptibility values of 0.4, 0.3, 0.1 and 0.01 (CGS) respectively. A similar set of results with the magnetization inclined at 31° and having an aximuth of 160° is shown in Figures 2.16a, 2.16b, 2.16c and 2.16d.

2.3.5.4 Comparison of Methods

Although the results presented so far have been obtained using the method of matrix inversion, similarly good results can be obtained using the methods of successive iteration and surface integrals. As has already been stated, the method of surface integrals is closely similar to the method of matrix inversion, the only difference being the nature of the matrix inversion and the method of computing the relevant coefficients used. An obvious
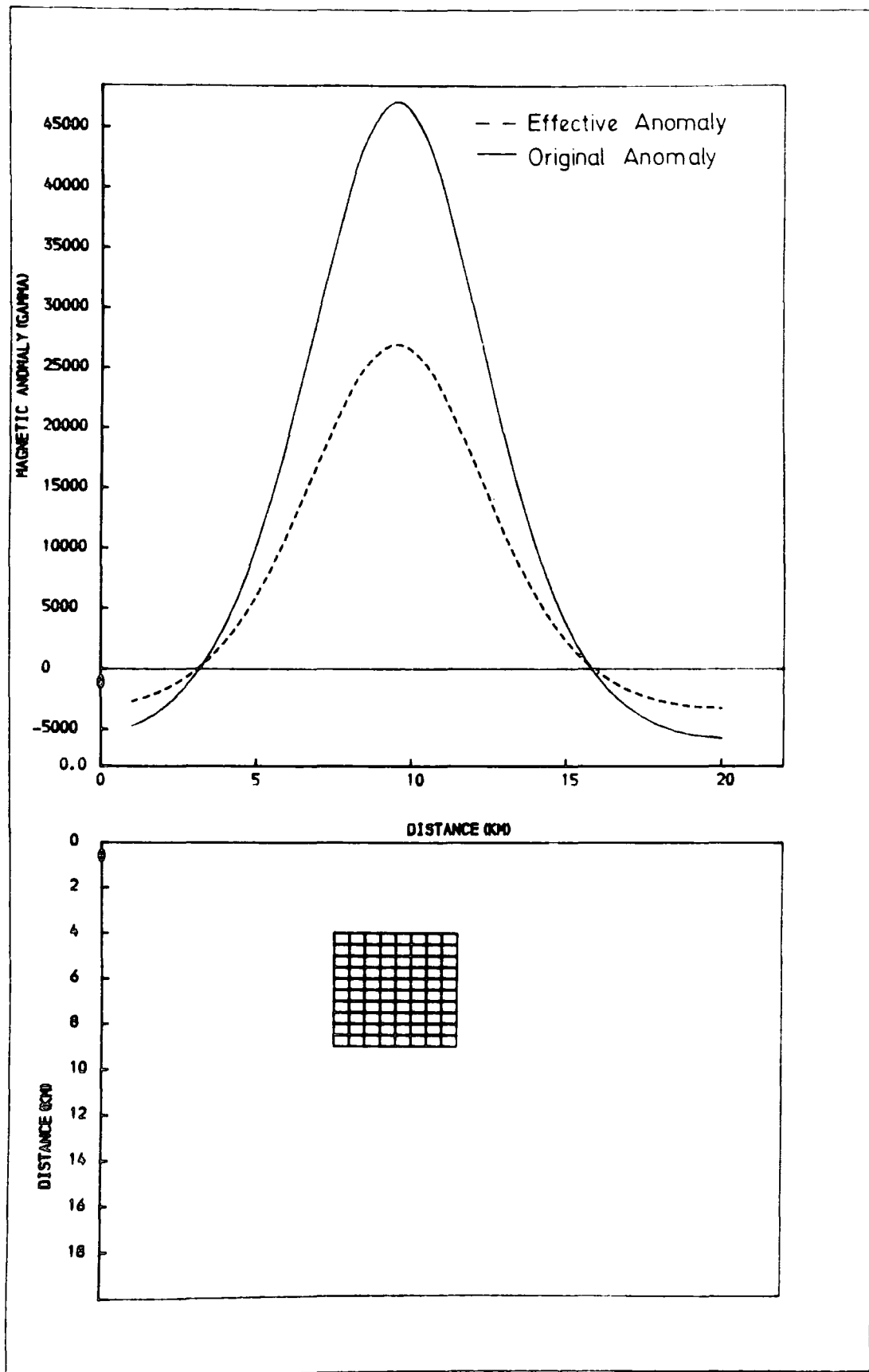
Figure 2.10   Plot of original and effective magnetic anomalies for a susceptibility of 4π(MKS) using eighty cells.
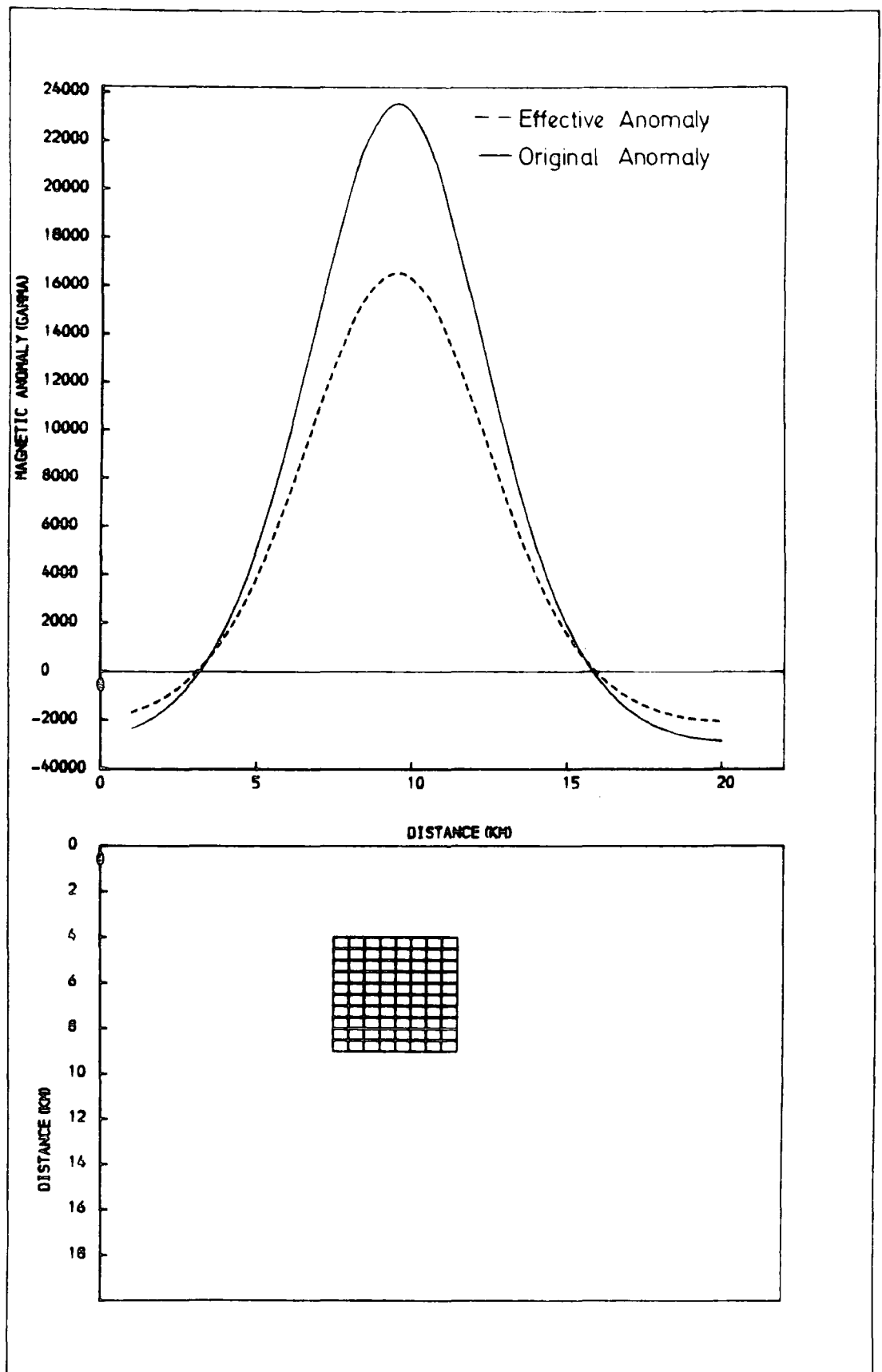
Figure 2.11   Plot of original and effective magnetic anomalies for a susceptibility of 2π(MKS) using eighty cells.
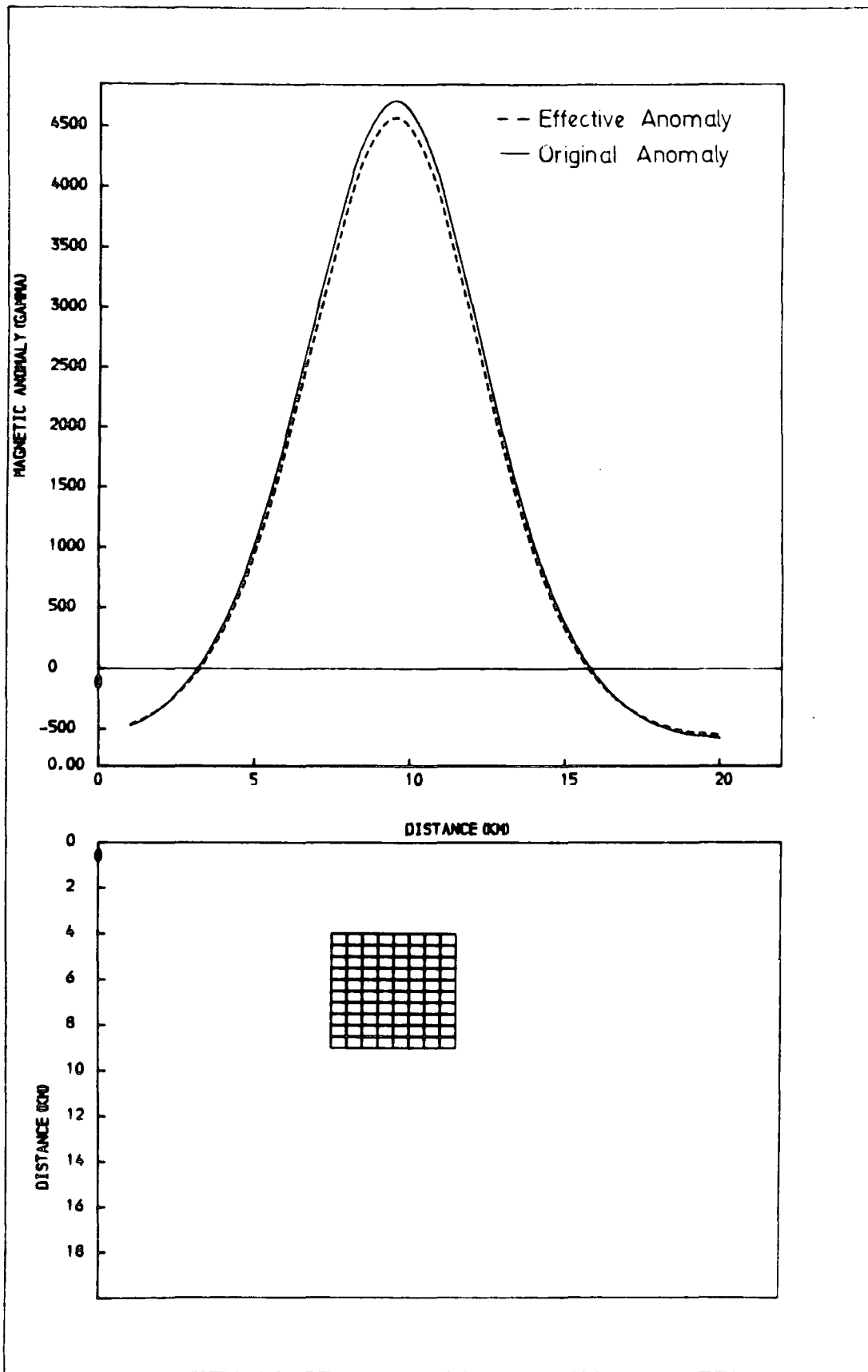
Figure 2.12   Plot of original and effective magnetic anomalies for a
susceptibility of $4\pi \times 10^{-1}$(MKS) using eighty cells.
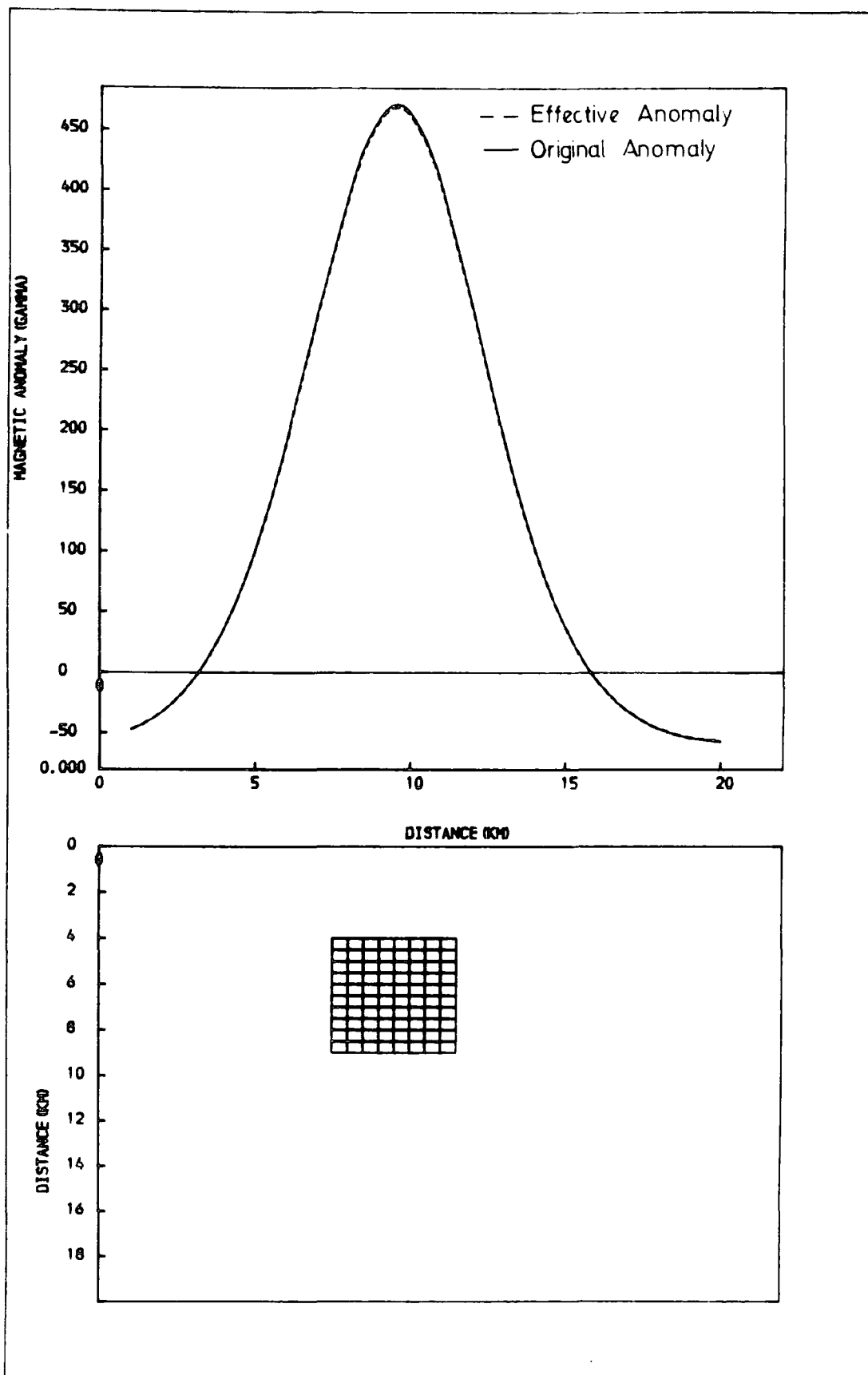
Figure 2.13 Plot of original and effective magnetic anomalies for a susceptibility of $4\pi \times 10^{-2}$(MKS) using eighty cells.
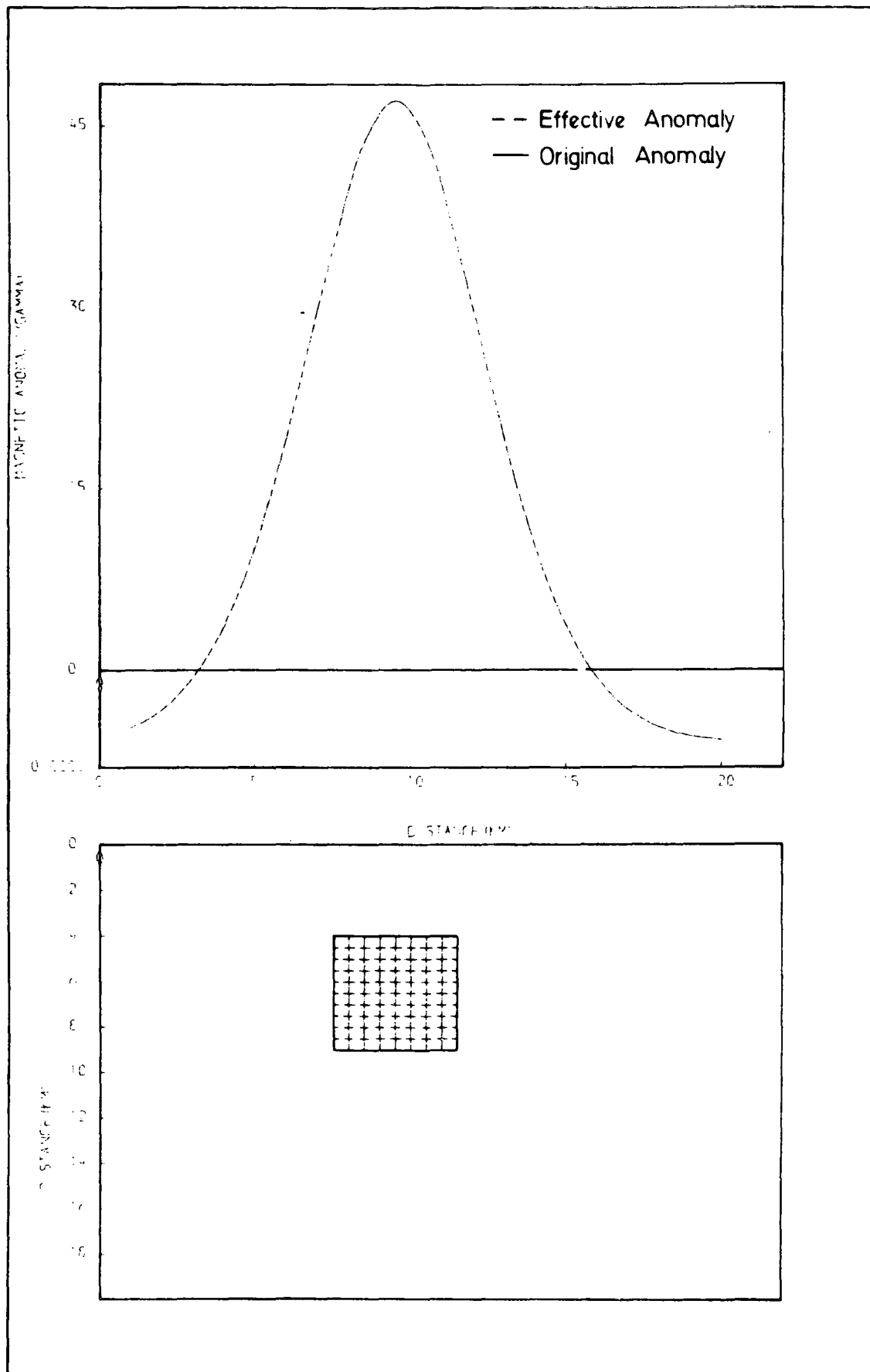
Figure 2.14 Plot of original and effective magnetic anomalies for a susceptibility of $4\pi \times 10^{-3}$(MKS) using eighty cells.
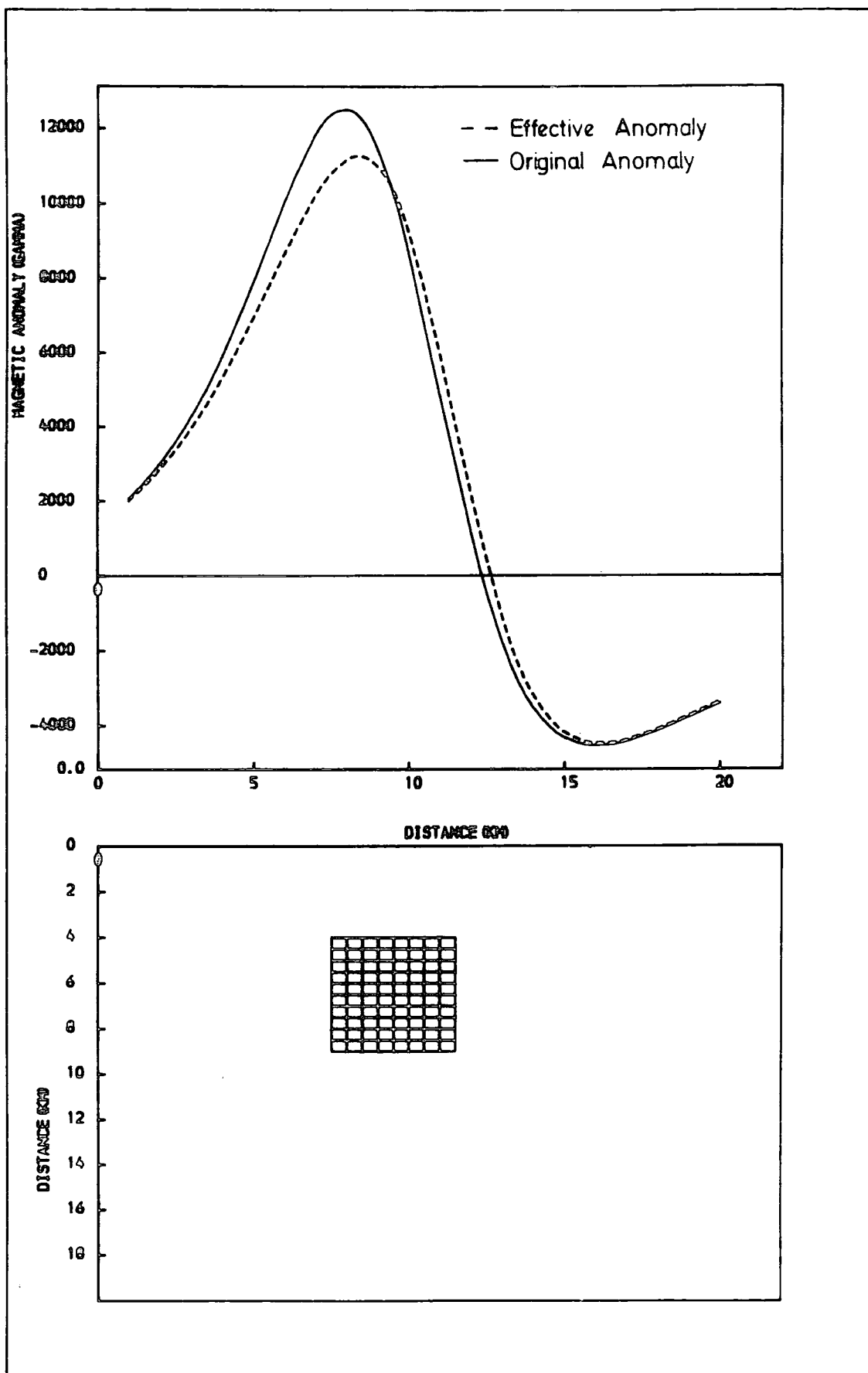
Figure 2.15a   Plot of original and effective magnetic anomalies for
a susceptibility of 0.4 (CGS).   Ie = 72°, αe = 20°;
Im = 62°, αe = 30°.
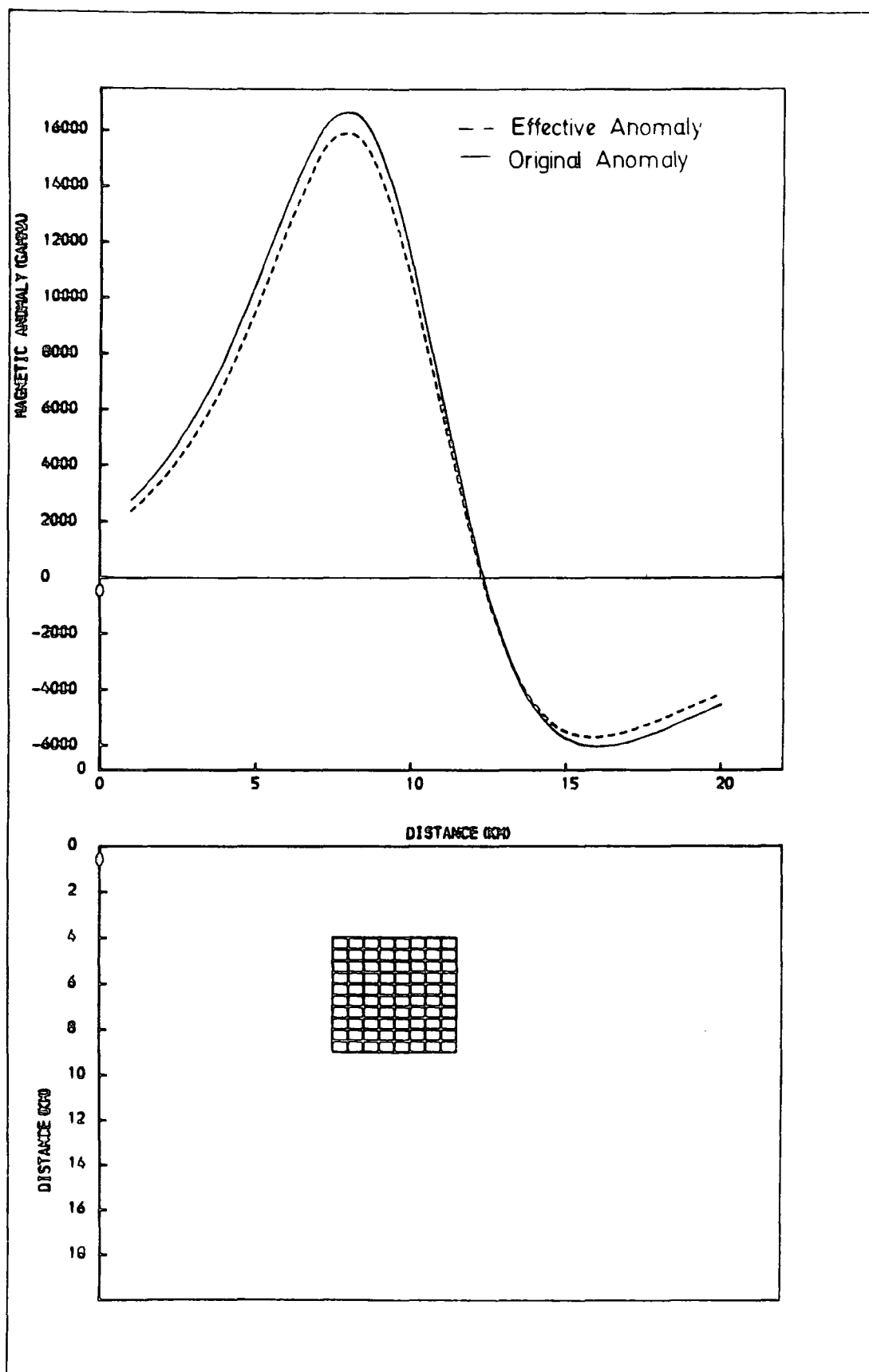
Figure 2.15b   Plot of original and effective magnetic anomalies for
a susceptibility of 0.3 (CGS).   Ie = 72°, αe = 20°;
Im = 62°, αe = 30°.
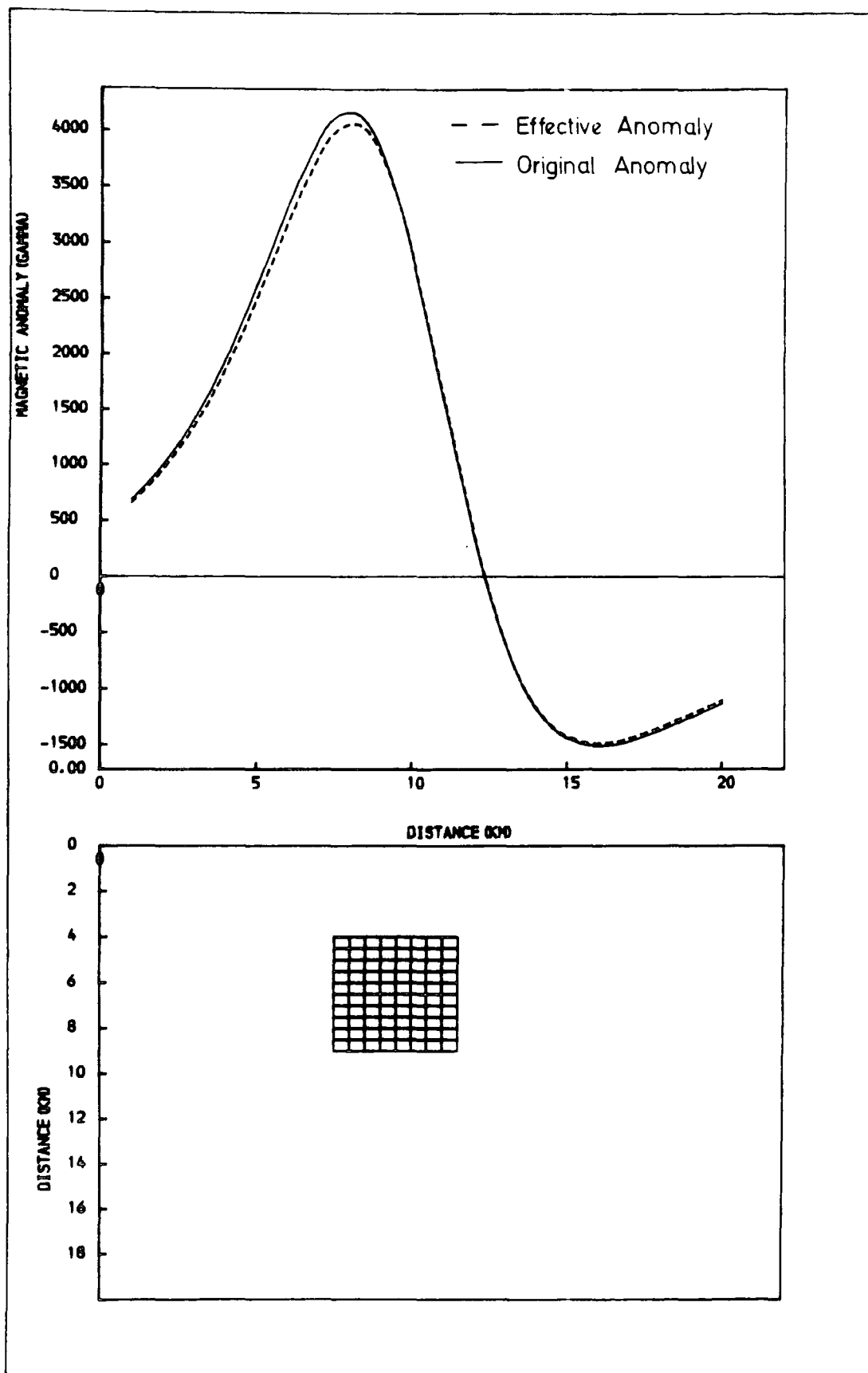
Figure 2.15c   Plot of original and effective magnetic anomalies for
a susceptibility of 0.1 (CGS).   Ie = 72°, αe = 20°;
Im = 62°, αe = 30°.
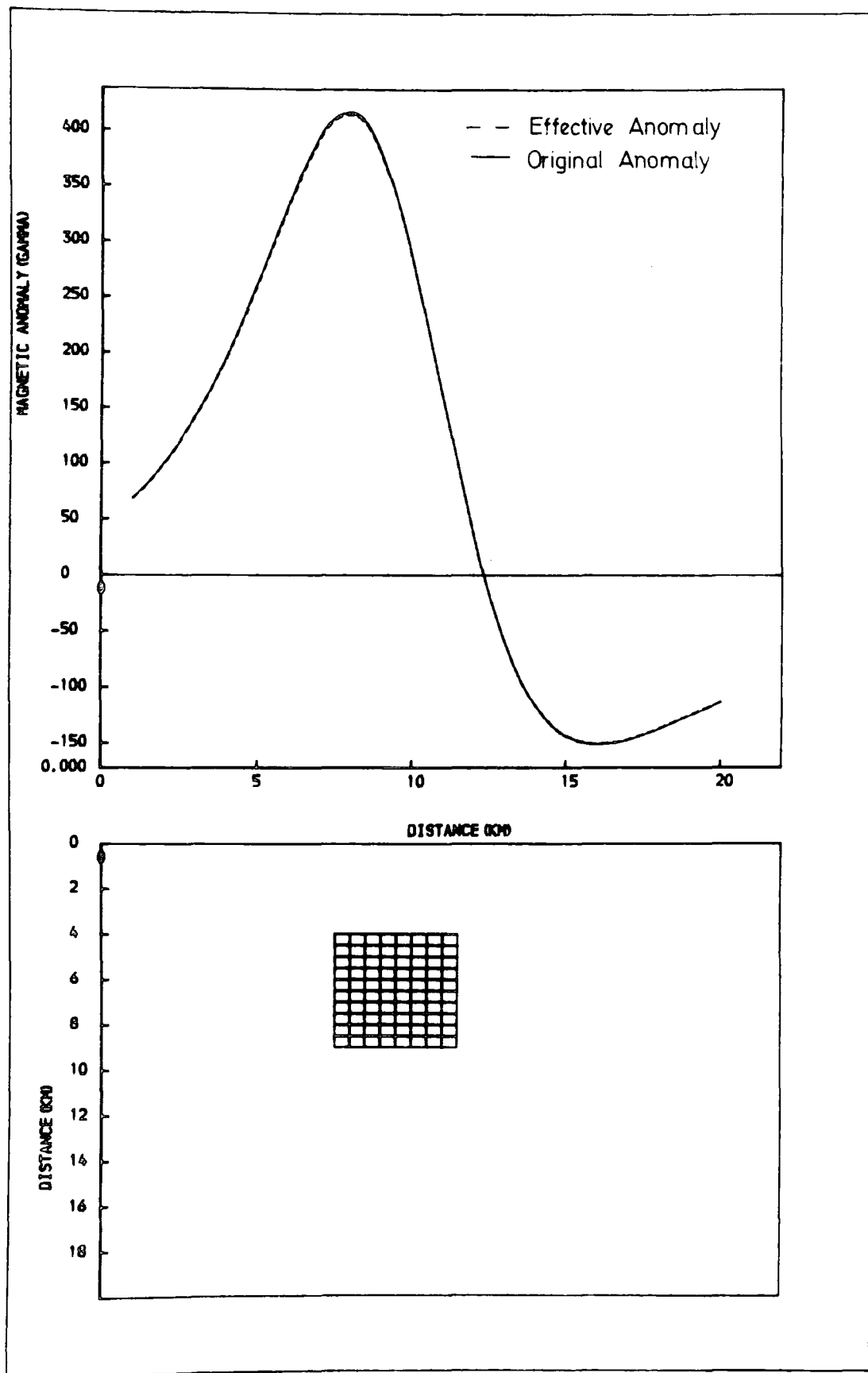
Figure 2.15d Plot of original and effective magnetic anomalies for a susceptibility of 0.01 (CGS). $Ie = 72^{\circ}$, $\alpha e = 20^{\circ}$; $Im = 62^{\circ}$, $\alpha e = 30^{\circ}$.
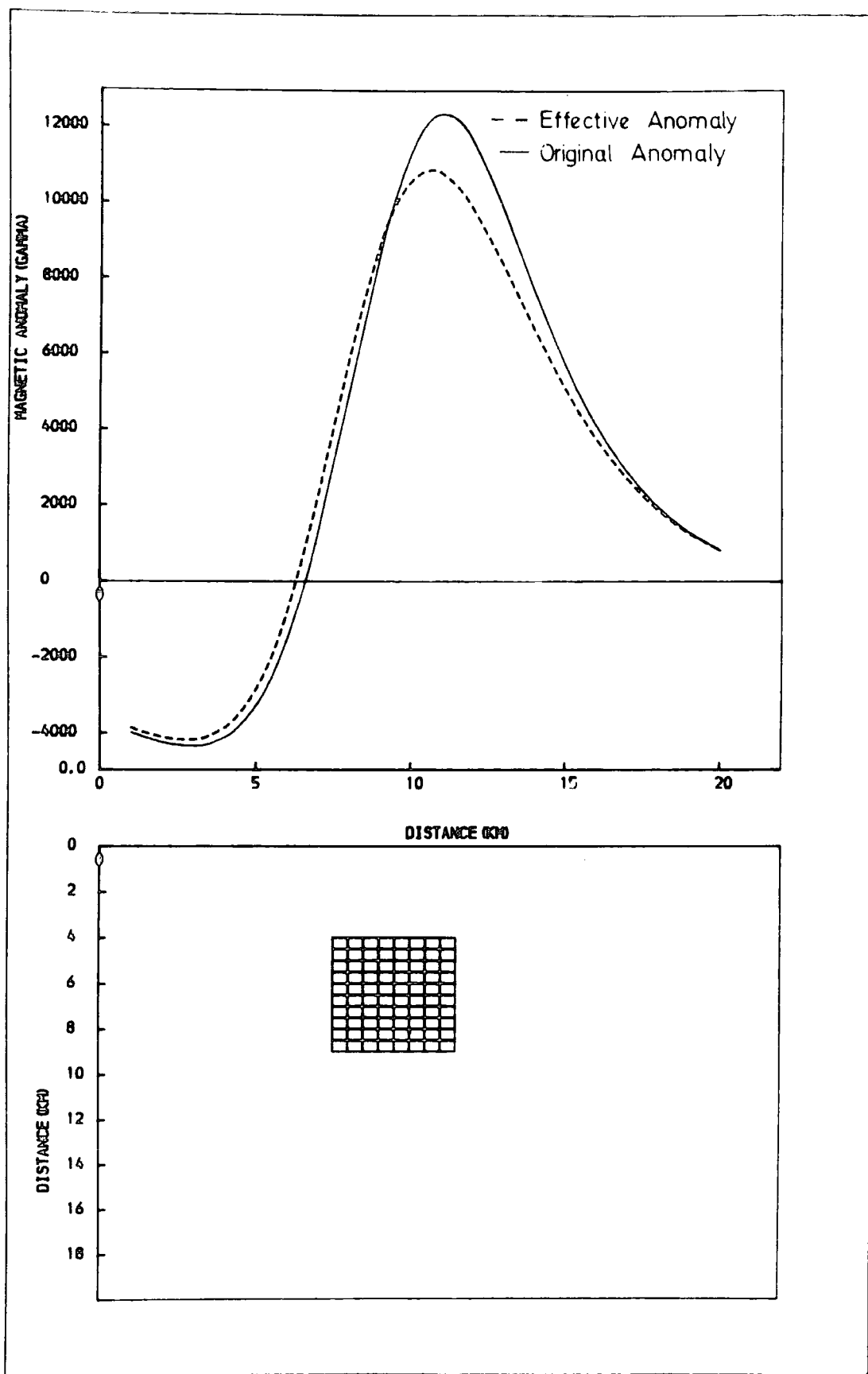
Figure 2.16a   Plot of original and effective magnetic anomalies for
a susceptibility of 0.4 (CGS).   Ie = 72°,   αe = 20°;
Im = 31°, αm = 160°.
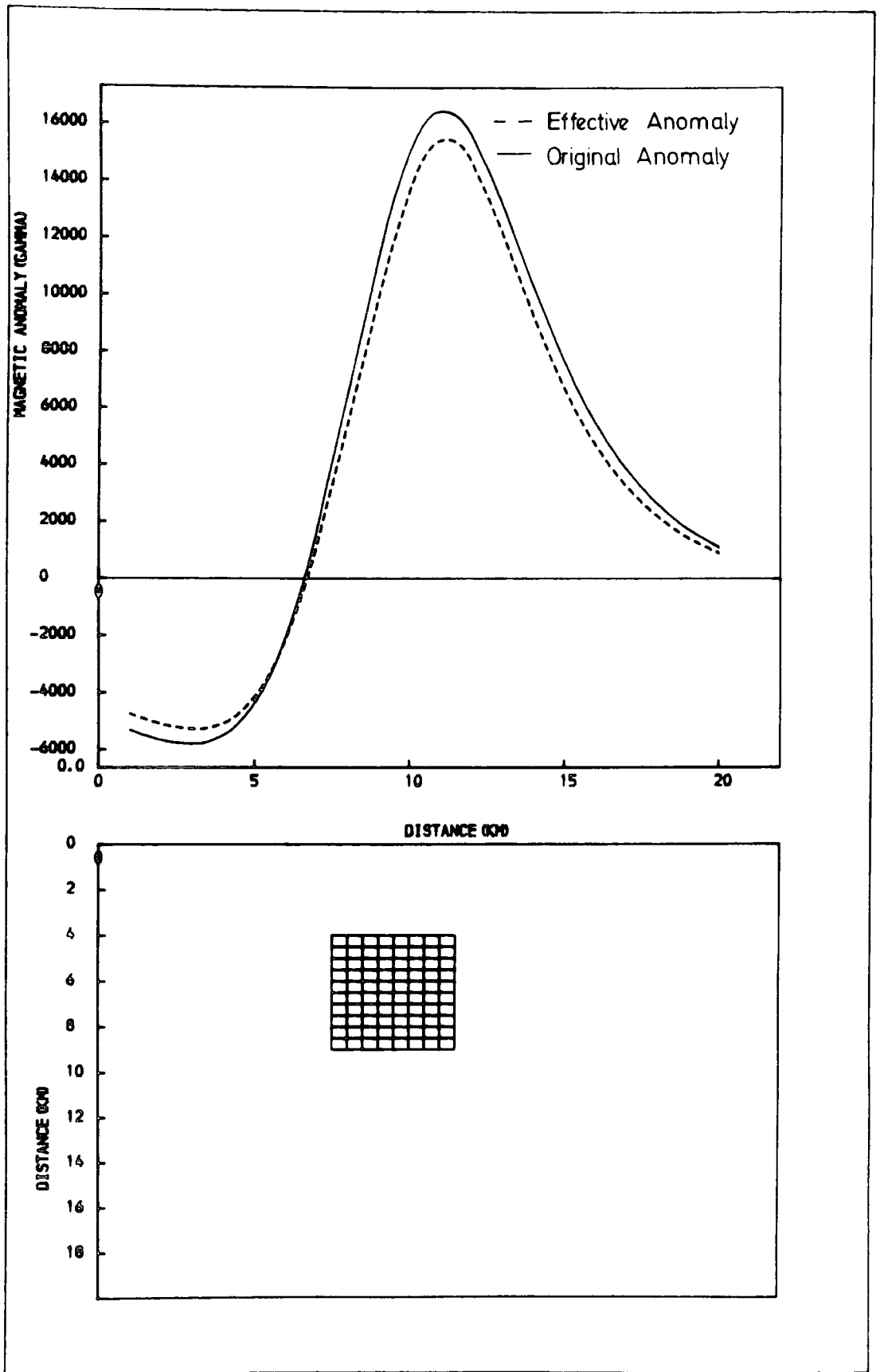
Figure 2.16b Plot of original and effective magnetic anomalies for a susceptibility of 0.3 (CGS). Ie = 72°, αe = 20°; Im = 31°, αm = 160°.
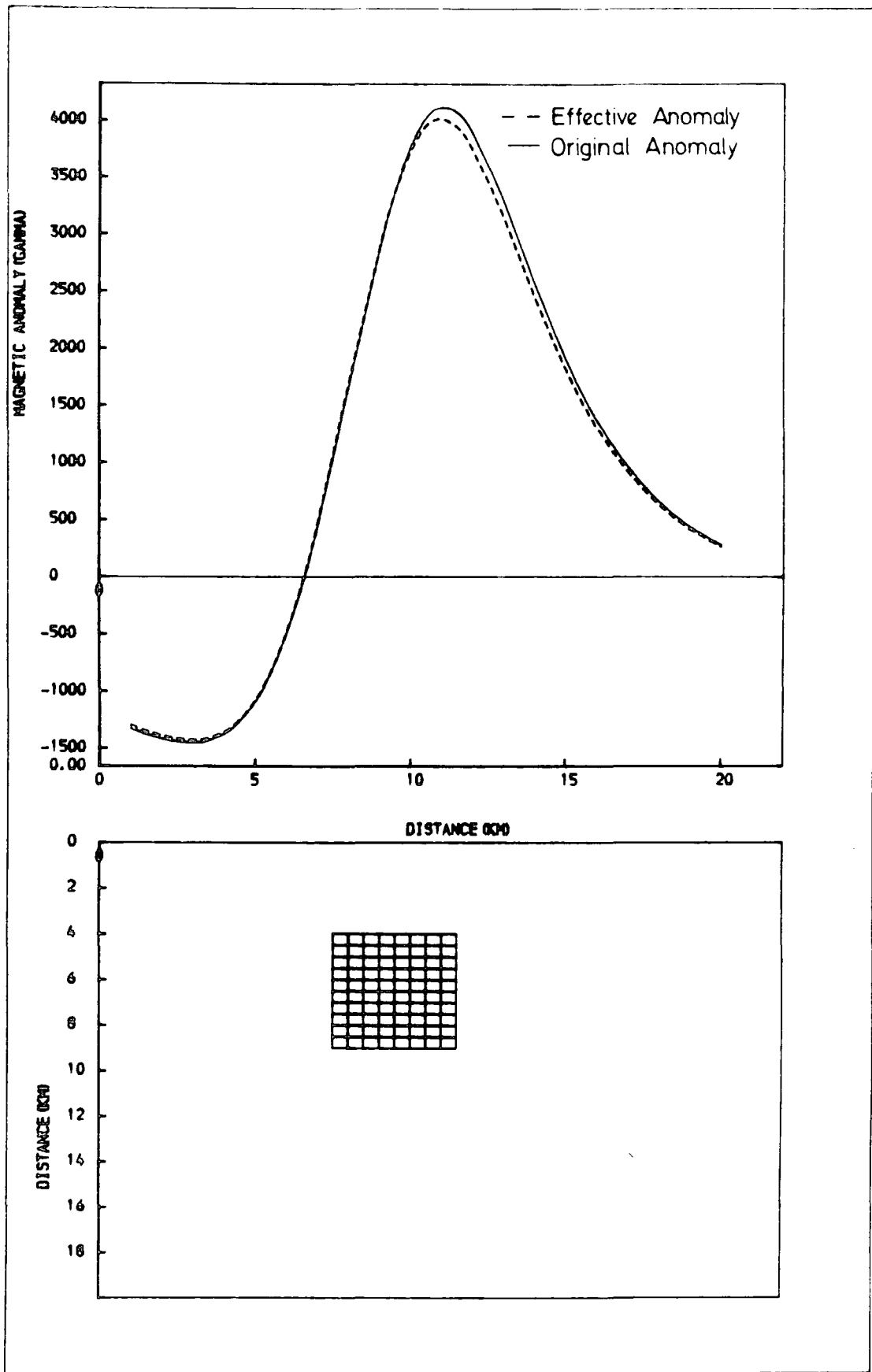
Figure 2.16c   Plot of original and effective magnetic anomalies for
a susceptibility of 0.1 (CGS). $I_e = 72^O$, $\alpha_e = 20^O$;
$I_m = 31^O$, $\alpha_m = 160^O$.
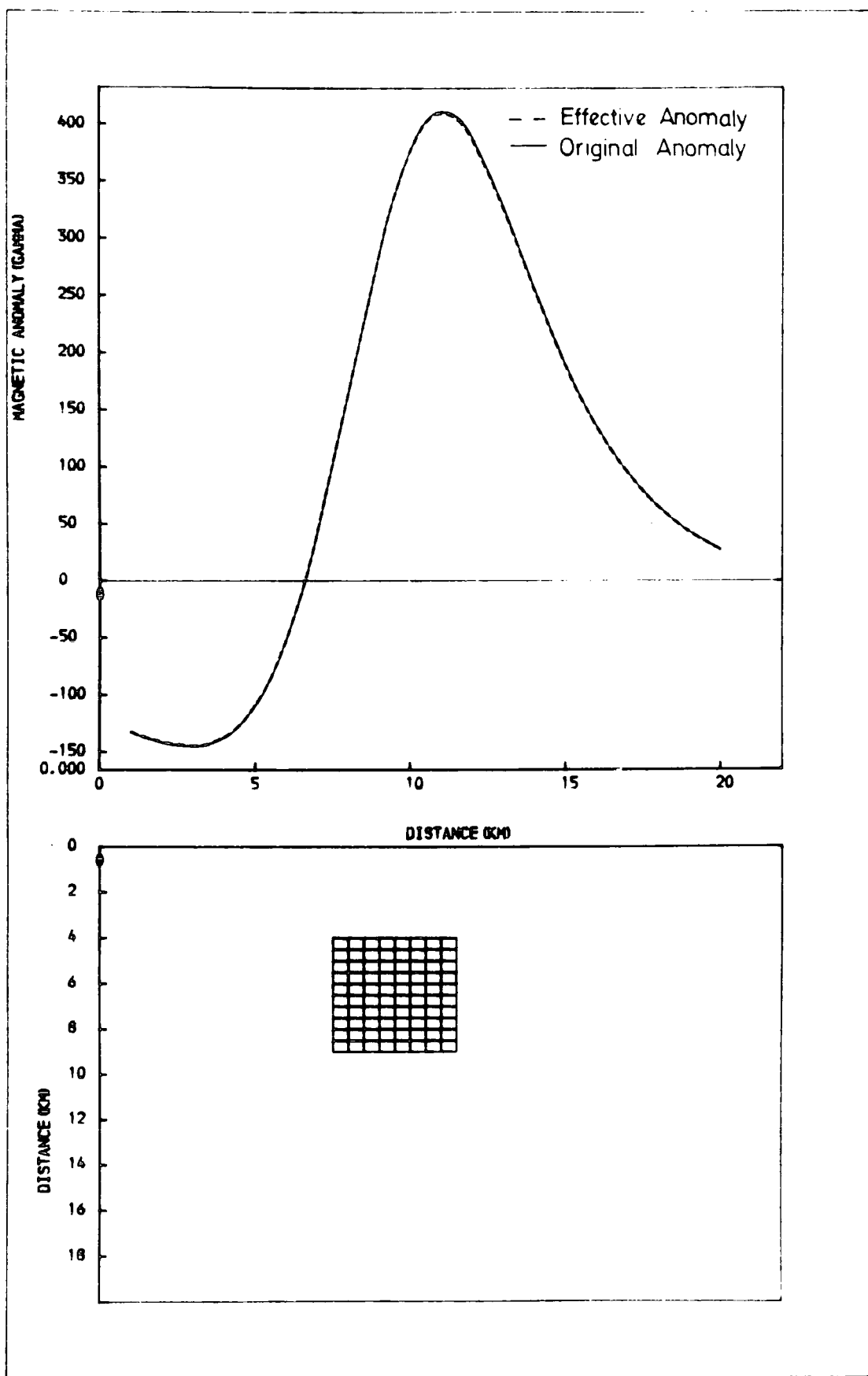
Figure 2.16d   Plot of original and effective magnetic anomalies for a susceptibility of 0.01 (CGS). Ie = 72°, αe = 20°; Im = 31°, αm = 160°.

advantage of the method of surface integrals lies in the fact that it does not assume the body to be in a medium of zero permeability.

The method of successive iteration depends on the reduction of the internal field by successive iterations to some acceptable value which in this case is to a value less than 1/1000th the original field. The fulfillment of this convergence criterion may therefore be a difficult and time consuming operation especially when the number of cells and the susceptibility are very high. For moderately low values of susceptibility however, the method was found to be as good as the methods involving matrix inversion. The results of a study using the method of successive iteration and the method of matrix inversion for a body divided into 80 cells – shown – for susceptibilities of 0.06, 0.05, 0.04 and 0.01 (CGS) are shown in Figures 2.17, 2.18, 2.19 and 2.20 respectively, where as was expected both results agree fairly well with each other. The method of successive iterations appeared to be faster and is expected to be more readily applicable to massive bodies than methods involving matrices since such methods would involve the solution of large numbers of equations.

2.4 Demagnetization Effects of Dykes

The difficulty involved in the evaluation of demagnetization effects in dykes depends to a great extent on whether the dyke is thin or thick. For a thin dyke, the computation of the effects of demagnetization and its inclusion in the interpretational scheme is simple and straightforward as it is usually sufficient to express the effects of demagnetization is such dykes in terms of the demagnetization factor (N). This demagnetization factor is zero when the components of magentization in the plane of a thin dyke is considered and has a value of unity (1.0) for components perpendicular to the
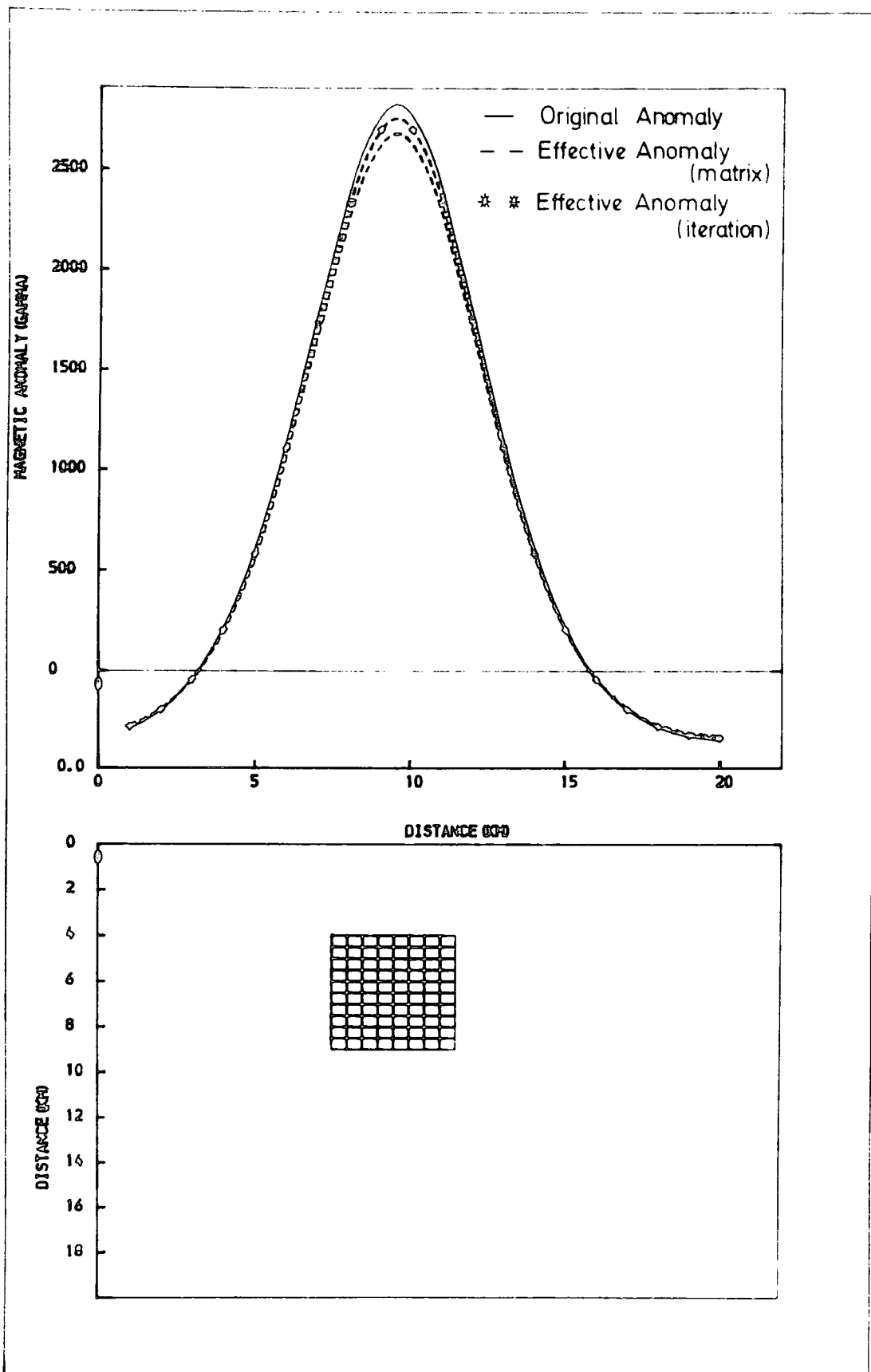
Figure 2.17   Comparison of the methods of successive   iteration and
              matrix inversion for a susceptibility of 0.06 (CGS).
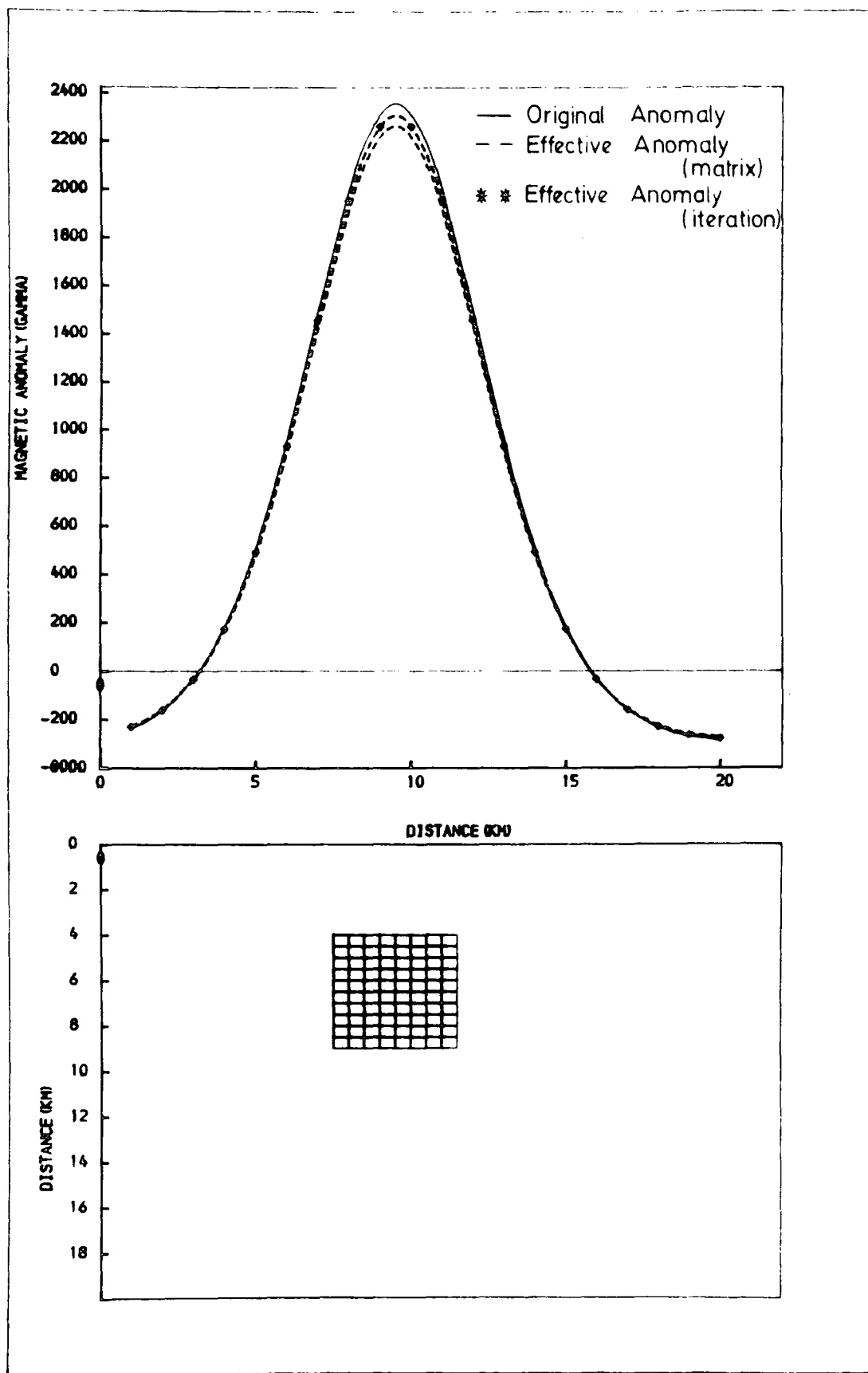
Figure 2.18   Comparison of the methods of successive   iteration and
matrix inversion for a susceptibility of 0.05 (CGS).
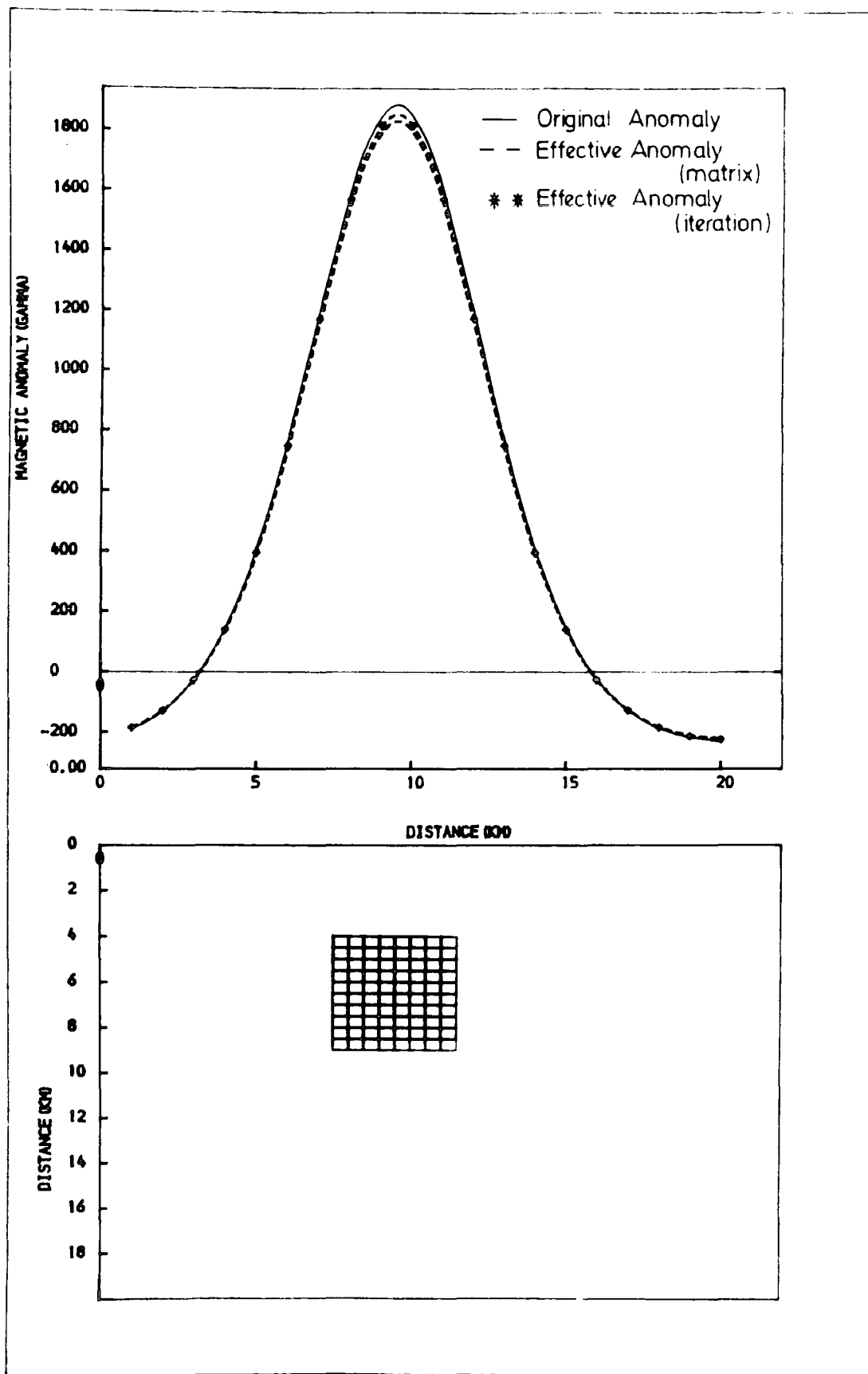
Figure 2.19 Comparison of the methods of successive iteration and matrix intersion for a susceptibility of 0.04 (CGS).
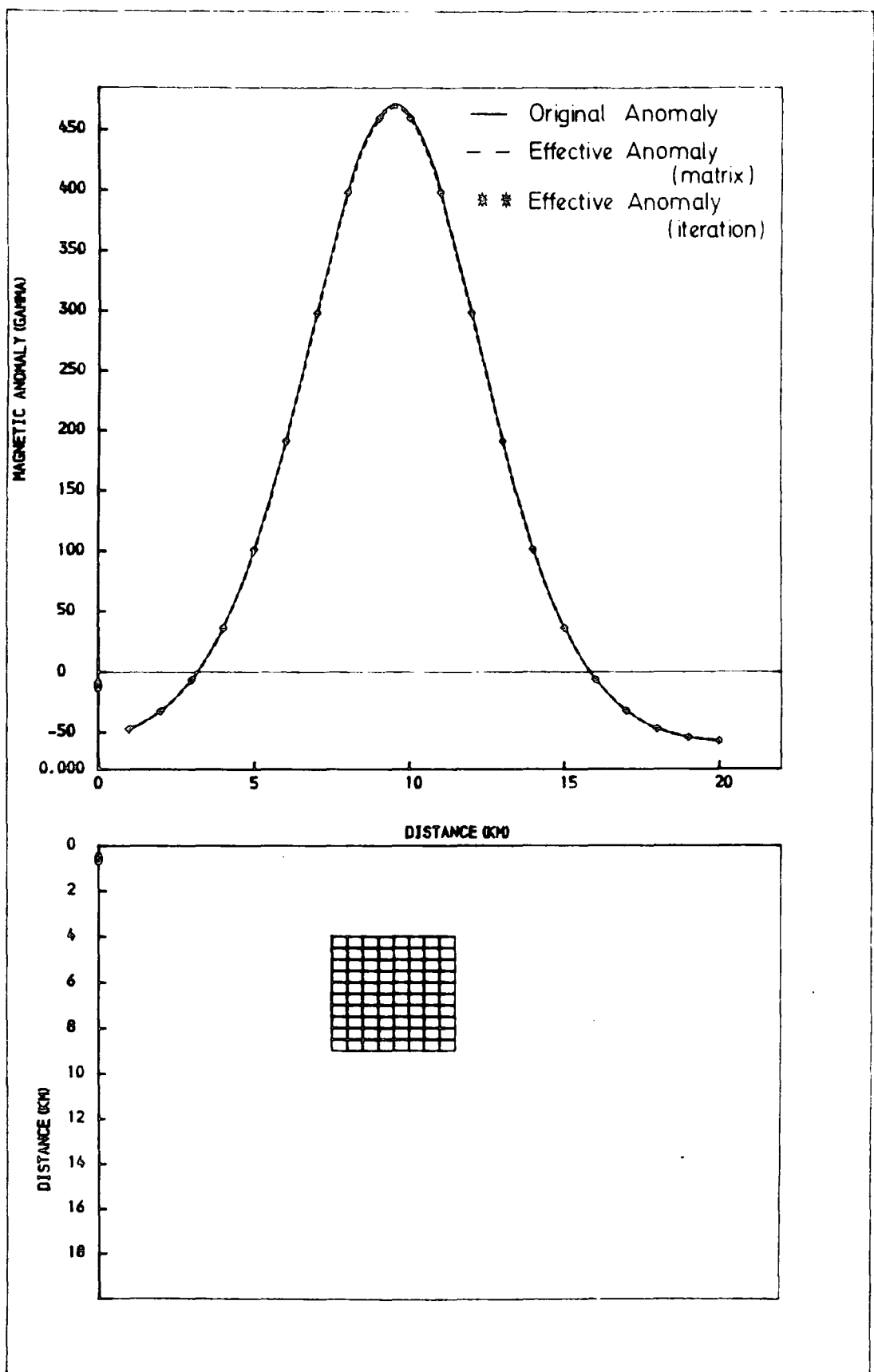
Figure 2.20   Comparison of the methods of successive iteration and matrix inversion for a susceptibility of 0.01 (CGS).

plane of the thin dyke (Parasnis, 1972). The departures expected from these values at the edge of the dyke are not serious as the thin dyke is assumed to be very thin compared to its depth of burial and the constant demagnetization factors equal to those of an infinite thin sheet hold good for a thin dyke. The susceptibility of the dyke is now modified to give an apparent susceptibility given as :

$$K' = K/(1 + K) \qquad\qquad 2.49$$

The problem of demagnetization in thick dykes is not, however, as straightforward as that of a thin dyke as an internal near surface magnetization which varies in both magnitude and direction is created in the thick dyke. To a first approximation, the demagnetization of a thick dyke may be expressed in terms of a demagnetization factor which for the cross components of magnetization has a value of 0.5 near the edge of the dyke (Gay, 1963). This approximation, however, becomes poor as the thickness and magnetization of the dyke increases, thus the need for alternative approaches to the problem of demagnetization in thick dykes. The techniques discussed in section 2.3 above represent very attractive alternatives to the use of an approximate demagnetization factor.

In general, the effect of demagnetization lowers the magnitude of the anomaly and the neglect of demagnetization effects when the later is appreciable may lead to an eroneously small thickness for the dyke while leaving the depth of burial and position of the dyke unaffected. The techniques discussed in Section 2.3 above, have been applied to a re-interpretation of some profiles taken across the Minch Dyke (Chapter Three) and the results of this study will be presented in that Chapter.

CHAPTER III

MAGNETIC INVESTIGATION OF THE MINCH DYKE

3.1 Introduction

On sheet 12 of the Aeromagnetic map of Great Britain and
Northern Ireland is a marked linear feature running from the
north of the Island of Lewis to Loch Ewe, a distance of about
110 km (Figure 3.1). The short wavelength anomalies over the
neighbouring land areas are associated with the Precambrian
basement and with lavas on Skye. For instance, the pronounced
positive anomaly over south Harris has been interpreted by
Westbrook (1974) as being closely related to the outcrop of
metagabbros which occur within the Lewisian igneous complex
of tonalites, anorthosites and gabbros bounded by metasediments.
In contrast, over the North Minch, the low amplitude magnetic
anomalies of rather gentle magnetic gradients reflect the develop-
ment of Mesozoic sediments underlain by Torridonian sediments
in the Minch Basin. An interpretation of the gravity field
(Figure 3.2) showed that the thickness of sediments in the
basin range from about 1.5 kms to about 4 kms (Allerton, 1968).
The prominent linear magnetic feature which crosses the basin
is here interpreted as being due to an unusually wide, reversely
magnetized dyke, probably of Tertiary age. The results of this
interpretation are presented in this chapter. An attempt has also
been made to include the effect of demagnetization of the dyke
in the interpretation. A brief outline of the geology of the
areas around the proposed Minch dyke is first given.

Figure 3.1   An aeromagnetic map of the area around the Minch Dyke
(taken from Sheet 12 of the Aeromagnetic Map of Great
Britain and Northern Ireland).

SCALE 250 000 : 1
BOUGUER ANOMALY
CONTOUR MAP
OF THE NORTH MINCH
Contours every 10 mgals.
· gravity stations
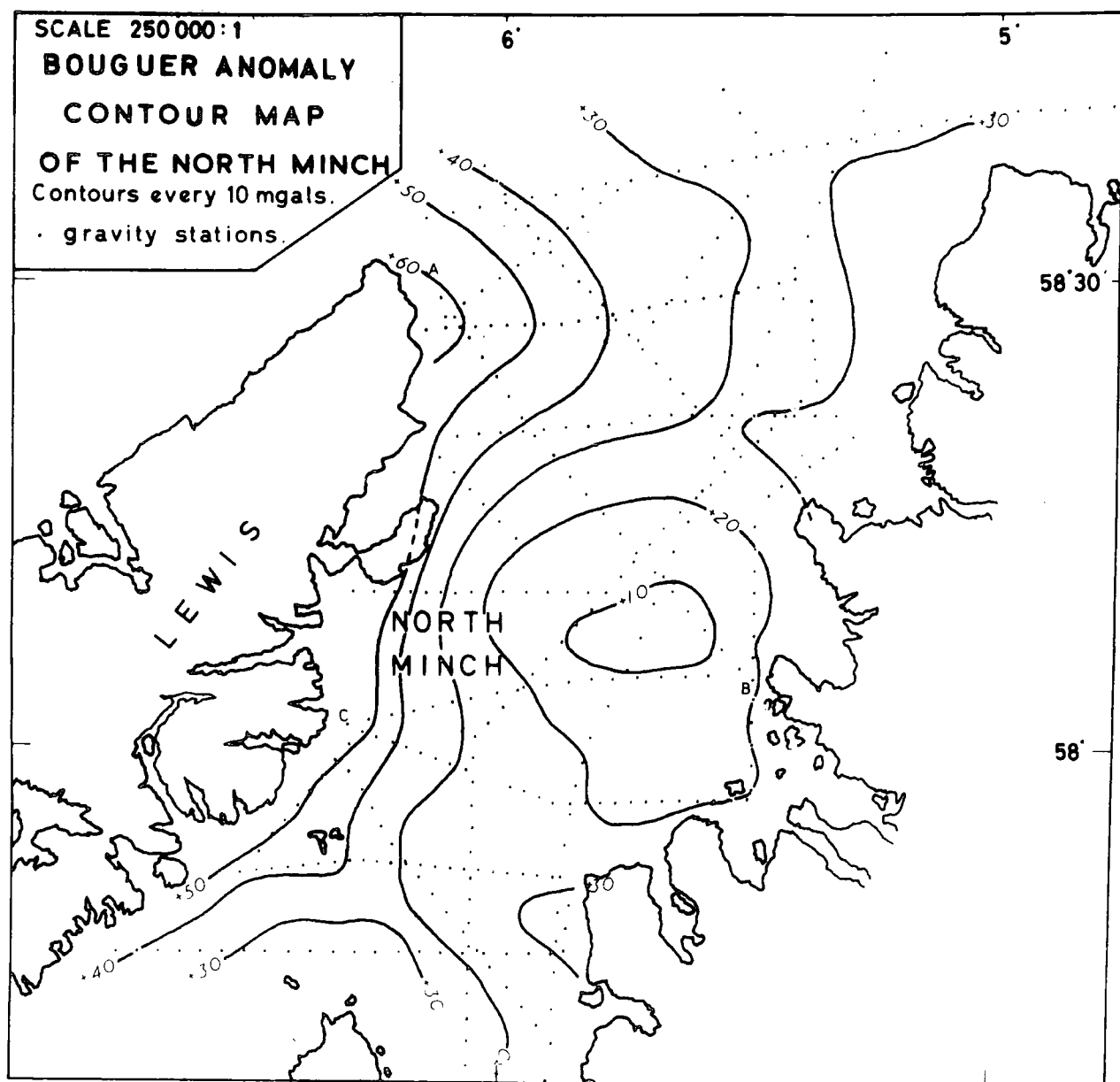
LEWIS

NORTH
MINCH

(After Allerton, 1968)

3.2   Geology of the Area Around the Minch Dyke

The Minch Basin across which the Minch anomaly runs is bordered by the Islands of Lewis and Harris to the west, Northern Skye to the south, the Shiant Isles as well as the north Scottish mainland. The geology of these areas which surround the Minch dyke has been presented in detail by several authors (Richey, 1961; Anderson and Dunham, 1966; Jehu and Craig, 1924; Binns et al., 1974).

3.2.1   The Outer Hebrides (Lewis and Harris)

The Islands of Lewis and Harris are essentially composed of Lewisian orthogneiss and a massive paragneiss which form most of the south-west Harris, (Jehu and Craig, 1924). South of Lewis and north of Harris there are massive granite intrusions. Sheets and dykes of varied rock types also intrude the gneiss of the Outer Hebrides. Most of these are late Lewisian in age although rocks of Caledonian, Permian and Tertiary ages are also to be found with Tertiary igneous rocks appearing as north-west trending dykes.

The Outer Isles Thrust Plane occurs to the south east of Lewis and Harris. This is gently inclined towards the south east and dates from Pre-Torridonian time. The Stornoway Beds lie to the north east of Lewis. The age of these beds is not definitely known but they have recently been described as Triassic based on sedimentological correlation (Steel, 1971). These sediments have been deposited in a graben like structure associated with the complex faulting along the Minch fault.

3.2.2. Northern Skye

Northern Skye is mainly composed of Tertiary basaltic lavas which overlie Jurassic rocks. Also lying on the peneplane of Jurassic rocks are the Tertiary sediments made up of volcanic dust, lapilli, bombs and tuffs ejected with explosive violence (Anderson and Dunham, 1966). These Tertiary sediments are similar to the tuffs of the Palagonite Formation of Iceland, (Wilson, 1937; Tyrrell, 1949).

East of Skye, is the Island of Rona which is formed of Lewisian gneiss. Mesozoic sediments are known to outcrop on the north and east coasts of Skye and intermittently along the west coast.

3.2.3 The Shiant Isles

The Shiant Isles are situated between the Outer Hebrides and Skye and have a geology closely related to that of Skye. They are formed of Tertiary igneous rocks (Craig, 1965). Massive sills of Tertiary crinanite occupy the bulk of the Shiant Isles and these outcrop on the seabed to the south of the Isles. Upper Lias shales though not in any great thickness are also present.

3.2.4 The North Scottish Mainland

The rocks of the Scottish mainland which form the eastern edge of the Minch Basin are mainly Precambrian in age. The Foreland complex in the north west is composed mainly of Lewisian gneiss which are unconformably overlain by Torridonian sediments. Nearer the Moine Thrust, Cambrian sediments unconformably overly the Lewisian and Torridonian of the Foreland Complex. The Moine sediments which occur east of the Moine Thrust, seem to have been laid down contemporaneously with the Torridonian sediments of the

Foreland complex. They were thrust to the northwest during the Caledonian movements. On the mainland between Gruinard Bay and Loch Ewe are found thin sequences of Triassic and Liassic sediments in down faulted tracts.

3.2.5 The North Minch Basin

Gravity and seismic studies of the North Minch indicate the presence of a sedimentary basin in the area. This basin is bounded on the west by the Minch Fault. A similar fault may also exist on the east side. The oldest sediments are probably of Torridonian age and the youngest sediments of Jurassic age. Thickness of these sediments have been estimated at between 1.5 kms and 3.7 kms (Allerton, 1968).

3.3 Interpretation of Magnetic Anomalies

Sixteen profiles have been taken across the linear magnetic feature which intersects the Minch Basin. These are spaced along the length of the feature as shown in Figure 3.3. The observed magnetic anomaly values were taken from the contours on the one inch compilation sheets for the 1:250,000 Aeromagnetic maps of Great Britain and Northern Ireland. To obtain equally spaced field points, values were interpolated between contours using a curve interpolation routine. The lengths of the observed profiles varied according to the position at which the profile was taken. The source of this anomaly is not exposed anywhere on land or at the seabed.

3.3.1 Method of Interpretation

The two-dimensional method of interpretation of magnetic
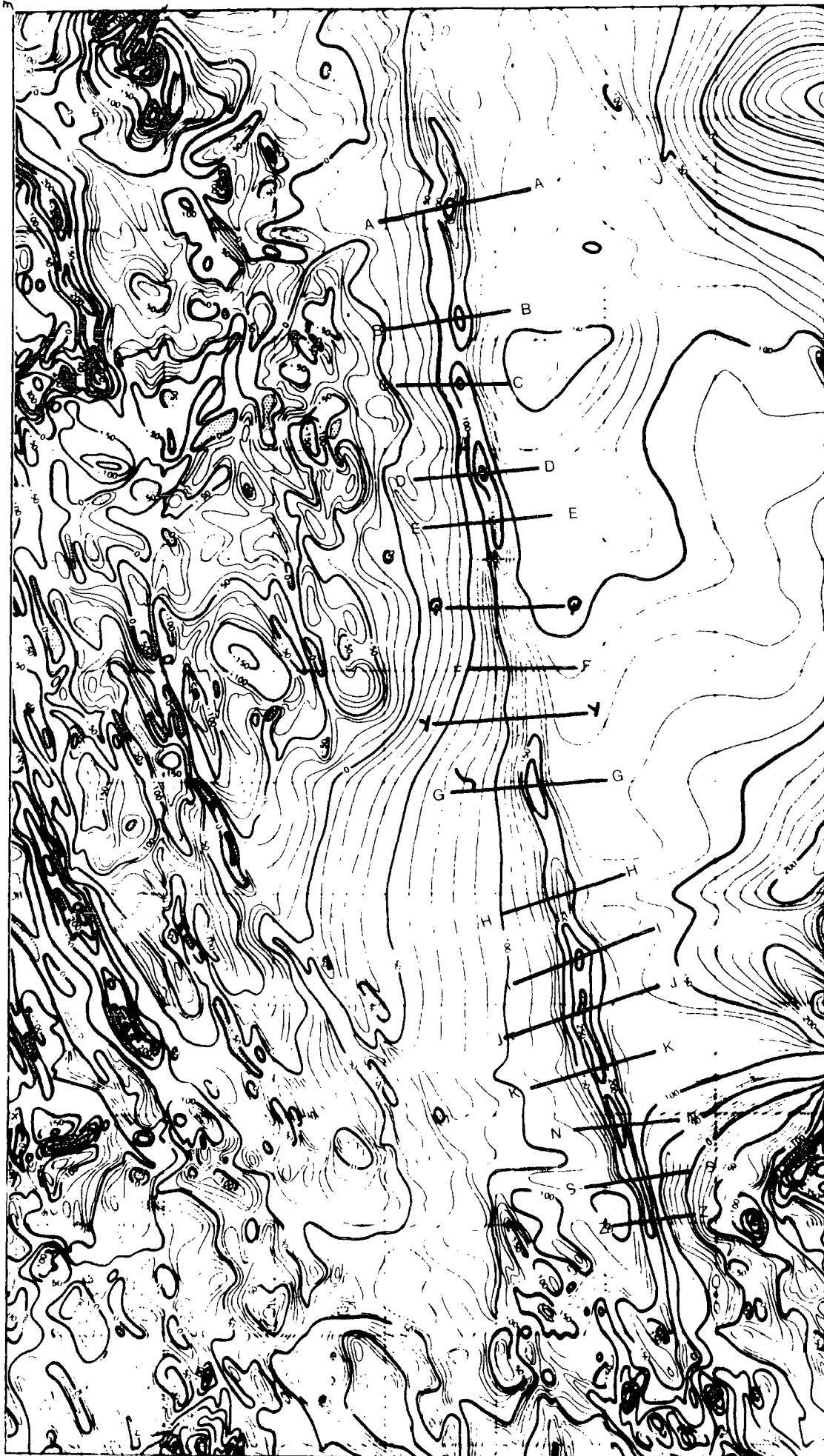
Figure 3.3 An aeromagnetic map of the area around the Minch Dyke
showing the positions of the profiles interpreted.

anomalies due to dykes described in Chapter I was used. The initial estimates of the parameters l, t, and z of the model dyke were obtained from the observed anomaly profile using the method of Bruckshaw and Kunaratnam (1963). Based on these initial estimates, lower and upper bounds were placed on permissible values of l, t and z. Starting with these initial estimate, the parameters l, t and z were varied until an acceptable fit was obtained between the observed and computed anomalies. A measure of this fit is given by the value of the objective function at the end of the optimization routine. A second order quadratic regional field was assumed throughout the interpretation. The removal of the regional field was carried out in the course of the interpretation process outlined in Chapter I (Section 1.3) of this thesis. Tests showed that for most of the profiles, the removal of only the zeroth order regional field does not adequately fit the observed anomaly. To illustrate this, an interpretation of the profile II' with only the zeroth order regional indicated removed is shown in Figure 3.4. The obvious inadequacy of the regional removed is evidently shown in the diagram. It was, however, found for most profiles that only the zeroth and first order regional fields were appreciable. The result of a re-interpretation of profile II' with higher order regional fields removed is shown in Figure 3.9.

3.3.2   Results of Interpretation

Seven profiles taken spacely across the entire length of the prominent linear negative magnetic anomaly which crosses the North Minch as interpreted by the non-linear optimization method (Chapter I, Section 1.3) are shown in Figures, 3.5 to 3.11.
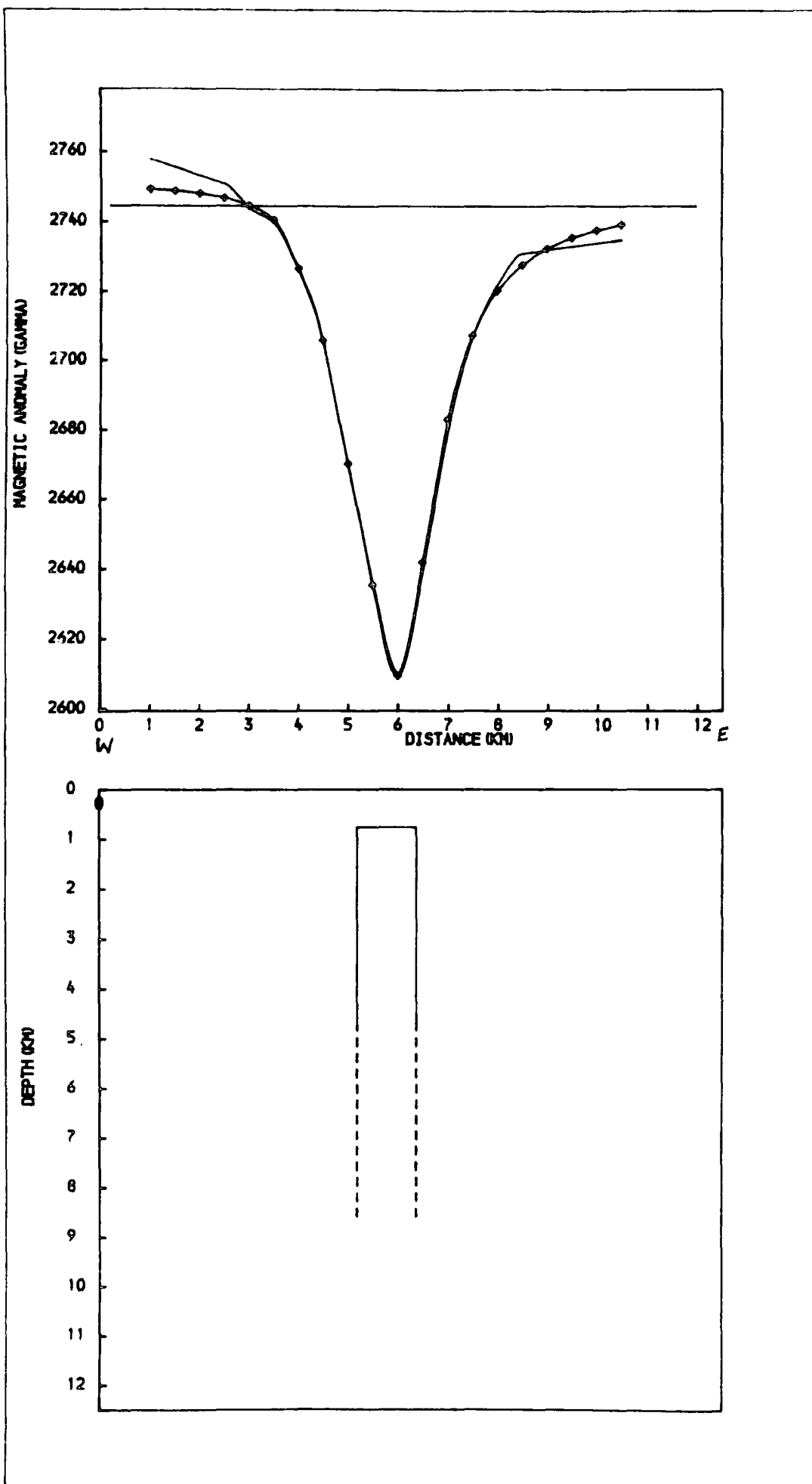
Figure 3.4   An interpretation of the profile II' with only the
zeroth order regional shown removed.
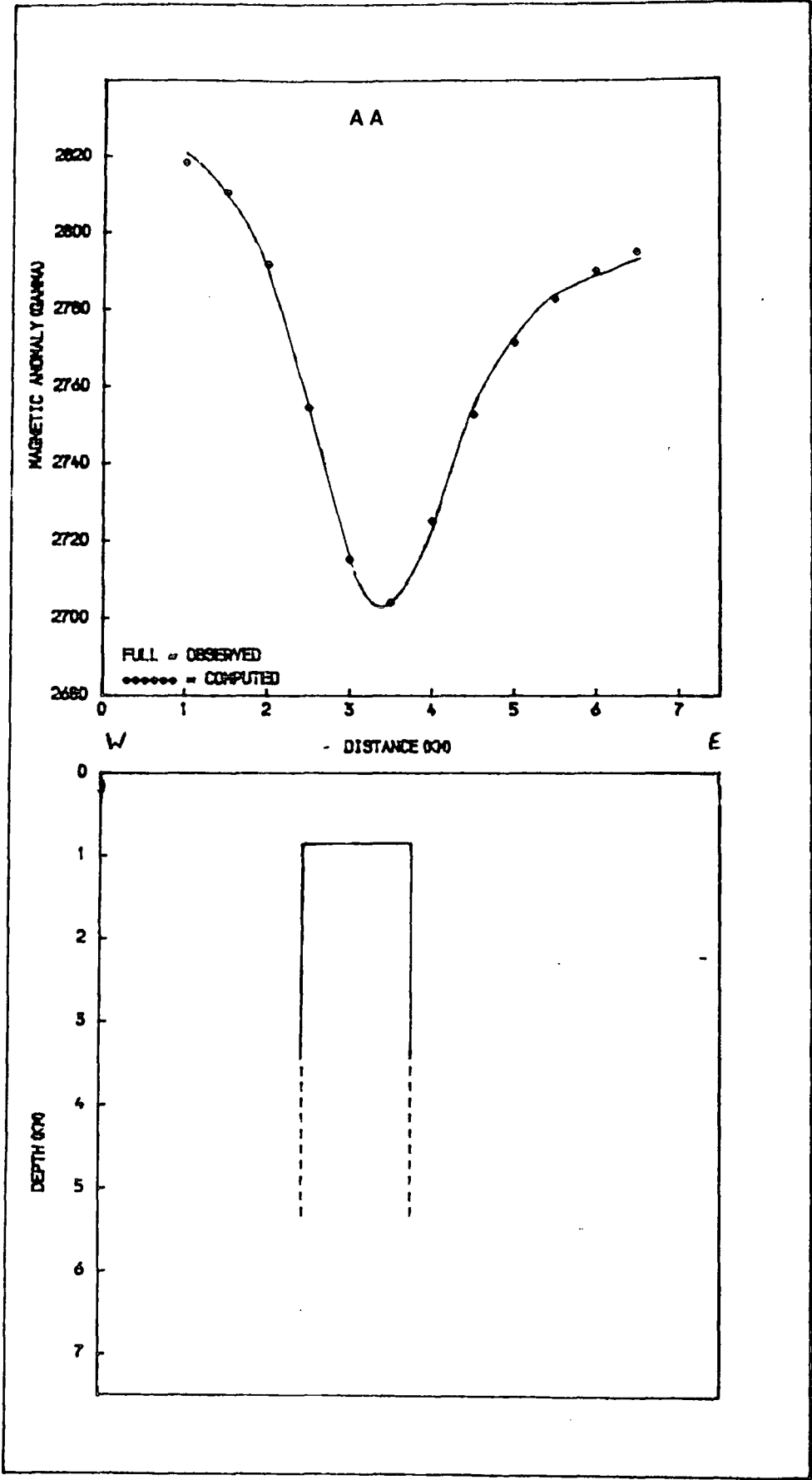
Figure 3.5 Optimal dyke model required to account for the profile AA'.

Figure 3.6   Optimal dyke model required to explain the profile BB'.
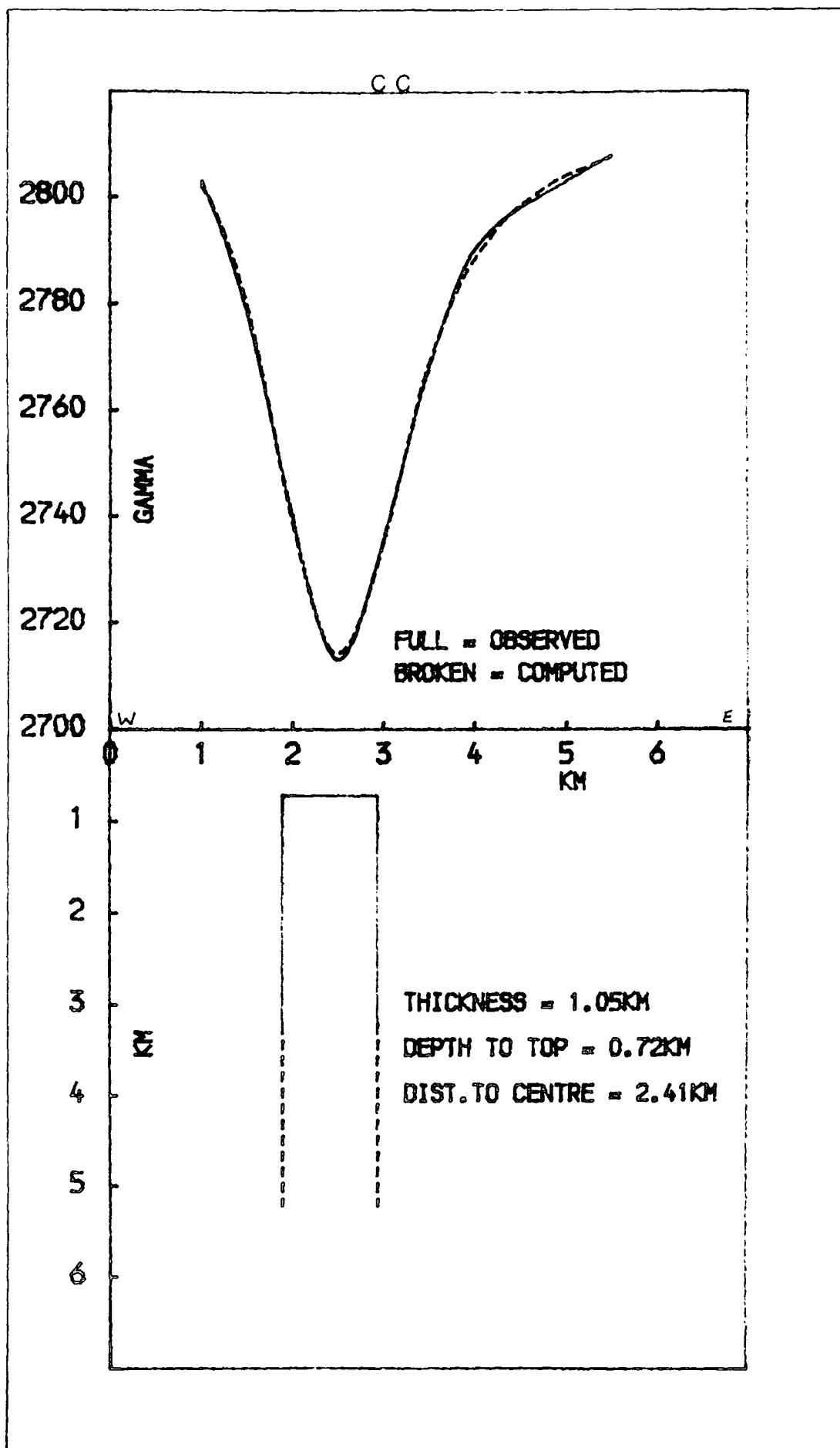
Figure 3.7 Optimal dyke model required to account for the profile
CC'.
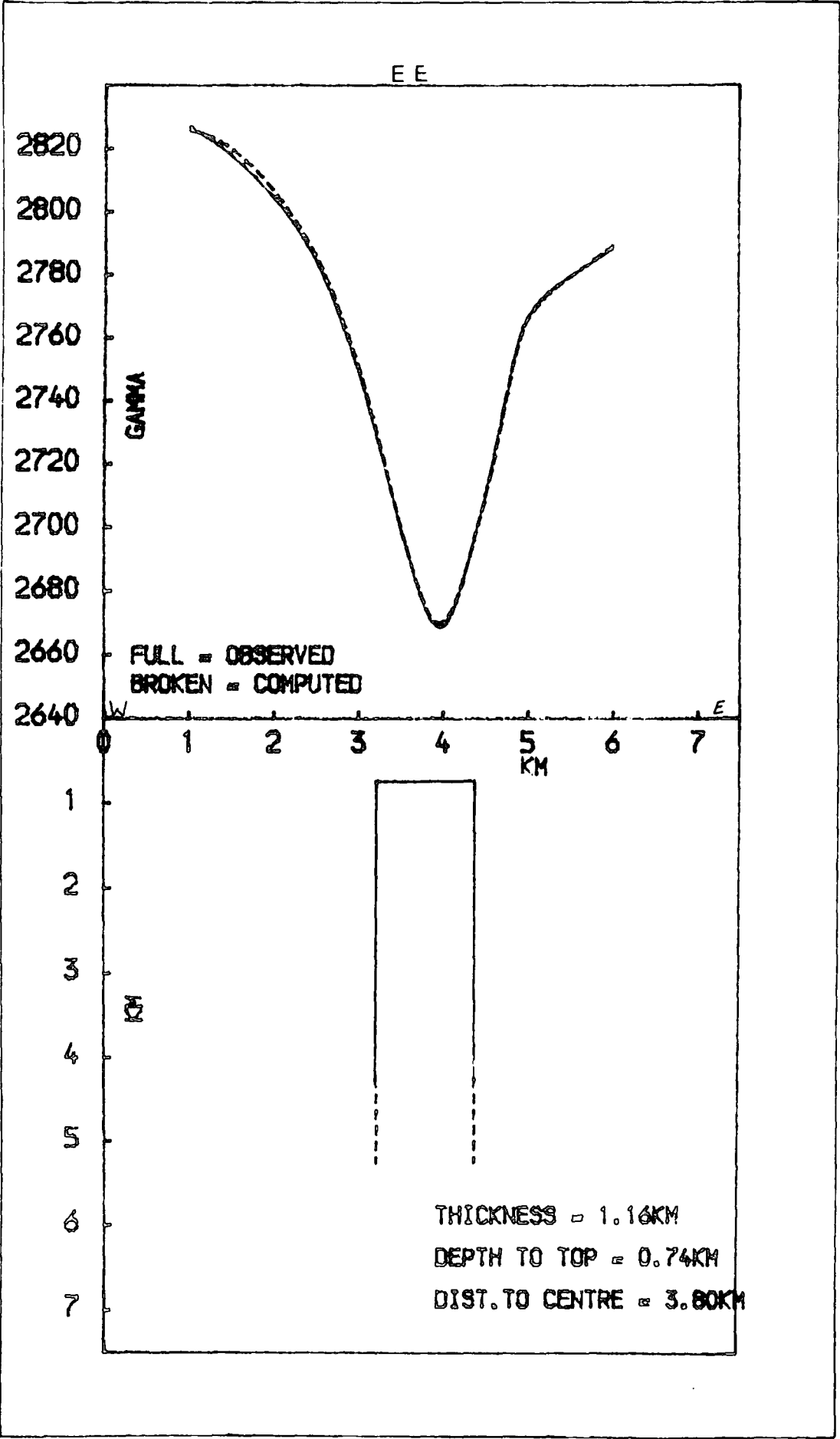
Figure 3.8 Optimal dyke model obtained for the profile EE'.
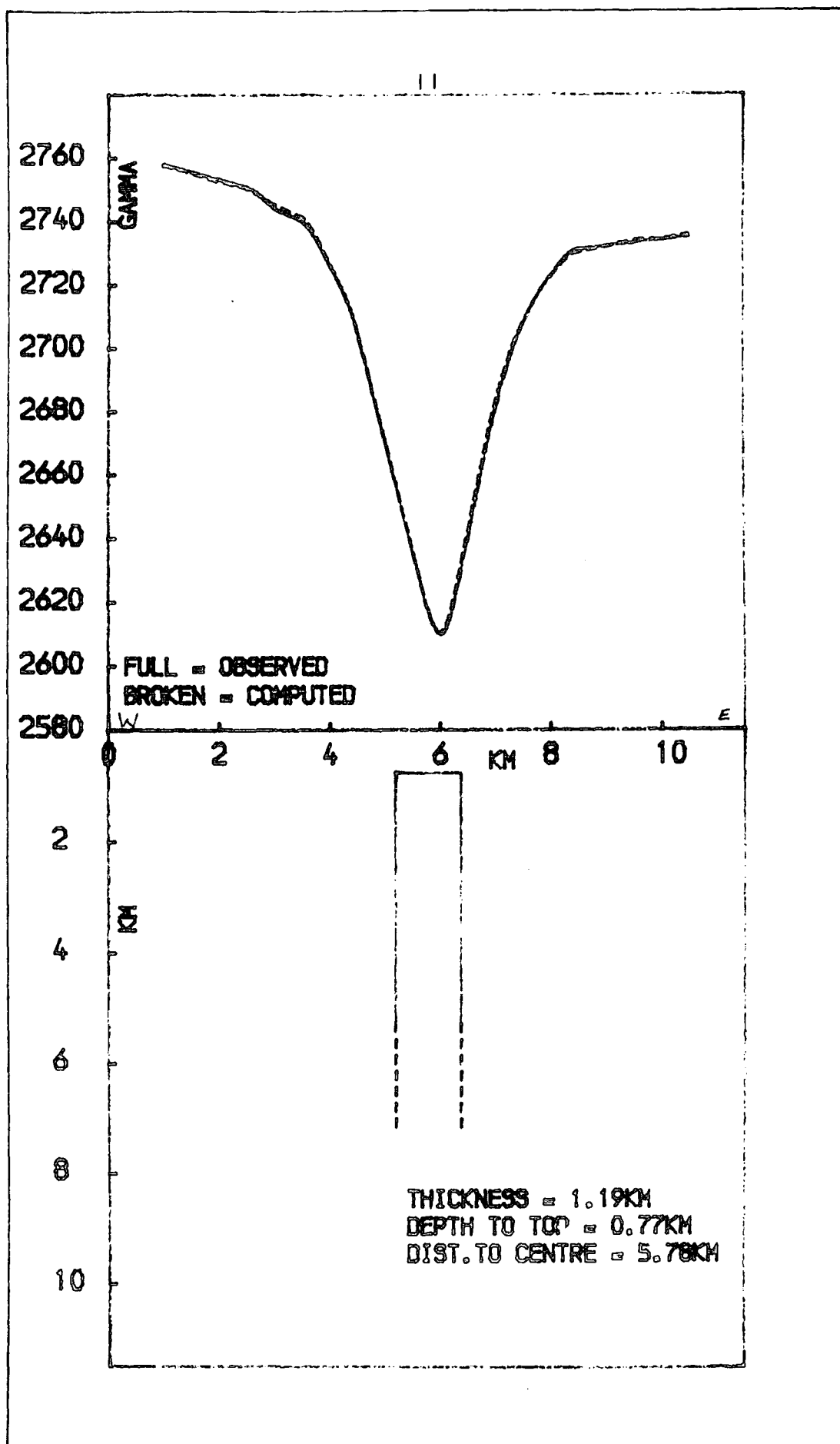
Figure 3.9 Optimal model required to account for the profile II'.
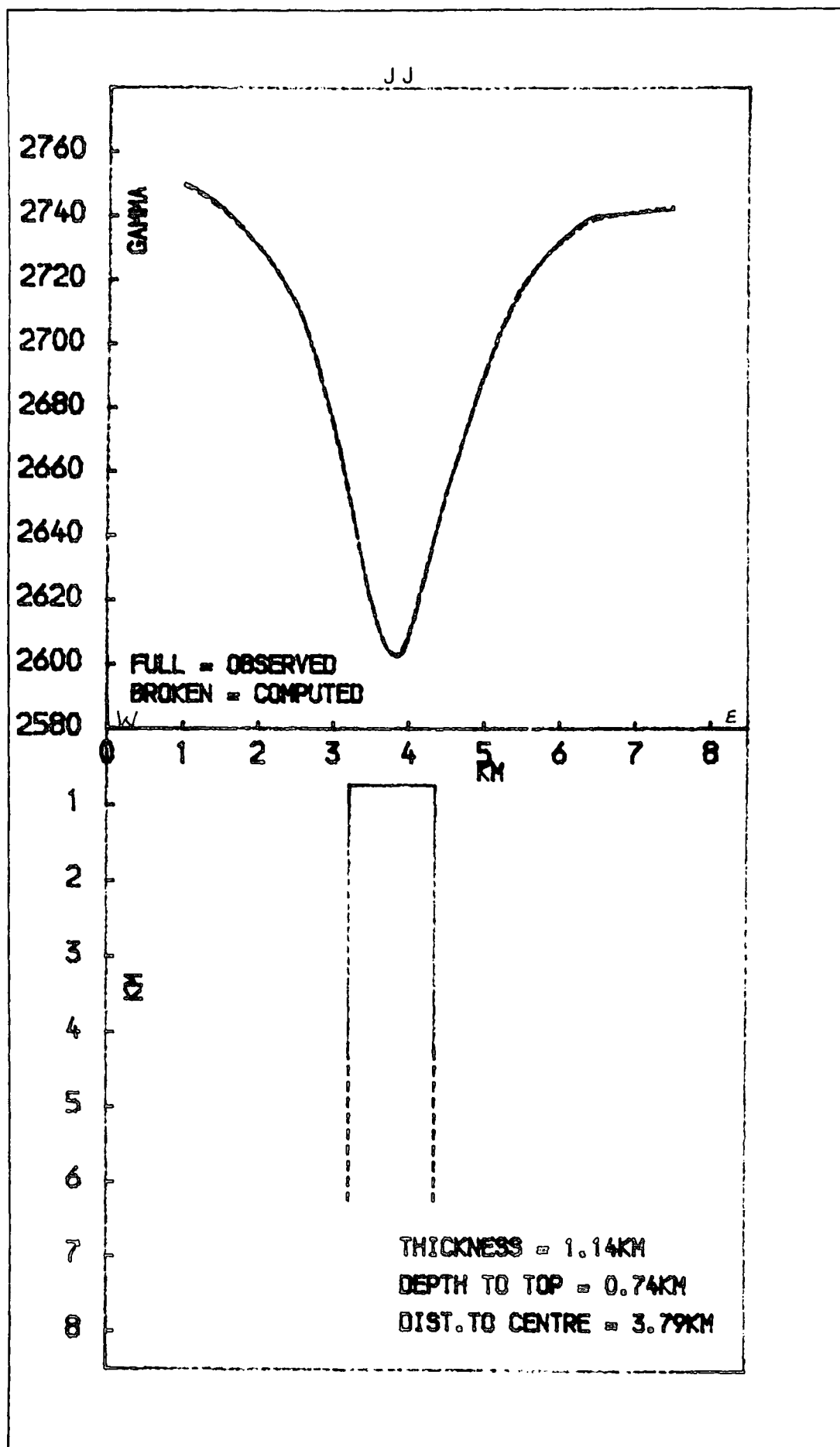
Figure 3.10 Optimal dyke model required to expalin the profile JJ'.
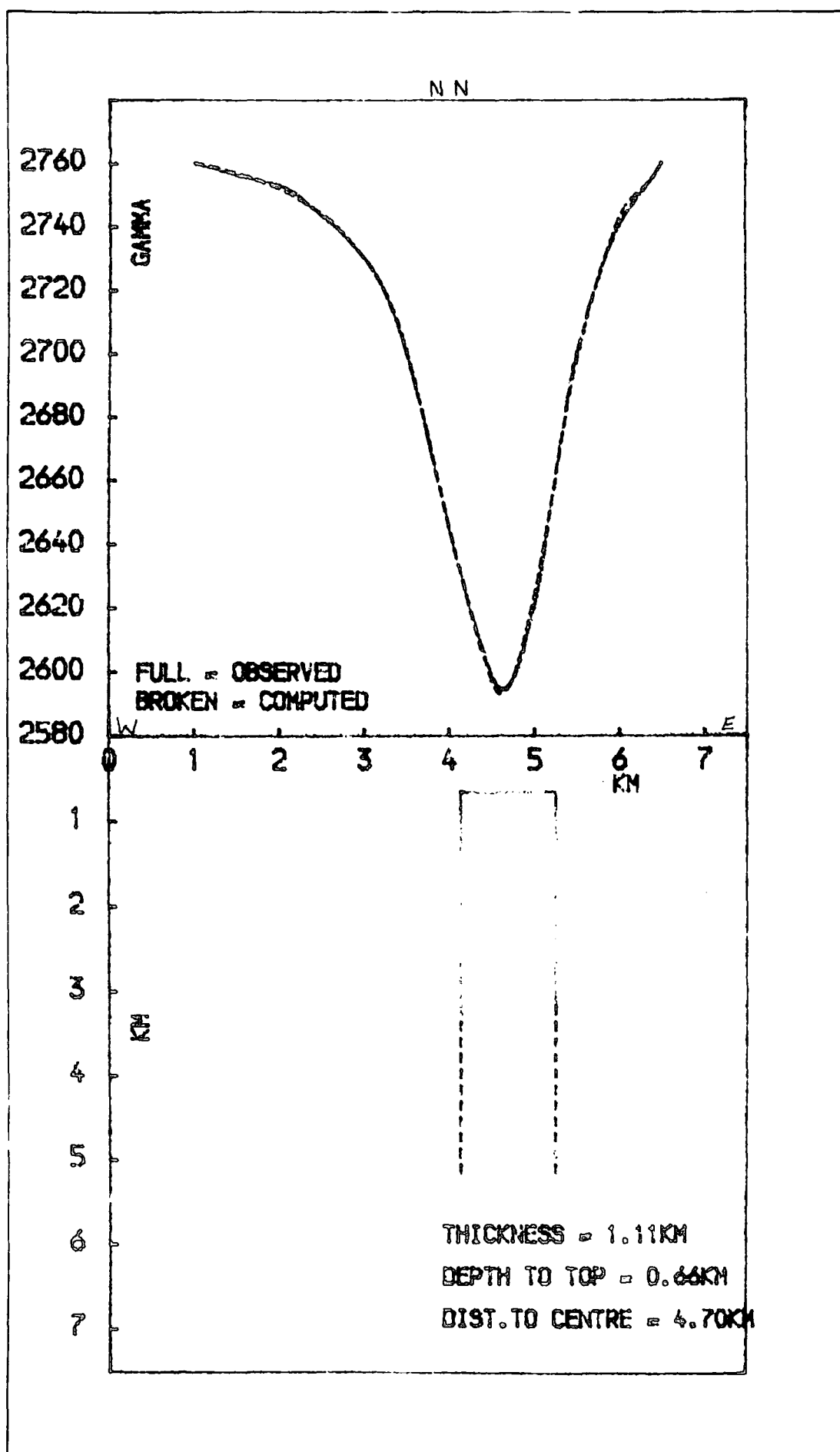
Figure 3.11 Optimal dyke model required to explain the profile NN'.

The interpretation of profile AA' located at the extreme northern end of the anomaly is shown in Figure 3.5. This indicates the dyke to be 1.30 km wide and 0.86 km deep. The angle β is estimated to be 297° and the magnetization within the vertical plane containing the profile is 0.61 A/m, assuming the dyke to be vertical. The optimal body shape produced for the profile BB' (Figure 3.6) indicates the dyke to have a thickness of 1.13 km, a depth of 1.02 km, a value of the angle β of 245° and magnetization in the plane of profile of 0.43 A/m.

The interpretation of profile CC' (Figure 3.7) shows the dyke to be 1.05 km thick and 0.72 km deep. The angle β for this profile is estimated to be 291° and the magnetization in the plane of the profile estimated at 0.59 A/m. Figure 3.8 gives the optimal model produced for the profile EE'. The model indicates a dyke of thickness 1.16 km, depth 0.74 km, a value of the angle β of 286° and magnetization in the plane of the profile of 0.81 A/m. The profile II' is best interpreted in terms of a dyke having a thickness of 1.19 km, depth to the top of 0.77 km, angle β of 280° and magnetization in the vertical plane of 0.80 km A/m (Figure 3.9). The corresponding optimal model for the profile JJ' indicates a dyke 1.14 km wide and 0.74 km deep (Figure 3.10). The angle β is estimated to be 274° and the magnetization in the plane of the profile estimated at 0.70 A/m.

An interpretation of the profile NN' is shown in Figure 3.11 where the dyke is seen to have a thickness of 1.11 km and depth to the top of 0.66 km. The angle β is here estimated to be 263°, and the magnetization estimated at 0.70 A/m in the plane of the profile.

Since it may be possible to model dykes whose parameters deviate from those of the models presented above owing to the problem of

ambiguity inherent in most potential field methods, it is useful
to place some bounds on the models.

In order to place lower and upper bounds on acceptable
models for the different profiles interpreted, a statistical
error analysis was carried out to determine the confidence intervals
for the parameters of the dyke as obtained from the interpretation.
This analysis was done following the procedures outlined in
section 1.3.6 of this thesis. Emphasis was laid on the thickness,
depth to the top and the angle (β) beta of the model dykes. A
95% confidence limit has been used throughout. The usual approach
is to compute the objective function value (Fc) using the
equation 1.18 (Chapter I, Section 1.3.6). A graph of the
objective function values against values of the parameters whose
confidence interval is required is now plotted with all other
parameters assumed to be fixed at their minimum values. The
function value Fc is marked out on the graph by a straight line
intersecting the curve of function values against parameter values.
The intercepts of the line representing the function value Fc on
the graph of function values against parameter values are now
produced to the parameter axis to give the limiting values of the
parameter and consequently the confidence interval assuming a
particular confidence limit (95% in this case).

Graphical representations of this statistical analysis for
the profile AA' are given in Figures 3.12a, 3.12b and 3.12c for
the thickness, depth to the top and the angle beta (β) respect-
ively. A similar set of plots for the profile NN' are given in
Figures 3.13a, 3.13b and 3.13c for the thickness, depth and the
angle beta (β) respectively. The position of the function value
Fc as well as the position of the lower and upper limits on the
values of the parameters are indicated. This analysis for the
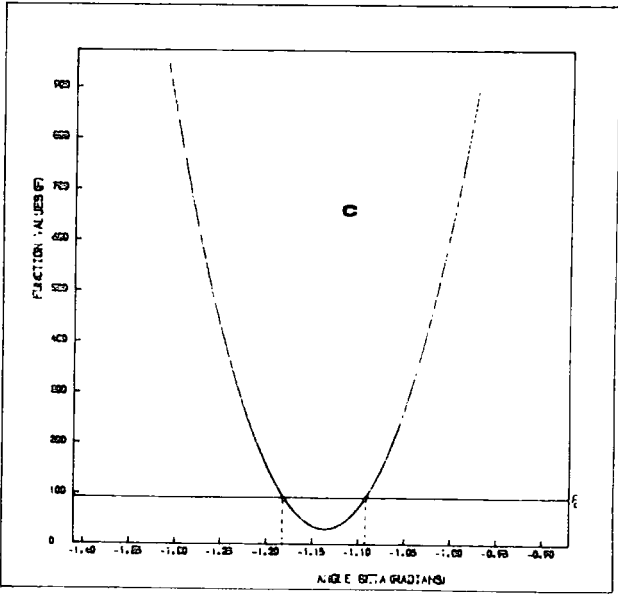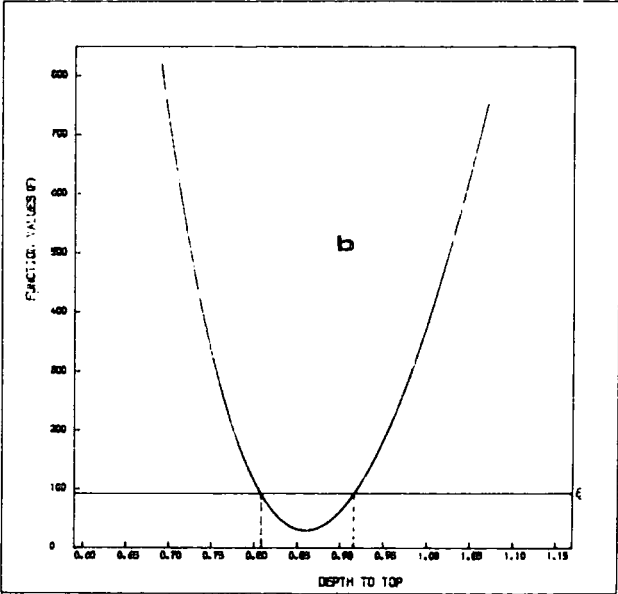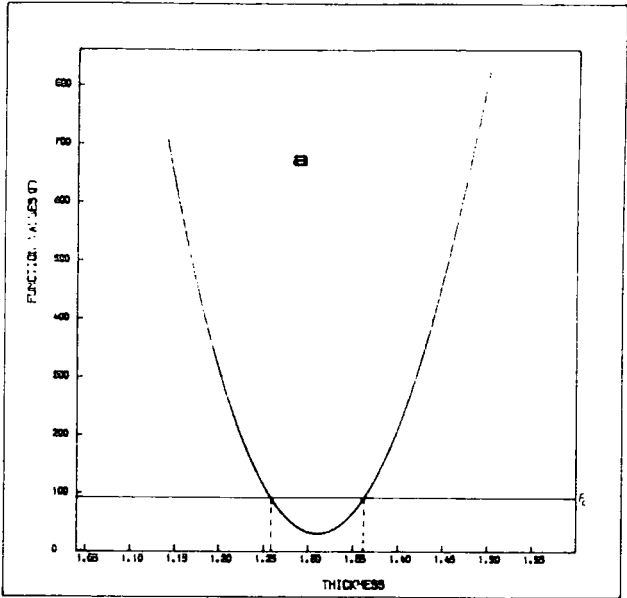
Figure 3.12 Graphical representation of the statistical analysis for theprofile AA'.
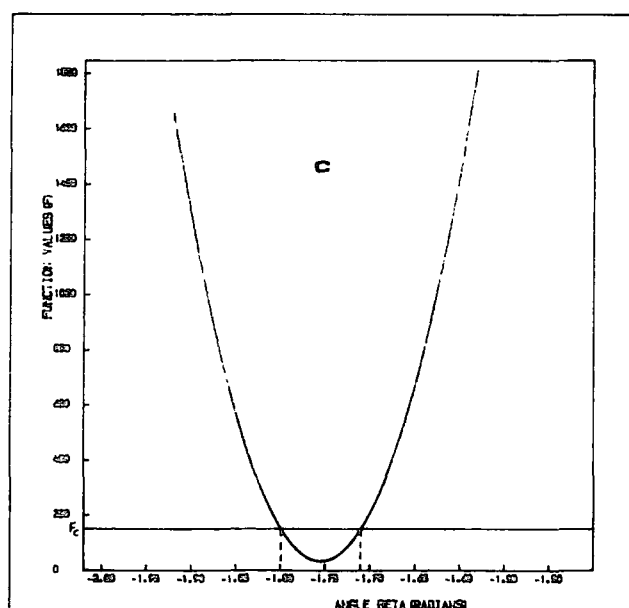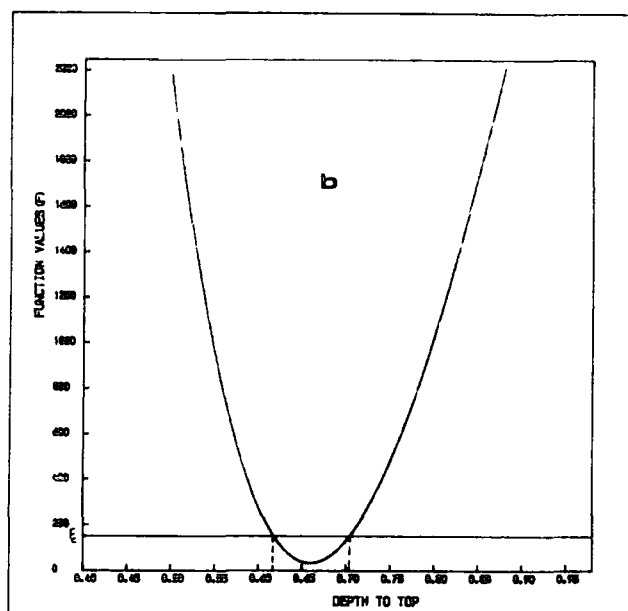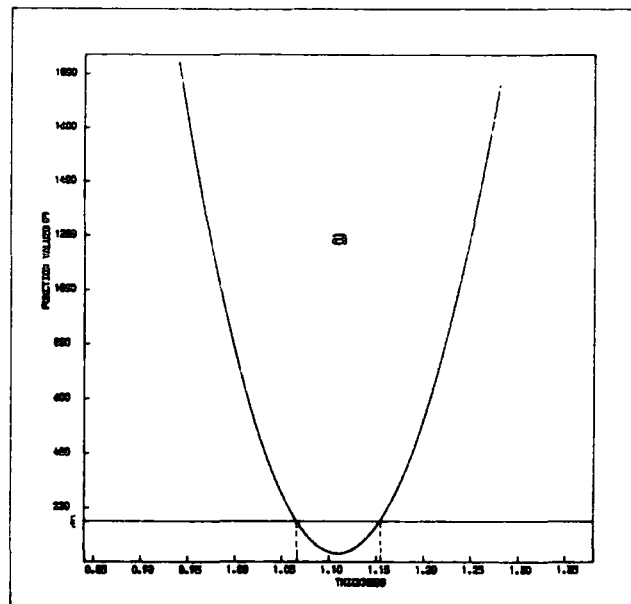
Figure 3.13   Graphical representation of the statistical analysis
              for the profile NN'.

profile AA' is based on the use of twenty (20) field points
and for the profile NN' is based on the use of sixteen (16) field
points. The confidence limit for both profiles and all other
cases was fixed at 95 per cent. The values of the corresponding
F-distribution parameter $F_{n, \, m-n-1}$ (1-x) were obtained using
Standard Statistical Tables (Neave, 1978). The value of the
parameter $F_{n, \, m-n-1}$ for the profile AA' as read from the tables
was 2.95 and for the profile NN', this was 3.73.

Table 3.1 is a table giving the optimal values of thickness,
depth to the top, magnetization values in the vertical plane
containing the profile as well as the values of the angle β of
the model dyke required to fit the different profiles interpreted.
It is evident from this table (Table 3.1) that the postulated
Minch dyke has a variable depth and thickness.

The angle I_e' which is the projection of the Earth's field
direction in the plane of the interpreted profile, is about 90°
(Ninety degrees). If the dyke is assumed to be vertical, then
the projection of the direction of magnetization in the plane of
the profile is given by the estimate of the angle (β) for the
different profiles. These estimates given in Table 3.1 are
approximately indicative of a direction consistent with reverse
magnetization along the present field direction.

TABLE 3.1 SUMMARY OF RESULTS

Profile	Thickness (KM)	Depth to Top (KM)	Angle β $\beta = I_e^1 + I_m^1 - d$	Magnetization A/M
A	1.30 ± 0.05	0.86 ± 0.06	296.68	0.61
B	1.13 ± 0.06	1.05 ± 0.04	245.10	0.43
C	1.05 ± 0.05	0.72 ± 0.03	291.24	0.59
D	1.05 ± 0.05	0.84 ± 0.04	268.40	0.64
E	1.16 ± 0.02	0.74 ± 0.01	285.50	0.81
F	1.05 ± 0.30	2.87 ± 0.41	337.65	0.499
G	1.23 ± 0.10	1.44 ± 0.12	322.18	0.72
H	1.05 ± 0.21	1.76 ± 0.24	290.67	0.70
I	1.19 ± 0.01	0.77 ± 0.08	279.78	0.80
J	1.14 ± 0.08	0.74 ± 0.04	274.05	0.70
K	1.16 ± 0.07	0.80 ± 0.15	264.88	0.60
N	1.11 ± 0.05	0.66 ± 0.42	262.59	0.70
Q	1.14 ± 0.34	1.45 ± 0.21	319.96	0.89
Y	1.20 ± 0.40	1.71 ± 0.53	303.27	0.77

N.B. Error limits shown have been obtained based on the method
discussed in Section 1.3.6 based on 95% confidence
limit.

3.3.3 Effects of Demagnetization

Four profiles across the Minch dyke have been re-interpreted with the effects of demagnetization considered. Evaluation of demagnetization of the Minch dyke was accomplished using methods described in Chapter II of this thesis. In carrying out this analysis, only the upper sections of the model dyke was considered to be giving rise to the anomaly and the upper part of the dyke was accordingly divided into rectangular blocks as required by the methods described in Chapter II. The program DEMAGN was used for this study. The results showed that the postulated Minch dyke was not appreciably demagnetized. The assumption of zero demagnetization effect made in the previous interpretation was therefore a valid one. The profile NN' on re-interpretation with the effect of demagnetization included, gave a thickness of 1.13 km, depth to the top of 0.65 km and an angle β of 267° (Figure 3.14).

3.3.4 Other Geophysical Evidence for the Minch Dyke

Additional evidence for the Minch dyke has been obtained from the results of seismic experiments carried out by the Shell and B.P., and the Institute of Geological Sciences, (I.G.S.) (McQuillin, personal communication). From one of the three seismic profiles on which evidence for the dyke is found, the dyke was interpreted as having a top at the base of the Jurassic and using a velocity of 2.4 km/sec, a depth to the top of 1.11 km has been estimated for the dyke at that point. The corresponding magnetic anomaly profile taken along this line has been interpreted in terms of a model dyke having a depth of 1.44 km (Profile HH'). This is in
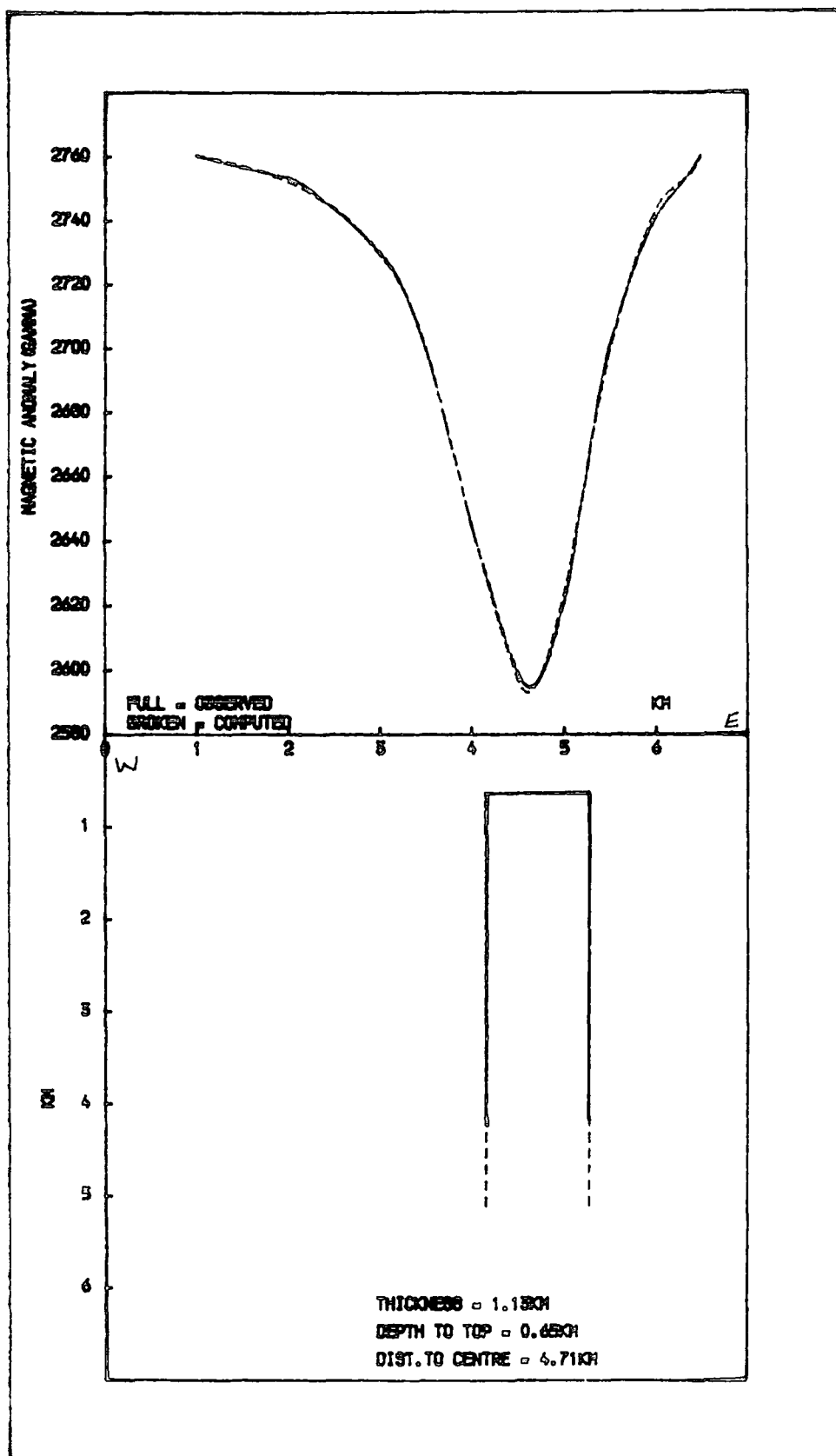
Figure 3.14   An interpretation of the profile NN' with the effects of demagnetization included.

a fairly good agreement with the results obtained from the seismic profile. Minor faulting that may have been associated with the emplacement of the dyke was also evident on the seismic profile.

3.4 <u>Interpretation of Linear Anomaly North of Lewis</u>

To the west of the linear magnetic feature associated with the Minch Dyke, is another linear magnetic feature which terminates close to the northern edge of the Island of Lewis (area A on Figure 3.1). Three profiles (Figure 3.1) across this feature have been interpreted in terms of a reversely magnetized dyke. The model dyke required to explain this anomaly was on the average, found to be thinner and deeper than the Minch Dyke. Figure 3.15 shows the result of an interpretation of the profile 1. The model dyke required to explain the anomaly here is of thickness 0.84 km, depth 1.01 km and the angle β has a value of 280°. The profile 2 on the other hand is best explained in terms of a dyke of thickness 0.70 km, depth 1.17 km and having an angle β of 260° (Figure 3.16). The optimal body required to account for the profile 3 has a thickness of 0.76 km, depth to the top of 0.81 km and the angle β of 290° (Figure 3.17).

3.5 <u>Discussion</u>

The conclusions drawn from this study of the Minch Dyke are that the linear magnetic anomaly which intersects the Minch Basin is related to a wide dyke of dimensions uncommon for dykes found in the British Isles. The dyke has a variable depth and thickness along its length and is reversely magnetized in a direction consistent with a Tertiary origin. It is observed that the values for the angle β obtained for the dyke north of Lewis (section 3.4) is close to those
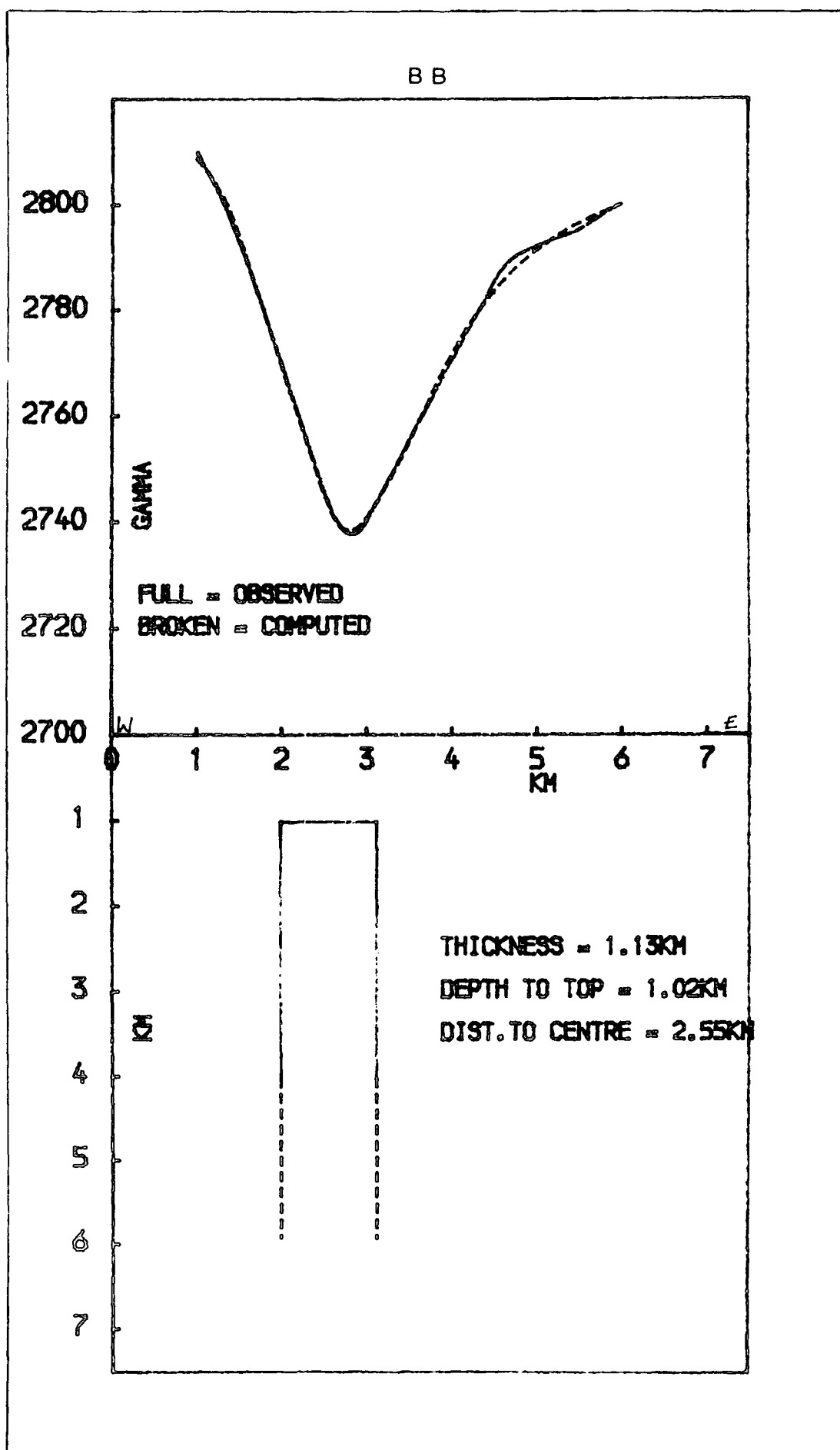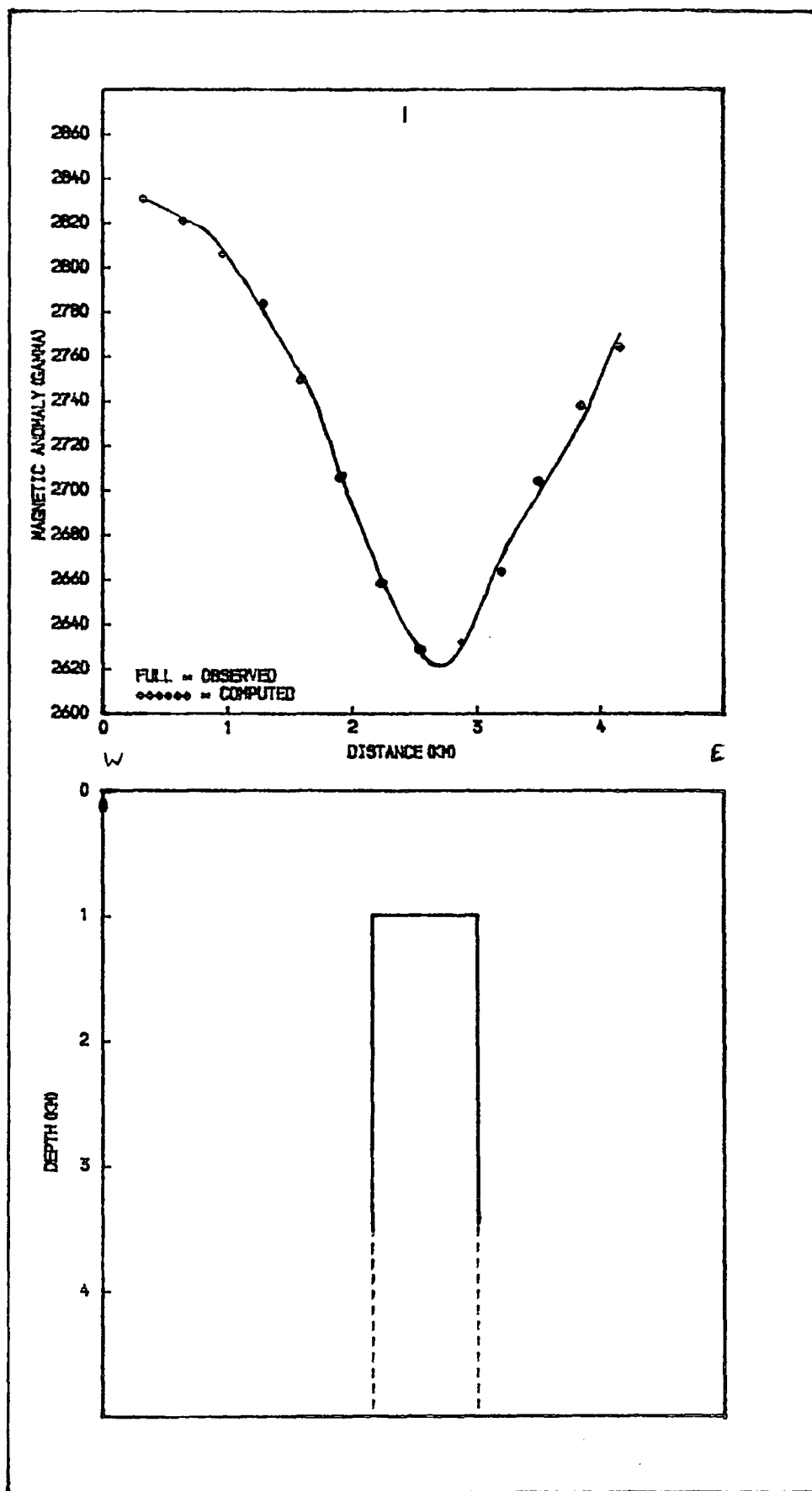
Figure 3.15 Optimal dyke model needed to explain the profile 1.
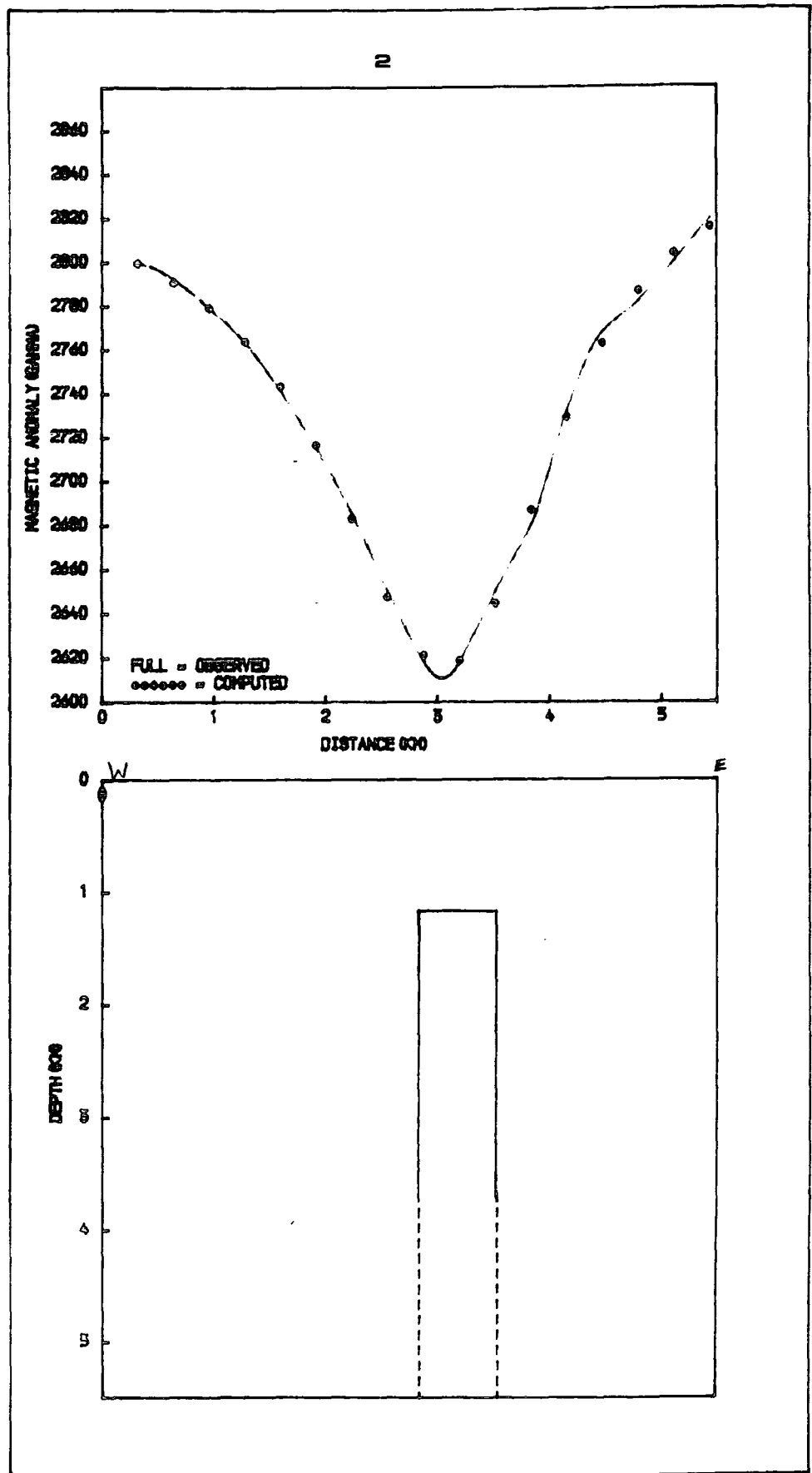
Figure 3.16 Optimal dyke model needed to account for the profile 2.
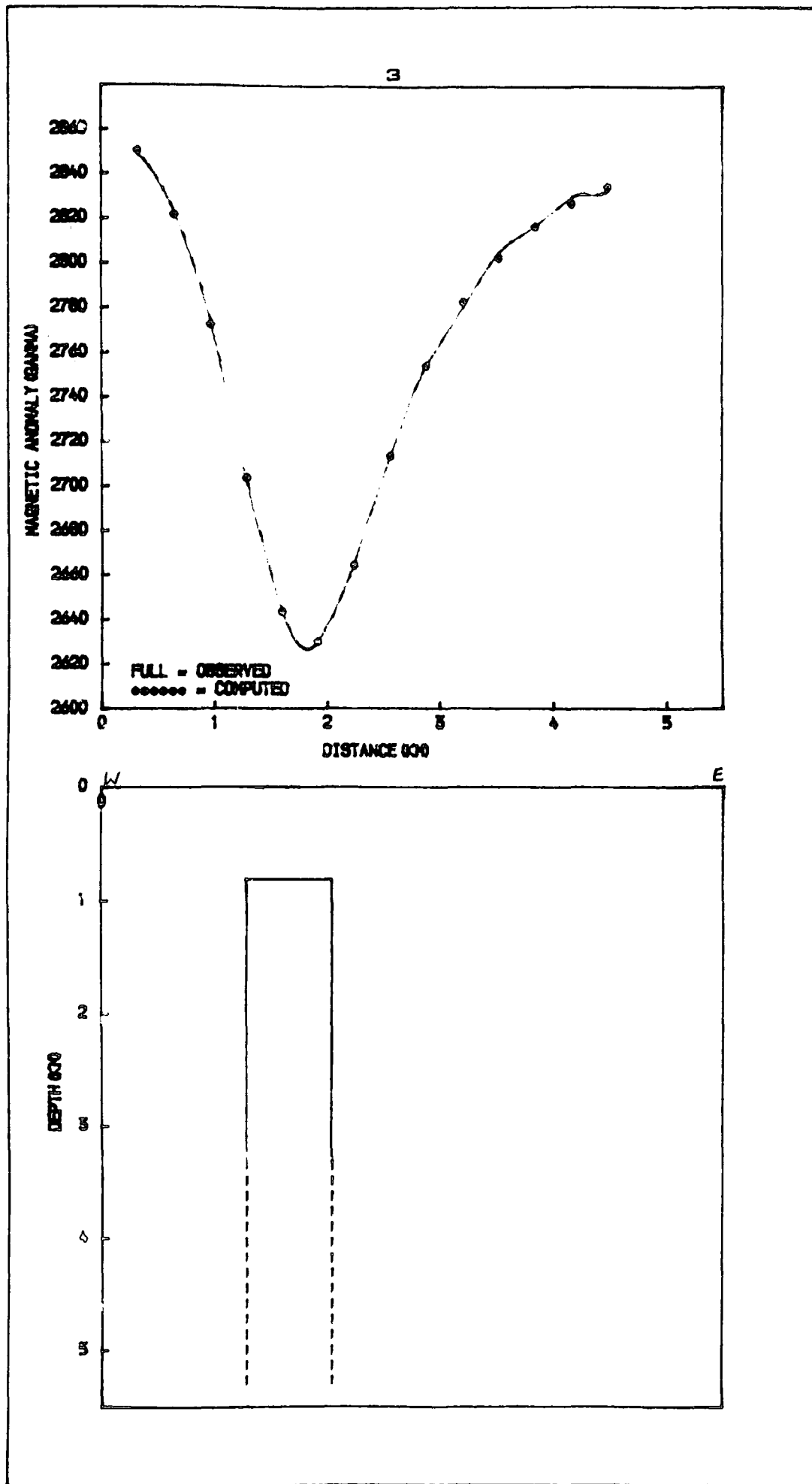
Figure 3.17 Optimal dyke model needed to account for the profile 3.

obtained for the Minch dyke (section 3.3.2). This suggests that both dykes may have been emplaced at the same time, probably in the Tertiary. Unusually wide dykes like the Minch Dyke and the dyke west of the Minch Dyke must be of some tectonic significance.

CHAPTER IV

THE GEOLOGY OF THE BENUE TROUGH REGION

4.1 Introduction

The Benue Trough is an elongated trough of subsidence. It
forms an important part of a system of linear sedimentary basins
which includes the Niger, Benue and Gongola Rivers. The Benue
Trough has a width of 130-150 km and trends north-easterly to
attain an approximate length of 800 km. The trough is filled
with Cretaceous rocks whose ages range from middle Albian to
Maestrichtian. It is bordered on either side by the granites and
gneisses of probable Proterozoic age which make up the crystalline
basement.

The stratigraphic and structural conditions are more or less
continuous from the south-west or Lower Benue, through the Middle
Benue to the north-east or Upper Benue and this is shown by the
continuity of palaeontological zonation within the marine form-
ations, the series of long narrow folds with ENE-WSW axes which
characterise the Cretaceous rocks from Abakaliki in the south-
west to Gombe in the north-east, and the narrow zone of lead-zinc
mineralization with associated intrusions which runs from
Abakaliki to Zurak (Figure 4.1) (Cratchley and Jones, 1965).
Special emphasis has been placed on the Middle and Lower Benue
area in the present work.

4.2 Basement Geology of the Benue Trough

In Nigeria over 90% of exposed rocks belong to the Basement
Complex which is believed to be mostly Precambrian (Oyawoye, 1972).
The Basement Complex over the Lower and Middle Benue
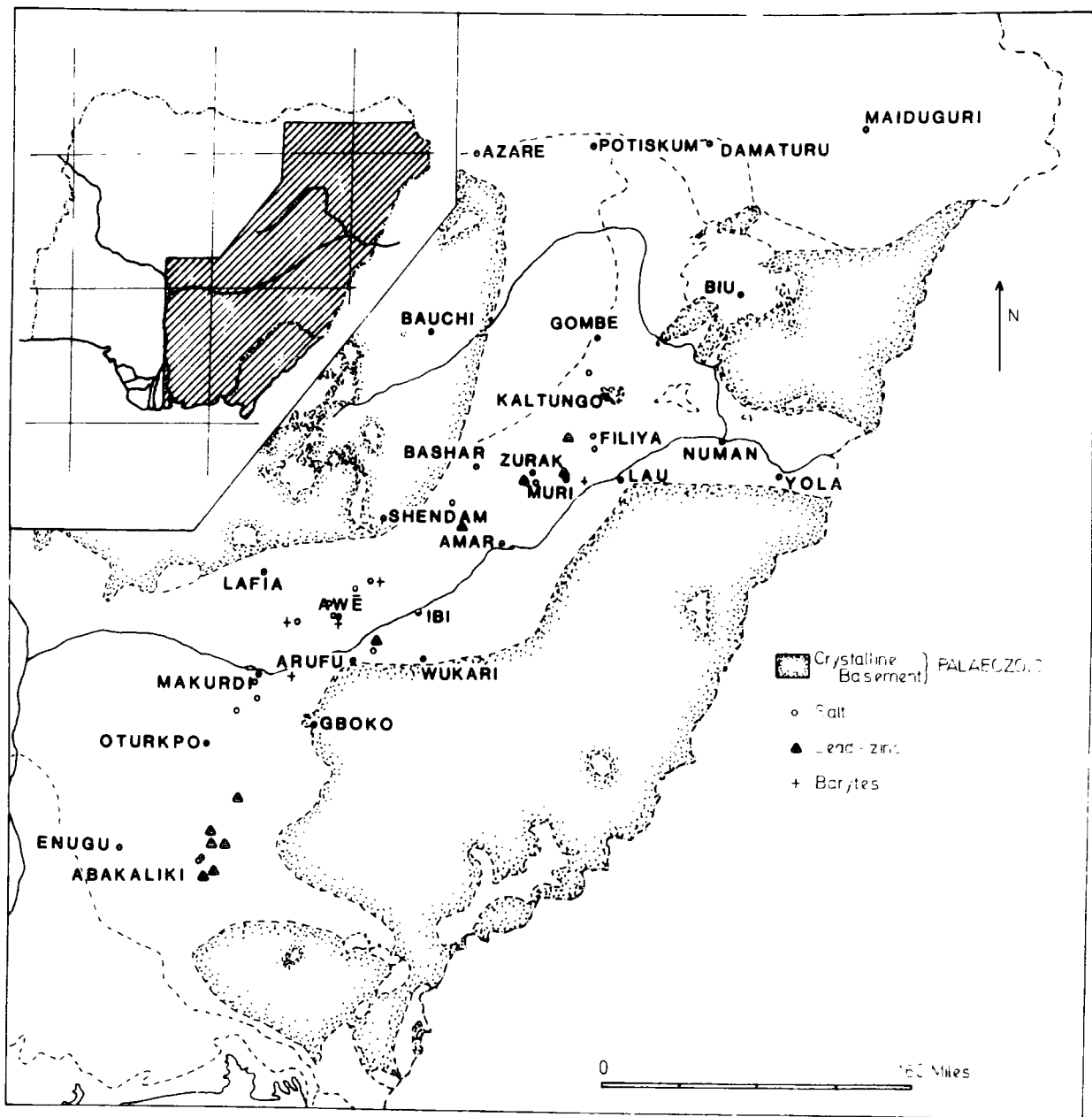
FIG· 4 -1   THE BENUE TROUGH AND ITS LEAD-ZINC FIELD.(AFTER CRATCHLEY AND JONES 1965)

consist mainly of quartzo-feldspathic migmatites and gneisses, with occasional quartzites, marbles and amphibolites. There are numerous Older Granite intrusions that range in composition from granite to granodiorite, quite a number of dioritic intrusions and a smaller number of gabbros and syenites.

The crystalline basement rocks over most of the Lower and Middle Benue area belong to two fairly well defined series. The first group is a less metamorphosed series, made up mainly of quartzites, schists and gneisses succession and this is probably of sedimentary origin (Falconer, 1911). The second group is a more highly metamorphosed series of banded and contorted gneisses which can be distinguished by the smooth and compact character of their exposed surfaces. The more highly metamorphosed gneisses which make up this second group are irregularly distributed throughout the micaceous and feldspathic gneisses of the first group (Falconer, 1911). Nowhere has the actual contact of the two groups been clearly exposed and its character is therefore subject to speculation (Oyawoye, 1972; Falconer, 1911).

In the Lower and Middle Benue areas, the crystalline basement, whose topography is believed to be irregular (Effeotor, 1974; Cratchley and Jones, 1965; Ayoola, 1978), is exposed in a number of places. It comes quite close to the surface at a few other places. Notable outcrops are the small inliers of biotite granite and gneisses that are found around the town of Arufu. Between Wukari and Ugba there are also numerous outcrops of the basement.

The crystalline basement over the Lower and Middle Benue, as in most other parts of Nigeria, contains many major and minor intrusives (Oyawoye, 1972; Carter et al., 1963; Cratchley and Jones, 1965; Reyment, 1965, McCurry, 1976). Many of the thin

bands of well foliated augen gneiss and granitoid gneiss enclosed within the metamorphic series are original granitic intrusions which are intimately associated with the adjoining gneisses and schists, making discrimination difficult. These can be separated into the younger and older intrusives. The older intrusives are largely granites while the younger intrusives include granitic, basic and diabasic types with numerous associated dyke-like bodies (Oyawoye, 1972; Falconer, 1911; McCurry, 1976; Wright, 1976).

The Older Granites, as the older intrusives are called (Falconer, 1911), represent a cycle of granite evolution in which all states of granitization and magmatic activity are displayed (Carter et al., 1963). These can hardly be distinguished from the metamorphic series and show a similar foliation. They may have been intruded at different times during the evolution of the gneisses and the amount of re-crystallisation varies depending on age (Carter et al., 1963; Falconer, 1911; Oyawoye, 1972). Vesicular micro-pegmatites found in the thoroughly foliated and reconstructed granites within banded and striated gneisses indicates the effects of minor crustal strains on these intrusives (Falconer, 1911). Falconer (1911) has described three easily distinguishable types of Older Granites based on their mode of emplacement and relationship with the crystalline gneisses that form the basement complex. These are the most altered types, the least altered types and the intermediate types.

The younger intrusives within the Basement Complex are mainly granitic and pegmatitic, although diorites, dolerites and some

syenites also occur. In addition to these are numerous associated

dyke-like bodies, which attain considerable size and may coalesce

to form massive bodies. Many younger intrusives of intermediate

to basic character have been reported to the south-west and to the

east of Gboko (Cratchley and Jones, 1965). The same authors have

interpreted a positive gravity anomaly over Gboko in terms of a

massive intrusive complex 30 km in diameter and about 5 km thick

which they believe is probably syenite because of its inferred maximum

density of 2.77 g cm^{-3}.
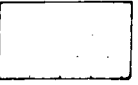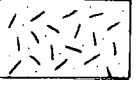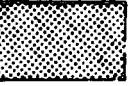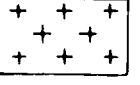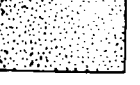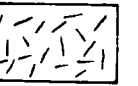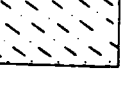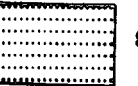
The pegmatite dykes are usually composed of microcline and

quartz and may be found in the vicinity of Older Granites (Oyawoye,

1972). They hardly exceed a few metres in thickness but may locally

be numerous, coalescing to form single massive bodies (Oyawoye, 1972).

The dolerite dykes rarely exceed a metre in width although they

may locally unite to form rather larger bodies (Oyawoye, 1972). They

usually exhibit forceful intrusive characteristics, by a

shattering of the host rock and the inclusion of numerous fragments

of various sizes as xenoliths. In summary, the basement of the

Middle and Lower Benue area is invaded by numerous intrusive bodies

whose sizes range from massive granitic bodies to thin dyke-like

bodies that may unite to form massive structures. The exact ages of

these intrusives are not known.

4.3 Cretaceous Stratigraphy of the Middle and Lower Benue Trough

Figure 4.2 is a map of the geology of the Benue Trough region of

Nigeria. The stratigraphic correlations for the Lower (south-west),

Middle, and Upper (north-east) Benue is given in Table 4.1 as

KEY TO FIGURE 4.2

Alluvium

Basalts,trachyte,rhyolite

Older basalts
(Jos Plateau)

Falsebedded sandstones
coal and shale

Shale and limestone

Clays and shale
with limestone

Coal,Sandstone and shale

Sandstone
shale and sandy shale

Sand,clays and shale

Undifferentiated
basement complex

Felspathic sandstone

Felspathic sandstone
and siltstone

Black shale and siltstone

Shale and limestone

Felspathic sandstone,
sandy clays,
calcareous sandstone
and shelly limestone

Older granites

Sands and clays

Granite(younger)

Grits,sand and clay

Shale and limestone

Bende -Ameki group

Shale and mudstone

Figure 4·2   Geology of the Benue Trough Region (AFTER GSN)

TABLE 4.1

STRATIGRAPHICAL CORRELATION (After Cratchley & Jones, 1965)

GEOLOGICAL STAGES		SOUTH-WEST	MIDDLE BENUE		NORTH-EAST	
		OTURKPO-MAKURDI	KEANA-AWE-ARUFU	BASHAR-MURI-AMAR	GOMBE	LAU
MAESTRICHTIAN		Upper Coal Measures	'Lafia Sandstone'	Gombe Sandstone	Gombe Sandstone	Lamja Sandstone
MAESTRICHTIAN		Falsebedded Sandstone	'Lafia Sandstone'	Gombe Sandstone	Gombe Sandstone	Lamja Sandstone
MAESTRICHTIAN		Lower Coal Measures	'Lafia Sandstone'			
SENONIAN	CAMPANIAN	Enugu-Nkporo Shales				Numanha Shale
SENONIAN	SANTONIAN		marine deposits	Kumberi Formation	Pindiga Formation	Sekule Formation
SENONIAN	CONIACIAN	Awgu-Ndeaboh Shales	marine deposits	Kumberi Formation	Pindiga Formation	Sekule Formation
TURONIAN	UPPER	Eze-Aku Shales	marine deposits	Kumberi Formation	Pindiga Formation	Jessu Formation
TURONIAN	LOWER	Eze-Aku Shales	marine deposits	Kumberi Formation	Pindiga Formation	Dukul Formation
CENOMANIAN		Makurdi Sandstone	transition deposits	'Passage beds'	Yolde Formation	Yolde Formation
CENOMANIAN		Makurdi Sandstone / Eze-Aku Shales	'Keana Sandstone'	Muri Sandstone	Bima Sandstone	Bima Sandstone
ALBIAN		Asu River Group	Asu River Group	marine deposits	marine deposits	marine and transition deposits
PALAEOZOIC and PRE-CAMBRIAN		Crystalline Basement	Crystalline Basement	Crystalline Basement	Crystalline Basement	Crystalline Basement

Note: Since this paper went to press Reyment (1965) has proposed certain changes in the formational names used here.

presented by Cratchley and Jones (1965). The present account only briefly covers the Upper Benue as there exists a considerable amount of published information on the area. However, to facilitate comparison with the Lower and Middle Benue areas, a geological sketch map of the area and geological sections across the region (Figure 4.3) are given.

4.3.1 The Middle Benue Trough

As there has been little systematic or detailed mapping of the Middle Benue area, it has remained perhaps the area for which the geology is least well known in Nigeria. Much of what is presented here is based mainly on the few published tentative correlations of the lithological sequences for the upper parts of the Middle Benue (Cratchley and Jones, 1965; Falconer, 1911; Offodile, 1976; Offodile and Reyment, 1978; Ayoola, 1978), and personal discussions with geologists working in the area (Wright, Cratchley, Jones, Muoto, Okoro, Ezepue and others).

Sedimentation in the Middle Benue area started in the Albian with the deposition of the Asu River Group whose age ranges from Middle Albian to Late Albian (Reyment, 1965; Offodile and Reyment, 1978). The Asu River Group, whose type section has been described for outcrops in the Asu River near Abakaliki in Anambra State (Offodile and Reyment, 1978), consists of dark shales, siltstones, fine grained sandstones and limestones which grade upwards into shales and limestones of Upper Albian age (Cratchley and Jones, 1965; Offodile, 1976). Typical exposures of this formation have been reported to the east of Keana and near Arufu where it overlaps the older sediments to rest unconformably on the crystalline basement rocks (Cratchley and Jones, 1965; Offodile, 1976; Offodile and
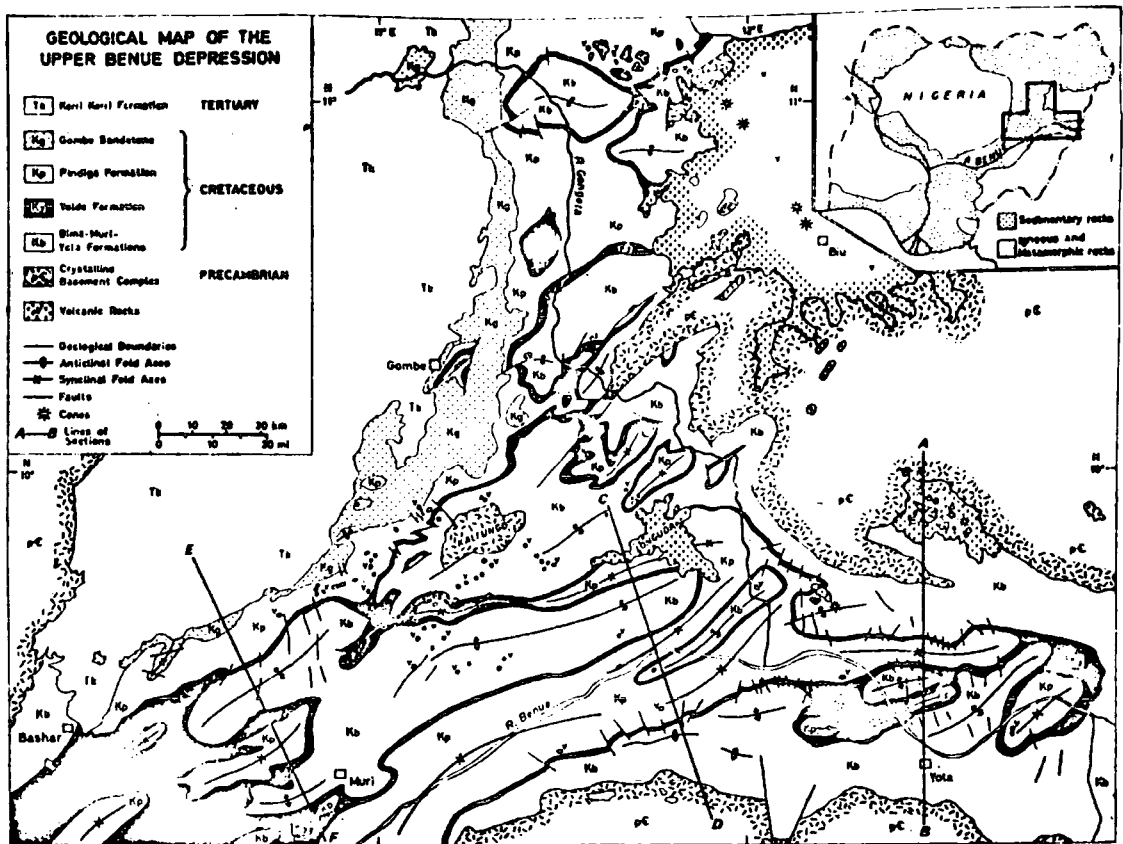
Figure 4.3a *Geological map of the Upper Benue Depression. Based on Geological Survey of Nigeria data and new data, University of Ibadan Benue Valley Project.*

(Burke et al.,1972)
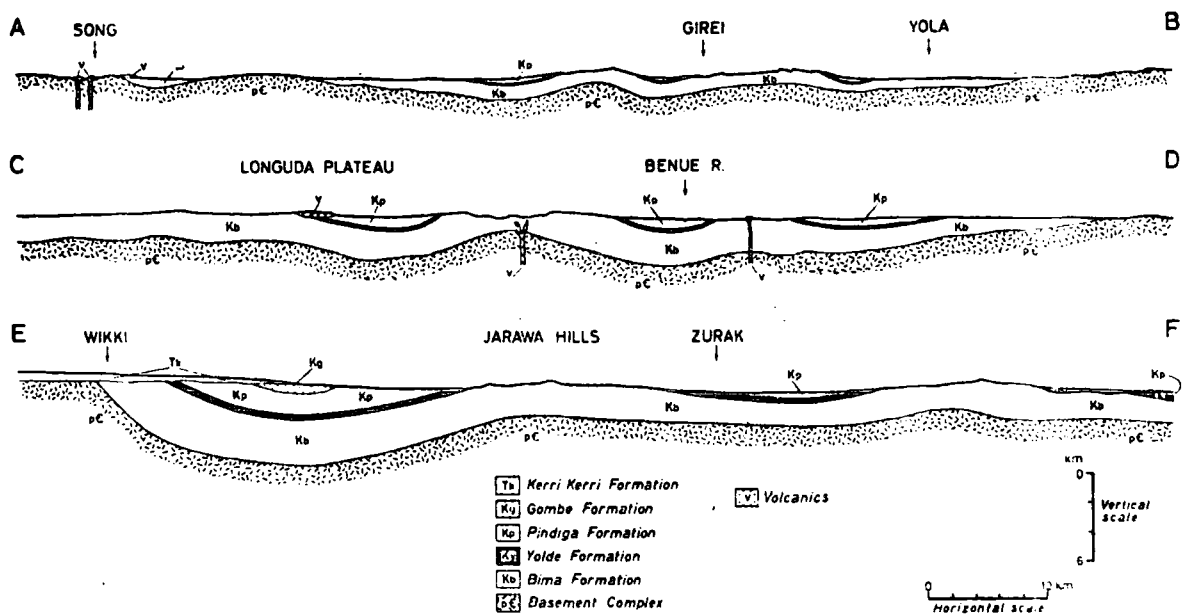
Figure 4.3b *Three geological cross sections of Upper Benue Depression. See fig. 8 for locations.*

(Burke et al.,1972)

Reyment, 1978). The exact thickness of this Asu River Group is not yet known or reported but it may attain an approximate thickness of 1500 m.

The Keana Sandstone is made up of poorly sorted feldspathic coarse grained gritty, commonly arkosic pebbly sandstones that sometimes contain pebbly conglomerates (Cratchley and Jones, 1965; Offodile and Reyment, 1978). The thickness of the Keana Formation has been estimated at 800 m around the Keana-Awe area. There has so far been no evidence reported for an unconformity between the Keana Formation and the underlying Asu River Group in the Middle Benue area, although such an unconformity was suggested by Cratchley and Jones (1965).

In the Keana-Awe area, the overlying "Passage Beds" or "Awe Formation" consist of flaggy, whitish coarse to medium grained sandstones, interbedded with carbonaceous shales, clays and sandy limestones (Cratchley and Jones, 1965; Offodile 1976; Offodile and Reyment, 1978; Ayoola, 1978). The lower part is associated with brine springs which are seen to issue near Awe (Offodile and Reyment, 1978). The exact position of this formation in the stratigraphic table is not generally agreed Offodile and Reyment (1978) reported that near the town of Awe, the inferred passage beds can be seen to lie between the older Asu River Group and the younger Keana Sandstone Formation. The thickness of these "Passage Beds" or "Awe Formation", which can be traced over large areas of the Benue Trough, has been put at about 1000 m (Offodile and Reyment, 1978).

Overlying the "Passage Beds" are unnamed marine deposits of Lower Turonian age which only rarely outcrop (Cratchley and Jones, 1965; Offodile, 1976). They consist mainly of shales, clays, siltstones and shelly limestones which are known to be mixed with

volcanic material to the south and south-west of Awe (Cratchley and Jones, 1965).

The Lafia Formation is the youngest reported formation in the Middle Benue and consists of coarse grained ferruginous sandstones, red, loose sands, flaggy mudstones and clays (Cratchley and Jones, 1965; Reyment, 1965; Offodile, 1976; Offodile and Reyment, 1978). The type locality is in and around the town of Lafia. Its thickness is estimated to be around 500-1500 m by Esso West Africa Inc. (Offodile and Reyment, 1978), though a wedge of this formation in the Lafia-Awe area hardly exceeds 50 m according to Offodile and Reyment (1978).

In addition to the major units generally known to exist within the Middle Benue are two other stratigraphic units that have been mapped by Offodile and Reyment (1978) in the Keana-Awe area. The Ezeaku Formation, whose thickness they estimated at around 95 m is composed mainly of shales. The Awgu Formation, whose thickness they estimated at 290 m, is composed of black shales, sandstones, seams of coal and subordinate limestones of Conacian age. These formations seem to have been recognised only in the Keana-Awe area.

4.3.2 The Lower Benue Trough

Sedimentation in the Lower Benue area began in the Albian times with the deposition of the Asu River Group which is inter-fingered by Aptian mafic volcanics (Uzuakpunwa, 1974). The Asu River Group consists of shales and siltstones and has an estimated thickness of about 2000 m in the Lower Benue (Adighije, 1981a).

Next to be deposited in the Lower Benue was the Ezeaku Shales/ Makurdi Sandstones/Ajali Sandstones sequence whose exact

relationship to the Asu River Group is not well known although they are generally regarded to be unconformable. The Ezeaku Shales consists of about 1000 m of calcareous, flaggy shales and siltstones, thin sandy and shelly limestone and calcareous sandstones. The equivalent of this in the Makurdi-Oturkpo area is the Makurdi Sandstones formation which consists of a thick mass of current-bedded, coarse-grained sandstone which, in places attain a thickness of about 900 m and is the lateral equivalent of the Keana Sandstone of the Middle Benue area (Cratchley and Jones, 1965; Offodile 1976; Reyment, 1965). The Ezeaku/Makurdi Formation has been assigned a Turonian age (Cratchley and Jones, 1965; Offodile, 1976; Adighije, 1981a).

Overlying the Ezeaku/Makurdi Formation is the Awgu Formation which consists of marine fossiliferous, grey bluish shales, lime-stones and calcareous sandstone whose age is probably Cenonian (Offodile, 1976). The Campanian sediment group which overlies the Awgu Formation is known as the Nkporo Shales. In the south these are marine shales (Offodile, 1976) but towards the south west, they pass into the arenaceous Otobi Sandstones.

The Nkporo Shales unit is unconformably overlain by dominant sandstone, carbonaceous shales, sandy shales and local coal seams which, together form the Mamu Formation or Lower Coal Measures (Cratchley and Jones, 1965; Offodile, 1976). The Mamu Formation has a thickness of about 400 m and is overlain by the 330 m of coarse-grained characteristically current-bedded sandstones, which make up the Ajali Formation (Offodile, 1976), or "False-Bedded Sandstones" (Cratchley and Jones, 1965).

Above the Ajali Formation, a thin coating of what has been

widely accepted as the latest sediments in the Lower Benue area was deposited. This is the Nsukka Formation, or the Upper Coal Measures, and consists of carbonaceous shales, sandstones and seams of coal; it has been assigned a Paleocene age (Cratchley and Jones, 1965).

4.4 Palaeogeography of the Benue Trough

The Pre-Cretaceous Benue Trough region, like the rest of Nigeria, consisted of a continental land mass composed of Precambrian crystalline basement on which Cretaceous sediments were unconformably laid down. Subsequently, the Benue Trough was subject to four main depositional cycles marked by the transgression and regression of the sea.

The first sedimentary cycle of the Benue Trough lasted from the Middle-Albian to the Cenomanian. These sediments were not deposited elsewhere in Nigeria except in parts of the south eastern Nigeria (Kogbe, 1976). This cycle began with a Middle-Albian marine transgression marked by the deposition in moderately deep marine environments of the Asu River Group and the Abakaliki Shales of the Lower and Middle Benue.

The end of the Albian period marked the start of the first regressive phase in the Benue Trough. This continued until about the end of the Cenomanian and was marked by extensive deltaic development (Murrat, 1972; Kogbe, 1976; Cratchley and Jones, 1965). This regressive phase was marked by the deposition of the Bima Sandstone in the Upper Benue, (Carter et al., 1963) and the Keana Sandstone in the Lower and Middle Benue (Falconer, 1911; Kogbe, 1976; Murrat, 1972).

The second sedimentary cycle began with a marine transgressive phase at the beginning of the Turonian. Associated with this transgression was the continued deposition of the Upper Limestones of the Calabar Flank (Murrat, 1972; Reyment, 1972; Falconer, 1911). The Ezeaku Shales were deposited within the nearby Abakaliki Trough during this transgression. The subsequent Lower Turonian regression led to deltaic deposition within the Benue Trough, represented by the Makurdi Sandstone formation (Murrat, 1972).

The third sedimentary cycle occurred from the Upper Turonian to the Lower Santonian. Most of the deposits of this cycle have been eroded as a result of the late Cretaceous tectonic activity and much of what is known of this cycle is based on palaeontological evidence which shows that the transgression reached as far as the Gongola Basin. The onset of folding and uplift involving the Abakaliki anticlinorium set the stage for the regressive stage that lasted well into Lower Santonian times (Ayoola, 1978) and was accompanied by volcanic activity in the Upper Benue (Carter et al., 1963).

The Lower Santonian uplift and folding which marked the end of the third sedimentary cycle was followed by a brief marine transgressive period in the Campanian. The Campanian transgression was marked by the deposition of the Nkporo Shales and Enugu Shales (Kogbe, 1976; Ayoola, 1978). The accompanying regression gave rise to the growth of deltaic conditions associated with the deposition of the Gombe Sandstones in the Upper Benue and the Mamu Formation and continental sequence of Ajali Sandstones in the Lower and parts of the Middle Benue in Maestrichtian times.

4.5 Structural Geology of the Benue Trough

The Benue Trough was subject to several folding episodes,
notably in the Cenomanian, Santonian, Post Maestrichtian and
Palaeocene. Numerous faults have also been reported within the
trough (Ajayi and Ajakaiye, 1981; Chukwu-Ike, 1977) and the
Cretaceous/crystalline basement contact which form the edges of
the trough is also thought to be faulted. Major anticlinal axes
and major faults found within the trough are shown in Figure 4.4.
Two geological sections across the trough showing the nature of
the edges of the trough and suspected faulting are also shown in
Figure 4.4 .

4.5.1 Cenomanian Folding Episode

Nwachukwu (1972) working in the southern portion of the Benue
Trough has provided evidence to suggest the existence of a folding
phase which may have taken place during the Cenomanian regression.
There seems to be evidence to support the claim of Nwachukwu (1972)
for the existence of a Cenomanian deformation, but whether or not
this affected parts of the Benue Trough other than the lowermost
portions.of the trough and to what scale, is not known.

4.5.2 Santonian Folding Episode

Of all the earth movements in the Benue Trough region, the
Santonian folding episode was the most severe (Burke et al., 1972;
Wright, 1976). The fold axes of the Santonian folding episode
have given the Benue Trough its unique character. This folding
took place as part of the major folding episode in the African
Continent since Palaeozoic times (Burke et al., 1972). Dips of
the Santonian folds hardly exceed 30° although dips in excess of
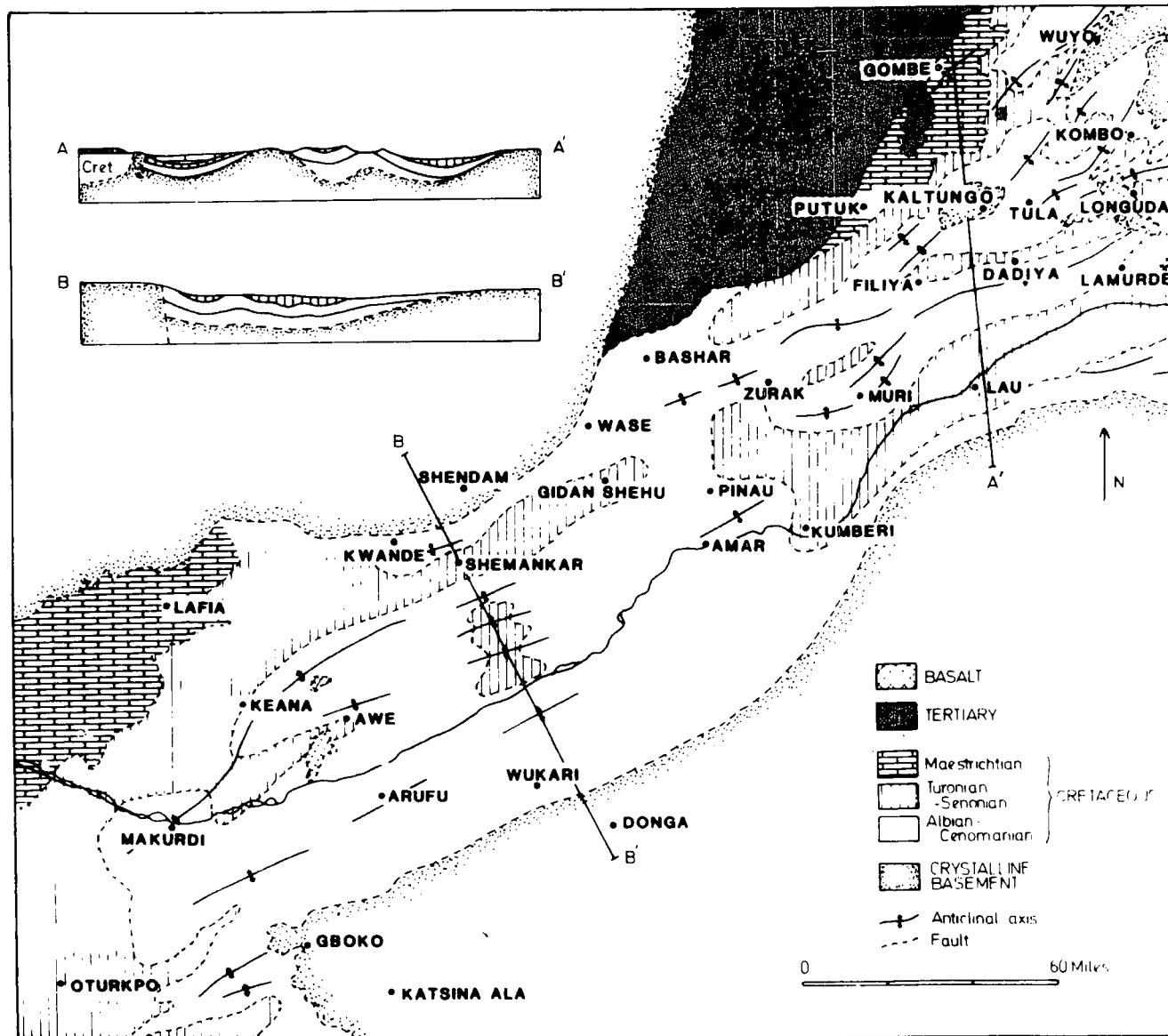
FIG·4 - 4 GEOLOGY OF THE BENUE VALLEY.(AFTER CRATCHLEY AND JONES 1965)

this have been locally reported in the Benue Trough. The number of
these folds, however, is large and some of them are over 60 km
long (Burke et al., 1972). Most of these folds have strike
directions along the trough and they are usually asymmetric.

An important measure of the scale of the Santonian folding
is the 2000 m of sediments removed from the Abakaliki anti-
clinorium. This was the largest structure produced by the
Santonian folding episode in the Lower and Middle Benue before
the deposition of Senonian sediments (Burke et al., 1972). During
and after this folding episode the margins of the Benue Trough were
uplifted and eroded with sandstones and coarse clastics spreading
throughout the trough (Burke et al., 1972). These include the
Gombe Sandstones and the Coal Measures of Enugu.

4.5.3 Post-Maestrichtian Folding Episode

This affected all the sediments in the Benue Trough but was
less intense than the Santonian folding discussed above. The
Upper Benue was not seriously affected by the Post-Maestrichtian
folding episode, its sediments being uniformly and only gently
folded. In the Lower Benue, and parts of the Middle Benue, however,
the Santonian and Older sediments are believed to have been folded
twice and so are more strongly deformed than the overlying younger
sediments (Wright, 1976). The older and younger sediments are
separated by a well marked erosional unconformity (Burke et al.,
1972; Wright, 1976).

4.5.4 Palaeocene Folding Episode

This gave rise to "Molasse" accumulations such as the Kerri-
Kerri Formation in the northern parts of the Benue Trough (Carter

et al., 1963; Wright, 1976).

Only very little information is available on the distribution of anticlines and synclines in the Benue Trough in general and the Lower and Middle Benue in particular. A major character of the folds in the Benue Trough is their somewhat consistent trend. In the Lower Benue, folding took place mainly along ENE-WSW axes particularly in the Abakaliki area. Folds have been reported in the Konshisha River area south-east of Oturkpo; these are small and closely spaced. Two anticlines have been reported to run, ENE on to the crystalline basement at Gboko suggesting that the structures may have a core of older rocks (Cratchley and Jones, 1965). Two other anticlines with axes having a NE-SW trend run through the towns of Wannune and Makurdi and have shallow dips that rarely exceed 10°. The folds in Abakaliki area have dips of $30-60^{\circ}$ (Nwachukwu, 1972). Severe faulting has not been reported in the Lower Benue.

In the Middle Benue, fold axes are reported to be in directions consistent with the Lower Benue. A large anticline trending about 64 Km in a northeast direction has been mapped from the east of the town of Keana (Cratchley and Jones, 1965), which the authors have correlated with another anticline in the Shemakar Valley sequence. In the Amar and Muri districts, anticlinal structures have been reported mainly in the resistant sandstones with axes trending ENE to NE (Cratchley and Jones, 1965). Faulting is more severe in the Middle Benue than in the Lower Benue, so that major E-W faulting may account for the complicated nature of the Muri and Ligri folds (Cratchley and Jones, 1965). The exact relationship between faulting and folding in the Benue Trough is not well known.

4.6 <u>Igneous Intrusion and Volcanic Activity in the Middle and
Lower Benue Trough</u>

Igneous rocks in the Benue Trough range from Cretaceous to
Tertiary in age. The extensive igneous activity which took
place in the Lower Cretaceous of Nigeria was concentrated within
the Benue Trough. This igneous phase was apparently most intense
during the late Albian times and it had ceased by the end of
the Turonian. Subsequent to this was the extensive volcanic
activity which has extended from Cretaceous to Recent times. The
younger of these volcanic ⌐ocks are of Miocene - Quaternary
age, and they are mainly basaltic. Some Younger Granites may
be buried beneath the Cretaceous sediments.

<u>Intrusive rocks</u> within the trough extend from Ishiagu in the
Lower Benue to Zurak in the Upper Benue, a distance of over 500
km. The number and extent of these occurrences increases from
Zurak towards the south-eastern part of the zone. Many igneous
rock types occur within this central zone of intrusives, but they
are predominantly basic to intermediate in composition (Farrington,
1952; Cratchley and Jones, 1965). Some of the complexes such as
the Aghilla Hill complex, exhibit a concentric arrangement of
igneous types, becoming more basic from the centre outwards with
types ranging from syenites to gabbros. The dolerites are
usually intruded into folded sediments which suggests that the
sedimentation, folding and intrusion are not widely separated in
time (Cratchley and Jones, 1965; Farrington, 1952; Falconer,
1911).

There is also marked association of the intrusions with
structure. The intrusions favour the well developed and steeper
anticlines (Farrington, 1952; Nwachukwu, 1972; Wright, 1976). They
were typically quietly emplaced, although, as Farrington (1952)

pointed out, local phases may have been violently emplaced.
Most of these intrusions take the form of sills, dykes, plugs or
bosses of up to a few kilometres in diameter (Wright, 1976).
The sills are mostly dolerite and follow the ENE trends of the
folds while the dykes have north-easterly trends. Trachyte
sills exhibiting flow structures have been observed, especially
in the Aghilla area (Farrington, 1952).

Although igneous bodies have not been recorded in some
sections of the trough, Farrington (1952) pointed out that
close examination of any area shows evidence of some igneous
bodies that do not outcrop. Many sizeable bodies may yet be
unmapped. One such body is thought to exist to the south-west
of Gboko. Some of these, especially the larger basic masses,
produce contact metamorphism in the sediments (Cratchley and Jones,
1965).

Extrusive volcanic activity has been widespread in
Cretaceous to recent times in the Benue Trough. The lavas
grade in time from acid to intermediate. Farrington, (1952),
whose description of the igneous and volcanic activity of the
Benue Trough still remains the only thorough description available
(Wright, 1976, personal communication) has listed the following
important basaltic occurrences : (a) South of Obubra, (b) Egede
Hills, (c) Lefin area, (d) NE of Ogoja, (e) Aghilla area, (f) South
of Makurdi, (g) Arufu area, (h) Awe area, (i) Gongola region.
In addition to these occurrences, basalt flows have been reported
in many other parts of the trough such as that resulting from a
central vent type eruption below Shemankar and occurring on
the floor of the trough (Cratchley and Jones, 1965). Basalt
cones have also been found over basement along a line which
runs NNW from Peshiep to Panyam.

As Farrington (1952) has said, "The lavas, for the most part, are typical olivine basalts that are rarely vesicular or amygdaloidal." These extrusives are thought to have emanated from a number of small volcanoes many of which are still recognisable. Only in the Aghilla and Egede areas are the extrusive bodies known to coincide well with the intrusives although some of the volcanic plugs may well be mingled with the igneous bosses known to exist in the trough.

The occurrences of igneous and volcanic activity within the trough tend to be closely associated with the lead-zinc mineralization. Both favour similar steeply dipping anticlines and are concentrated within the central portion of the trough.

4.7 Lead-Zinc Mineralization of the Benue Trough

One of the major features of the Benue Trough is the central zone of lead-zinc mineralization which is about 80 km wide and extends from Abakaliki in the south to Zurak in the north-east, a distance of about 560 km (Figure 4.1). The mineralization tends to be restricted to strata of Albian to Cenomanian age. The better defined occurrences are located in steeply dipping, fracture-filling veins which frequently strike north-south and tend to be associated with the axes of the major anticlines.

McConnell (1949) concluded that the mineralization is of hydrothermal origin and deposited under mesothermal conditions. This conclusion was based on : (a) the mineralization is vertically zoned with lead-zinc ratio and silver content decreasing with depth, (b) the mineral assemblages resemble the lead-zinc deposits of the Mississippi Valley, (c) evident crustification of the lead-zinc minerals and close association of the mineralization

with saline springs and Tertiary volcanic activity.

Farrington (1952) also suggested a medium to low temperature origin under mesothermal conditions of deposition. It has recently been suggested that the origin of the lead-zinc mineralization is likely to involve geothermal heavy metal bearing brines circulating under the influence of a deeper geothermal reservoir such as is known to occur at several locations along the present day lines of lithospheric separation as in the Red Sea and Salton Sea north of the Gulf of California (Grant, 1971).

Although the exact age of the mineralization is not known, it is agreed that it took place at the end of the Santonian folding (Wright, 1968) and after the period of basic to intermediate igneous activity (Cratchley and Jones, 1965). Nwachukwu (1972) reported evidence of post mineralization deformation in the Enyegba, Ameri and Ameka areas of Abakaliki province where the minerals show coarsely crystalline and extensively sheared, striated and grooved granular forms that are suggestive of post-depositional deformation. The lead-zinc veins are extensively oxidised above the water table (Farrington, 1952) and closely associated with igneous and volcanic activity in the trough.

4.8 Origin of the Benue Trough

The elongated shape of the Benue Trough, its position and consistent mineralization, igneous activity, fold axes and structural lineaments have been given considerable attention by geologists interested in its mode of formation and its possible relationship to other similar structures in the world.

The earliest theories on the origin of the Benue Trough were

based mainly on geomorphological evidence, the first being that
of King (1950) who suggested that the trough originated as a
rift structure associated with stresses which accompanied the
separation of Africa and South America. According to King
(1950), the bounding faults of this buried rift system have been
obliterated by subsequent erosion and any remaining traces masked
by the sedimentary rocks now filling the trough.

The absence of any then known major normal faults led to
doubts about the rift nature of the Benue depression as
presented by King (1950) and led Farrington (1952) to contend
that, in view of the deposition of sediments in a long narrow
belt, their longitudinal folding and roughly medial arrangement
of associated mineralization and intrusives, the trough
originated as a geosyncline. Lees (1952) based on geomorphological
evidence, supported the idea of a minor geosyncline in which
compressive forces played a major role. According to Lees (1952),
the crystalline basement underlying the Cretaceous sediments
took part in the general folding of the sedimentary rocks.

A gravity survey was undertaken by Cratchley and Jones
(1965) to obtain new evidence. The gravity field over parts
of the trough shows a characteristic central positive, flanked
on either side by elongated negatives. Cratchley and Jones
(1965) suggested that the Benue Trough originated as a rift
valley under tension which subsided while the sediments were
being laid down, the folding and uplift being later events.

Perhaps the first attempt at explaining in any detail the
mechanism of the evolution of the Benue Trough was that of
Wright (1968). He considered the trough as a sediment filled
inter-cratonic rift lying between the Congo and West African
Cratons in which the release of torsional stresses associated

with the separation of Africa from South America and the ensuing

crust readjustment of Africa led to a slight deformation,

closing the trough and folding the sediments within it.

Wright (1968, 1976) estimated that the amount of closure

was not more than 6-8 km and that separation took place in the

Lower Turonian times, an argument borne out by palaeontological

evidence (Reyment, 1969; Reyment and Tait, 1972).

The theory of plate tectonics stimulated renewed interest

in the origin and mechanism of evolution of the Benue Trough and

has led to a number of hypotheses, differing only in the

mechanism of achieving a commonly accepted structure.

Grant (1971) proposed a model similar to the earlier one

of Wright (1968) but differing in suggesting that the South

Atlantic, Benue Trough and the Gulf of Guinea formed an unstable

RRF triple junction which underlay the present day Niger Delta

of Nigeria. This involved a number of transform faults along

the North Gulf of Guinea Coast. This RRF triple junction may

have caused internal strain in the African plate and a possible

dilation of the Gulf of Guinea transform faults, which with the

short-lived intervening ridge segments, helped to localize

Cretaceous volcanic activity responsible for the newly found

North Brazilian Ridge. Grant (1971) suggested a 30 million

year spreading time for the trough from Albian to Santonian

times during which the continents were either in contact or

closely proximate along transform faults. This model involves

crustal thinning (Cratchley and Jones, 1965) and concomitant

subsidence (Wright, 1976).

Burke et al. (1970, 1971, 1972) proposed an open and close mechanism for the evolution of the Benue Trough which involved short-lived lithospheric spreading and subduction. They suggested that the right angled bends of South American and African coasts resulted from three Cretaceous rift systems (RRR) which met at the point of the present day Niger Delta. Two arms of this RRR triple junction continued to spread while the third arm, the Benue Trough, ceased spreading after about 30 million years. To complement this idea, the authors point to the magnetic anomaly pattern of three positives and three negative anomalies each of about 70 km wavelength and above 40 gamma amplitude over the Niger Delta as suggesting that a spreading oceanic ridge underlay the Niger Delta. This model, accepting a 30 million year spreading time from Albian to Santonian, involved the generation of about 200 km of oceanic crust beneath the trough in comparison with the measured amount of crustal extension of 8-10 km (Nwachukwu, 1972; Uzuakpunwa, 1974; Wright, 1968, 1976). According to Burke et al. (1970, 1971, 1972), this 200 km of oceanic crust was eliminated by subduction evidenced by the presence of andesitic materials around Abakaliki. The accompanying intra-continental collision led to a folding of the sediments. Although the basic idea of an RRR triple junction underlying the Niger Delta has been generally accepted, later workers still believe that there are flaws in the idea of generation and subduction of about 200 km of newly generated oceanic crust.

Perhaps the most cogent criticism of the model due to Burke et al (1970, 1971, 1972) is that of Wright, (1976) who argued that the hypothesis cannot be completely correct because the trough closed in Santonian times implying that it took much

shorter time to close than the estimated 20 million years
required to subduct 200 km of oceanic crust at a rate of 1 cm per
year. The Cretaceous magmatic rocks reported within the
trough are highly altered with no petrological or geochemical
evidence that the reported andesites are of calc-alkaline
affinity. Further, the rotation of the African plate involved
in this model has not been recorded elsewhere in Africa.

Nwachukwu (1972) proposed that the deformation of the
sediments was caused by repeated collision of two continental
plates. According to him, this collision took place in the
form of a two stage disruptive and convergent plate interaction,
the first being a post-Albian-pre-Turonian event giving rise
to Albian folds and early lead-zinc mineralization (Farrington,
1952) and the second being a Santonian event which gave rise to
Santonian folding and a newer generation of ore bodies and
intrusions.

Olade, (1975, 1978) proposed, a hypothesis involving mantle
plumes. The first stage involved the rise of a mantle plume
beneath the Niger Delta. This led to a doming of the Benue region
and formation of an RRR triple junction involving the Gulf of
Guinea and the South Atlantic during Aptian to Albian time
(Burke and Whiteman, 1973). Associated with this doming and
rifting was the outpouring of alkaline mafic lava and volcano-
clastics such as are found around Abakaliki (Olade, 1978). The
growth of the Benue Trough into an ocean was inhibited by the
stresses associated with the opening of the Atlantic and the
Benue was consequently filled by sediments (Hoffman, 1972) during
an episode of rapid subsidence and deposition of inmature clastic
sediments of the Asu River Group (Uzuakpunwa, 1974; Olade, 1975,
1978) (Figure 4.5). This mantle upwelling ceased temporarily in
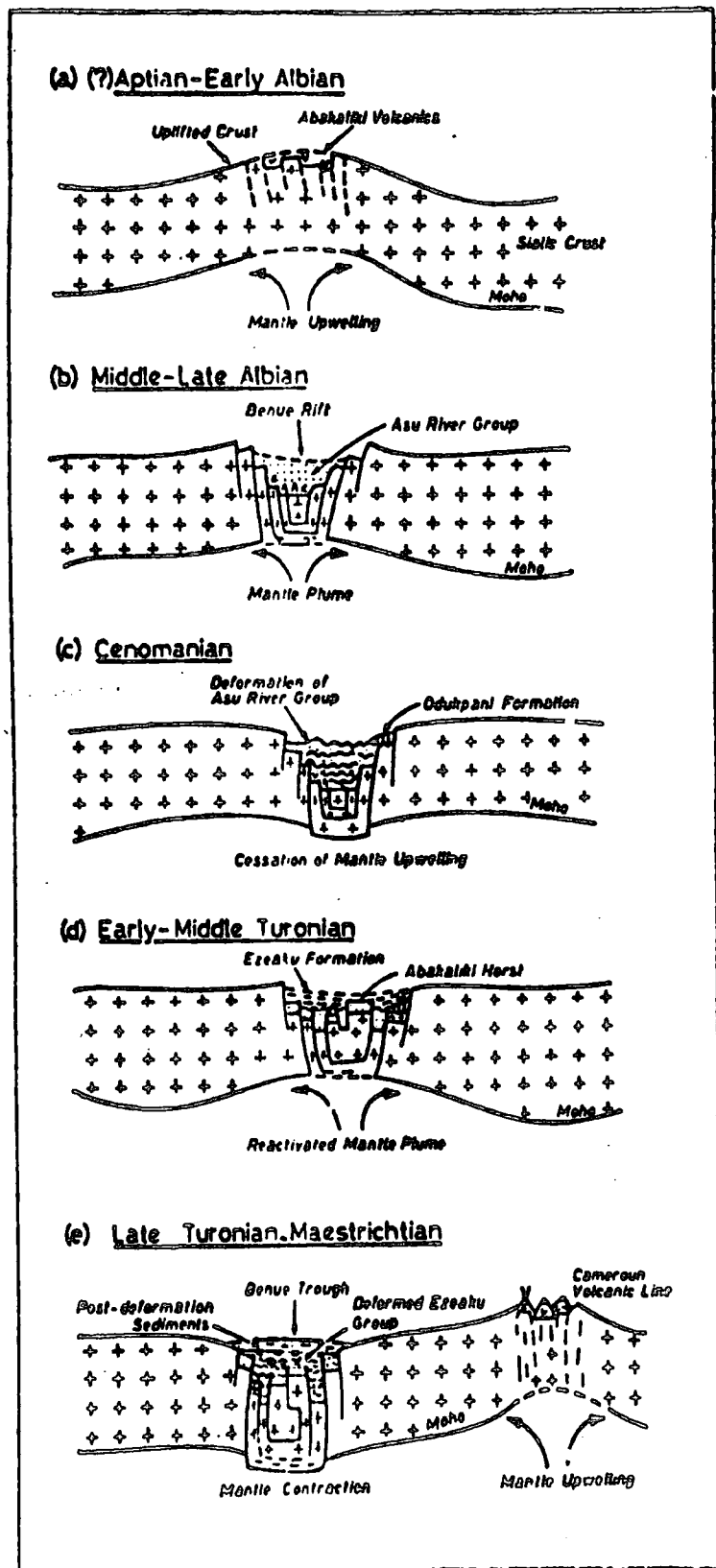
Fig 4·5 Proposed stages in the tectonic evolution of Nigeria's Benue Trough.
(After Olade, 1975)

the Cenomanian, when sub-crustal contractions and compressive folding of Albian sediments and the deposition of the marine Odukpani Formation took place.

The second stage of this hypothesis began in early Turonian times when mantle upwelling was again reactivated and rifting along earlier lines of weakness produced unstable tectonic conditions suitable for the deposition of the Eze-Aku Formation on the Asu River Group (Nwachukwu, 1972; Ogbukagu, 1974; Olade, 1975). This Turonian upwelling ceased in the Senonian because of the rotation of the African plate. The accompanying loss of momentum led to a collapse of the trough to form the present downwarp, accompanied by Senonian and Maestrichtian depositon.

Fitton (1980) has further suggested that the origins of the Cameroon Mountain system lies in its relationship with the Benue Trough. According to him a Y-shaped hot zone which underlaid the Benue Trough in Cretaceous times has been displaced to lie beneath the present day Cameroon mountains and the Gulf of Cuinea. This may have taken place during the cessation of rifting in the Benue Trough and the clockwise rotation of the African plate relative to the asthenosphere, thus initiating igneous activity as the Cameroon line and over the southern edge of the Benue Trough. This removal of the hot spot led to subsidence and folding of sediments as suggested by other authors.

Norman et al. (1977) have also suggested that the Benue Trough was part of an Astron System. They contended that the trough is a graben associated with a peripheral fracture. This resulted from the collision of a large cosmic body with the African plate during the Cretaceous. In the last stages of this work, the following paper dealing with the origin of the Benue Trough came to the author's attention:

Benkhelil, J., 1982. Benue Trough and Benue chain, Geol.Mag. 119, 155-168.

CHAPTER V

INTERPRETATION OF MAGNETIC ANOMALIES OVER THE LOWER AND MIDDLE

BENUE TROUGH, NIGERIA

5.1 Introduction

As described in Chapter Four, the Benue Trough of Nigeria is

an elongated trough of subsidence which trends north-easterly to

attain an approximate length of 800 km and is filled by Cretaceous

rocks whose ages range from middle Albian to Maestrichtian.

Despite the structural significance of the Benue Trough, interest

in the area has been concentrated on putting together the scanty

geological information available in an attempt to explain its

origin. Previous geophysical studies of the subsurface structure in

the area have been confined to gravity measurements and their

interpretation in terms of the subsurface structure.

An aeromagnetic study of the Lower and Middle Benue Trough of

Nigeria is here presented. Regions of high and low magnetic anomalies

have been correlated in an effort to find trends. Two-dimensional

interpretation of several aeromagnetic profiles across the trough

has been carried out using different geophysical techniques. An

attempt to account for the observed anomalies in terms of topo-

graphic variations of the basement leads to rather unreasonable models.

The anomalies are best interpreted in terms of basic intrusive bodies

which occur either within the Cretaceous sediments or within the

metamorphic basement. The model intrusives have variable thicknesses

and directions of magnetization, suggesting that although derived

from the same basic mantle material, the intrusions were emplaced at

different polarity epochs. The observed aeromagnetic profiles

across the trough have been transformed to the corresponding pseudo-

gravity anomalies over the trough and the result of this transformation for some of the profiles are presented. In addition to these profiles taken across the trough, are other shorter profiles which have been taken across smaller features on the aeromagnetic map. These have been interpreted either in terms of dykes or volcanic plugs using non-linear optimization techniques. An attempt has also been made to explain the tectonic evolution of the Benue Trough in terms of the models obtained from the present study of magnetic anomalies over the trough. A review of previous geophysical work done in the area is first presented.

5.2 Review of Previous Geophysical Work

The only interpreted geophysical measurements over the Benue Trough are to the author's best knowledge, the gravity anomalies and some local magnetic anomalies.

5.2.1 Gravity Studies

Published results of gravity studies on the Benue Trough are due to Cratchley and Jones (1965), Adighije (1979, 1981a, 1981b) and Artsybashev and Kogbe (1975). These authors have reported a central axial positive anomaly, flanked on either side by a number of elongated negative anomalies (Figure 5.1). The characteristic shape of the gravity field over the trough is closely similar to that over other rift systems, notably the Red Sea and the East African Rift (Adighije, 1981b).

The belt of positive anomalies coincides with the central zone of known tectonic activity, mineralization, uplift, erosion, numerous mafic intrusives and basaltic lavas (Olade, 1978; Adighije, 1981b).

The geological and geophysical interpretations of Cratchley and Jones (1965) was the first published gravity study of the Middle
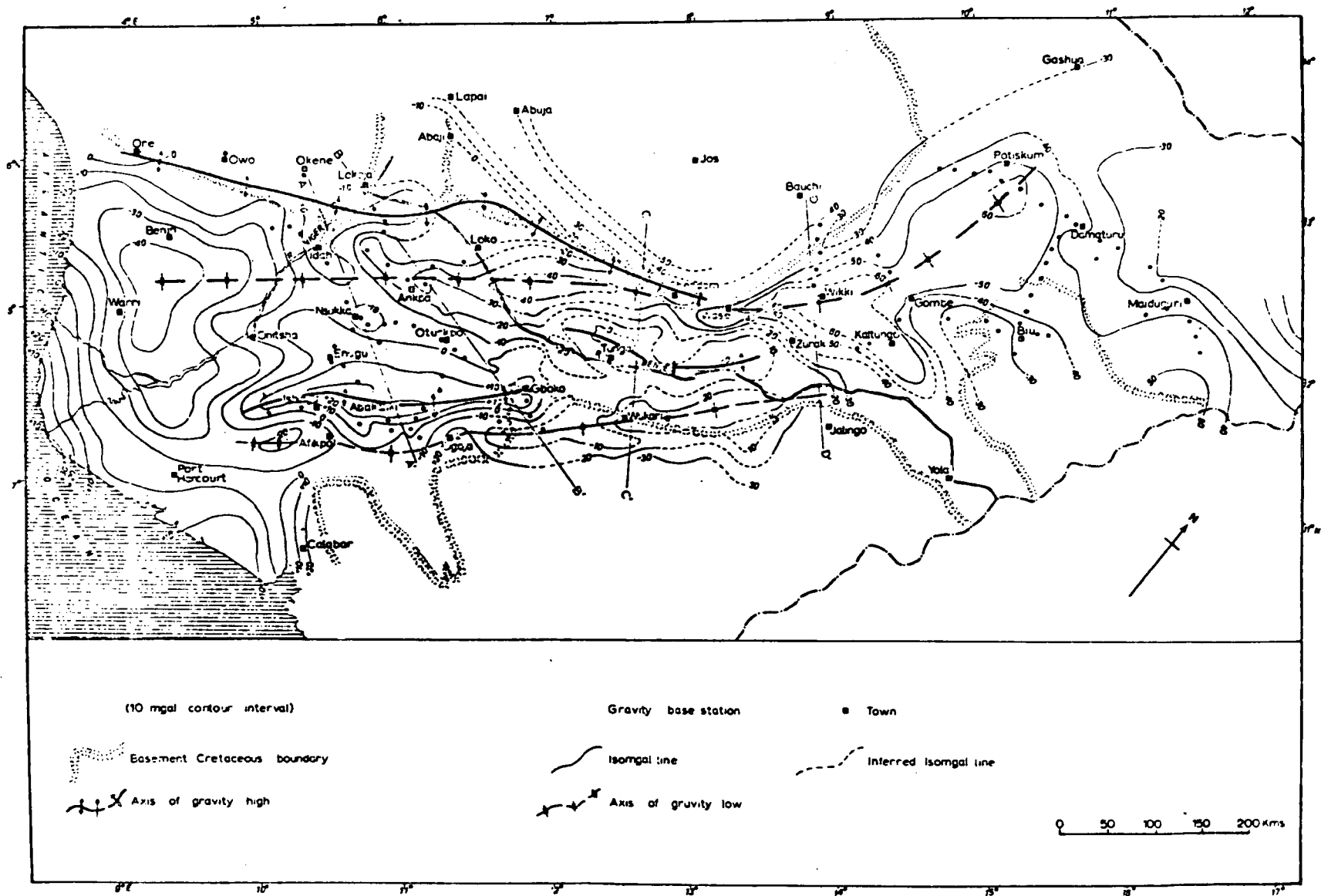
Figure 5.I. Bouguer anomaly of Benue Trough using a density of 2.67gcm^{-3} (After Adighije, 1981b)

Benue and parts of the Upper Benue. This remains the most widely accepted geophysical study of the Benue Trough in general and the Middle Benue in particular. From a consideration of the scant geological information and the gravity evidence, Cratchley and Jones interpreted the central positive anomaly in terms of the combined effect of (a) zone of basic to intermediate intrusions occuring either within the basement or within the sedimentary basin, (b) a possibly shllow basement and (c) a thin crust as an approximate compension for topography and the sedimentary basin. Local positive anomalies were also interptreted as being due to the numerous minor intrusions which abound within the trough. The flanking negative anomalies were interpreted as being due to increased thickness of Cretaceous sediments averaging about 5200 m in the Upper Benue and 3500 m in the Middle Benue. All subsequent workers have sought to complement the above interpretation (Artsybashev and Kogbe, 1975; Adighije, 1979, 1981a, 1981b).

Artsybashev and Kogbe (1975) interpreted the central regional positive anomaly recorded by Cratchley and Jones (1965) as being due to a shallowing of 10-12 km of the Moho due to the spreading and contemporaneous thinning of the crust under the trough. Their estimate of the uplift, however, appears too large on account of the very low density contrast of 0.17 g cm^{-3} which they have assumed between crust and mantle (Adighije, 1979). The depth to the Moho as computed by Artshybashev and Kogbe varies from 22-27 km in the north to 31-37 km in the south (Figure 5.2).

Adighije (1979), while accepting an uprise of the mantle as explaining the central regional positive anomaly, estimated that the amount of uprise does not exceed 1.5 km in the Lower Benue assuming a density contrast of 0.57 g cm^{-3}. He also interpreted the strong positive anomaly around Abakaliki as being due to a high density body (Figure 5.3). The very large size of this body, according to
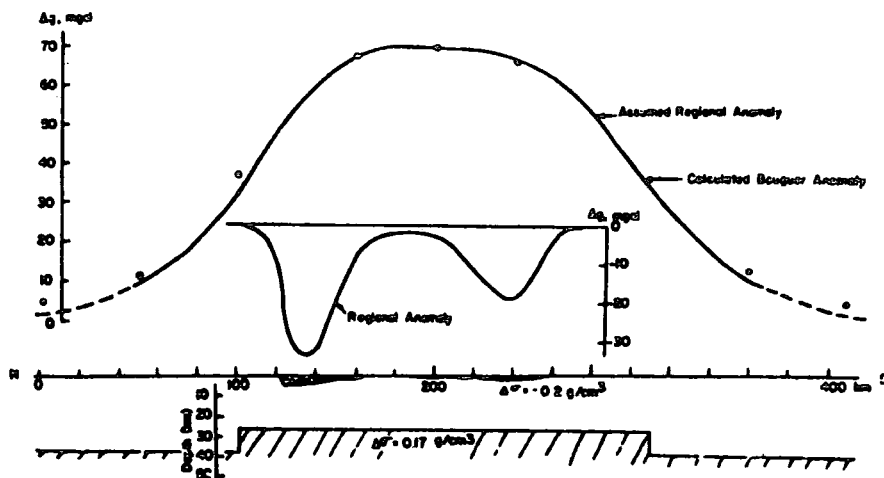
Figure 5.2. Generalized crustal section and gravity profile across Benue Valley.
(After Artsybashev and Kogbe, 1975).

Crustal models of Benue Trough.
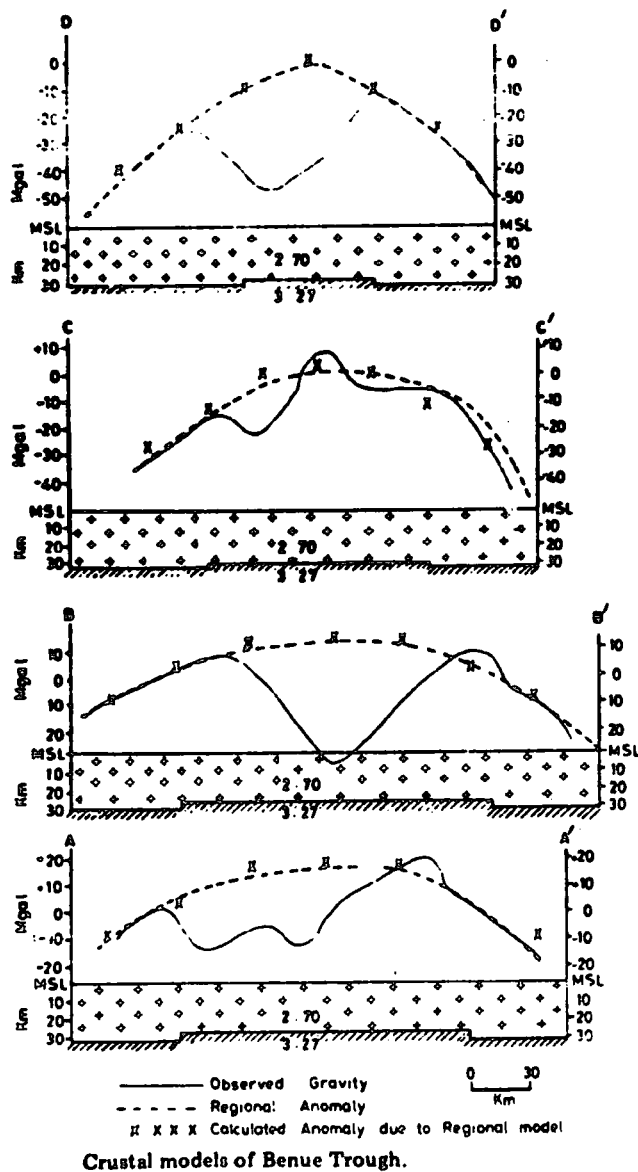
Figure 5.3   Crustal models for the Benue Trough (After
              Adighije, 1979).

Adighije (1979), does not justify interpretation as an intrusive but rather as a mantle diapir which may have been the source of the volcanic pyroclastics reported over the area (Nwachukwu, 1972; Uzuakpunwa, 1974; Olade, 1978). Adighije interpreted an E-W profile across the Lower Benue from Gboko - Nsukka - Auchi in terms of a basement of variable topography, this being shallower near the axis than on both flanks.

Adighije (1981b) presented a comprehensive gravity anomaly map for the whole of the Benue Trough area and made qualitative and quantitative interpretations of several profiles across the trough. He interpreted the axial positive anomaly as being due to an intrusive body at depth in the crust and extending linearly towards the north-east for over 350 km from Abakaliki. The intrusive body required to explain this positive anomaly is probably gabbroic on account of its density of 2.90 gcm^{-3} and may have originated from magma produced in the underlying mantle. The size of this body decreases northwards from the Cretaceous triple junction located near the present day Niger Delta (Wright, 1968, 1976). The body may be associated with an unsuccessful attempt to open the Benue Trough into a proto-ocean during Late Cretaceous times (Adighije, 1981b). The same author, (Adighije, 1981a, 1981b) has also interpreted the lateral negative anomalies in terms of great thickness of sediments, the maximum thickness being about 6000 m in the Upper Benue and 3000 m in the Middle Benue (Figure 5.4).

5.2.2 Magnetic and Other Studies

Apart from the gravity studies discussed in the last section, there has been no other published geophysical study of the Benue Trough known to the author. However, a number of reconnaissance magnetic measurements have been carried out by different authors
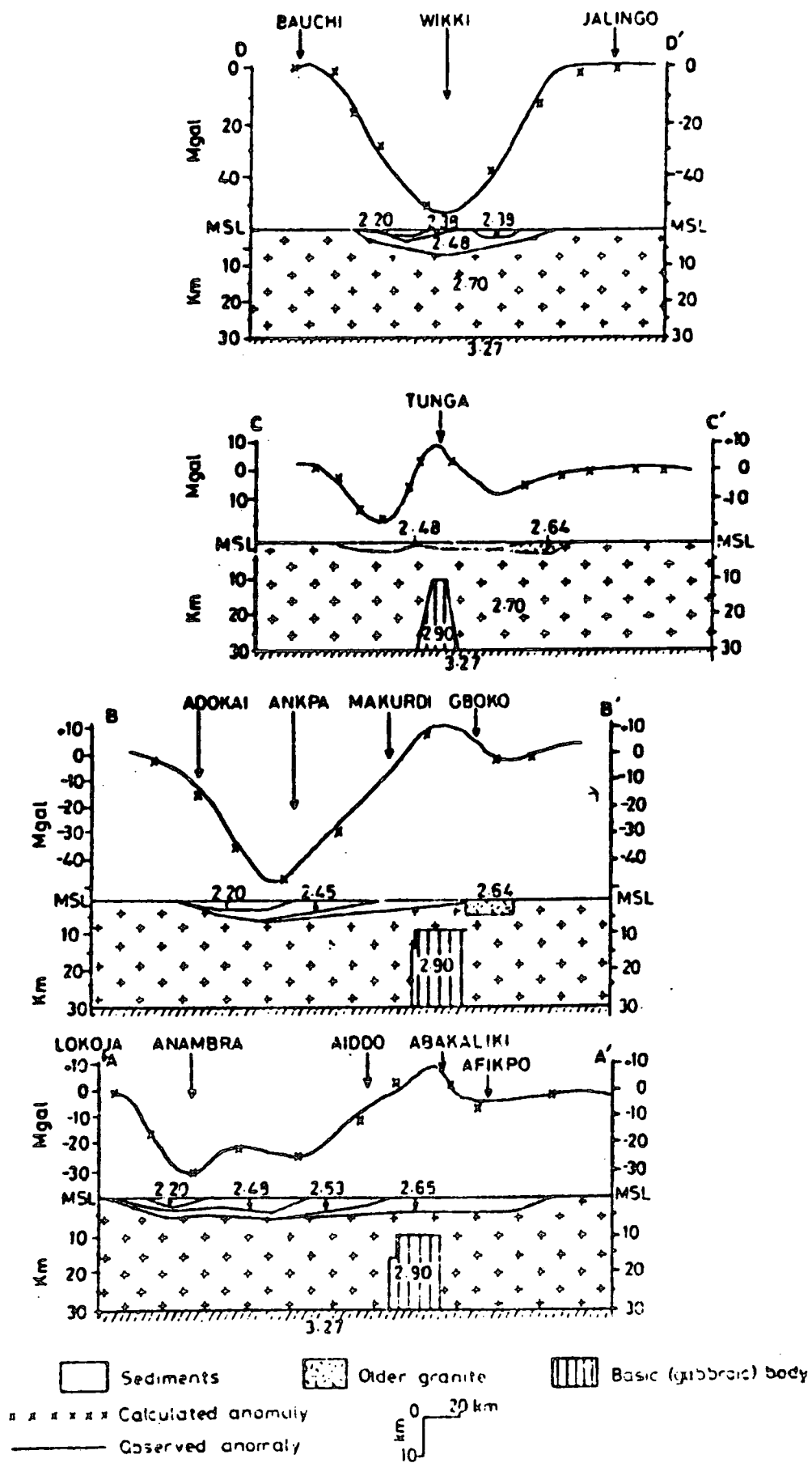
Figure 5.4   Interpretation of observed gravity anomalies over
The Benue Trough (After Adighije, 1981b).

although none of these were interpreted in any detail or published (Cratchley and Jones, personal communication).

Cole, in 1958 interpreted a negative magnetic anomaly about 9 km south-east of Shendam in terms of a southerly dipping dyke-like body approximately 2 km wide and of basic composition which could be related to a volcanic centre beneath Shenmanker postulated by Cratchley and Jones (1965). A few ground magnetic tra verses were carried out across the trough by Cratcley and Jones (Cratchley, personal communication) while working on the geology and gravity field and these showed no appreciable magnetic variations. Variations of $\pm$ 100 gamma across Awe were explained in terms of relatively thin basalt flows and small cones (Cratchley and Jones, 1965).

A reconnaissance aeromagnetic survey was carried out in 1965 along 8,500 miles of flight lines by Geophysicists of the Canadian Ministry of Mines and Technical Surveys under the supervision of Mr. Alan Gregory, over most of the basement rocks of Nigeria and parts of the Benue Trough. The results of this survey were correlated with the regional geology but this was not published (Cratchley - personal communication). The present magnetic study therefore appears to be the first attempt at interpreting in any detail the magnetic anomalies over the Benue Trough in terms of the sparsely known geology.

A seismic refraction experiment is being contemplated by the Geology and Physics Departments of University of Nigeria, Nsukka in the Lower Benue (Chukwudebelu - personal communication). A similar experiment is planned jointly by the Physics Department of Ahmadu Bello University, Zaria and the Department of Geological Sciences, of University of Durham for the Upper and parts of the Middle Benue Trough (Dr. Long, personal communication).

5.3 Interpretation of Magnetic Anomalies

Figure 5.5 shows the aeromagnetic map of the area covered in this study. To produce this map, sixty four 1:100,000 sheets of the Aeromagnetic Map of Nigeria have been stacked together. The positions of the profiles interpreted are shown. The lengths of the observed profiles which were taken directly from the 1:100,000 sheets of the Aeromagnetic Map of Nigeria published by the Geological Survey of Nigeria, varied according to the position along the trough.

5.3.1 Collection and Analysis of Data

The data used was in the form of aeromagnetic maps which were kindly provided by the Geological Survey of Nigeria, Kaduna. The collection of these maps was the most time consuming single aspect of this work, having taken almost one year of letter writing, telephoning and a visit to Kaduna.

Several methods of magnetic interpretation have been used in the analysis of the data. The methods used included the linear inverse methods, non-linear optimization techniques, pseudo-gravity transformation and interactive techniques (Chapter One). Fortran programming of most of these methods was carried out during the course of this work and details of these and other programs used are given in the Appendix. In addition to the programs written by the author, a few existing programs were used, including MAGN, GRAVN and INTERGRAM. The programs MAGN and GRAVN were mostly used for cross checking the programs developed. The program INTERGRAM on the other hand is a very versatile graphic oriented interactive program suitable for the interpretation of both gravity and magnetic data using the trial and error method. This program was used extensively. The use of non-linear optimization was restricted to the modelling of dykes and plugs and the interpretation of some of the profiles in terms of models

requiring not more than three separate bodies and a total of eighteen body points. It was, however, found that most of the interpreted profiles could only be explained in terms of several different bodies and the use of non-linear optimization techniques in their interpretation was extremely time consuming. More use was therefore made of the interactive techniques.

The aeromagnetic profiles taken from the aeromagnetic map (Figure 5.5) were complicated by the presence of short wavelength anomalies which would have made their interpretation virtually impossible. This particularly applied to the profiles taken across the Middle Benue Trough. To filter off these short wavelength anomalies, most of the profiles had to be upward continued. In order to carry out this upward continuation, the program UPCON was developed. The program is an upward/downward continuation routine applicable to both gravity and magnetic data. The height to which the profiles were upward continued varied from profile to profile depending on the degree of complexity. Table 5.1 shows the heights to which the different interpreted profiles were upward continued. These heights have been allowed for during the interpretation of the profiles.

TABLE 5.1

Heights of Upward Continuation for Different Profiles

Profile	Height of Continuation
LB1	0.85 km
LB2	1.0 km
LB3	3.0 km
LB4	0.9 km
MB1	5.0 km
MB2	5.3 km
MB3	4.0 km
MB4	4.0 km
MB5	3.0 km

The removal of the regional field prior to interpretation was carried out by least-squares regression analysis using programs which compute and remove the first and second order regional fields.

5.3.2 Limitations on Interpretation

The interpretation of the aeromagnetic anomalies over the Lower and Middle Benue Trough was not without constraints. The greatest limitation was the absence of sufficiently detailed background geological information due to lack of much previous work. Modelling has therefore been carried out from first principles. The gravity studies of Cratchley and Jones (1965), Adighije (1981a, 1981b) and others were, however, useful in estimating probable depths to the basement at different portions of the trough.

Although the observed aeromagnetic anomalies appear to be three-dimensional, interpretation has been carried out in terms of two dimensional structures in view of the massive nature of the area covered and difficulties involved in the modelling of several three dimensional bodies to explain a single profile. This use of two dimensional bodies to explain the observed anomalies would affect the depth estimates made in the present study. Furthermore, the short wavelength anomalies removed by upward continuation are important in placing depth limits to the models required to explain a given observed anomaly and their removal may have an effect on the resolution of depth limits obtained in this study.

No known palaeomagnetic studies have been carried out in the area and it was not possible to assert with any confidence, the approximate directions of magnetization. For most models, it was therefore necessary to constrain the directions of magnetization to as close as possible to the direction of the Earth's field, which in Nigeria, has an inclination of about -7.5° and a declination of -7.4°

as recorded at Ibadan in 1975 (I.G.S. Geomagnetic Bulletin 10, 1979).

The actual values of inclination and declination used were inter-

polated from contours published by the United States Naval

Oceanographic Office. The position of Nigeria has not changed much

from its palaeolatitude in Cretaceous times. Although a northward

shift has been suggested, any such deviation hardly exceeds 10-15°

(Tarling - personal communication) and the assumption of directions

of magnetization closely parallel or against the present days field

direction is a fairly valid one.

5.3.3 Description of Anomalies and Discussion of Trends

Presentation of any detailed trend analysis of the aeromagnetic

anomlies over the Lower and Middle Benue Trough is a difficult task

at the present stage because of the size of the area and the difficul-

ties of synthesis of one single sheet. The aeromagnetic map

presented in Figure 5.5 is compiled from sixty four different

1:100,000 sheets each covering an area of 3,600 km^2. The brief

qualitative description of the anomalies given here aims to show

the broad distribution of magnetic anomalies over the area. To

facilitate this description, regions of high and low magnetic

anomalies are labelled "H" and "L" respectively in Figure 5.5. The

positions of key towns in the area are also shown (Figure 5.5).

5.3.3.1 Magnetic Anomalies Over the Basement

The basement area bordering the Lower and Middle Benue Trough

is characterised by short wavelength anomalies which are probably

caused either by susceptibility changes within the basement or by

near surface intrusives. These anomalies have a distinct lineation

along the trend of the Benue Trough (Figure 5.5). In contrast to

these short wavelength anomalies are the smoother magnetic anomalies which characterise the sedimentary basin area. These long wavelength anomalies whose average width is about 40 km are probably mainly caused by deep seated bodies below the sediments. It is on the interpretation of these anomalies that special emphasis is placed.

5.3.3.2   Basement/Cretaceous Basin Boundary

The boundary between the basement complex and the sedimentary basin is for most parts of the Lower and Middle Benue, characterised by a belt of magnetic lows shown on Figure 6.5 by the peripheral chain of the letter "L" to the north and south.

A chain of the magnetic lows characterizing the contact of the basement with the sedimentary basin can be traced from the area to the south east of Gboko through Kado to beyond Donga (Figure 5.5). This belt of magnetic lows in the south corresponds remarkably closely with the Cretaceous - Basement contact indicated on the Geological Map except in the area around Donga, south of Wukari. The position of the line of magnetic lows indicates that the position of the basement - basin boundary is slightly displaced towards Donga, suggesting that the boundary as it appears on the Geological Map of Nigeria needs to be moved southwards.   Cratchley and Jones (1965), from an analysis of the distribution of gravity anomalies (Figure 5.1), had observed a similar difference between the basement-Cretaceous contact on the Geological Map and the contact obtained from the gravity analysis in the area south of Wukari.   They considered that the actual basement-basin contact may be further south towards Donga, in agreement with the present analysis of magnetic anomalies. A similar conclusion was also drawn by Alan Gregory in 1966 from a preliminary study of the reconnaisance aeromagnetic survey (Cratchley - personal communication).   The belt of magnetic

low can be traced further through Ugba and beyonds Gboko where it is interrupted by a rather complex magnetic high which may correspond to the positive gravity anomaly observed over Gboko (Cratchley and Jones, 1965). It was not possible to investigate the magnetic character of the basement-basin contact in the lower portions of the trough as the boundary was not transversed. However, the belt of magnetic low characterising the contact in the Middle Benue could be followed all the way down into a line of magnetic lows beginning at Oturkpo, running through Odoba, Otukpa, Enugu-Ezike to Idah (Figure 5.5).

The basement - Cretaceous contact in the north of the area is also characterised by a belt of generally low magnetic anomalies which, unlike the lows in the south, can be traced from the Lower Benue to the uppermost portions of the Middle Benue. This belt of magnetic lows (Figure 5.5) is locally interrupted by small regions of short wavelength anomalies. This chain of magnetic lows can be traced from Lokoja through Bagana to Udegi and beyond. The belt then runs from the north of Doma, north of Lafia, through Adogi, Ajaikia, Namu, above Bakin-Chiawa, south of Shendam, through Lantang to the north of Yuli. The basement-Cretaceous contact in the north appears rather better defined than it is in the south and in both cases the belt of magnetic lows defining the contact correspond closely to the belt of negative gravity anomalies observed over the contact (Cratchley and Jones, 1965; Adighije, 1979, 1981a, 1981b).

5.3.3.3 Magnetic Anomalies over the Sedimentary Trough

In general, the sedimentary trough is characterised by a sequence of belts of positive and negative magnetic anomalies. These belts are not continuous but appear to be made up of several elongated lobes of varying lengths. These can be traced for varying distances

along the trough before being interrupted by the occasional occurrence

of short wavelength anomalies which may be due to near surface

intrusives, volcanic plugs and thin basalt flows. An interesting

feature of the anomaly belts lies in the fact that they trend sub-

parallel to the trough.

South of the belt of magnetic lows indicating the basement/

Cretaceous contact to the north, is a line of magnetic highs. This

belt of magnetic maxima can be traced from well beyond Dekina in the

Lower Benue through Abejuko to the north east of Onugba, before

being interrupted by an area of generally low magnetic features whose

trend is not well defined. This same belt of magnetic highs continues

again from Obi, through Rufai, Akiri, Azara and Yamini, to the town

of Amar beyond where it passes into linear short wavelength anomalies.

To the south of this line of magnetic highs, is a belt of magnetic

lows (Figure 5.5) which begins from the southwest of Dekina and

can be traced through Oliya and terminates just to the east of Onugba,

west of Makurdi. Not directly linked with this chain is another chain

of magnetic lows which runs through the Middle Benue. This chain begins

at Udei, passes through Keana, Kanje, Awe, Ibi, Jubu, Sussanne and

Lampar (Figure 5.5).

To the south of this belt of minima, is a belt of magnetic

highs which can be traced from around Idah and terminates at Adum in

the Lower Benue. Anomaly lobes of this belt can be seen to begin

again at Akwana in the Middle Benue and continues through the area

north-west of Wukari, through Batanji and beyond; where it terminates

into an area of short wavelength anomalies caused by near surface

igneous bodies.

A closer look at the aeromagnetic map showed that there were

differences between the character of the long wavelength anomalies

over the sedimentary trough and those over the surrounding basement. To demonstrate this, an aeromagnetic profile was taken across the area covered by Figure 5.5. The length of the profile (Profile AB in Figure 5.5) was such that it covered as much as possible, the basement areas flanking the trough. The profile AB is shown in Figure 5.6a. To clearly demonstrate the differences in character of the long wavelength anomalies over the sedimentary trough and basement, the profile AB was upward continued by a height of 1.0 km to eliminate short wavelength anomalies and the resultant profile is given in Figure 5.6b, where the difference in character of the long wavelength anomalies is clearly manifest.

This apparent variation in the nature of the long wavelength anomalies observed over the sedimentary trough and flanking basement area (Figure 5.6) as well as the non-continuity of the belts of the magnetic highs and lows and their trend sub-parallel to the trough suggests that the anomalies over the Benue Trough do not represent typical oceanic magnetic anomaly and the extensional hypothesis of Burke et al. (1970, 1971, 1972) may not adequately explain the tectonic evolution of the Benue Trough (see Chapter Four).

5.3.4 Interpretation of Magnetic Anomalies in Terms of Basement Topography

The first attempt at interpreting the magnetic anomalies over the Lower and Middle Benue Trough was based on the assumption that the anomalies can be interpreted strictly in terms of the underlying metamorphic basement. This would involve either of two possible models:-

(a) A block of strongly magnetized basement whose magnetization and composition may vary laterally. Such a block would be required to occupy the entire width of the trough.
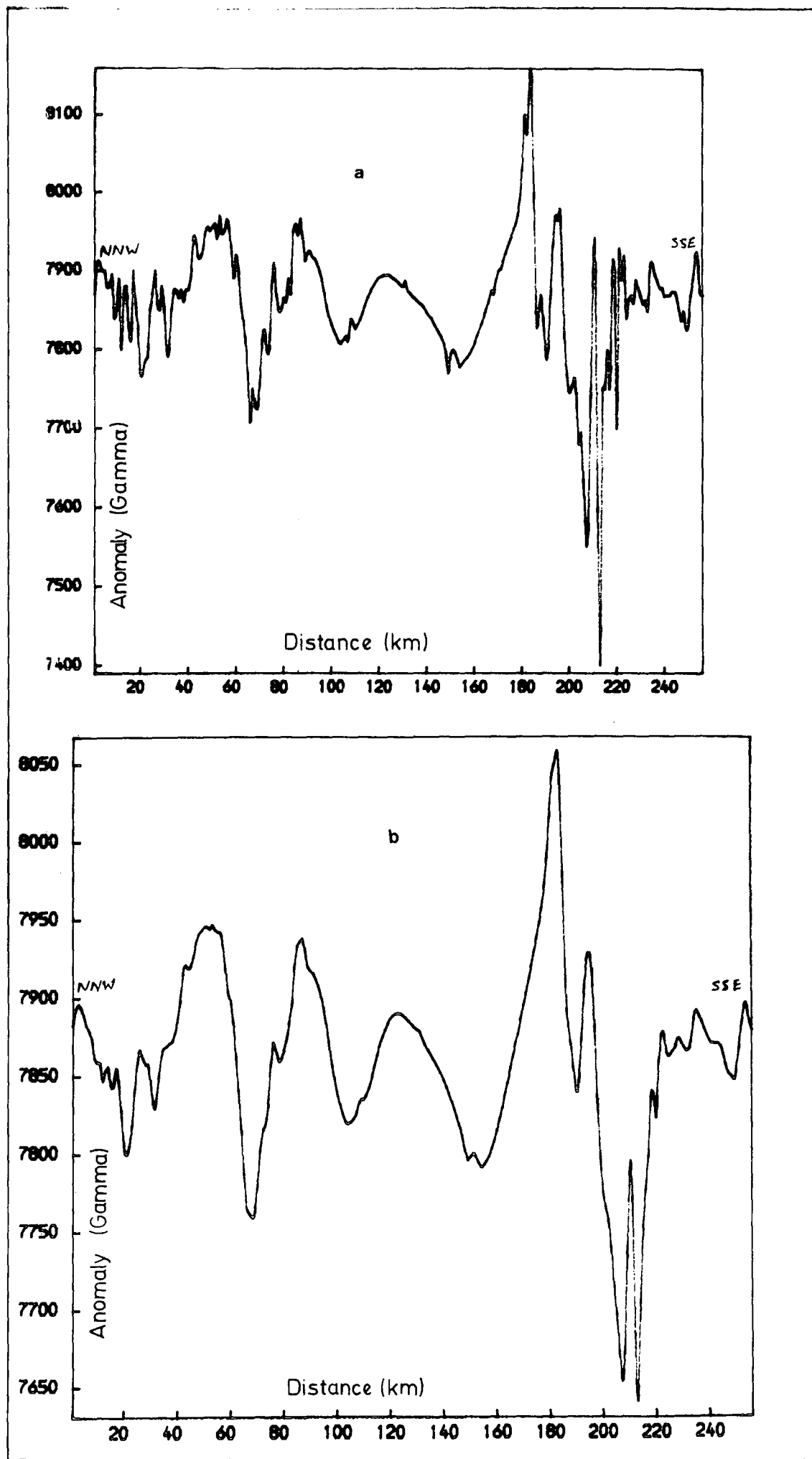
Figure 5.6 Profile AB taken across the Benue Trough and flanking basement to demonstrate the variation in the long wavelength anomalies found over the basement and over the sedimentary trough.

(b)   A block of normal metamorphic basement of variable depth.

There is no evidence to support a strongly magnetized basement block underneath the sediments filling the Benue Trough and this model was therefore discarded. An attempt was made to explain the observed anomalies in terms of a uniformly magnetized metamorphic basement of variable topography. Three profiles, MB1, MB2 and MB4 taken over the Middle Benue Trough have been used in this study. The positions of these and other interpreted profiles are given in Figures 5.5 and 5.7.

Figure 5.8a shows a possible interpretation of profile MB4 (Figure 5.5) in terms of the basement topography. To produce this model required a magnetization of 1.30 A/m and assumes a magnetization in the direction of the Earth's field. The model gives a reasonably good fit between the observed and computed anomalies. The ends of the model correspond closely to the expected basement/Cretaceous contacts although without a good fit towards the southern end of the profile. The maximum sediment thickness of about 4.10 km appears too great compared with known estimates in the area. Furthermore, to obtain this fit between the observed and calculated anomalies required a basement outcrop in the area around Jobu (Figure 5.5). This is not in agreement with the known geology of the area. An attempt shown in Figure 5.8b to reduce the maximum thickness of sedimentary rocks around Batanji (Figure 5.5) proved unsuccessful as this required the basement to outcrop east of Shemanker and increasing the area of outcrop in the previous model (Figure 5.8a).

Figures 5.9a, 5.9b and 5.9c show models required to explain profile MB2 in terms of basement topography. These models give a good fit between the observed and computed anomalies, but are not geologically feasible. The model of Figure 5.9a required a magnetization of 2.5 A/m, having a dip of -4.0° which does not differ much
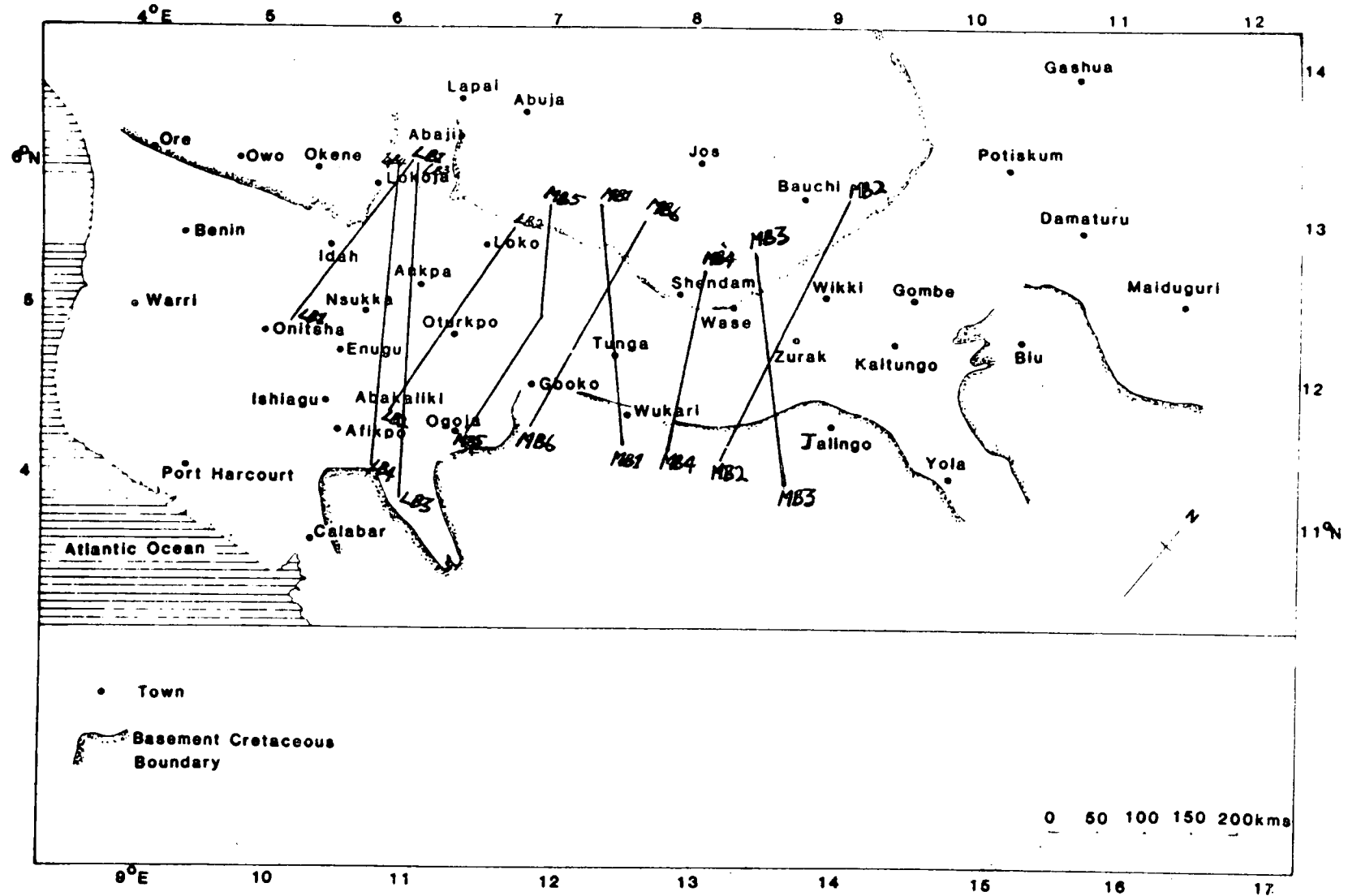
Figure 5.7   Map of the Benue Trough showing the positions of the
profiles interpreted.
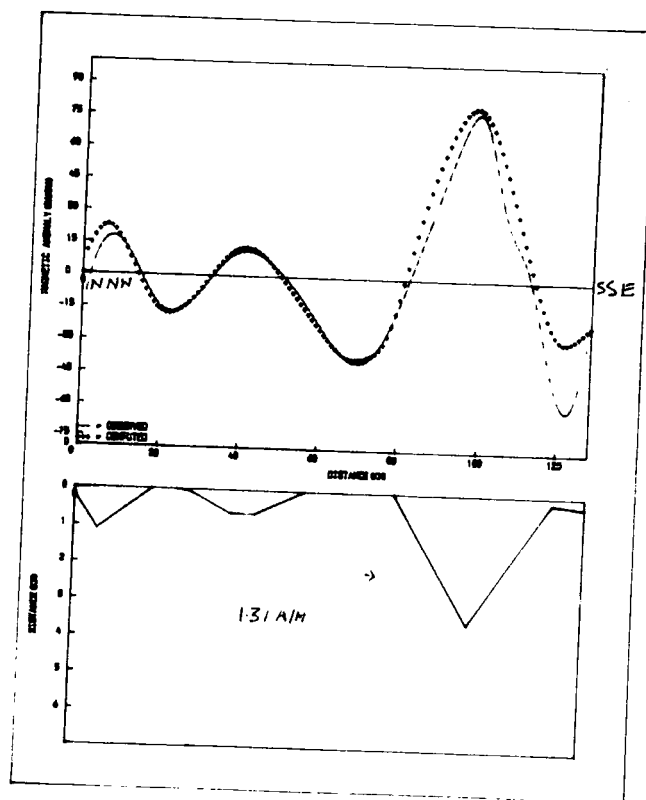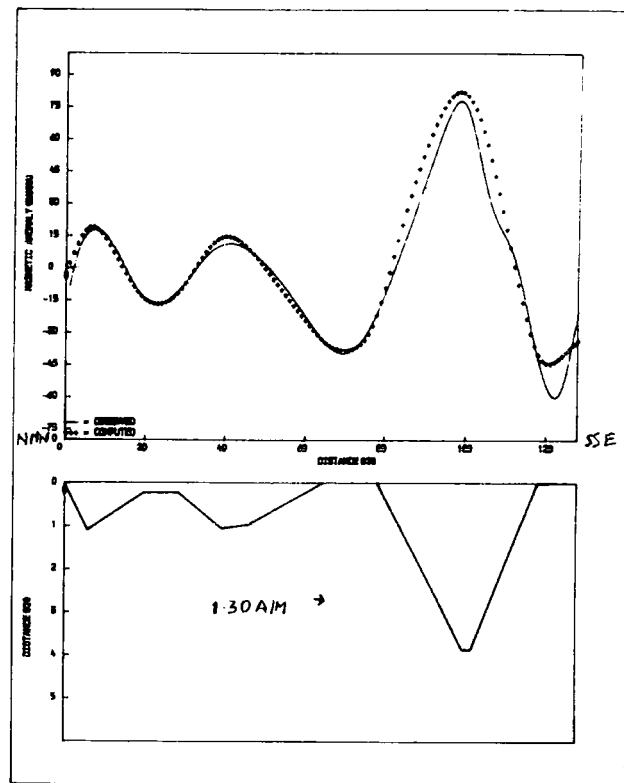
Figure 5.8   Possible models required to explain the profile MB4 in
terms of the underlying basement.
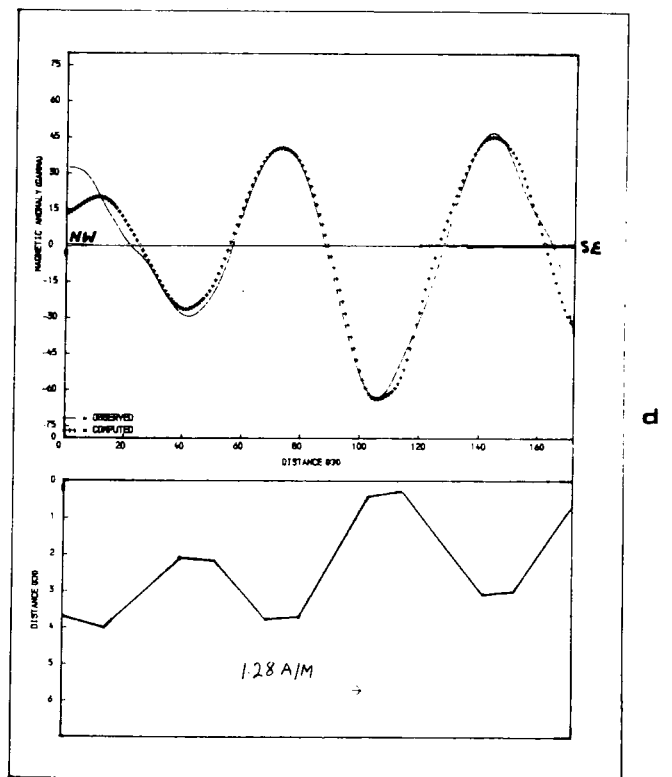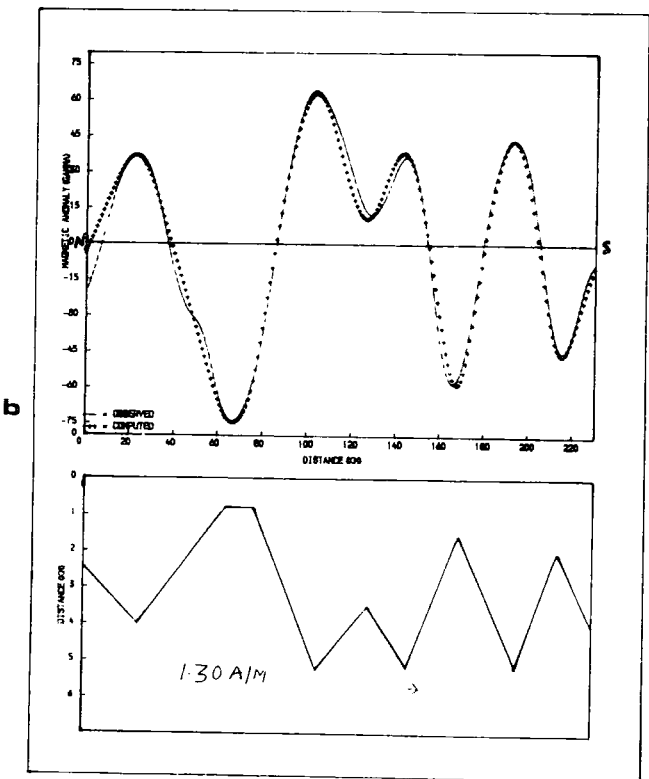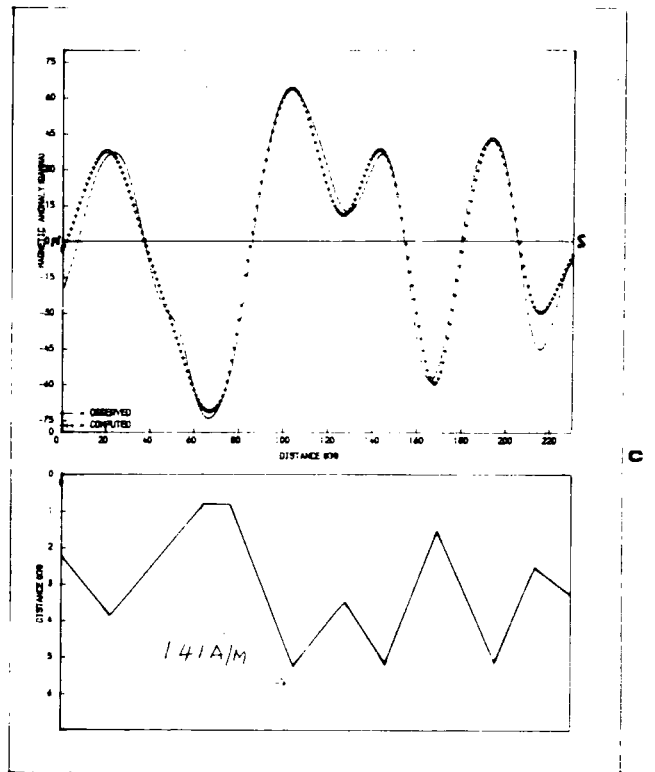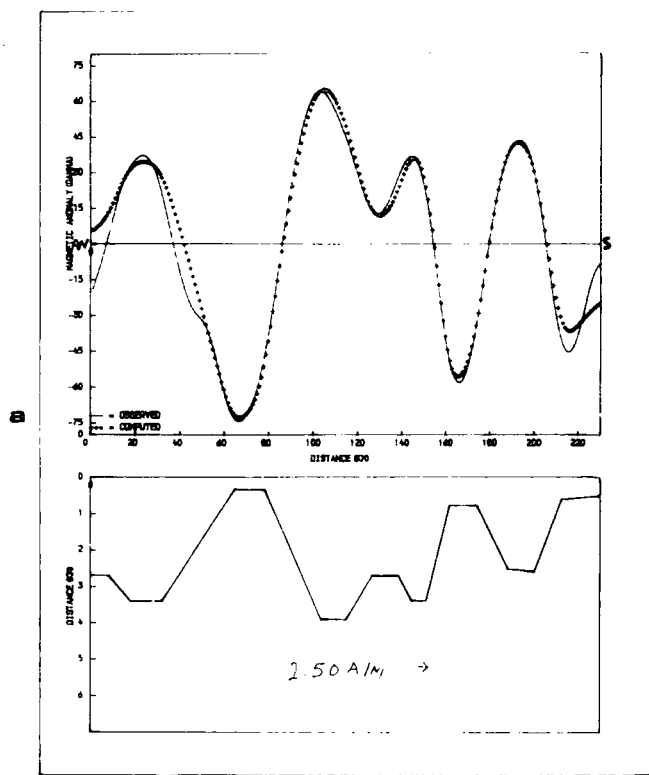
Figure 5.9   Possible models required to account for the profiles
MB2 and MB1 in terms of the underlying basement.

from the direction of the Earth's field. Although the average sediment thickness of 3.11 km is in close agreement with known average thickness in the area, the model does not account well for the edges of the trough and involves a magnetization of rather too high a value. The models of Figures 5.9b and 5.9c require magnetizations of 1.30 A/m and 1.41 A/m in the direction of the Earth's field. Both models involve too great a thickness of the sedimentary cover in the area and like the previous model cannot account for the position of the edges of the trough.

The profile MB1 which runs through Wamba, Ajaikia, Rufai, Wukari and Kado (Figure 5.5) has also been interpreted in terms of a basement of variable topography. Figure 5.9d shows one such interpretation in which the basement has been assigned a magnetization of 1.28 A/m. As for profile MB4, the basement is assumed to be magnetized in the Earth's field direction. This model does not account well for both extreme ends of the profile. Furthermore, the closeness of the basement to the surface and maximum thickness of sediments conflict with the geological knowledge of the area. A model using a magnetization of 0.9 A/m also led to outcrop of the basement around Awe which do not agree with the known geology of the area. A model allowing a reduction in the depth range between the peaks and the troughs in the basement required a magnetization as high as 2.3 A/m which is unreasonably high for a crystalline basement.

The conclusion drawn from this section is that variation in the basement topography could contribute to the observed anomalies, but such changes cannot in themselves fully account for the observed anomalies. The anomalies must therefore, be due to highly magnetic bodies occupying much of the entire width of the trough. The observed profiles across the trough were therefore interpreted in terms of discrete intrusive bodies and the results of this interpretation for the different profiles are described in the following sections.

5.3.5 Interpretation of Anomalies in Terms of Intrusive Bodies

The aeromagnetic anomalies over the Lower and Middle Benue Trough are best accounted for in terms of basic intrusive bodies which may occur either within the Cretaceous rocks or within the basement, or both. These intrusive bodies have variable thicknesses and are magnetised in directions close to or opposite to, the direction of the present Earth's field.

5.3.5.1 Interpretaion of Profile LB1

This profile lies to the east of Lokoja and Idah and runs through the town of Dekina, ending north of Adani (Figures 5.5 and 5.7). The observed anomaly profile has been interpreted in terms of three intrusive bodies magnetized in opposite directions. The model bodies required to explain this profile are thought to be deep seated bodies with the depth to the top surface lying between 2 km and 8 km. Figures 5.10a, 5.10b, 5.10c and 5.10d show possible model bodies required to account for this profile. Figure 5.10a shows the bodies at their minimum possible depths if a good fit is to be obtained between the observed and computed anomalies. The central body in this model has a magnetization of 1.60 A/m while the bodies to its right and left have magnetizations of 1.25 A/m and 1.60 A/m respectively. While the model of Figure 5.10a gives a reasonably good fit it does not account equally well for all the wavelengths in the profile. Figure 5.10b shows the intrusive bodies at greater depths and gives a better fit to the observed anomaly than the previous model. The central body here has a magnetization of 2.15 A/m. The model bodies of Figure 5.10c are even deeper than those of Figure 5.10b. The central body in this model has an increased magnetization of 2.5 A/m. Figure 5.10d shows a model in which the intrusive bodies required to account for the observed profile have
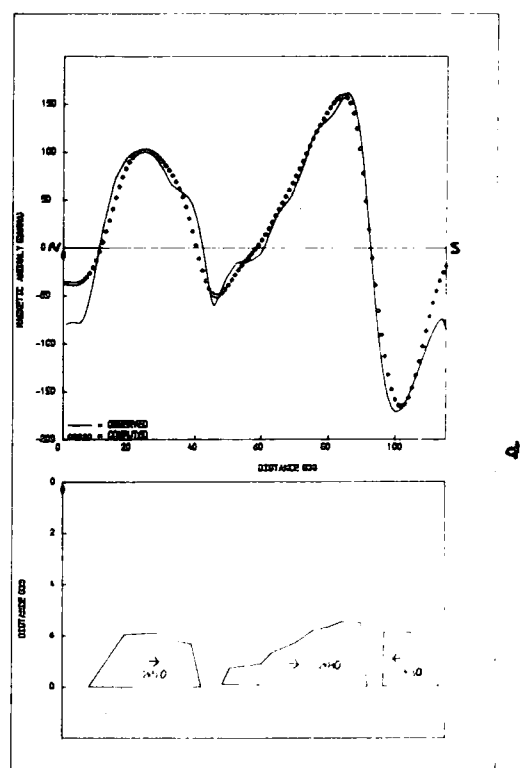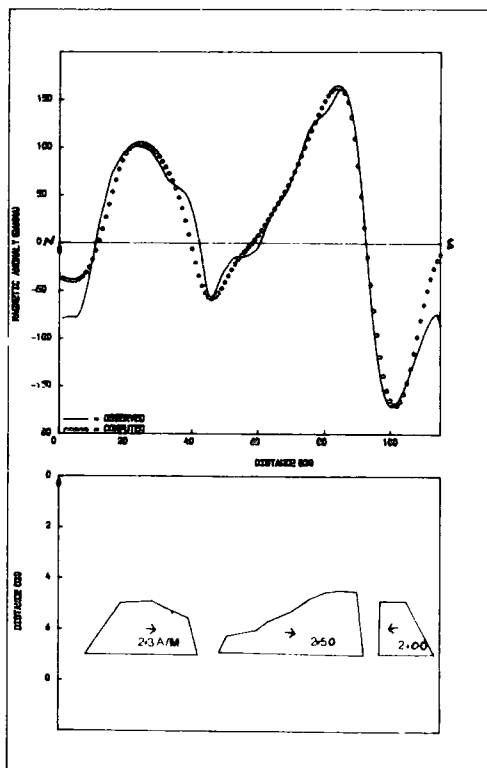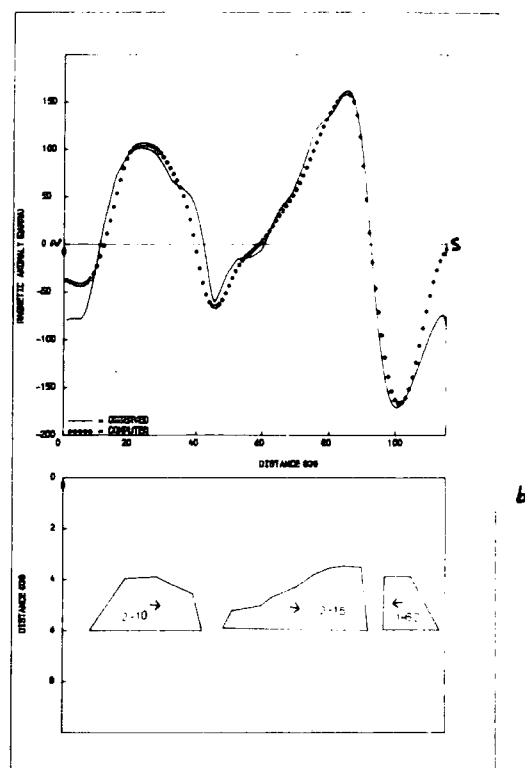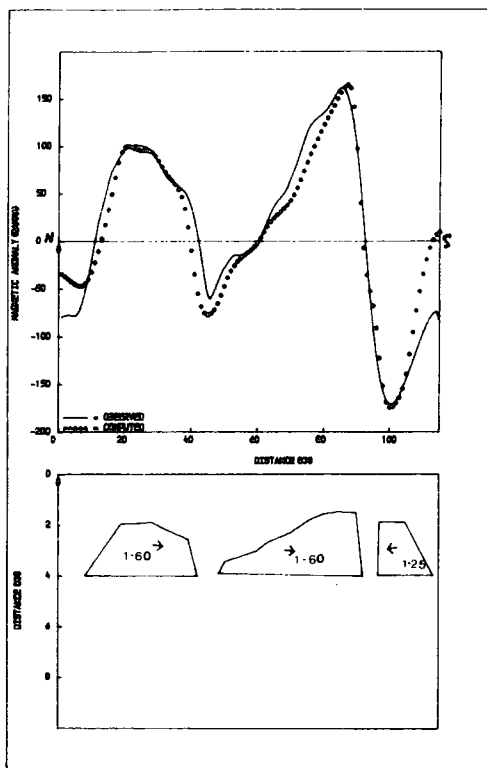
Figure 5.10   Possible models required to account for the profile
                LB1 in terms of discrete intrusive bodies.

a minimum depth of about 6.0 km. This model requires more strongly magnetized bodies and has a central body having a magnetization of 2.8 A/m. These intrusive bodies could be placed further down the crust but it was found that at average depths of about 9 km and above, the model intrusive bodies require rather high values of magnetization reaching for the central body a value of 3.50 A/m at 9 km depth and 4.17 A/m at a depth of about 12.0 km. It was also found that beyond the depth of 8 km, it is no longer possible to account for all the short wavelengths in the profile.

5.3.5.2   Interpretation of Profile LB2

The profile LB2 is a NS profile across the Lower Benue Trough. The profile lies east of Kuri and passes through Udegi, Onugba, Boju and ends south of the town of Igumale. Like the profile LB1, it has been interpreted in terms of deep seated intrusive bodies at varying depths and of varying magnetization. Figures 5.11a, 5.11b, 5.11c and 5.11d show model intrusive bodies with depth to the top of the intrusive bodies progressively increased, required to account for the observed profile. The values of magnetization for the different bodies are also shown in the figure. The magnetizations of the model intrusives progressively increase as their depths increase. The prominent magnetic low in Figure 5.11a must be accounted for by an intrusive body whose top lies well within the sediments (2.0 km) and having a magnetization of 1.4 A/m. The model intrusive required to account for this prominent anomaly in Figures 5.11b and 5.11c have magnetization of 1.55 A/m and 1.75 A/m respectively. Figure 5.11d shows a model similar to that of Figure 5.11c but having the body accounting for the prominent anomaly at about the same depth as the other bodies. This body has a magnetization of 2.17 A/m.
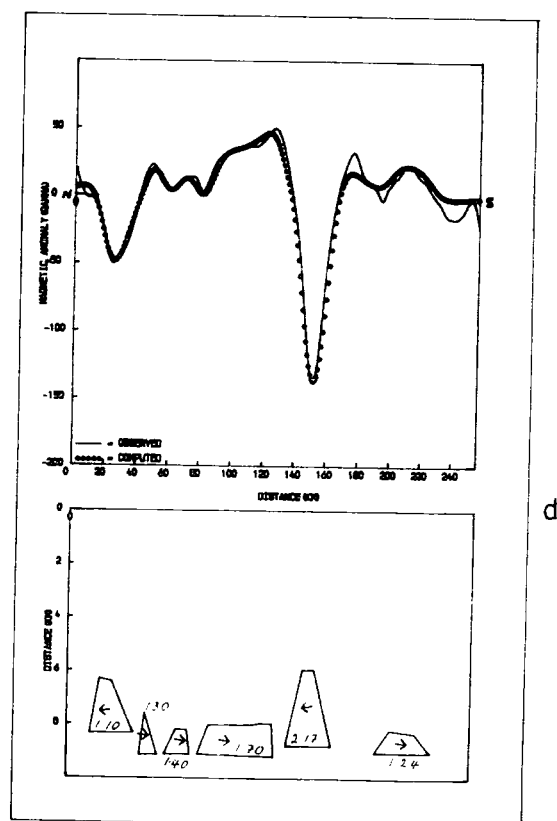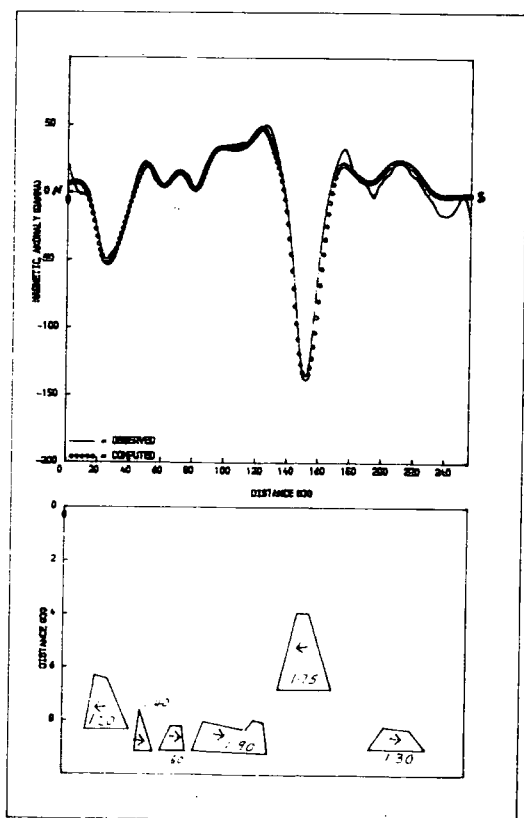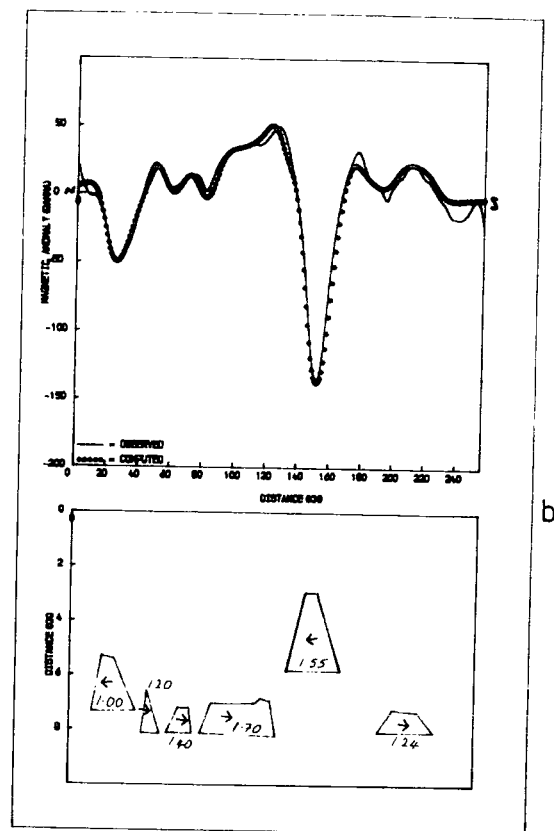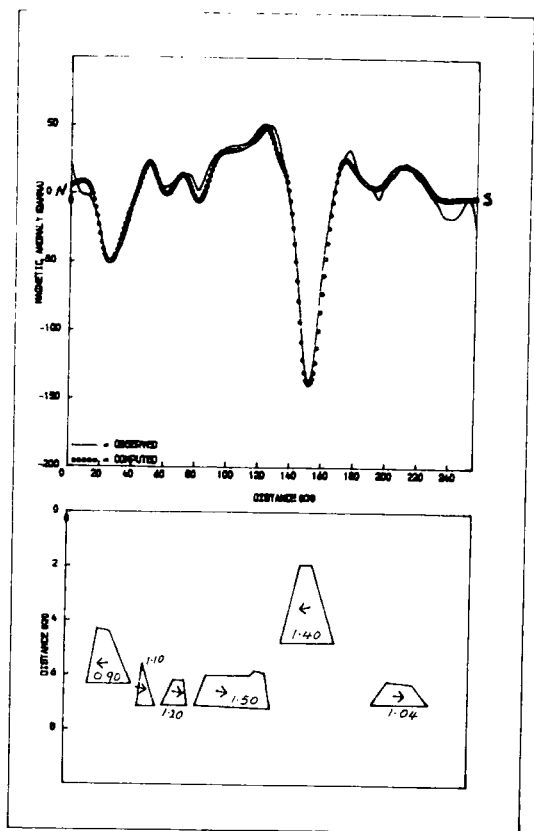
Figure 5.11   Possible interpretation of the profile LB2 in terms
of basic intrusive bodies.

5.3.5.3 Interpretation of Profiles LB3 and LB4

Profile LB3 is a NW-SE profile which passes through Imane, Odoba, Otukpa and Abakaliki. The profile LB4 on the other hand runs nearly parallel to the west of profile LB3 (Figures 5.5 and 5.7) and passes through Enugu-Ezike. Both profiles have been interpreted in terms of intrusive bodies of varying sizes and magnetization. The model intrusives are assumed to be magnetized in directions closely parallel to or opposite to the direction of the Earth's field. Figures 5.12a, 5.12b, 5.12c and 5.12d show possible model intrusives and their magnetizations required to account for the observed profile LB3. The causative intrusives in Figure 5.12a have their upper surfaces at an approximate depth of 1.7 km and magnetizations ranging from 0.61 A/m to 1.75 A/m. Figure 5.12b shows a model for which the causative bodies exist deeper within the crust with their top surfaces at approximately 3.8 km below the surface. The magnetization of the bodies range from 0.90 A/m to 2.01 A/m. Figure 5.12c represents the effect of further increasing the depth of the bodies required to account for the profile LB3. The bodies here are about 5.0 km below the surface and have magnetization values lying between 1.05 A/m and 2.23 A/m. With the bodies at a depth of about 7.30 km (Figure 5.12d) magnetization values of 1.30 A/m to 2.61 A/m were needed to account for the observed anomaly.

The several possible models of intrusions required to explain the profile LB4 are shown in Figures 5.13a, 5.13b, 5.13c and 5.13d. The intrusive bodies of Figure 5.13a have their top surfaces at depths of between 1.50 km and 3.80 km and magnetization ranging from 1.10 A/m to 2.20 A/m. Figures 5.13b, 5.13c and 5.13d show the same set of bodies at greater depths. The bodies in Figure 5.13b are at depths of 3.50 km to 5.40 km and have magnetization values lying between 1.12 A/m and 2.75 A/m. The magnetization values of the intrusive
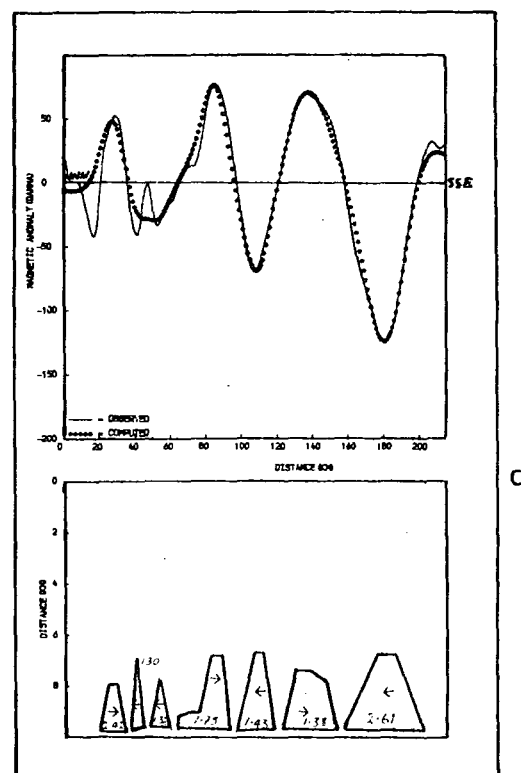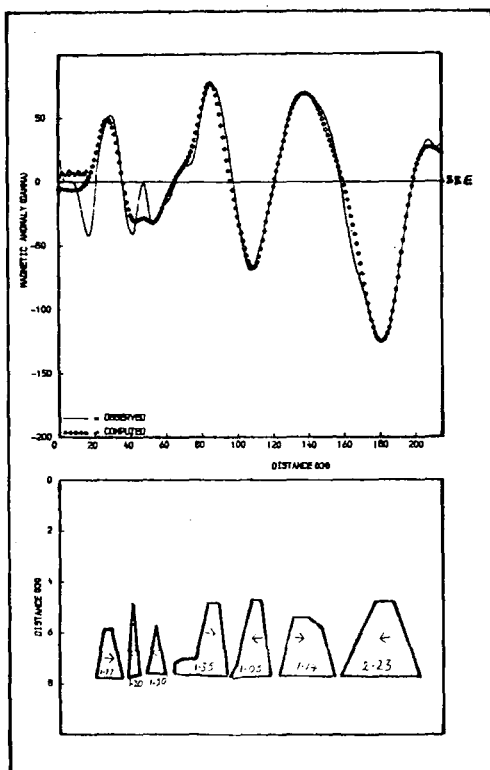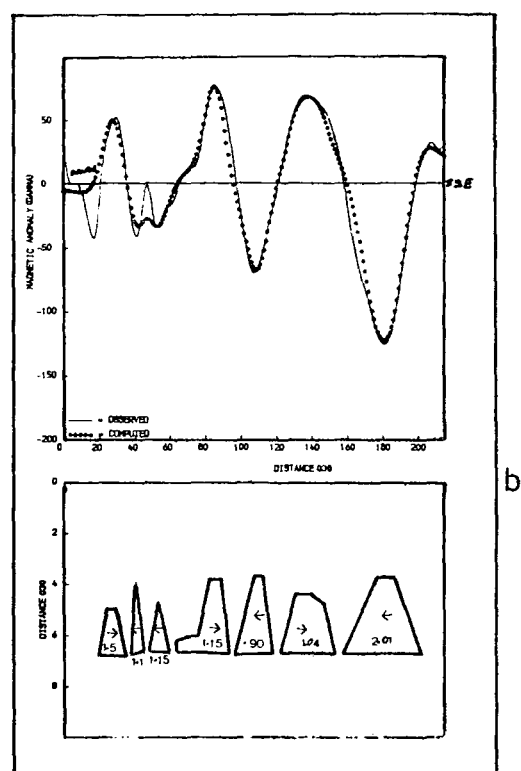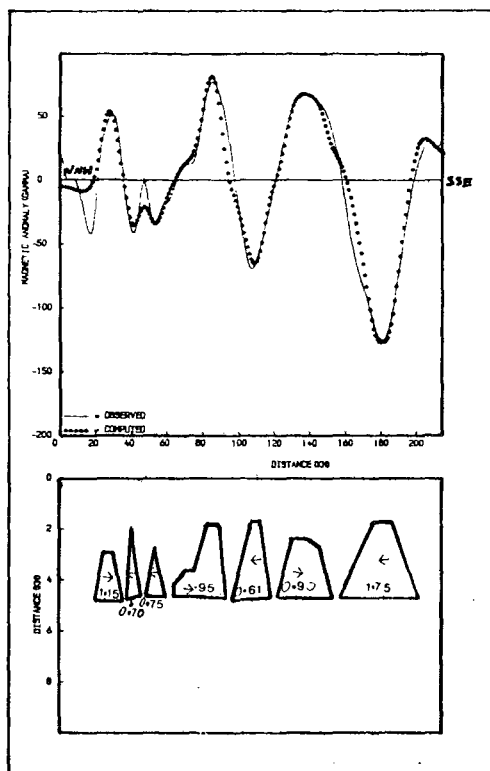
Figure 5.12   Possible models required to explain the profile LB3
in terms of intrusive bodies.
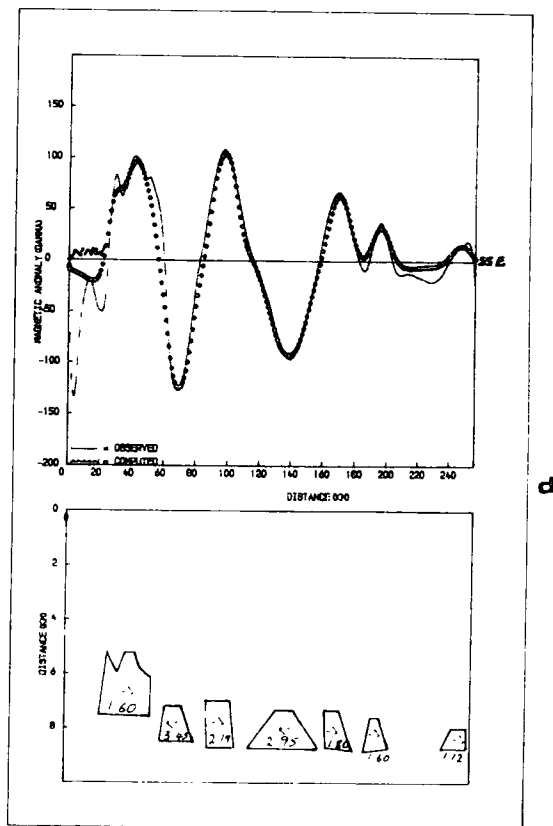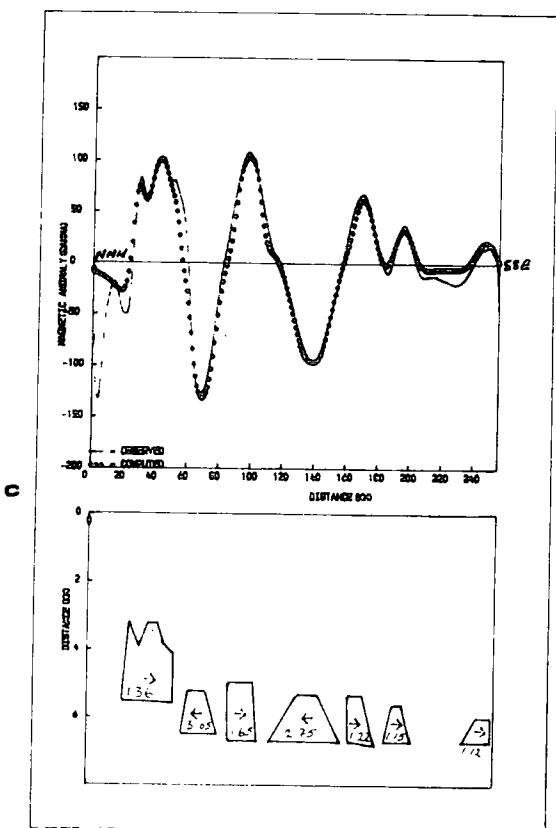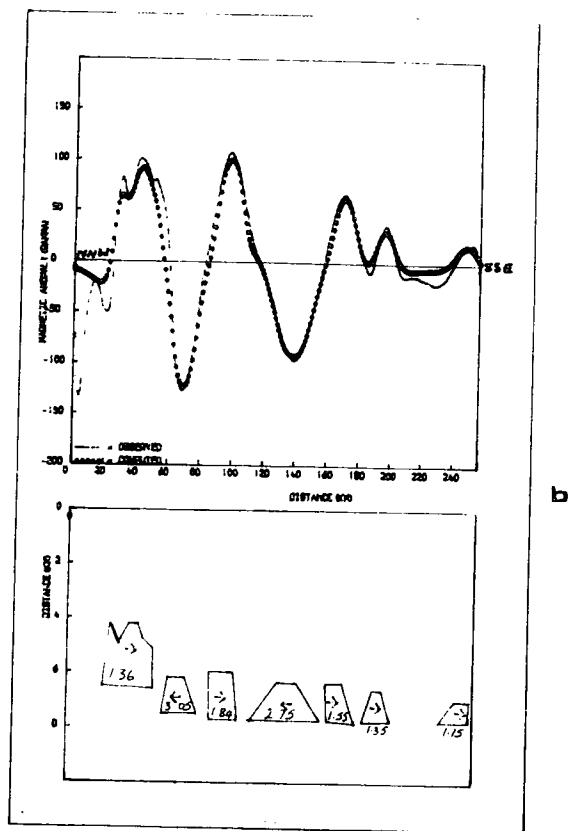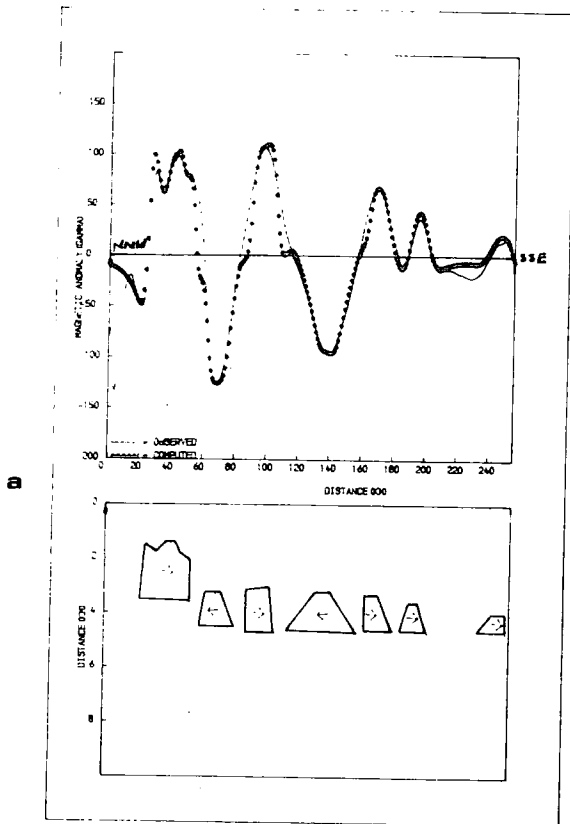
Figure 5.13   Possible moa⸗ls required to account for the profile
LB4 in terms of intrusive bodies.

bodies in Figure 5.13c range from 1.12 A/m to 3.05 A/m while the bodies modelled in Figure 5.13d which are at depths of the order of 7.0 km have magnetization values ranging from 1.12 A/m to as high as 3.45 A/m.

5.3.5.4   Interpretation of Profile MB1

Possible interpretations of the profile MB1 (Figure 5.7) are given in Figures 5.14a, 5.14b, 5.14c and 5.14d. The profile traverses the Awe area within which near surface basalt flows have been reported (Cratchley and Jones, 1965). The lack of conspicuous short wavelength anomalies suggests that the near surface lavas do not cause the main anomaly but it could be caused by related deeper-seated intrusions extending to depth beneath. The fact that the basalts seen on the surface around Awe are Tertiary in age (Cratchley and Jones, 1965) may however rule out any relationship between the model bodies required to account for the anomalies and the surface basalts seen in the area. The profile however, is here interpreted in terms of intrusive bodies existing either very close to the surface, deep down the sedimentary basin and beyond. Figure 5.14a shows a set of model bodies explaining the observed anomaly. Figure 5.14b shows a similar model to that of Figure 5.14a but with the thickness of the bodies reduced. This however, led to an appreciable increase in the magnetization values of the bodies with the central body now having a magnetization of 3.13 A/m. Figures 5.14c and 5.14d represent models for which the causative bodies are made to lie well below the surface.

5.3.5.5   Interpretation of Profiles MB2 and MB3

Profile MB2 is a NS profile in the Middle Benue Trough (Figure 5.5) which passes through Gaji, Bashar, Dinya, Amar and Dampar and
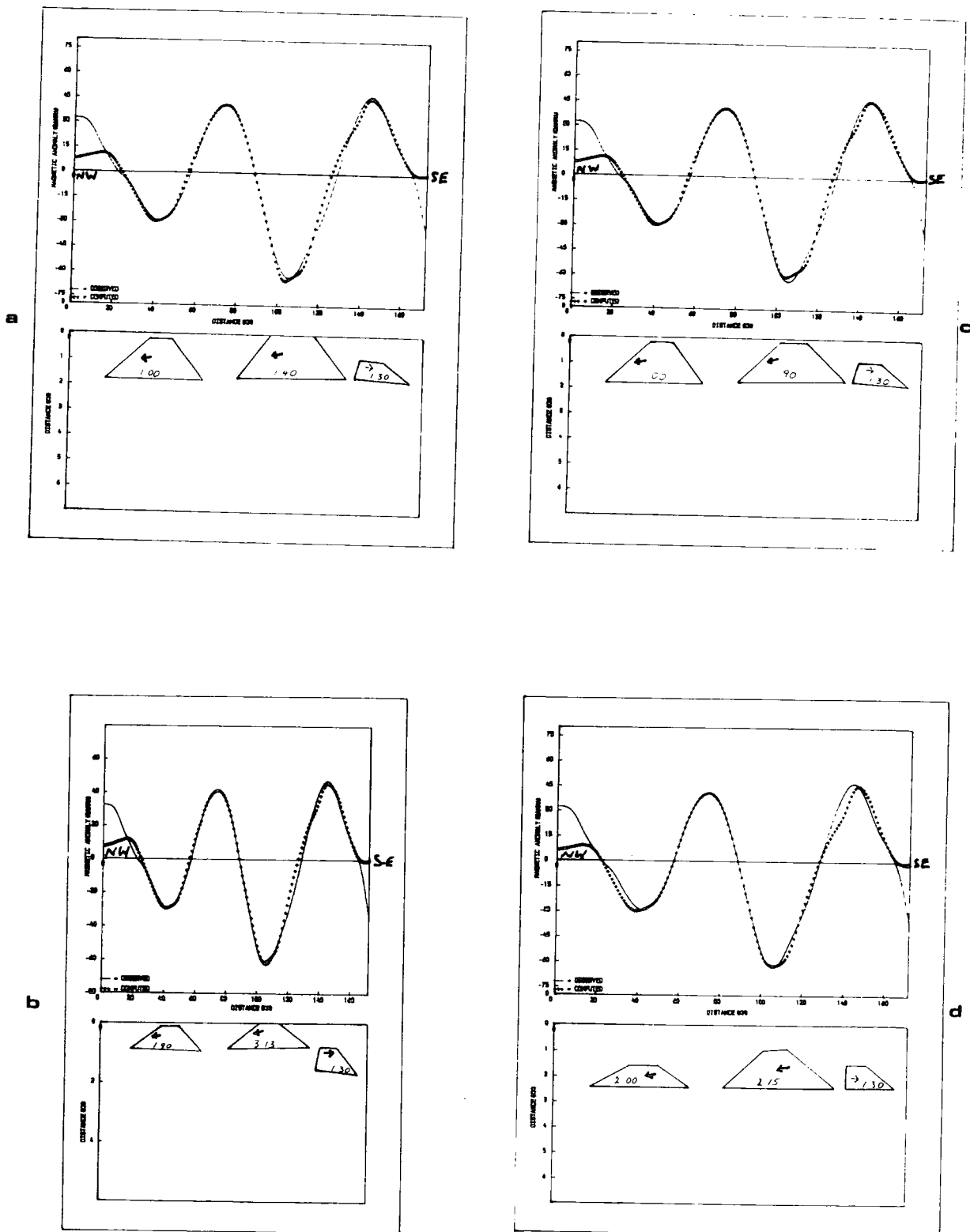
Figure 5.14 Possible interpretation of the profile MB1 in terms
of intrusive bodies.

ends south of Batanji. The profile MB3 on the other hand, passes

through Lantang and Amar (Figure 5.5). Both profiles have been

interpreted in terms of basic intrusive bodies which could lie either

within the sedimentary rocks or deep down the crust. The size and

magnetization of the bodies are variable and all directions of

magnetization have been confined to be closely along or opposite to,

the direction of the Earth's field. An interpretation of the profile

MB2 in terms of intrusive bodies which are about 300 m below the

surface are given in Figure 5.15a. A minimum of five different

intrusive bodies was required to account fully for the observed

profile. The large central body required in this model has a

magnetization of 2.31 A/m. Figure 5.15b shows a model for the

profile MB2 for which the causative intrusive bodies exist at depths

of the order of 2.0 km. The large central body here requires a

magnetization of 2.50 A/m and all other bodies in the model have

magnetization lying between 1.10 A/m and 1.76 A/m. With the

intrusive bodies required to account for the observed anomaly

profile MB2 at a depth of nearly 4.0 km, their magnetization values

lie between 1.70 A/m and 2.80 A/m (Figure 5.15c). Figure 5.15d shows a

model for which the intrusive bodies are below 6.0 km of the surface.

The magnetization values here range from 2.32 A/m to 3.10 A/m. The

central body under Amar is here assigned a magnetization of 3.10 A/m.

Figures 5.16a, 5.16b, 5.16c and 5.16d show model intrusive

bodies at varying depths required to account for the observed

anomaly MB3. The large central body which forms part of each of

these models lies adjacent to the magnetic high over Amar (Figure 5.5)

and is coincident with the central body of profile MB2 which also

coincides with the magnetic high over Amar. The model intrusive

bodies of Figure 5.16a exist at about 3.0 kms below the surface and

have their magnetization in the range of 1.00 A/m to 2.11 A/m for the

central body under Amar. Figure 5.16b represents a model for
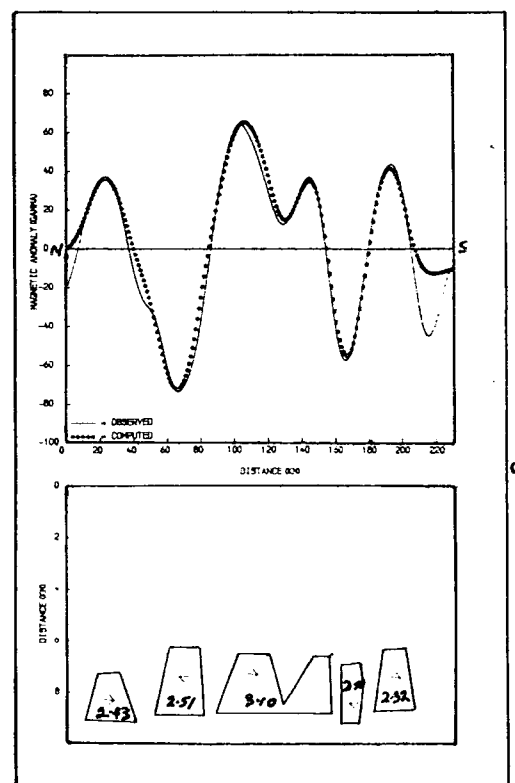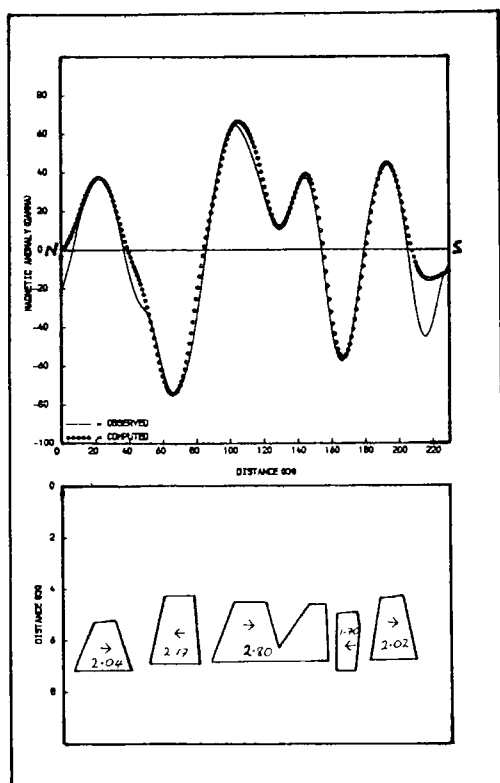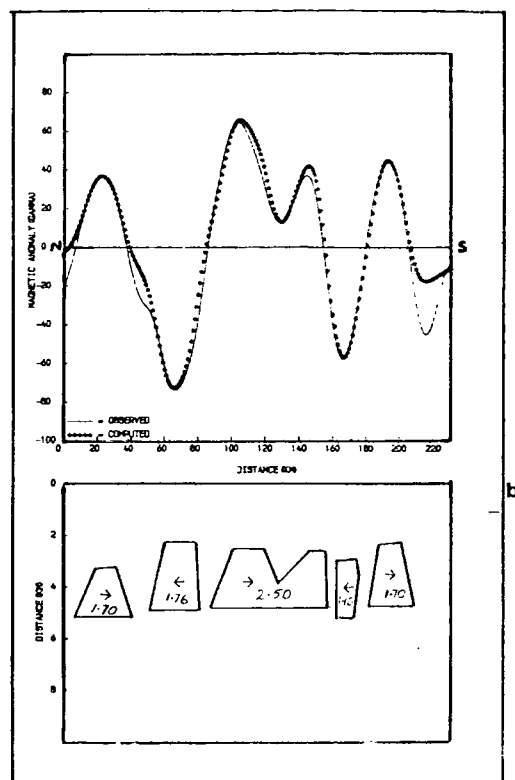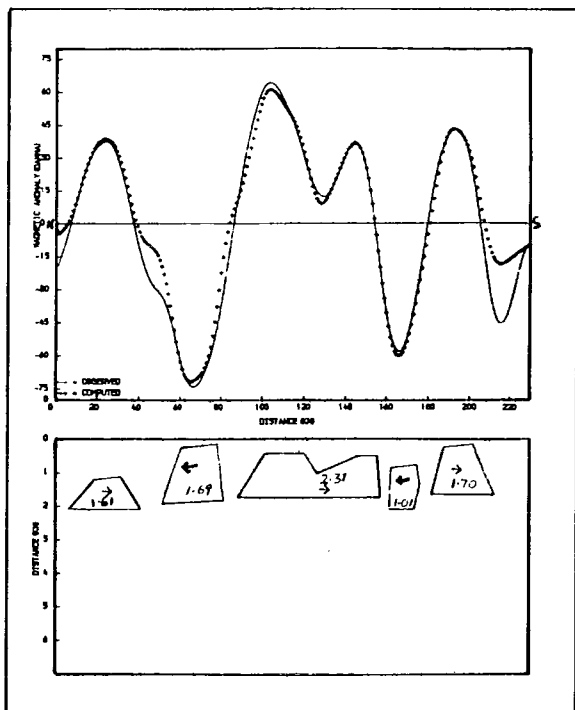
Figure 5.15   Possible models required to explain the profile MB2
in terms of basic intrusive bodies.
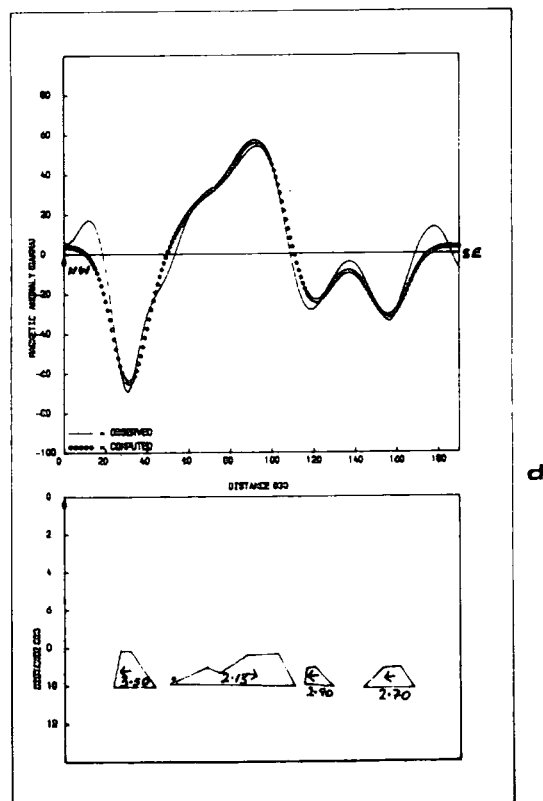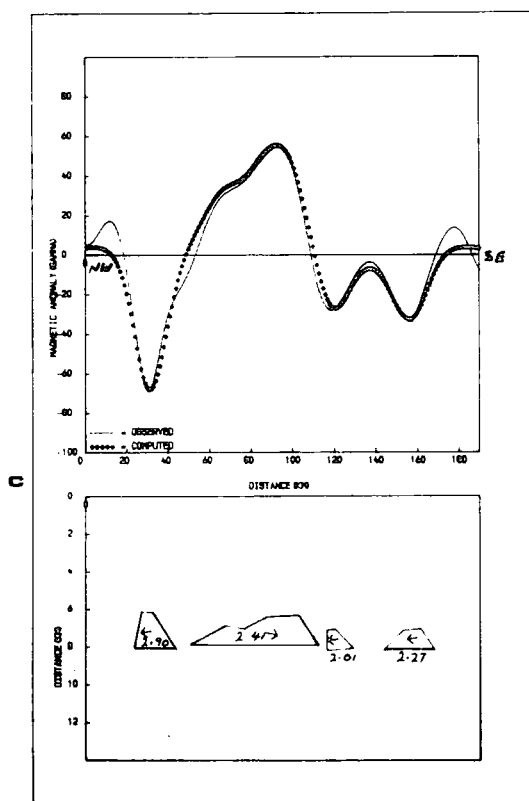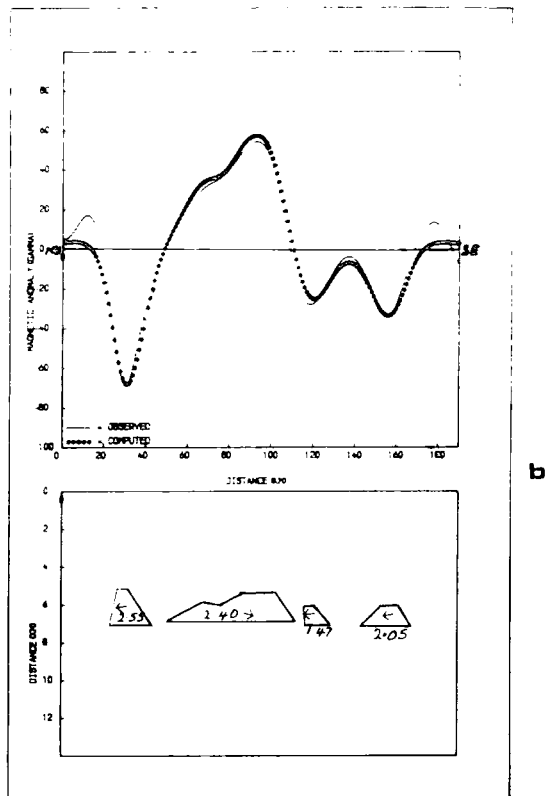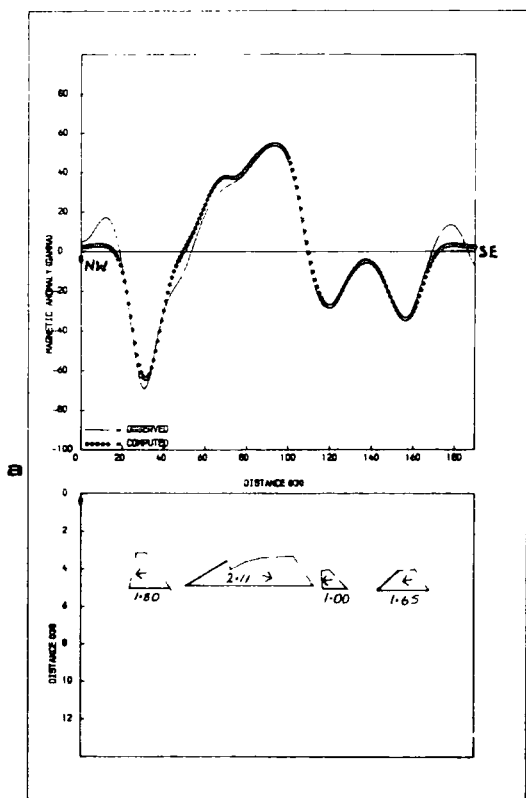
Figure 5.16   Possible interpretations of the profile MB3 in terms
              of intrusive bodies.

which the intrusive bodies needed to account for the observed
anomaly profile MB3 are about 5.0 km below the surface and
magnetization values here range from 1.47 A/m to 2.55 A/m. The
magnetization values in the case of the models in Figure 5.16c
range from 2.01 A/m to 2.90 A/m and with the intrusive bodies below
8.0 km of the surface the magnetization of the model bodies lie
between 2.70 A/m and 3.50 A/m (Figure 5.16d).

5.3.5.6   Interpretation of Profiles MB4 and MB5

Profile MB4 is the Shendam-Donga profile which passes through
Shemanker and Jobu. Profile MB5 lies to the west of Lafia and passes
through Udei, Keana and Akpagher, west of Gboko (Figure 5.5). Like
all other profiles, both profiles have been interpreted in terms of
basic intrusive bodies of varying magnetization. The different
possible models required to explain the profile MB4 are given in
Figures 5.17a, 5.17b, 5.17c and 5.17d. The magnetization values of
the bodies are also given.

Profile MB5 has been interpreted in terms of a combination of
intrusive bodies and a sill which is known to exist south of the
town of Lafia (Offodile and Reyment, 1978). The model required to
account for this profile is shown in Figure 5.18. The model sill has
a magnetization of 2.01 A/m and is less than 200 m from the surface.

5.3.5.7   Interpretation of Anomalies in terms of a Single Body Model

The possibility of interpreting the magnetic anomalies over the
Lower and Middle Benue in terms of a single body, has been
investigated. The profile LB1 was re-interpreted in terms of a single
body which could either be at a shallow depth or at a great depth.
Figure 5.19a shows such a model body at a shallow depth. The body
of the model in Figure 5.19a has a magnetization of 1.20 A/m and in
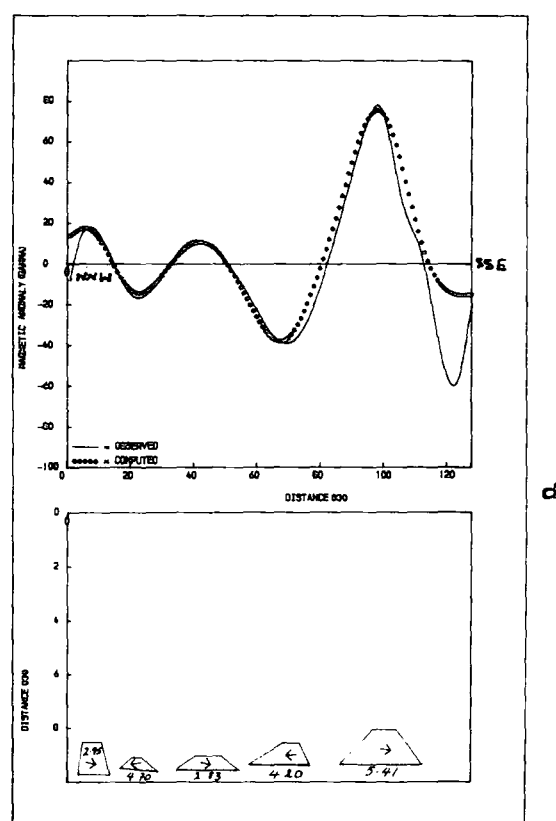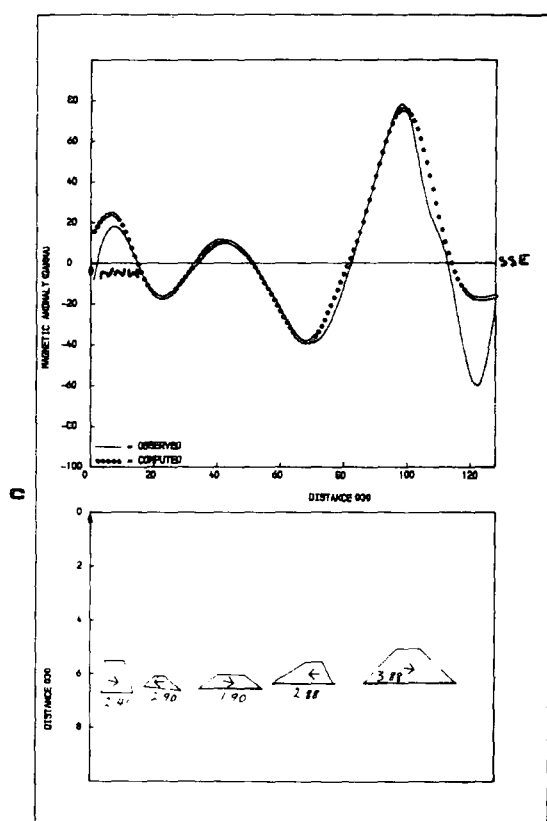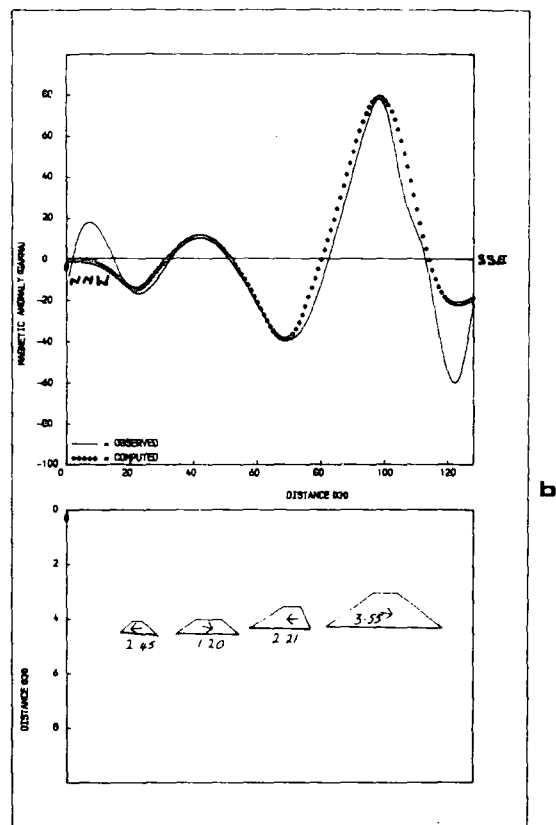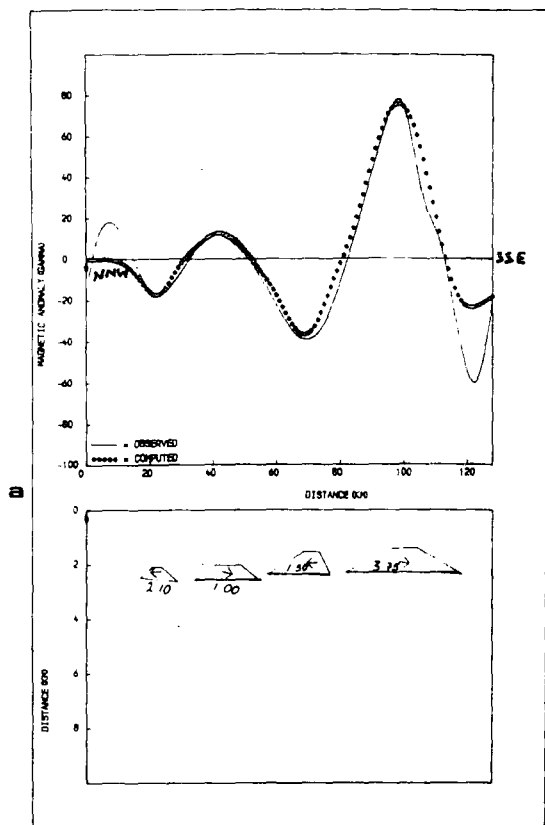
Figure 5.17   Possible interpretations of the profile MB4 in terms
of intrusive bodies.
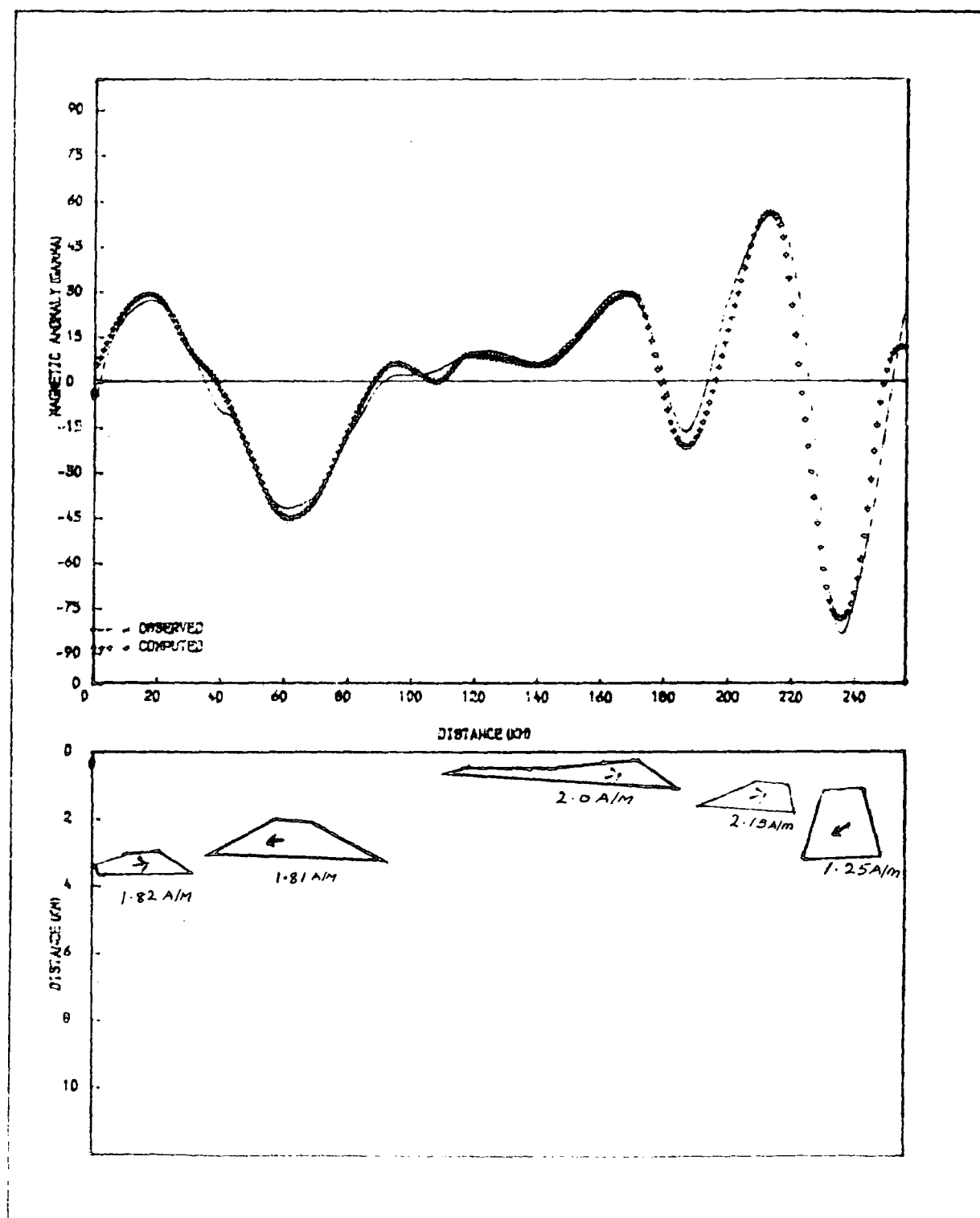
Figure 5.18 An interpretation of the profile MB5.
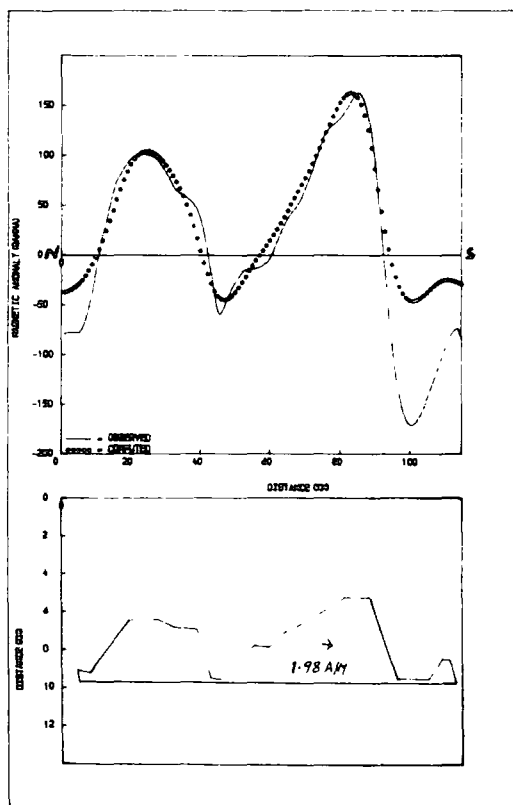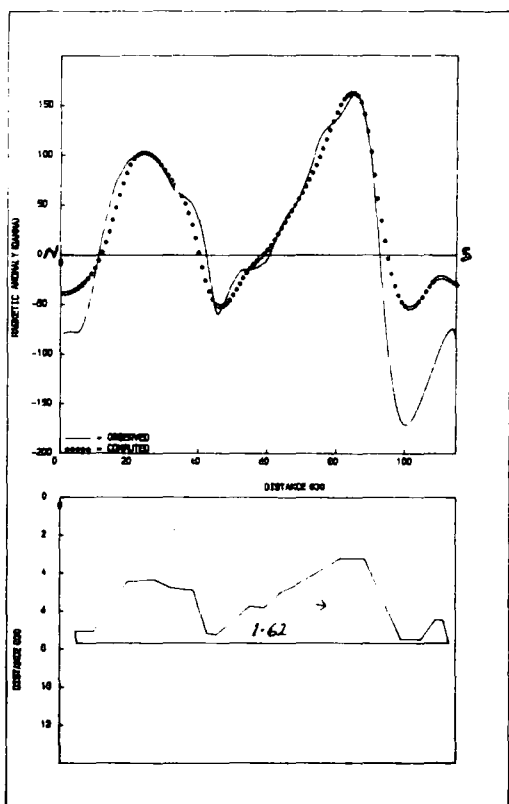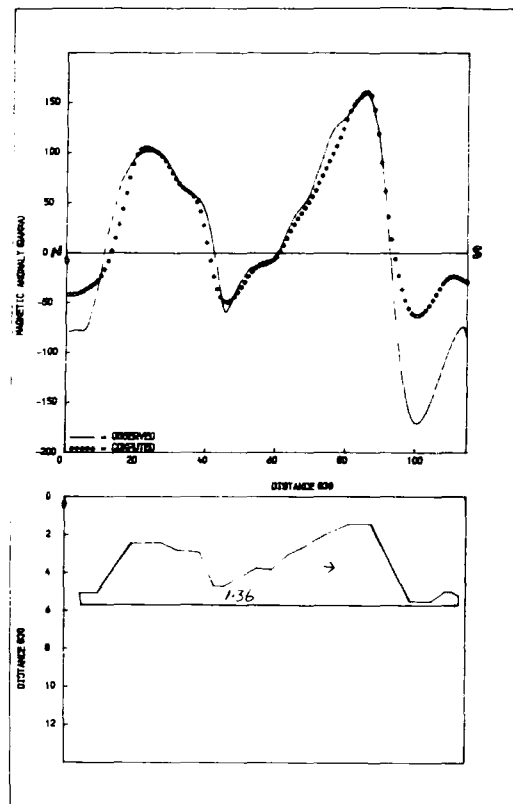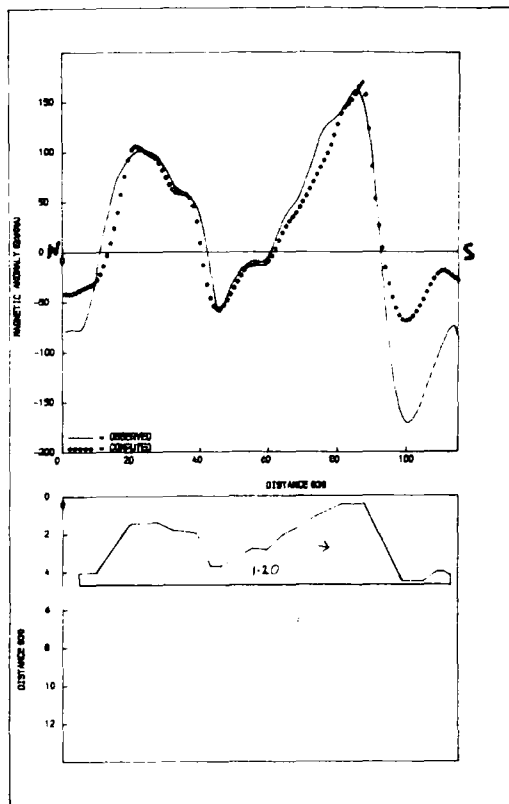
Figure 5.19   Possible interpretations of the profile LB1 in terms
of a single body.

places comes as close as 0.40 km to the surface. The mismatch to the
right of the profile is suggestive of the fact that at least two sep-
arate bodies would be required to account for the anomaly at this
depth. The position of the body required to explain the observed
anomaly was changed by increasing the depth and consequently
increasing the magnetization and changing some dimensions of the body.
It was found that with the causative body at a minimum depth of 2.0 km
a magnetization of 1.36 A/m was needed for the model body (Figure 5.19b).
Obtaining an adequately good fit for the magnetic low in the middle
of the profile however, becomes increasingly difficult as the body becomes
deeper. Figure 5.19c shows this for a model of a causative body at
about 4.0 km depth with a magnetization of 1.62 A/m. In figure 5.19d
it is about 6.0 km deep with a magnetization of 1.98 A/m. It becomes
difficult to obtain a good fit in the middle and at the right end of
the profile. This suggests more than one body in agreement with the
previous interpretation of the profile (Section 5.3.5.1). Although
the use of a shallower body may have improved the fit over the middle
of the profile, it would have also led to greater misfit over other
sections of the profile.

5.4   Interpretation of Minor Features in the Area

In addition to long wavelength magnetic features over the
Lower and Middle Benue, there are several minor features scattered
over the area. These anomalies have been interepreted in terms of
thin dykes and volcanic plugs. The dykes modelled hardly exceeded
50 m in thickness and have depths varying from the surface to few
tens of metres. These minor features have been interpreted using
non-linear optimization techniques (Chapter One). The anomaly close

to the town of Buruku has been interpreted in terms of a volcanic

plug (Figure 5.20) of thickness 0.46 km and existing at a depth of

0.60 km below the surface. The model body has a magnetization of

2.91 A/m inclined at -7.17°. The striking anomaly over Mkar has been

interpreted both in terms of a massive dyke (Figure 5.21a) and in

terms of a massive intrusive body (Figure 5.21b) exposed at the

surface in each case. This anomaly coincides well with the Mkar

Hill, about 7.0 km east of Gboko, which rises about 270 m over the

surrounding plane. The model dyke of Figure 5.21a has a thickness

of 1.15 km. The model intrusive plug in Figure 5.21b has a thickness

of 1.85 km and a magnetization of 0.6 A/m inclined at -31.82°.

5.5 Pseudogravtiy Transformation of the Magnetic Anomalies over Lower and Middle Benue

The aeromagnetic profiles interpreted in Section 5.3 were

transformed using the program MGRAV, the theory of which is described

in Chapter One (1.4), to obtain the corresponding pseudogravity

anomalies. This transformation was carried out with a view to

comparing the resultant pseudogravity anomalies with the observed

gravity anomalies over the trough. Good gravity data on the trough

was not, however, available and this pseudogravity study ended with the

computation of the pseudogravity anomalies. The results of the

transformation of the observed aeromagnetic profiles LB1, LB3, LB4 and

MB2 and distribution of blocks used for their transformation are shown

in Figures 5.22a, 5.22b, 5.22c, and 5.22d. It is hoped that the

results of this pseudogravity transformation will be found useful in

any future work on the Benue Trough when adequate gravity data becomes

available.
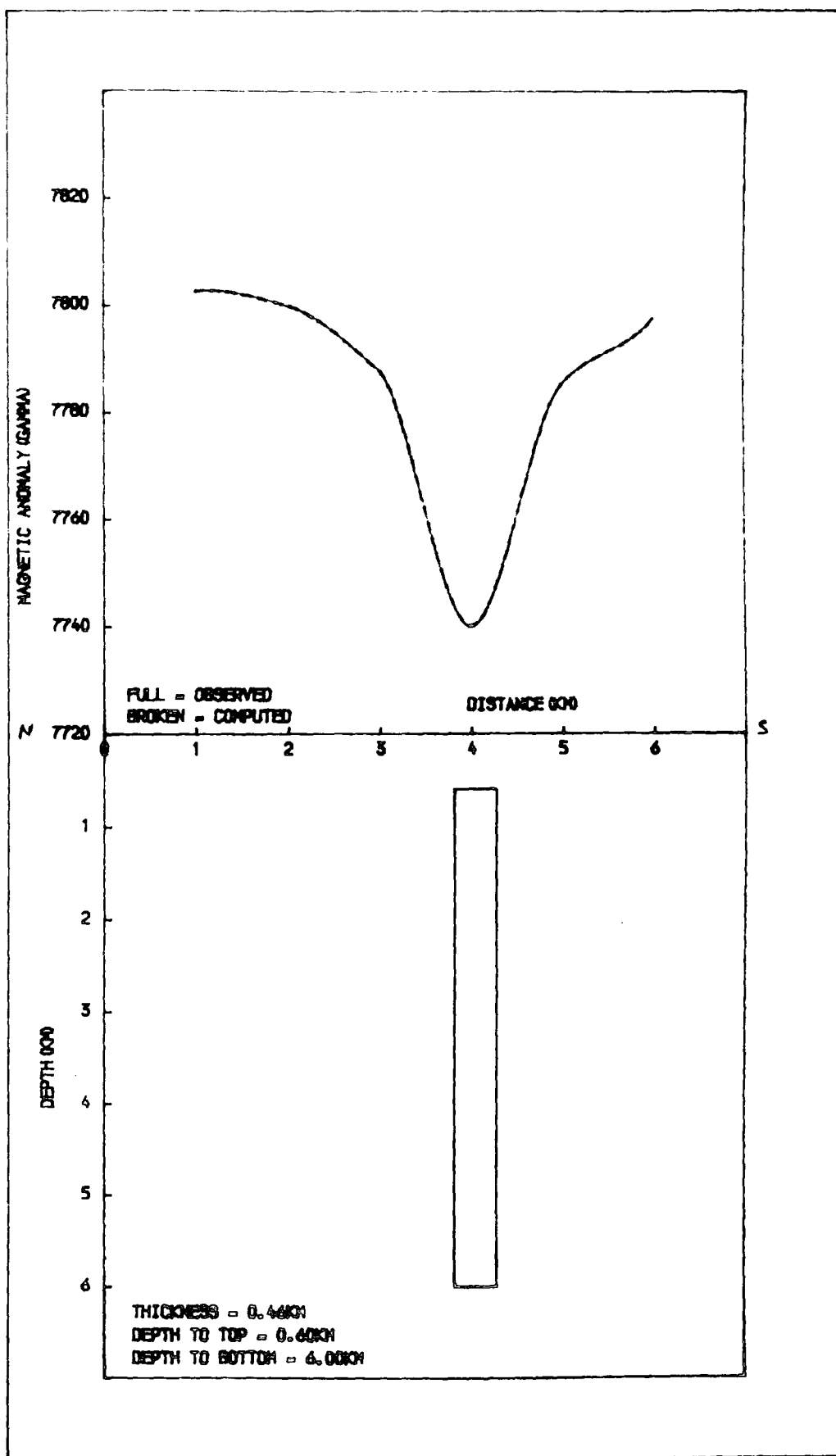
Figure 5.20 An interpretation of the Buruku anomaly in terms of
a volcanic plug.
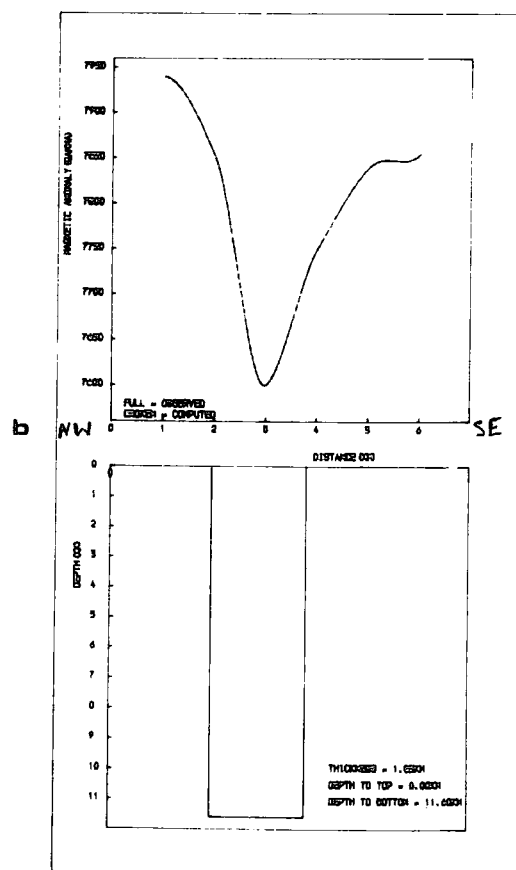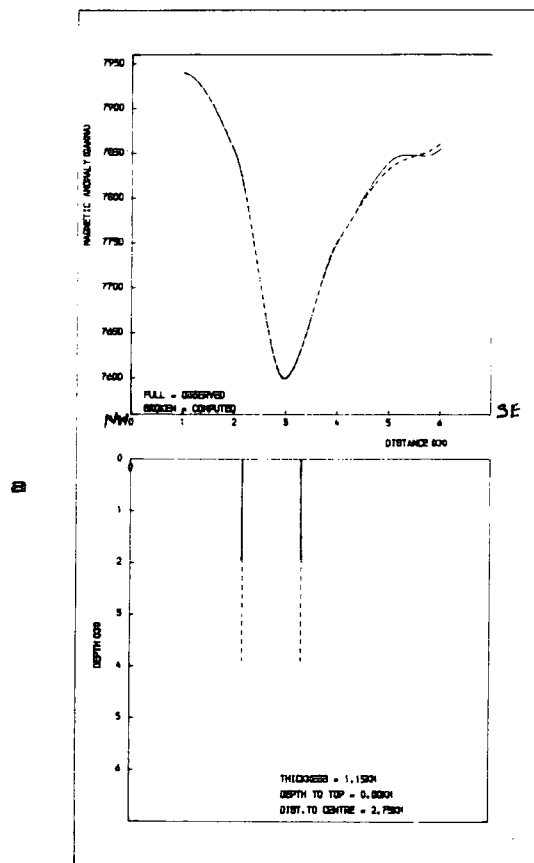
Figure 5.21   Possible models to explain the Mkar anomaly.
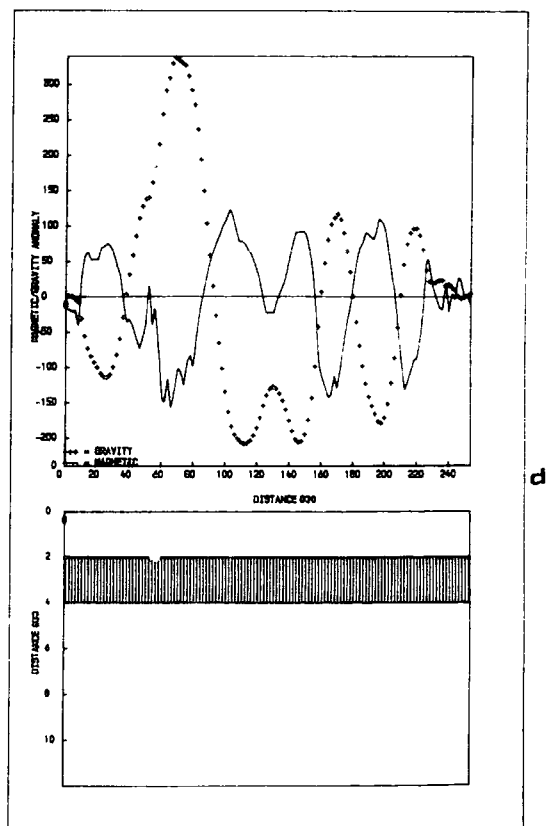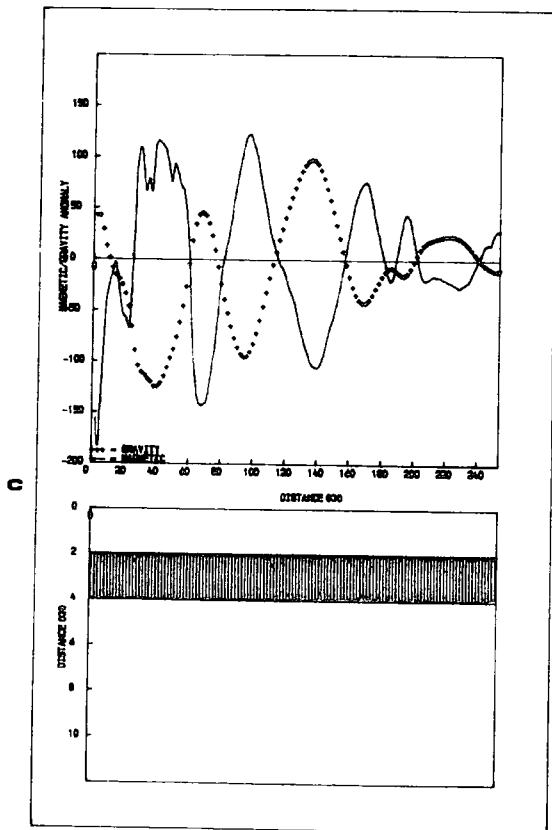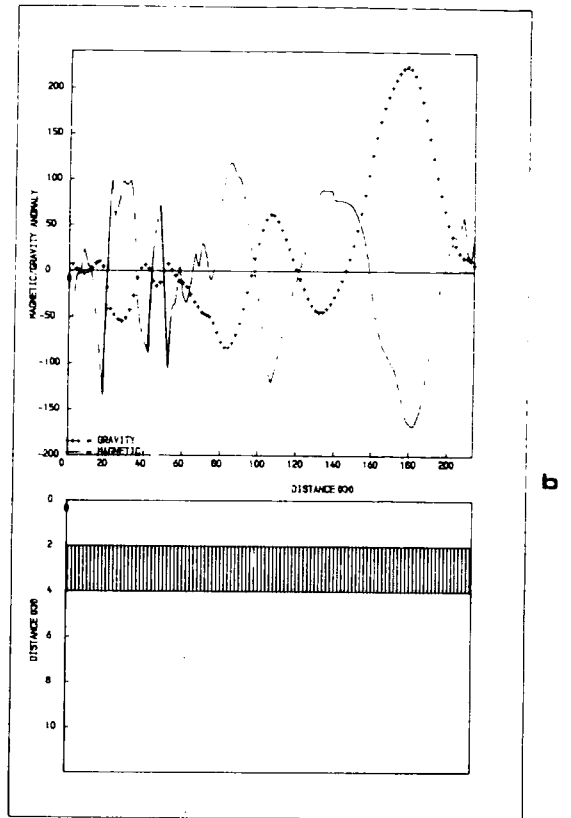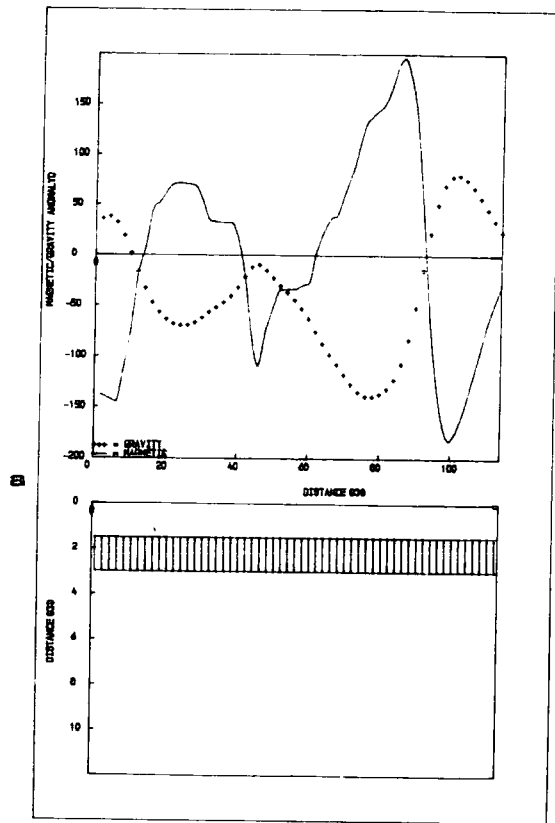
Figure 5.22   Results of the pseudo-gravity transformation for the
profiles LB1, LB3, LB4 and MB2.

5.6 Discussion of Interpretations and a Model on the Tectonic Evolution of the Benue Trough

The results of the interpretation described above suggest that the magnetic anomalies over the Lower and Middle Benue are best accounted for by intrusive bodies existing beneath the trough. It was found that the magnetization of the bodies modelled here for all the profiles on the average lie between 1.5 A/m and 3.40 A/m although a few cases of magnetization below 1.0 A/m and above 4.0 A/m were obtained and $\overset{the\ bodies}{\wedge}$ have an average width of about 10 km. These bodies may exist predominantly within the basement or within the sedimentary basin.

These intrusive bodies may possibly extend to greater depths than shown in the plots, but without greatly affecting the conlusions drawn. The model intrusive bodies required to account for the magnetic anomalies over the Lower and Middle Benue are probably of basic composition (gabbroic).

The interpretation in terms of intrusive bodies can be justified from the available geological information on the trough. Outcrop of sediments from SW Gboko to Awe contain numerous minor intrusions whose composition range from intermediate to basic. Furthermore, the positive gravity anomaly over Gboko has been interpreted in terms of an intrusive body of probably intermediate composition having a width of 30 km and a thickness of 5 km. This intrusive body may be associated with some of those modelled in the present study.

The results of the present study are in good agreement with the interpretation of gravity anomalies over the trough (Cratchley and Jones, 1965, Adighije, 1981b). Cratchley and Jones (1965) interpreted the positive anomaly over Amar which is typical of the Benue Trough in terms of a zone of basic intrusive which may lie either within the basement or with the sedimentary rocks. Additional positive anomalies

which flank the elongated negative anomalies on either side of the axial positive anomaly. These and other minor positive anomalies over the Trough (Figure 5.23) may be due to additional basic intrusive bodies within either the basement or the sedimentary rocks (Cratchley and Jones, personal communication). There is also a close agreement between the positioning of the central intrusive body modelled by Cratchley and Jones (1965) and the large intrusive body which characterises most of the interpretations presented in this Chapter. Adighije (1981b) has also explained the central positive gravity anomaly in terms of an intrusive body at depth in the crust which extends northwards for about 350 km from Abakaliki. This intrusive body is probably of gabbroic composition on account of its inferred density of about 2.90 gm cm^{-3}. Support for the basic intrusive bodies can also be found from the results of studies over various rift systems such as the Baikal Rift and the Rift Valley in Kenya.

From an interpretation of airborne magnetometer measurements over the Upper Rhine Graben, Bosum and Hahn (1967, 1970) have suggested the existence of underlying intrusive bodies, probably of basic compositon. These bodies have their top surfaces at variable depth of between 400 m and 3000 m. Roche and Wohlenberg (1970) have also interpreted the aeromagnetic anomalies over the Alsace, Baden and Pfalz areas of the Rhine Graben in terms of rocks with high magnetic susceptibility, probably of basic composition with roofs about 2 km below the surface and having widths in the range of 6 - 10 km. A magnetic profile between Kaiserslautern and Stuttgart shows a prominent anomaly which has been interpreted in terms of a dyke-shaped intrusive body along marginal faults of the Rhine Graben (Roche and Wohlenberg, 1970).

The presence of intrusive bodies in the Baikal Rift has been demonstrated from both gravimetric and magnetometric data (Zorin,

(a) Profile A-B across the Gboko anomaly

(b) Profile C-D across the Awe anomaly

(c) Profile E-F across the Amar anomaly

(d) Profile E-F. Residual and Free Air anomalies

MILES

KILOMETRES
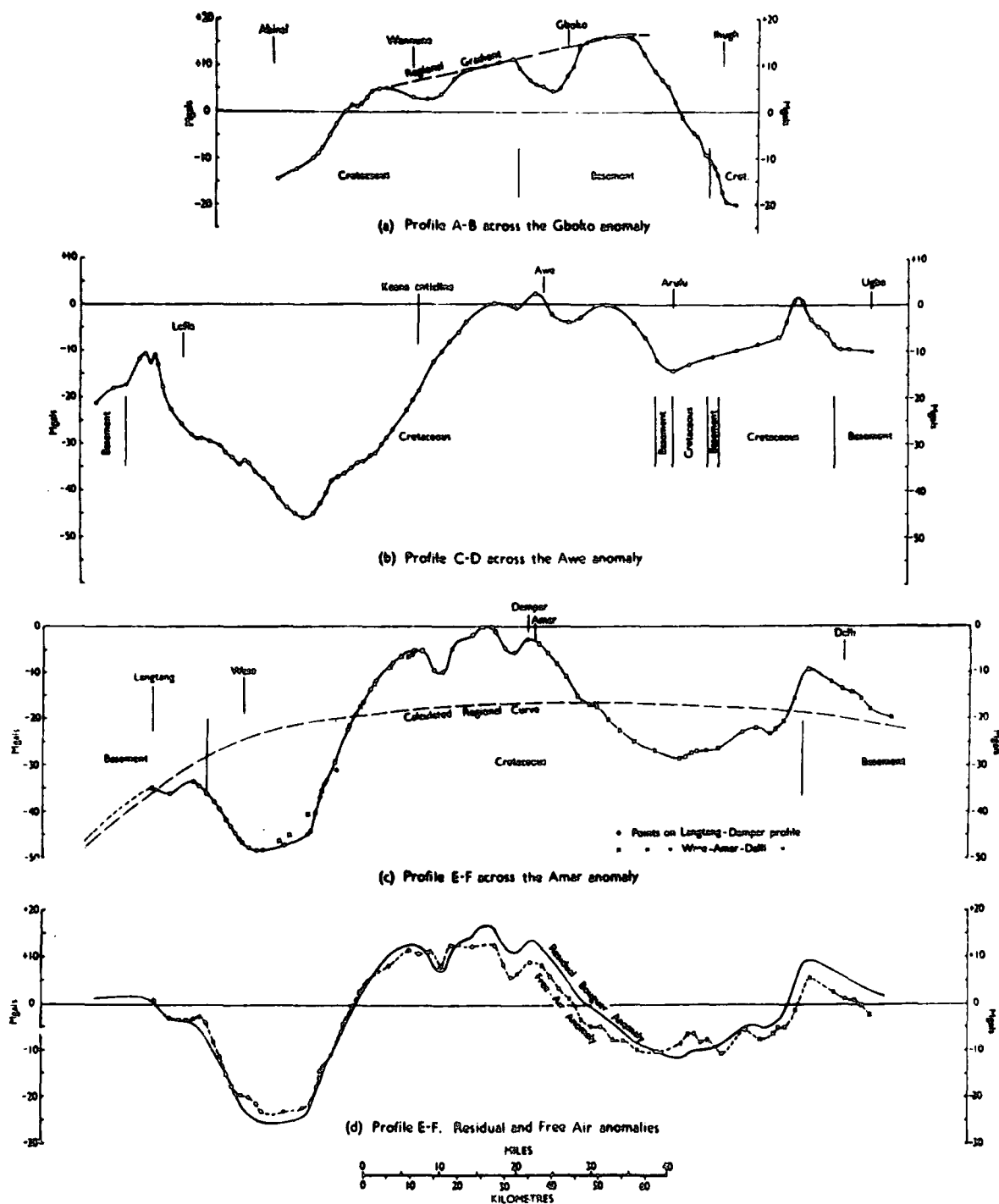
Figure 5.23   Bouguer anomaly profiles across the Benue Trough
              (After Cratchley and Jones, 1965).

1971; Zorin and Rogozhina, 1978; Zorin, 1981). Zorin et al. (1975) have also interpreted observed geothermal anomalies over the Baikal Rift depression in terms of linear intrusive bodies of the form of vertical dykes within the underlying crust. However, these bodies occur within the lower, more dense part of the crust and may imply that the intrusions may be more dense than normal gabbro (Zorin, 1971).

Searle (1969, 1970) from an interpretation of gravity and magnetic anomalies over the Rift Valley in Kenya, has suggested the existence of dense intrusive bodies underneath the Rift Valley (Figure 5.24) whose upper surface may be as close as 2 km from the surface. The model intrusive bodies are probably gabbroic due to its density of 2.90 gm cm^{-3}.

The magnetic anomalies over the Lower and Middle Benue Trough are most probably caused by sizeable intrusive bodies of basic composition. The existence of such bodies has implications for the evolution of the Benue Trough. An attempt is now made to explain the tectonic evolution of the Benue Trough, taking into account the models obtained from the interpretation of the magnetic anomalies.

5.6.1 A Tectonic Model for the Evolution of the Benue Trough, Nigeria

Rift Valley systems represent one of the main structural features of the continental crust. In many cases, they are formed in updomed regions associated with strong tensile stresses and accompanied by basaltic volcanism which suggests the existence of an anomalously hot mentle underneath. Recent studies of continental rifts such as the Baikal Rift and the Rhine Graben have shown that associated with this updoming is an intrusion of materials of probably asthenospheric origin into the lithosphere and a thinning of the crust (Zorin, 1981; Zorin et al., 1975, Zorin and Rogozhina, 1978; Artyushkov, 1981; Neugebaure and Temme, 1981; Burke, 1978; Bott, 1976, 1981; Searle, 1969, 1970). Significant
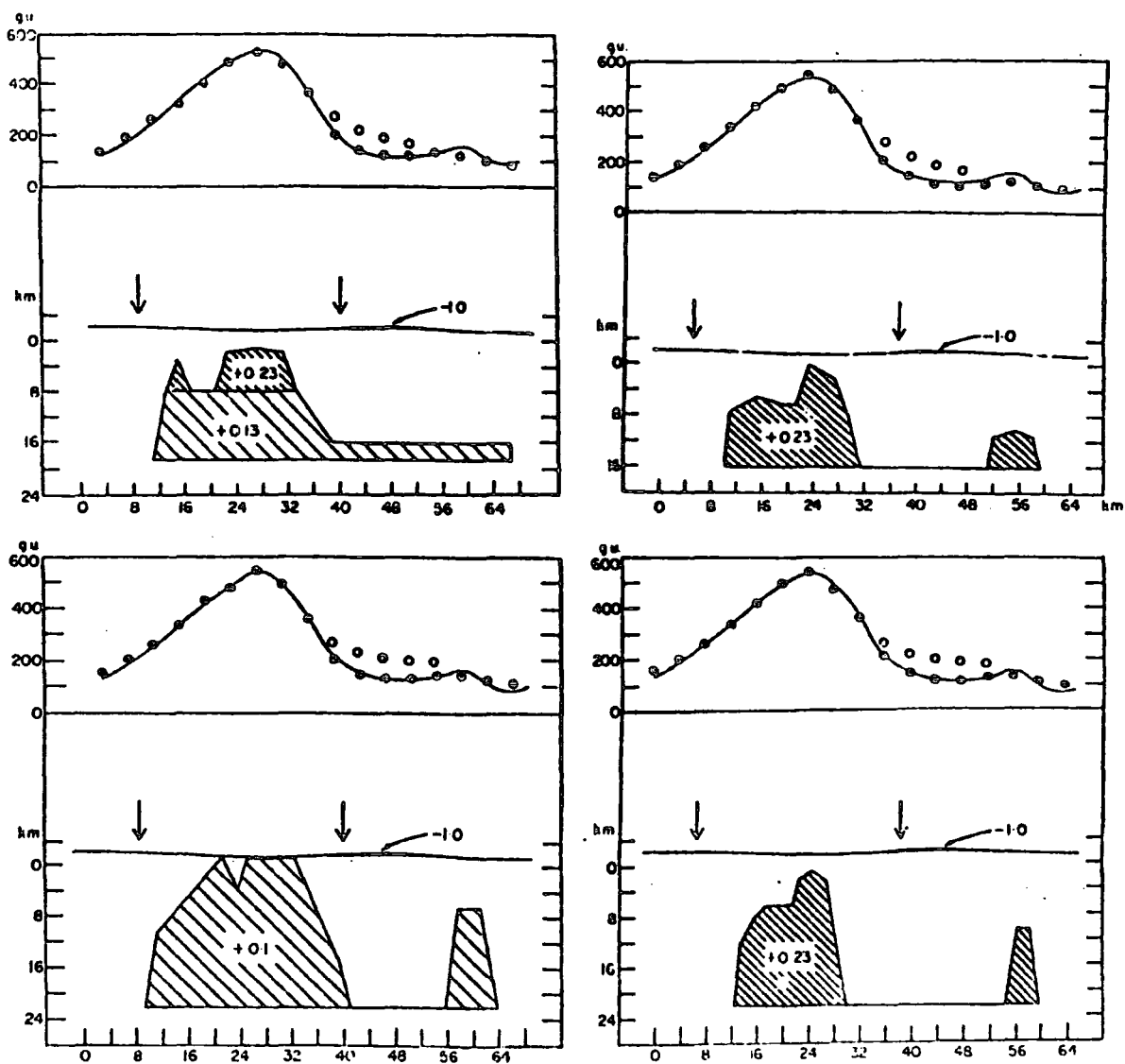
Figure 5.24   Possible models to account for the gravity anomaly
over the Rift Valley in Kenya (After Searle, 1970).

gravity, magnetic, seismic and heat flow anomalies and the frequent association of asthenospheric intrusions, volcanism and volcanic centres in time and space indicate an intimate relationship between mantle updoming, igneous activity and the mechanisms of rift genesis.

Most of the present day ideas on the mechanism of graben formation and continental rift genesis are based on the wedge subsidence hypothesis originally put forward by Vening Meinesz (1950) and modified by Bott (1976). From an analysis of the energy budget of the process of wedge subsidence, Bott (1976) has shown that the tensile stress needed to cause a subsidence with sediment infill up to 5 km or more must be a continually renewable one, persisting throughout the process of rifting. Bott estimated that a basin subsidence of about 5 km with sediment fill requires tensile stresses of the order of 1 to 2 Kbar.

Upwelling of mantle material with excess mantle pressure is capable of inducing thermo-mechanical stresses on the lithospheric plate. Bhattacharji and Koide (1978) studied the resulting stress contours and elastic displacement vectors, and showed that an area of relative subsidence would generally occur in the centre of the domal uplift. This could later evolve into an elongated rift valley bounded by marginal inward dipping faults. However, tensile stresses associated with lithospheric uparching can probably only account for graben subsidence not exceeding 200 m (Bott, 1981) and can therefore, only play a minor contributary role in the formation of rift valleys with several kilometers of sediment such as the Benue Trough. However, there are additional stresses that may be associated with uplifted regions arising from the additional surface load of the updomed topography and the upthrust of the underlying isostatic compensation

in a purely elastic lithosphere (Bott, 1981; Artyushkov, 1973). These stresses cannot, however, account for a rift valley of more than 2 km sediment infill unless the lower part of the crustal lithosphere deforms by creep (Bott and Kusznir, 1979). It seems, therefore, unlikely that the tectonic model of Olade (1975), which involves the rise and cessation of mantle upwelling and its attendant pattern of doming and rifting, can explain the evolution of the Benue Trough in itself completely.

The heating and thinning of continental lithosphere by thermal conduction from below would entail an unrealistically long time scale for sufficient uplift. This time scale can, however, be reduced if the lithosphere is net-veined by rising magma which leads to a replacement of loose blocks by asthenospheric material from below. Furthermore, the tensile stress sytem associated with rift valley formation, favours the emplacement of dyke-like bodies which could lead to a further stretching of the brittle upper crust, significant extension of the underlying part of the lithosphere by ductile necking and consequently, rifting. Depending on the amount of magma present, such a structure might develop into a split continent. Bhattacharji and Koide (1978) have shown that an excess magma pressure of the order of 1 Kbar or more can originate due to vertical dyke-like intrusions from the upper mantle into the crust. It can therefore be assumed that the stresses generated and imparted to the lithospheric plate by asthenospheric upwell, doming and protrusion of dyke-like bodies could be sufficient to lead to the formation of rift structures with sediment infill as large as is found over the Benue Trough. Based on this assumption, a tectonic model for the evolution of the Benue Trough is now discussed.

It is here suggested that the tectonic evolution of the Benue Trough involved the rise of a mantle plume or mantle upwelling which

gave rise to doming, emplacement of intrusive igneous material in the crust, thinning and consequently, rifting. It is thought that this sequence of events may have been repeated in a cyclic manner with structural deformation taking place in between any two cycles.

The evolution of the Benue Trough began with the rise of a mantle plume under the present day Niger Delta (Burke and Dewey, 1973). This gave rise to doming and uplift of continental lithosphere, emplacement of mafic and maybe felsic igneous material, crustal thinning and subsequently rifting and the formation of an RRR (rift - rift - rift) triple junction which involved the Benue Trough, the South Atlantic and the Gulf of Guinea (Burke et al., 1970, 1971, 1972; Burke, 1976). This event took place during Aptian to Albian times and was accompanied by the deposition of sediments of the Asu River Group and the release of alkaline-mafic lavas and volcaniclastics as are found around Abakaliki (Uzuakpunwa, 1974).

In the Cenomanian, prior to the initiation of renewed mantle upwelling, there was a reduction of the tension in the Benue Trough and the accompanying lithospheric contraction gave rise to a folding of Albian sediments and associated with this, was the marine regression which gave rise to the deposition of the Odukpani Formation on the Calabar Flank. (See Section 4.4).

Renewed mantle upwelling, doming and associated emplacement of igneous material along earlier lines of weakness took place in Turonian times although on a slightly reduced scale and this led to renewed rifting in the Benue Trough. This cycle of tectonic activity continued until about the start of the Santonian and was accompanied by a marine transgression culminating in the deposition of the Ezeaku Shales on the already deformed Asu River Group (Ayoola, 1978; Murrat, 1972; Reyment, 1972). The reduction or complete cessure of mantle upwelling in the Benue Trough during Senonian times gave rise to a marine regression in Santonian - Maestrichtian times, which gave rise to the

deposition of younger sediments and a deformation of the older sediments. It is thought that the centre of tectonic activity at the thin stage shifted eastwards as the result of the migration of the mantle plume caused by a rotation of the African plate, (Fitton, 1980; Olade, 1975; Adighije, 1981b) to give rise to the Cameroon line.

From this point onwards, there may have been minor crustal movements, continued emplacement of minor intrusives, sedimentation and minor faulting along earlier lines of weakness. It is also thought that the migration of the centre of tectonic activity eastwards due to the rotation of the continent may have given rise to a marginal or flank uplift which was accompanied by marginal volcanism and intrusive bodies such as are seen around Gboko and Shemanker and marginal fractures. Some of these fractures have been mapped by Chukwu-Ike (1978a, 1978b) using satellite imagery studies.

5.6.2 Limitations of Model Proposed

The tectonic model proposed above has its limitations. Firstly, the model as it now stands, does not take into account the tensional stresses that may be associated with the bend in the Atlantic. The folding of sediments within the trough has also not been fully accounted for by this model in its present form. Furthermore, the width of the Benue Trough appears too large when compared to typical widths of rift structures and, it is possible that the Benue Trough represents two rift structures running parallel to one another.

CHAPTER VI

SUMMARY AND CONCLUSIONS

A discussion of the results of the different aspects of this thesis is given at the end of the relevant chapter. A general summary and synthesis of all aspects covered by this thesis and the conclusions drawn from them is presented in this final chapter. Suggestions on available scopes for future work on the topics covered are also given at the end.

6.1 Methods of Magnetic Interpretation

Several methods for the interpretation of magnetic anomalies as well as programs based on them were developed in the course of the work. These include, non-linear optimization techniques, linear inversion, pseudogravity and methods for the evaluation of demagnetization effects of arbitrarily shaped bodies.

6.1.1 Use of Non-linear Optimization Techniques in the Interpretation of Magnetic Anomalies

The use of non-linear optimization techniques in the interpretation of magnetic anomalies was discussed in Chapter One. A method of interpreting magnetic anomalies due to dykes by non-linear optimization techniques was developed. The method makes a combined use of non-linear optimization and least squares analysis. It seeks to minimize a non-linear objective function which represents the difference between the observed and calculated anomalies due to a dyke by iteratively varying the non-linear parameters of the dyke, while obtaining optimum values of the linear parameters of the dyke by at least squares analysis until an acceptable fit is obtained between the observed and the computed anomalies.

The problem of ambiguity as encountered in the interpretation of magnetic anomalies due to dykes was studied. This study was carried out through a study of the behaviour of the objective function geometrically by plotting the values of the objective function as a function of any two chosen parameters of a model dyke for varying thickness - depth ratios. It was found that the degree of uniqueness of the solution obtained for a dyke increases with increasing thickness - depth ratio.

The method of dyke interpretation developed uses all points on a given profile to obtain a solution and guarantees convergence to a minimum. The method also allows the geological feasibility of the solution to be taken into account and requires initial estimates for only three non-linear parameters, the thickness, the depth to the top and the location of the centre of the dyke with respect to the origin. The method was tested on field data collected over the Minch and Hett dykes in Britain and several dykes within the Benue Trough of Nigeria. It was found to be much quicker and less expensive than most other approaches to dyke interpretation. The method was found to take on the average, less than one CPU seconds to arrive at a solution compared to a time of 10-20 CPU seconds used by most other techniques for a typical profile of about one hundred field points.

In addition to methods making use of non-linear optimization techniques, a number of other techniques were applied. These include the linear inverse method and its application to the joint analysis of gravity and magnetic data.

6.1.2 Evaluation of Demagnetization Effects

The effects of demagnetization in both ellipsoidal and non-ellipsoidal bodies was studied. Three methods for the evaluation of demagnetization effects in arbitrarily shaped two dimensional

bodies magnetized in an arbitrary direction were developed. The
methods were applied to the study of demagnetization effects in
two dimensional bodies. The effect of demagnetization was found to
be appreciable only when the susceptibility exceeds 1.2 MKS and at
such susceptibilities, values of magnetization of a body is far
from being uniform. The methods were applied to profiles taken
across the Minch dyke.

6.2 Magnetic Study of the Minch Dyke

A linear magnetic feature which extends from the north of the
Island of Lewis to Loch Ewe was interpreted in terms of an unusually
wide dyke using the non-linear optimization methods developed. An
interpretation of sixteen profiles across this feature suggests that
the proposed dyke has a thickness of 1.05-1.30 km and a depth to the
top of 0.66-2.87 km. The dyke is reversely magnetized and the
magnetization in the plane of the profiles ranges from 0.43 A/M to
0.89 A/M. The dyke was found not to be appreciably demagnetized and
the assumption of uniform magnetization made in the interpretation
was therefore, probably valid. The angle beta ($\beta = Ie' + Im' - d$;
Chaper One) obtained from the interpretation range from 245°-337° and
this, combined with the fact that the dyke comes up to the base of
the Jurassic sediments which are disturbed on the seismic section,
suggests that the dyke is probably of Tertiary origin.

West of the Minch dyke and of Lewis is another linear magnetic
feature. Three profiles across this feature were interpreted in terms
of a reversely magnetized dyke whose thickness range from 0.70 km to
0.84 km and having a depth to the top of 0.81 km to 1.17 km. The
angle beta for this dyke was interpreted as being 260°-390°. The
closeness of this angle for both dykes suggests that they may have

been emplaced at the same time, probably in the Tertiary and may have been associated with the Tertiary igneous activity of North Britain.

6.3 Aeromagnetic Study of the Lower and Middle Benue Trough of Nigeria

6.3.1 Geology of the Benue Trough

The geology of the Benue Trough has hitherto remain poorly known as very little published information exists. The absence of detailed geological information on the Benue Trough has inhibited would-be researchers on different aspects, and has presented the most serious limitation on geophysical interpretations of the area. An attempt has therefore been made to assemble a review of the known geology of the Benue Trough in general, and for the Lower and Middle Benue in particular, based on the few published papers and on oral discussions with geologists and geophysicists interested in the area. This review is presented in Chapter Four. It should contribute towards an understanding of the geology of the Trough.

6.3.2 Interpretation of Aeromagnetic Anomalies Over the Lower and Middle Benue Trough

A study of the aeromagnetic anomalies over the Lower and Middle Benue Trough has been made. An analysis and description of regions of low and high magnetic anomalies was carried out in an effort to determine their trends. The result of this analysis showed that (a) the basement area surrounding the Benue Trough is characterised by a complicated distribution of short wavelength anomalies which are either due to near surface intrusions or susceptibility variations in the basement, (b) the basement/Cretaceous contact can be roughly identified with a sequence of magnetic lows except in the area around Donga where it is thought that the contact as shown on the geology map needs to be moved southwards by about 15 km, (c) the belts of magnetic highs and

lows alternatively distributed over the Cretaceous trough are not continuous but exist as elongated anomalies, (d) the belts of magnetic highs and lows have trends sub-parallel to the trend of the trough and (e) the character of the long wavelength anomalies found over the basement differs significantly from those over the sedimentary basin.

It is thought from the findings given above, that the magnetic anomalies over the Lower and Middle Benue, do not represent typical oceanic anomalies and cannot be treated as such.

Several aeromagnetic profiles across the trough were interpreted. These profiles could not be satisfactorily explained solely in terms of topographic variations of the underlying basement. Such an interpretation leads to a basement having too high a magnetization, too thick a sedimentary sequence in some regions, and outcrops of the basement not in agreement with the known geology of the trough. The profiles were best interpreted in terms of discrete intrusive bodies existing beneath the trough. It was found that the model intrusives on the average have magnetizations ranging from 1.5 A/M to 3.4 A/M except for exceptional cases where values below 1.0 A/M and above 4.0 A/M were obtained. The modelled intrusive bodies have variable widths which average about 10 km. These bodies may exist predominantly within the sedimentary rocks or within the crystalline basement or both. The magnetization suggest that they are probably basic in composition and may well be gabbroic.

The interpretation of the anomalies in terms of basic intrusive bodies is in good agreement with the interpretations of gravity anomalies over the trough (Cratchley and Jones, 1965; Adighije, 1981b) as well as results of gravity and magnetic interpretations obtained for other rifts such as the Baikal Rift and the Rift Valley in Kenya (Bosum and Hahn, 1967, 1970; Roche and Wohlenberg, 1970; Zorin, 1971, 1981; Zorin et al., 1975; Searle, 1969, 1970).

6.3.3 A model for the Tectonic Evolution of the Benue Trough

A model for the tectonic evolution of the Benue Trough was proposed taking into account the models obtained from the interpretation of the aeromagnetic anomalies. In arriving at this model, it was assumed that the stresses generated and imparted to the lithospheric plate by asthenospheric upwell, doming and protrusion of dyke-like bodies could be sufficient to lead to the formation of rift structures with sediment infill as large as is found over the Benue Trough. The proposed model involves the rise of a mantle plume or mantle upwelling which gave rise to doming, emplacement of intrusive igneous materials in the crust, thinning and consequently rifting. This sequence of events may have been repeated in a cyclic manner accompanied by structural deformations which took place in between any two cycles. The model does not appear to have accounted fully well for the stresses associated with the bends in the Atlantic and the folds found in the Benue Trough.

6.4 Suggestion for Future Work

Although most of the topics dealt with in this thesis have been in some detail, there still exists scope for future work. The dyke interpretation method developed could be further modified such that the parameters of the dyke are expressed in terms of depth units and hence allowing for automation in the determination of the initial estimates needed from the observed profile. The basic approach might be adapted for use in the frequency domain.

In the area around the Minch dyke are several linear magnetic features of varying lengths which are probably due to dykes. Their interpretation and correlation with the Minch dyke could be carried out in future. The tectonic significance of a dyke the size of the

Minch dyke has been recognised by the present author and Bott (1973b), and the determination of this represent a challenge to future workers.

The study of the Benue Trough, being a pioneer attempt, should help open up a discussion on the magnetic character of the trough and should serve as a stepping stone to future work. A magnetic study of the intrusive centres that have been suggested by several authors would form an interesting study. Also, in addition to the minor features interpreted here, there exist several other such features and dyke like anomalies whose interpretation would form a useful project. A comparison of the pseudogravity anomaly over the trough with observed gravity and its interpretation represent a scope for further work. Furthermore, the model for the evolution of the Benue Trough presented here has its limitations and these might be reduced through further geophysical and geological study so as to obtain a more comprehensive account of the evolution of the trough.

REFERENCES

Adighije, C., 1979. Gravity field of Benue Trough, Nigeria.
Nature Phys. Sci., 282, 199-201.

Adighije, C., 1981a. Gravity study of Lower Benue Trough, Nigeria.
Geol. Mag., 118, 59-67.

Adighije, C., 1981b. A gravity interpretation of the Benue Trough,
Nigeria. Tectonophysics, 79, 109-128.

Ajayi, C.O. and Ajakaiye, D.E., 1981. The origin and peculiarities
of the Nigerian Benue Trough: another look from recent
gravity data obtained from the Middle Benue. Tectonophysics,
80, 285-303.

Al-Chalabi, M., 1971. Some studies relating to non uniqueness in
gravity and magnetic inverse problems. Geophysics, 36, 835-855.

Al-Chalabi, M., 1970. The application of non-linear optimization
techniques in geophysics. Unpublished Ph.D. thesis, University
of Durham.

Allerton, H.A., 1968. An interpretation of the gravity field of the
North Minch. Unpublished M.Sc. thesis, University of Durham.

Åm, K., 1972. The arbitrarily magnetized dyke: interpretation by
characteristics. Geoexploration, 10, 63-90.

Åm, K. and Stenland, R.O., 1965. Experimental determination of
effective demagnetization factors for a short cylinder.
Geophysics, 40, 527-529.

Anderson, F.W. and Dunham, K.C., 1966. The geology of Northern
Skye. Mem. geol. Surv. Scotland.

Artyushkov, E.V., 1973. Stresses in the lithosphere caused by
crustal thickness inhomogeneities. J. geophys. Res., 78,
7675-7708.

Artyushkov, E.V. 1981. Mechanism of continental riftogenesis.
Tectonophysics, 73, 9-14.

Ayoola, E.O., 1978. Sedimentology of the Middle Benue Trough, Nigeria.

    Unpublished Ph.D. thesis, University of London.

Barford, N.C., 1967. Experimental measurements: precision, error and

    truth. Addison-Wesley Pub. Co., London.

Barnes, J.G.P., 1965. An algorithm for solving non-linear equations

    based on the secant method. Comput. J., 8, 66-72.

Barnett, C.T. 1972. Theoretical modelling of induced polarization

    effects due to arbitrarily shaped bodies. Unpublished Ph.D.

    thesis, Colorado School of Mines.

Bhattacharji, S. and Koide, H., 1978. The origin and evolution of

    rifts and rift valley structures: A mechanistic interpretation.

    In: Tectonics and geophysics of continental rifts, PP 29-39,

    edited by Ramberg, I.B. and Neumann, E.R., D. Reidel Pub. Co.,

    London.

Binns, P.E., McQuillin, R., and Kenolty, N., 1974. The geology of

    The Sea of the Hebrides. Rep. Inst. geol. Sci., No. 73/14.

Books, K.G., 1962. Remanent magnetization as a contributor to some

    magnetic anomalies. Geophysics, 27, 359-375.

Bosum, W. and Hahn, A., 1967. Aeromagnetic surveying in the Upper

    Rhine graben.   Abh. geol. Landesamt Baden-Wurtt., 6, 89-91

Bosum, W. and Hahn, A., 1970. Interpretation der Flugmagnetometer -

    Vermessung des Oberrhein-grabens. In: Graben Problems, pp.

    219-223, edited by Illies, J.H. and Mueller, St., E.

    Schweizerbartsche Verlagsbuchhand lung, Stuttgart.

Bott, M.H.P., 1967. Solution of the linear inverse problems in

    magnetic interpretation with application to oceanic magnetic

    anomalies. Geophys. J.R. astr. Soc., 13, 313-323.

Bott, M.H.P., 1969a. GRAVN. Durham geophysical computer program

    specification 1.

Bott, M.H.P., 1969b. MAGN. Durham geophysical computer program
specification 2.

Bott, M.H.P., 1973a. Inverse methods in the interpretation of
magnetic and gravity anomalies. In: Methods in computational
physics, 13, pp. 133-162, edited by Botten, B.A., Alder, B.,
Fernbach, S., and Rotenberg, M.

Bott, M.H.P. 1973b. The evolution of the Atlantic north of the
Faeroe Islands. In: Implications of continental drift to
the earth sciences, pp. 175-189, edited by Tarling, D.H. and
Runcorn, S.K., Academic Press, London.

Bott, M.H.P., 1976. Formation of sedimentary basins of graben type
by extension of the continental crust. Tectonophysics, 36,
77-86.

Bott, M.H.P., 1981. Crustal doming and the mecnahism of continental
rifting. Tectonophysics, 73, 1-8.

Bott, M.H.P. and Hutton, M.A., 1970. A matrix method for interpreting
oceanic magnetic anomalies. Geophys. J.R. astr. Soc., 20,
149-157.

Bott, M.H.P. and Ingles, A., 1972. Matrix methods for joint
interpretation of two dimensional gravity and magnetic
anomalies with application to the Iceland-Faeroe ridge.
Geophys. J.R. astr. Soc., 30, 55-67.

Bott, M.H.P. and Kusznir, N.J., 1979. Stress distributions associated
with compensated plateau uplift structures with application
to the continental splitting mechanism. Geophys. J.R. astr. Soc.,
56, 451-459.

Box, M.J., 1965. A new method of constrained optimization and a
comparison with other methods. Comput. J., 8, 42-52.

Box, M.J., 1966. A comparison of several current optimization methods
and the use of tranformations in constrained problems. Comput. J.,
9, 67-77.

Box, M.J., Davies, D. and Swann, W.H., 1969. Non-linear optimization
techniques. I.C.I. Monographs No. 5, Oliver and Boyd, London.

Brown, W.F., 1962. Magnetostatic principles in ferromagnetism.
North-Holland Pub. Co., Amsterdam.

Broyden, C.G., 1965. A class of methods for solving non-linear
simultaneous equations. Math. Comp., 19, 577-593.

Broyden, C.G., 1967. Quasi-Newton methods and their application
to function minimization. Math. Comp. 21, 368-381.

Broyden, C.G., 1970. The convergence of single rank Quasi-Newton
methods. Math. Comp., 24, 365-382.

Bruckshaw, J.M. and Kunaratnam, K., 1963. The interpretation of
magnetic anomalies due to dykes. Geophys. Prospect., 11,
509-522.

Burke, K., 1976. Development of graben associated with the initial
ruptures of the Atlantic ocean. Tectonophysics, 36, 93-112.

Burke, K., 1978. Evolution of continental rift systems in the light
of plate tectonics. In: Tectonics and geophysics of continental
rifts. pp. 1-9, edited by Ramberg, I.B. and Neumann, E.R.,
D. Reidel Pub. Co., London.

Burke, K., Dessauvagie, T.F.J. and Whiteman, A.J., 1970. Geological
history of the Benue Valley and adjacent areas. In: Conference
on African geology, Commonw. geol. Liaison Off. London.

Burke, K., Dessauvagie, T.F.J. and Whiteman, A.J., 1971. Opening of
the Gulf of Guinea and the geological history of the Benue
depression and Niger Delta. Nature Phys. Sci., 233, 51-55.

Burke, K., Dessauvagie, T.F.J. and Whiteman, A.J., 1972. Geological
history of the Benue Valley and adjacent areas. In: African
Geology, pp. 187-206, edited by Dessauvagie, T.F.J. and
Whiteman, A.J., Ibadan University Press, Ibadan.

Burke, K. and Dewey, J.F., 1973. Plume - generated triple junctions: Key indicators in applying plate tectonics to old rocks. J. Geol., 81, 406-433.

Burke, K. and Whiteman, A.J., 1973. Uplift, rifting and the break up of Africa. In: Implications of continental drift to the earth sciences, pp. 735-755, edited by Tarling, D.H. and Runcorn, S.K., Academic Press, London.

Butler, P.F., 1968. The interpretation of magnetic field anomalies over dykes by optimization procedures. Unpublished M.Sc. thesis, University of Durham.

Campey, I.G. and Nickols, D.G., 1961. Simplex minimization. Program specification, Imperial Chemical Industries Ltd.

Carter, J.D., Barber, W. and Tait, E.A., 1963. The geology of parts of Adamawa, Bauchi and Bornu provinces in Northern Nigeria. Bull. geol. Surv. Nigeria, No. 30.

Chukwu-Ike, I.M., 1977. Regional photogeological interpretation of the tectonic features of the Central Nigerian basement complex - a statistical imagery based study. Unpublished Ph.D. thesis, University of London.

Chukwa-Ike, I.M., 1978a. Interpetation of marginal en-echelon lineaments in the Mid-Benue Trough, Nigeria. Nig. J. Ming. geol. 5, 14-18.

Chukwu-Ike, I.M., 1978b. The regional tectonic setting of Northwestern Nigeria low grade metasedimentary belt. Nig. J. Ming. geol., 5, 19-22.

Corbato, C.E., 1965. A least squares procedure for gravity inter-pretation. Geophysics, 30, 228-233.

Craig, G.Y., 1965. The geology of Scotland. Oliver and Boyd, Edinburgh.

Cratchley, C.R. and Jones, G.P., 1965. An interpretation of the geology and gravity anomalies of the Benue Valley, Nigeria. Geophys. Pap. Overseas geol. Surv. London, No. 1.

Davidon, W.C., 1959. Variable metric method for minimization. Argonne National Laboratory Report, No. ANL-5990.

Davidon, W.C., 1968. Variance algorithm for minimisation. Comput. J., 10, 406-410.

Eadie, W.T., Dryard, D., James, F.E., Roos, M. and Sadoulet, B., 1971. Statistical methods in experimental physics. North-Holland Pub. Co., Amsterdam.

Effeotor, O.E., 1974. Sedimentological studies of the Bima Sandstones (Sheets 193 and 172) N.E. Nigeria. Unpublished Ph.D. thesis, University of London.

Emilia, D.A. and Bodvarsson, G., 1969. Numerical methods in the direct interpretation of marine magnetic anomalies. Earth planet. Sci. Lett., 7, 194-200.

Falconer, J.D., 1911. The geology and geography of Northern Nigeria. MacMillan and Sons, London.

Farrington, J.L., 1952. A preliminary description of the Nigerian lead-zinc field. Econ. Geol., 47, 583-608.

Fitton, J.G., 1980. The Benue Trough and Cameroon line - a migrating rift system in West Africa. Earth planet. Sci. Lett., 51, 132-138.

Fletcher, R., 1970. A new approach to variable metric algorithms. Comput. J., 13, 317-322.

Fletcher, R. and Powell, M.J.D., 1963. A rapidly convergent descent method for optimization. Comput. J., 6, 163-168.

Fletcher, R., 1965. Function minimization without evaluating derivatives - a review. Comput. J., 8, 33-41.

Gay, S.P., 1963. Standard curves for interpretation of magnetic anomalies over long tabular bodies. Geophysics, 28, 161-200.

Gill, P.E. and Murray, W., 1974. Sagefuarded steplength algorithms for optimization using descent methods. National Physical Laboratory Report, No. NAC 37.

Gill, P.E. and Murray, W., 1977. The computation of Long range - multiplier estimates for constrained optimization. National Physical Laboratory Report, No. NAC 77.

Grant, N.G., 1971. South Atlantic Benue Trough and Gulf of Guinea Cretaceous triple junction. Bull. geol. Soc. Am., 82, 2295-2298.

Greenstadt, J., 1967. One the relative efficiencies of gradient methods. Math. Comp., 21, 360-367.

Greenstadt, J., 1970. Variations on variable metric methods. Math. Comp., 24, 1-22.

Hall, D.H., 1968. A magnetic interpretation method for calculating body parameters for buried sloping steps and thick sheets. Geoexploration, 6, 187-206.

Hoffman, P., 1972. Aulacogens and the evolution of continental margins (Unpublished).

Jehu, T.J. and Craig, R.M., 1924. Geology of the Outer Hebrides. Trans. R. Soc. Edinburgh, 53, 419-441, 615-641.

Johnson, W.W., 1969. A least squares method of interpreting magnetic anomalies caused by two dimensional structures. Geophysics, 34, 65-74.

Joseph, R.I., 1966. Ballistic demagnetizing factors in uniformly magnetized cylinders. J. Appl. Phys., 37, 4639-4643.

Joseph, R.I., 1967. Ballistic demagnetising factors in uniformly magnetized rectangular prisms. J. Appl. Phys., 38, 2405-2406.

Joseph, R.I., 1976. Demagnetizing factors in non-ellipsoidal samples - a review. Geophysics, 41, 1052-1054.

Joseph, R.I. and Schlomann, E., 1965. Demagnetizing field in non-ellipsoidal bodies. J. Appl. Phys., 36, 1579-1593.

Kellog, O., 1929. Foundations of potential theory. Julius Springer, Berlin.

Khurana, K.K., Rao, S.V.S. and Pal, P.C., 1981. Frequency domain least-squares inversion ofthick dyke magnetic anomalies using Marquardt algorithm. Geophysics, 46, 1745-1748.

King, L.C., 1950. Outline and deposition of Gondwanaland. Geol. Mag., Mag., 87, 353-359.

Kogbe, C.A., 1976. Palaeogeographic history of Nigeria from Albian times. In: Geology of Nigeria, pp. 337-353, edited by Kogbe, C.A., Elizabethan Pub. Co., Lagos.

Kunaratnam, K., 1972. An iterative method for the solution of a non-linear inverse problem in magnetic interpretation. Geophys. Prospect., 20, 439-447.

Lee, T., 1972. A general technique for the direct interpretation of resistivity data over two dimensional structures. Geophys. Prospect., 20, 847-859.

Lee, T., 1975. An integral equation and its solution for some two and three dimensional problems in resistivity and indirect polarization. Geophys. J. R. astr. Soc., 42, 81-95.

Lee., T.J., 1980. Rapid computation of magnetic anomalies with demagnetization include for arbitrarily shaped magnetic bodies. Geophys. J. R. astr. Soc., 60, 67-75.

Lees, G.M., 1952. Foreland folding. Q.J. geol. Soc. London, 108, 1-34.

Marquardt, D.W., 1963. An algorithm for least squares estimation of non-linear parameters. J. Soc. Indust. Appl. Maths., 11, 431-441.

Maxwell, J.C., 1904. Electricity and magnetism. The Clarendon Press, Oxford.

McConnell, R.B., 1949. Notes on lead-zinc deposits of Nigeria and Cretaceous stratigraphy of Benue and Cross River Valleys. Rep. geol. Surv. Nigeria, No. 752.

McCurry, P., 1976. The geology of the Precambrian to Lower Palaeozoic rocks of Northern Nigeria - a review. In: Geology of Nigeria, pp. 15-39, edited by Kogbe, C.A., Elizabethan Pub. Co., Lagos.

McGrath, P.H. and Hood, P.J., 1970. The dipping dyke case - a computer curve matching method of magnetic interpretation. Geophysics, 35, 831-848.

Moo, J.K.C., 1965. Analytical aeromagnetic interpretation of the inclined prism. Geophys. Prospect., 13, 203-224.

Mood, A.M., Graybill, F.A. and Boes, D.C., 1974. An introduction to the theory of statistics. McGraw-Hill Kogakusha, Tokyo.

Murrat, R.C., 1972. Stratigraphy and palaeogeography of Cretaceous and Lower Tertiary in Southern Nigeria. In: African Geology, pp. 251-269, edited by Dessauvagie, T.F.J., and Whiteman, A.J., Ibadan University Press, Ibadan.

Neave, H.R. 1978. Statistical tables for mathematicians, engineers, economists and behavioural and management sciences. George Allen and Unwin, London.

Nelder, J.A. and Mead, R., 1965. A simplex method for function minimization. Comput. J., 7, 308-313.

Neugebauer, H.J. and Temme, P., 1981. Crustal uplift and the propagation of failure zones. Tectonophysics, 73, 35-51.

Norman, J., Price, N. and Chukwu-Ike, M., 1977. Astrons – the earth's oldest scars? New Scientist, 73, 689-692.

Nwachukwu, S.O., 1972. The tectonic evolution of the southern portion of the Benue Trough, Nigeria. Geol. Mag., 109, 411-419.

Offodile, M.E., 1976. A review of the geology of the Cretaceous of the Benue Trough. In: Geology of Nigeria. pp. 319-330, edited by Kogbe, C.A., Elizabethan Pub. Co., Lagos.

Offodile, M.E. and Reyment, R.A., 1978. Stratigraphy of the Keana-Awe area of the Middle Benue region of Nigeria. Bull. geol. Inst. Univ. Uppsala, 7, 37-66.

Ogbukagu, K.N., 1974. Preliminary investigation on the benefication of some Cretaceous shales in parts of East-Central State. Nig. J. Ming. Geol., 1, 5-16

Olade, M.A., 1975. Evolution of Nigeria's Benue Trough (Aulacogen): a tectonic model. Geol. Mag., 112, 575-583.

Olade, M.A., 1978. Early Cretaceous basalt volcanism and initial continental rifting in Benue Trough, Nigeria. Nature Phys. Sci., 273, 458-559.

Oyawoye, M.O., 1972. The basement complex of Nigeria. In: African Geology, pp. 67-103, edited by Dessauvagie, T.F.J., and Whiteman, A.J., Ibadan University Press, Ibadan.

Osborn, J.A., 1945. Demagnetizing factors of the general ellipsoid. Phys. Review, 67, 351-357.

Parasnis, D.S., 1972. Principles of applied geophysics. Chapman and Hall, London.

Peters, L.J., 1949. The direct approach to magnetic interpretation and its practical applications. Geophysics, 30, 403-410.

Powell, M.J.D., 1964. An efficient method for finding the minimum
of a function of several variables without calculating deriv-
atives. Comput. J., 7, 155-162.

Powell, M.J.D., 1965. A method for minimizing a sum of squares of
non-linear functions without calculating derivatives. Comput. J.,
8, 303-307.

Ramsey, A.S., 1952. An Introduction to the theory of Newtonian
attraction. Cambridge University Press, Cambridge.

Rao, D.A., Babu, H.V.R. and Narayan, P.V.S., 1981. Interpretation
of magnetic anomalies due to dykes: the complex gradient method.
Geophysics, 46, 1572-1578.

Rao, B.S.R., Murphy, I.V.R. and Rao, C.V., 1973. Two methods for
computer interpretation of magnetic anomalies of dykes.
Geophysics, 38, 710-718.

Reyment, R.A., 1965. Aspects of the geology of Nigeria. Ibadan
University Press, Ibadan.

Reyment, R.A., 1969. Ammonite biostratigraphy, continental drift
and oscillatory transgressions. Nature, 224, 137-140.

Reyment, R.A., 1972. Cretaceous (Albian-Turonian) geology of the
South Atlantic. In: African Geology, pp. 505-513, edited by
Dessauvagie, T.F.J. and Whiteman, A.J., Ibadan University
Press, Ibadan.

Reyment, R.A. and Tait, E.A., 1972. Biostatigraphical dating of the
early history of the South Atlantic Ocean. Phil. Trans. R.
Soc. London, 264, 55-95.

Richey, J.E. 1961. British regional geology. Scotland : the Tertiary
volcanic districts. H.M.S.O.

Roy, A., 1962. Ambiguity in geophysical interpretation. Geophysics, 27, 90-99.

Roche, A. and Wohlenberg, J., 1970. Magnetic measurements in Alsace, Baden and Pfalz. In: Graben Problems, pp. 224-234, edited by Illies, J.H. and Mueller, St., E. Schweizerbart'sche Verlagsbuchhandlung, Stuttgart.

Scheffe, H., 1963. Analysis of variance. Wiley, New York.

Searle, R.C., 1969. Barometric hypsometry and a geophysical study of part of the Gregory Rift Valley in Kenya. Unpublished Ph.D. thesis, University of Newcastle upon Tyne.

Searle, R.C., 1970. Evidence from gravity anomalies for thinning of the lithosphere beneath the rift valley in Kenya. Geophys. J. R. astr. Soc., 21, 13-31.

Sharma, P.V., 1966. Rpaid computation of magnetic anomalies and demagnetization effects caused by bodies of arbtirary shape. Pure and Appl. Geophys, 64, 89-109.

Sharma, P.V., 1968. Demagnetization effect of a rectangular prism. Geophysics, 33, 132-134.

Silvey, S.D., 1975. Statistical inference. Chapman and Hall, London.

Skeels, D.C., 1947. Ambiguity in gravity interpretation. Geophysics, 12, 43-56.

Skeels, D.C., 1963. An approximate solution of the problem of maximum depth in gravity interpretation. Geophysics, 28, 724-735.

Smith, R.A., 1978. Non-uniqueness in the inverse gravity problem for infinite polygonal cylinders. J. Inst. Maths. Applics., 21, 61-65.

Spendley, W., Hext, G.R. and Himsworth, F.R., 1962. Sequential application of simplex designs in optimization and evolutionary operation. Technometrics, 4, 441-461.

Steel, R.J., 1971. New Red Sandstone movement on the Minch fault. Nature Phys. Sci., 234, 158-159.

Stoner, E.C., 1945. The demagnetizing factors for ellipsoids. Phil. Mag., 36, 803-821.

Straton, E.C., 1941. Electromagnetic theory. McGraw-Hill Book Co., New York.

Talwani, M. and Heirtzler, J.K., 1964. Computation of magnetic anomalies caused by two dimensional structures of arbitrary shape. In: Computers in Mineral Industries part 1, Stanford Univ. Publ. Geol. Sci., 9, 464-480.

Tanner, J.E., 1967. An automated method of gravity interpretation. Geophys. J.R. astr. Soc., 13, 339-347.

Topping, J., 1978. Errors of observation and their treatment. Chapman and Hall, London.

Tyrrell, G.W., 1949. The Tertiary igneous rocks of Scotland in relation to Iceland and Greenland. Med^d· Dansk. geol. Foren., 11, 413-440.

Uzuakpunwa, A.B., 1974. The Abakaliki pyroclastics, Eastern Nigeria: new ageand tectonic implication. Geol. Mag., 111, 65-70.

Venning Meinesz, F.A., 1950. Les graben africains, resultat de compression ou de tension dans la croute' terrestre? Bull Inst. R. Colonial Belge, 21, 539-552.

Vogel, A., 1963. The application of electronic computers to the calculation of effective magnetization. Geophys. Prospect., 11, 51-58.

Westbrook, G.K., 1974. The South Harris magnetic anomaly. Proc. Geol. 85, 1-12.

Westbrook, G.K., 1977. Joint interpretation of gravity and magnetic anomalies using non-linear optimization. Geophys. J.R. astr. Soc., 49, 267-268.

Westbrook, G.K., 1980. Non-linear methods for geophysical inversion.

   Unpublished manuscript.

Wilson, G.V., 1937. Sheets,80-90,Scotland. Summ. Prog. geol. Surv. G.B.

   (1937), 73-74.

Won, I.J., 1981. Application of Gauss's method to magnetic anomalies

   of dipping dykes. Geophysics, 46, 211-215.

Wright, J.B., 1968. South Atlantic continental drift and the

   Benue Trough. Tectonophysics, 6, 301-309.

Wright, J.B., 1976. Origins of the Benue Trough: a critical review.

   In : Geology of Nigeria, pp. 309-317, edited by Kogbe, C.A.,

   Elizabethan Pub. Co., Lagos.

Zeitz, I. and Henderson, R.G., 1956. A preliminary report on model

   studies of magnetic anomalies of three-dimensional bodies.

   Geophysics, 21, 794-814.

Zorin, Yu. A., 1971. Recent structure and isostasty of the Baikal

   Rift Zone and adjacent areas. Nauka, Moscow.

Zorin, Yu.A., 1981. The Baikal Rift: an example of the intrusion of

   asthenospheric material into the lithosphere as the cause of

   disruption of lithospheric plates. Tectonophysics, 73, 91-104.

Zorin, Yu.A., Lysak, S.V. and Golubev, V.A., 1975. On the nature of

   the geothermal anomaly in Baikal area. In: Baikalsky Rift,

   pp. 66-73, Nauka, Novosibirsk.

Zorin, Yu.A. and Rogozhina, V.A., 1978. Mechanism of rifting and some

   features of the deep-seated structure of the Baikal rift zone.

   Tectonophysics, 45, 23-30.

APPENDIX A

Derivation of Expressions for the Ballistic and Magnetometric

Demagnetization Factors for a Uniformly Magnetized Cylinder -

(Equations 2.6 and 2.7)

Joseph and Schlomann (1965) have shown that the demagnetization tensor for a sample assumed to be uniformly magnetized, is given as follows :

$$N(r,z) = \tfrac{1}{2}a \int_{0}^{\infty} J_0(tr)J_1(ta) \left[e^{-tz} + e^{-t(L-z)} \right] dt \qquad A1$$

where $J_0(x)$ and $J_1(x)$ are the Bessel functions of the real argument of order zero and unity respectively and a, z, r and L are as in Figure 2.1b. The term $t = z/b$.

The ballistic demagnetization factor is defined as the spatially varying demagnetization factor in a plane perpendicular to the direction of the applied field and midway between the endfaces of the samples (Joseph, 1966) and is given by the following integral :

$$N_b = {}^{1}/A \int N (r, {}^{L}/2) dA \qquad A2$$

Combining A1 and A2 and making use of the fact that

$$rJ_1(r) {}^{d}/dr = rJ_0(r)$$

$$N_b = 2 \int_{0}^{\infty} J_1{}^2(t\,a) t^{-1} e^{-\frac{1}{2}tL} dt \qquad A3$$

The integral equation A3, is a standard integral of Bessel Functions whose exact solution can be found in standard tables of integrals and on reduction gives the following equation :

$$N_b = 1 - (2/\pi)(P/K_1)(E_1(K_1) - E_2(K_1)) \qquad A4$$

where

$$K_1^2 = (1 + \tfrac{1}{4}P^2)^{-1}$$

$$P = L/2a$$

and $E_1(K)$ and $E_2(K)$ are complete elliptical integrals of the first and second kinds respectively and putting their values into equation A4 gives the following expressions for the ballistic demagnetization factor :

$$N_b = 1 - (2P/\pi)(\ln(8/P) - 1) \; ; \; P \ll 1$$

$$N_b = (\tfrac{1}{2}P^2)(1 - (3/2P^2) + (25/8P^4)) \; ; \quad P \gg 1 \qquad A5$$

The magnetometric demagnetization factor Nm is defined as the volume average of the spatially varying demagnetization factor and is given thus :

$$Nm = \frac{1}{V} \int_V N(r,z) \, dV \qquad A6$$

combining A1 and A5 and carrying out the integrations in r and z, we get :

$$Nm = \frac{2}{L} \int_0^\infty J_1^2(ta) \, t^{-2}(1 - e^{-tL})dt \qquad A7$$

which on evaluation using tables gives the following expression:

$$Nm = 1 - (4/3\pi P)\{(1 + P^2)^{\frac{1}{2}} \times (P^2 E_1(K_2) + (1 - P^2)E_2(K_2))-1\}$$

$$A8$$

where $K_2^2 = (1 + P^2)^{-1}$ and P is as given previously. Putting in the values of $E_1(K)$ and $E_2(K)$ the following expressions for the magnetometric demagnetization factor results :

$$Nm = 1 - (2P/\pi)(\ln(4/P) - \tfrac{1}{2}) \; ; \quad P << 1$$

$$Nm = (4/3\pi P) - (\tfrac{1}{8}P^2) \; ; \; P >> 1 \qquad\qquad A9$$

APPENDIX B1

The following programs though developed, were not used to any great extent in this work and are not listed in this thesis. Listings of them and their implementation details are however, available in the Department of Geological Sciences, University of Durham.

OP·MAG: This program interprets the magnetic anomaly due to two-dimensional bodies of arbitrary cross-section by non-linear optimization techniques.

REG1:   This program calculates and removes the zeroth and first order regional fields from a given gravity or magnetic anomaly.

REG2:   This program calculates and removes the zeroth, first and second order regional fields from a given gravity or magnetic anomaly.

OPDYE9:   This program is similar to the program OPDYE8 but uses the Simplex Method.

ANOM2:   This program calculates the magnetic anomaly due to a system of two-dimensional prisms of rectangular cross-section.

ANOM3:   This is the three-dimensional equivalent of the program ANOM2.

DMAGFIELD2:   This computes the components of the effective magnetization for a two-dimensional body divided into rectangular cells using the method of matrix inversion.

DMAGFIELD3:   This computes the components of the effective magnetization for a three-dimensional body divided into rectangular prisms using the method of matrix inversion.

PLOT1:   This is an adaptation of the Ghost plotting routines and gives a plot of the output from the program INTERGRAM to an A4 scale. It could be used to generate a plot of the observed and computed anomaly and the model bodies.

PLOT2:   This gives a plot of the observed and computed anomaly due to a dyke as well as the model dyke arising from a run of the dyke interpretation programs.

PLOT3:   This gives a plot of the magnetic anomaly and its corresponding pseudogravity anomaly as well as the block distribution using the output from the program MGRAV.

APPENDIX B2

In this appendix, a listing of computer programs developed and used during this work is given. A brief introduction of these programs and the necessary run commands for the NUMAC IBM 370/168 computer are first given below. All input formats are free although provision has been made in each program for easy conversion to a formatted input.

OPDYE2:   is a dyke interpretation program using non-linear optimization technique. The program obtains optimal values for the non-linear parameters of the dyke (thickness, depth to top and location of centre w.r.t. origin) by non-linear optimization while obtaining optimal values for the linear parameters (components of the magnetization in the plane of the profile, the zeroth, first and second order regional fields) by least-squares analysis. It uses the Quasi-Newton's method (see Chapter One).

OPDYE5:   is similar to the program OPDYE2 but considers only the zeroth order regional field neglecting the first and second order regional fields. It also uses the Quasi-Newton method.

OPDYE7:   is a dyke interpretation program similar to the program OPDYE2. It however, considers the angle beta (Chapter One) as an additional non-linear parameter and together with the thickness, depth to the top and location of the centre of the dyke w.r.t. the origin is found by non-linear optimization. The linear parameters optimized by OPDYE7 are the magnetization in the plane of the profile, the zeroth and first order regional fields. It uses the Quasi-Newton's method.

OPDYE8:   is similar to the program OPDYE2 but assumes that the given anomaly is already corrected for the regional level. It uses the Quasi-Newton's method.

The following run command is used for OPDYE2, OPDYE5, OPDYE7 and OPDYE8:

$ RUN OBJ. + * NAG + * GHOST 5 = INPUT1

6 = OUTPUT1   9 = PLOT1

Description of files:

INPUT1 contains the title, number of non-linear parameters, initial estimates of the non-linear parameters, their scaling factors and their bounds as well as the values of the observed anomaly and weighting factors (as the case maybe) (see listing of programs).

OUTPUT1 contains the result of the run of any of the programs which includes the optimal parameters for the dyke as well as the observed, calculated and residual anomaly values (see program listings).

PLOT1 contains a plot of the observed and computed anomalies and the optimum model dyke assumed vertical.

OPDYE4:   is similar to the program OPDYE2 but uses the Simplex Method instead of the Quasi-Newton's method.

OPDYE6:   is similar to the program OPDYE5 but uses the Simplex Method instead of the Quasi-Newton's method.

$ RUN OBJ. + * NAG + * GHOST 5 = INPUT2

6 = OUTPUT2   9 = PLOT 2

File description:

INPUT2 contains the title, number of non-linear parameters, FLAG, maximum number of function calls,

initial estimates of the non-linear parameters and
their scaling factors as well as the values of the
observed anomaly and weighting factors (as the case
maybe)(see listing of programs).

OUTPUT2 is similar to OUTPUT1 but in addition
contains the values of the objective function and
the vertices of the corresponding simplex after a
specified number of function calls (see listing of
programs).

PLOT2 is similar to PLOT1

DMAGN   evaluates the effective magnetization and anomaly for
a two-dimensional body made up of a system of
rectangular cells or elements using the method of
matrix inversion (see Chapter Two).

DMAGN2   is similar to the program DMAGN but uses the method
of successive iterations (see Chapter Two).

The run command for DMAGN is as follows:

$ RUN OBJ. + * NAG + * GHOST 5 = INFILE

6 = OUTFILED   9 = PLOTFILE

The run command for DMAGN2 is as follows:

$ RUN OBJ. + * GHOST 5 = INFILE

6 = OUTFILE   9 = PLOTFILE

File description:

INFILE contains information about the elements
making up the body as well as information about the
original inducing field (see listing of programs).
OUTFILE contains the result of any run of the programs
DMAGN and DMAGN2 such as the values of the inner and
effective magnetization and values of the original
and effective anomalies (see listing of programs.

PLOTFILE contains a plot of the original and effective anomalies and the cell distribution used in calculations.

UPCON: upward or downward continues a given gravity or magnetic anomaly by a specified height.

Run command:

$ RUN OBJ. + * GHOST   5   = DATA1

6 = DATA2   7 = DATA3   9 = PLOT

File description:

DATA1 contains information regarding the anomaly to to upward or downward continued (see listing of program).

DATA2 contains the values of the original anomaly and the upward or downward continued anomaly (see program listing).

DATA3 contains the real and imaginary parts of the fourier transform of the given anomaly as well as its inverse.

PLOT gives a plot of the original anomaly and its upward or downward continued version.

MGRAV: computes the pseudogravity anomaly corresponding to a given magnetic anomaly using the equivalent layer theory (Bott, 1973a; Ingles, 1971).

Run command:

$ RUN OBJ. + * NAG   5 = FILE1   6 = FILE2

File description:

FILE1 contains information about the distribution of blocks making up the equivalent layer as well as the values of the given magnetic anomaly (see listing of programs).

FILE2 contains information about the given distribution of blocks and the values of the given magnetic anomaly and the corresponding pseudogravity anomaly (see listing of program).

MANOM: calculates the magnetic anomaly due to an arbitrarily shaped two-dimensional body of polygonal cross-section. Run command:

$ RUN OBJ. 5 = INPUT 6 = OUTPUT

INPUT and OUTPUT contains the input and output data for the program as explained in the program listing.

FACT1: evaluates the ballistic and magnetometric demagnetization factors for a cylinder (see Chapter Two). Run command:

$ RUN OBJ. 5 = INPUT 6 = OUTPUT

The files INPUT and OUTPUT contain the input and output data respectively as explained in the program listing.

```
C                    PROGRAM OPDYE2
C                    ==================
C
C           THIS PROGRAM IS A TWO DIMENSIONAL DYKE INTERPRETATION
C           PROGRAM USING THE NON LINEAR OPTIMIZATION TECHNIQUES
C           THE PARAMETERS OPTIMIZED ARE: THE COMPONENTS OF THE
C           MAGNETIZATION OF THE DYKE IN THE PLANE OF THE PROFILE
C           ,THE THICKNESS,DEPTH TO TOP,AND POSITION OF THE -
C           CENTRE OF THE DYKE AS WELL AS THE ZEROTH,FIRST AND
C           SECOND ORDER REGIONAL FIELDS,THE QUASI-NEWTON'S METHOD
C           IS USED,THE INPUT DATA IS AS FOLLOWS:
C           (1)    TITLE:(NOT MORE THAN 40 CHARACTERS)
C           (2)    NM,FLAG,KTOT:
C                  NM=NO. OF NON-LINEAR PARAMETERS(USUALLY THREE)
C                  FLAG:=0.0(NO WEIGHTING OF FIELD POINTS
C                          ,N.E. 0.0(FIELD POINTS WEIGHTED)
C                  KTOT=NO.OF FIELD POINTS-NOT MORE THAN 300
C           (3)    AX,BX,CX:
C                  AX=INITIAL ESTIMATE OF LOCATION W.R.T ORIGIN
C                  BX=    "         "      OF THICKNESS
C                  CX=    "         "      OF DEPTH TO THE TOP
C           (4)    SC1,SC2,SC3 (SCALING FACTORS FOR AX,BX,CX
C                  RESPECTIVELY-SEE CHAPT. ONE)
C           (5)    X11,X12:-LOWER & UPPER LIMITS OF LOCATION
C                  X21,X22:-   "     "    "       "     " THICKNESS
C                  X31,X32:-   "     "    "       "     " DEPTH
C           (6)    FX(K),FTOB(K)(IF FLAG .EQ. 0.0)
C                  FX(K),FTOB(K),WHT(K)(IF FLAG .N.E. 0.0)
C                  FX(K)=ARRAY OF X-CORD. OF FIELD POINTS
C                  FTOB(K)=ARRAY OF OBSERVED ANOMALY
C                  WHT(K)=ARRAY OF WEIGHTING OF FIELD POINTS
C       THE OUTPUT IS AS FOLLOWS:
C           (1)    TITLE:(AS IN INPUT)
C           (2)    F :- OBJECTIVE FUNCTION VALUE ON EXIT
C           (3)    X(I):ARRAY OF VALUES OF NON-LINEAR
C                  PARAMETERS(SCALED) ON EXIT
C           (4)    FXL,FXT,FD:
C                  FXL =OPTIMUM VALUE OF LOCATION W.R.T ORIGIN
C                  FXT =    "         "    OF THICKNESS
C                  FD  =    "         "    OF DEPTH TO TOP
C           (5)    KTOT (AS IN INPUT)
C           (6)    RJ1,RJ2,FOT,FIT,F2T,BETA
C                  RJ1,RJ2 :COMPONENTS OF MAGNETIZATION IN PLANE
C                  OF PROFILE(CHAP. ONE)
C                  FOT,FIT,F2T :REGIONAL FIELD LEVELS
C                  BETA :ANGLE BETA(SEE CHAP. ONE)
C           (7)    FX(K),FTOB(K),FTOT(K),FRES(K)
C                  FX(K) & FTOB(K) : (AS IN INPUT)
C                  FTOT(K) : ARRAY OF COMPUTED ANOMALY
C                  FRES(K) : ARRAY OF RESIDUALS(FTOB(K)-FTOT(K))
C
C       WRITTEN BY OFOEGBU JAN. 1981
C
       IMPLICIT REAL*8(A-H,O-Z)
       REAL*4 FTOT2,FDT4,FXT1,FXT2,FDT1,FDT2,FUT3,FTOB2,FX2
       DIMENSION BL(3),BU(3),W(39),X(3),FX(300),FTOB(300)
      1,WHT(300),TITLE(10),FTOT(300),FRES(300),IW(9)
      2,FTOB2(300),FTOT2(300),FX2(300)
C
C       DECLARATION OF COMMON BLOCKS BEGINS
```

```
C
      COMMON/SC1/SC1
      COMMON/SC2/SC2
      COMMON/SC3/SC3
      COMMON/FX/FX
      COMMON/FTOB/FTOB
      COMMON/KTOT/KTOT
      COMMON/FTOT/FTOT
      COMMON/RJ1/RJ1
      COMMON/RJ2/RJ2
      COMMON/FOT/FOT
      COMMON/FIT/FIT
      COMMON/F2T/F2T
      COMMON/WHT/WHT           .
      COMMON/FLAG/FLAG
C
C     READ IN INPUT PARAMETERS
C
      READ(5,11)TITLE
   11 FORMAT(10A4)
      WRITE(6,11)TITLE
      READ(5,*)NM,FLAG,KTOT
      READ(5,*)AX,BX,CX
      READ(5,*)SC1,SC2,SC3
      READ(5,*)X11,X12
      READ(5,*)X21,X22
      READ(5,*)X31,X32
      IF(FLAG.NE.0.0)GO TO 710
      READ(5,*)(FX(K),FTOB(K),K=1,KTOT)
      GO TO 712
  710 READ(5,*)(FX(K),FTOB(K),WHT(K),K=1,KTOT)
  114 FORMAT(F10.2,F10.2)
  712 N=NM
C
C        SET UP AND SCALE INITIAL ESTIMATES OF PARAMETERS
C
      X(1)=AX/SC1
      X(2)=BX/SC2
      X(3)=CX/SC3
      IBOUND=0.0
C
C        SET UP AND SCALE BOUNDS ON PARAMETERS
C
      BL(1)=X11/SC1
      BU(1)=X12/SC1
      BL(2)=X21/SC2
      BU(2)=X22/SC2
      BL(3)=X31/SC3
      BU(3)=X32/SC3
      LIW=NM+2
      LW=39
      IFAIL=1
      CALL TIME(0)
      CALL E04JAF(N,IBOUND,BL,BU,X,F,IW,LIW,W,LW,IFAIL)
      CALL TIME(1,1)
      IF(IFAIL.NE.0)WRITE(6,12)IFAIL
      IF(IFAIL.EQ.1)GO TO 20
C
C        RESTORE RESULTANT VALUES OF PARAMETERS TO ACTUAL VALUES
C
```

```
      FXL=X(1)*SC1
      FXT=X(2)*SC2
      FD=X(3)*SC3
      FXT1=FXL-FXT/2
      FXT2=FXL+FXT/2
      FDT4=FD
      PIE=3.1415926
      IF(RJ2.EQ.0.0)GO TO 900
      BETA=DATAN2(RJ1,RJ2)
      GO TO 901
  900 BETA=PIE/2
C
C
C         COMPUTATION OF RESIDUALS BEGINS
C
  901 DO 25 K=1,KTOT
      FRES(K)=FTOT(K)-FTOB(K)
   25 CONTINUE
C
C         RESULTS OF COMPUTATIONS ARE NOW WRITTEN OUT
C
      WRITE(6,14)F
      WRITE(6,16)(X(J),J=1,N)
      WRITE(6,230)
      WRITE(6,160)FXL,FXT,FD
      WRITE(6,170)KTOT
      WRITE(6,190)RJ1,RJ2,FOT,FIT,F2T,BETA
      WRITE(6,210)
      WRITE(6,220)
      WRITE(6,200)(FX(K),FTOB(K),FTOT(K),FRES(K),K=1,KTOT)
  135 FORMAT(5F10.2)
      DO 117 K=1,KTOT
      FTOT2(K)=FTOT(K)
      FTOB2(K)=FTOB(K)
      FX2(K)=FX(K)
  117 CONTINUE
      YMA=FTOB2(1)
      YMI=FTOB2(1)
      XMI=FX2(1)
      XMA=FX2(1)
      DO 119 K=2,KTOT
      IF(FTOT2(K).GT.YMA)YMA=FTOT2(K)
      IF(FTOB2(K).GT.YMA)YMA=FTOB2(K)
      IF(FTOT2(K).LT.YMI)YMI=FTOT2(K)
      IF(FTOB2(K).LT.YMI)YMI=FTOB2(K)
      IF(FX2(K).GT.XMA)XMA=FX2(K)
      IF(FX2(K).LT.XMI)XMI=FX2(K)
  119 CONTINUE
      XMIN=0.0
      XMAX=XMA+2.0
      YMAX=YMA+20.0
      YMIN=YMI-10.0
      YMA4=(YMAX-YMIN)/3+YMIN
      XMA7=XMAX/13
      XMA3=XMAX/9
      XMA4=XMAX/8
      YMA5=XMAX/2
      FDT1=FDT4
      FDT2=FDT4+(XMAX-FDT4)/3
      FDT3=FDT2+(XMAX-FDT4)/3
      CALL PAPER(1)
```

```
      CALL PSPACE(0.20,0.60,0.55,0.95)
      CALL CTRMAG(7)
      CALL MAP(XMIN,XMAX,YMIN,YMAX)
      CALL BORDER
      CALL AXESSI(1.0,20.0)
      CALL CTRORI(1.0)
      CALL PLOTCS(-XMA4,YMA4,'MAGNETIC ANOMALY(GAMMA)',24)
      CALL CTRORI(0.0)
      CALL NSCURV(FX2,FTOB2,1,KTOT)
      CALL PTPLOT(FX2,FTOT2,1,KTOT,45)
      CALL FULL
      CALL BLKPEN
      CALL PSPACE(0.20,0.60,0.10,0.50)
      CALL MAP(XMIN,XMAX,XMAX,XMIN)
      CALL BORDER
      CALL AXESSI(50.0,1.0)
      CALL POSITN(FXT1,FDT1)
      CALL JOIN(FXT2,FDT1)
      CALL POSITN(FXT2,FDT1)
      CALL JOIN(FXT2,FDT2)
      CALL POSITN(FXT1,FDT1)
      CALL JOIN(FXT1,FDT2)
      CALL BROKEN(5,5,5,5)
      CALL POSITN(FXT1,FDT2)
      CALL JOIN(FXT1,FDT3)
      CALL POSITN(FXT2,FDT2)
      CALL JOIN(FXT2,FDT3)
      CALL PLOTCS(YMA5,-XMA7,'DISTANCE(KM)',12)
      CALL CTRORI(1.0)
      CALL PLOTCS(-XMA3,YMA5,'DEPTH(KM)',9)
      CALL CTRORI(0.0)
      CALL FULL
      CALL PSPACE(0.14,0.66,0.05,1.00)
      CALL BORDER
      CALL GREND
   20 STOP
   12 FORMAT(//'ERROR IN E04JAF 1H IFAIL=',I2/)
   14 FORMAT(///27H FUNCTION VALUE ON EXIT IS,F13.4)
   16 FORMAT(13H AT THE POINT,7F9.4)
  110 FORMAT(I3)
  120 FORMAT(3F10.2)
  130 FORMAT(2F10.2)
  160 FORMAT(3F10.2)
  170 FORMAT(I3)
  190 FORMAT(2F10.4,F10.3,3F10.2)
  200 FORMAT(F10.2,2F13.4,F10.4)
  210 FORMAT(10X//'OBSERVED,COMPUTED,AND RESIDUALSIN GAMMA'/)
  220 FORMAT(10X//'  DIST      OBSERV       COMPUTED       RESIDUAL
  230 FORMAT(10X//'PARAMETER VALUES OBTAINED AFTER OPTIMIZATION'/)
      END
C
C     SUBROUTINE FUNCTION
C     =====================
C
C     THIS SUBROUTINE COMPUTES THE OBJECTIVE FUNCTION
C     TO BE MINIMIZED BY THE MAIN PROGRAM.
C
      SUBROUTINE FUNCT1(N,XC,FC)
      IMPLICIT REAL*8(A-H,O-Z)
      DIMENSION XC(N),FTOC(300),FTOT(300),QSUM(300),PSUM(300)
```

```
      1,A(5,6),FTOB(300),FX(300)
      2,WHT(300),ALPHA(5,6),WKS1(5),WKS2(5),C(5,1)
C
C         DECLARATION OF COMMON BLOCKS BEGIN
C
      COMMON/SC1/SC1
      COMMON/SC2/SC2
      COMMON/SC3/SC3
      COMMON/FX/FX
      COMMON/FTOB/FTOB
      COMMON/KTOT/KTOT
      COMMON/FTOT/FTOT
      COMMON/RJ1/RJ1
      COMMON/RJ2/RJ2
      COMMON/FOT/FOT
      COMMON/FIT/FIT
      COMMON/F2T/F2T
      COMMON/WHT/WHT
      COMMON/FLAG/FLAG
      COM=1.E+2
C
C         DESCALING OF NON-LINEAR PARAMETERS BEGINS
C
      XL=XC(1)*SC1
      XT=XC(2)*SC2
      D=XC(3)*SC3
C
C         LEAST SQUARES COMPUTATION BEGINS
C
      SUMQ1=0.0
      SUMQ2=0.0
      SUMQT=0.0
      SUMQP=0.0
      SUMP1=0.0
      SUMP2=0.0
      SUMPT=0.0
      SUMT1=0.0
      SUMX1=0.0
      SUMX2=0.0
      SUMXT=0.0
      SUMXP=0.0
      SUMXQ=0.0
      SUMX2=0.0
      SUMX2T=0.0
      SUMX2P=0.0
      SUMX2Q=0.0
      SUMX3=0.0
      SUMX4=0.0
      DO 50 K=1,KTOT
      XX1=XL-XT/2-FX(K)
      XX2=XL+XT/2-FX(K)
      XX3=XX1*XX2
      RR1=DSQRT(D**2+XX1**2)
      RR2=DSQRT(D**2+XX2**2)
      IF(DABS(RR1).LT.0.0000001)RR1=0.0000001
      IF(DABS(RR2).LT.0.0000001)RR2=0.0000001
      TD=XT*D
      DXX=D**2+XX3
      PI=3.1415926/2
      ALG=2*COM*DLOG(RR2/RR1)
```

```
      IF(DXX.EQ.0.0)GO TO 510
      ATN=2*COM*DATAN2(TD,DXX)
      GO TO 512
510   ATN=2*COM*PI
512   SUMQ1=SUMQ1+ALG
      SUMQ2=SUMQ2+ALG**2
      SUMQP=SUMQP+ALG*ATN
      SUMQT=SUMQT+ALG*FTOB(K)
      SUMP1=SUMP1+ATN
      SUMP2=SUMP2+ATN**2
      SUMPT=SUMPT+ATN*FTOB(K)
      SUMT1=SUMT1+FTOB(K)
      SUMX1=SUMX1+FX(K)
      SUMX2=SUMX2+(FX(K)**2)
      SUMX3=SUMX3+(FX(K)**3)
      SUMX4=SUMX4+(FX(K)**4)
      SUMXT=SUMXT+FTOB(K)*FX(K)
      SUMXP=SUMXP+ATN*FX(K)
      SUMXQ=SUMXQ+ALG*FX(K)
      SUMX2T=SUMX2T+FTOB(K)*FX(K)*FX(K)
      SUMX2P=SUMX2P+FX(K)*FX(K)*ATN
      SUMX2Q=SUMX2Q+FX(K)*FX(K)*ALG
50    CONTINUE
      TOT=KTOT
      A(1,1)=SUMP2
      A(1,2)=SUMQP
      A(1,3)=SUMP1
      A(1,4)=SUMXP
      A(1,5)=SUMX2P
      A(2,1)=A(1,2)
      A(2,2)=SUMQ2
      A(2,3)=SUMQ1
      A(2,4)=SUMXQ
      A(2,5)=SUMX2Q
      A(3,1)=A(1,3)
      A(3,2)=A(2,3)
      A(3,3)=TOT
      A(3,4)=SUMX1
      A(3,5)=SUMX2
      A(4,1)=A(1,4)
      A(4,2)=A(2,4)
      A(4,3)=A(3,4)
      A(4,4)=SUMX2
      A(4,5)=SUMX3
      A(5,1)=A(1,5)
      A(5,2)=A(2,5)
      A(5,3)=A(3,5)
      A(5,4)=A(4,5)
      A(5,5)=SUMX4
      A(1,6)=SUMPT
      A(2,6)=SUMQT
      A(3,6)=SUMT1
      A(4,6)=SUMXT
      A(5,6)=SUMX2T
      N1=6
      M1=5
      NSYS=1
      DO 1 I=1,M1
1     ALPHA(I,1)=A(I,1)
      DO 2 J=2,N1
```

```
  2 ALPHA(1,J)=A(1,J)/ALPHA(1,1)
    IF(M1.EQ.1)GO TO 9
    DO 6 K=2,M1
    KP=K+1
    KM=K-1
    DO 4 I=K,M1
    SUM=0.0
    DO 3 L=1,KM
  3 SUM=SUM+ALPHA(I,L)*ALPHA(L,K)
  4 ALPHA(I,K)=A(I,K)-SUM
    DO 6 J=KP,N1
    SUM=0.0
    DO 5 L=1,KM
  5 SUM=SUM+ALPHA(K,L)*ALPHA(L,J)
  6 ALPHA(K,J)=(A(K,J)-SUM)/ALPHA(K,K)
    DO 8 IT=1,NSYS
    J=M1+IT
    C(M1,IT)=ALPHA(M1,J)
    DO 8 I=2,M1
    K=M1+1-I
    KP=K+1
    SUM=0.0
    DO 7 L=KP,M1
  7 SUM=SUM+ALPHA(K,L)*C(L,IT)
  8 C(K,IT)=ALPHA(K,J)-SUM
    DO 11 J=1,NSYS
    RJ1=C(1,J)
    RJ2=C(2,J)
    F0T=C(3,J)
    F1T=C(4,J)
    F2T=C(5,J)
 11 CONTINUE
    GO TO 21
  9 DO 10 IT=1,NSYS
 10 C(1,IT)=ALPHA(1,IT+1)
    DO 17 J=1,NSYS
    RJ1=C(1,J)
    RJ2=C(2,J)
    F0T=C(3,J)
    F1T=C(4,J)
    F2T=C(5,J)
 17 CONTINUE
C
C
C     COMPUTATION OF OBJECTIVE FUNCTION NOW BEGINS
C
 21 FT=0.0
    DO 60 K=1,KTOT
    XX1=XL-XT/2-FX(K)
    XX2=XT/2+XL-FX(K)
    XX3=XX1*XX2
    RR1=DSQRT(D**2+XX1**2)
    RR2=DSQRT(D**2+XX2**2)
    IF(DABS(RR1).LT.0.000001)RR1=0.000001
    IF(DABS(RR2).LT.0.000001)RR2=0.000001
    TD=XT*D
    DXX=D**2+XX3
    ALOG=DLOG(RR2/RR1)
    IF(DXX.EQ.0.0)GO TO 514
    ATAN=DATAN2(TD,DXX)
    GO TO 516
```

```
  514  ATAN=PI
  516  QSUM(K)=2*COM*ATAN*RJ1
       PSUM(K)=2*COM*ALOG*RJ2
       FTOT(K)=QSUM(K)+PSUM(K)+FOT+FIT*FX(K)+F2T*FX(K)*FX(K)
       IF(FLAG.NE.0.0)GO TO 612
       FTOC(K)=(FTOB(K)-FTOT(K))**2
       GO TO 614
  612  FTOC(K)=((FTOB(K)-FTOT(K))*WHT(K))**2
  614  FT=FT+FTOC(K)
   60  CONTINUE
       FC=FT
       RETURN
       END
```

```
C                      PROGRAM OPDYE4
C                      =================
C
C         THIS PROGRAM IS A TWO DIMENSIONAL DYKE INTERPRETATION
C         PROGRAM USING THE NON LINEAR OPTIMIZATION TECHNIQUES
C         THE PARAMETERS OPTIMIZED ARE: THE COMPONENTS OF THE
C         MAGNETIZATION OF THE DYKE IN THE PLANE OF THE PROFILE
C         ,THE THICKNESS,DEPTH TO TOP,AND POSITION OF THE
C         CENTRE OF THE DYKE AS WELL AS THE ZEROTH,FIRST AND
C         SECOND ORDER REGIONAL FIELDS,THE SIMPLEX METHOD
C         IS USED,THE INPUT DATA IS AS FOLLOWS:
C         (1)    TITLE:(NOT MORE THAN 40 CHARACTERS)
C         (2)    NM,FLAG,MAXCAL,KTOT:
C                NM=NO. OF NON-LINEAR PARAMETERS(USUALLY THREE)
C                FLAG:=0.0(NO WEIGHTING OF FIELD POINTS
C                       ,N.E. 0.0(FIELD POINTS WEIGHTED)
C                MAXCAL=MAXIMUM NO. OF ITERATIONS(TRY 500)
C                KTOT=NO.OF FIELD POINTS-NOT MORE THAN 300
C         (3)    AX,BX,CX:
C                AX=INITIAL ESTIMATE OF LOCATION W.R.T ORIGIN
C                BX=    "          "      OF THICKNESS
C                CX=    "          "      OF DEPTH TO THE TOP
C         (4)    SC1,SC2,SC3 (SCALING FACTORS FOR AX,BX,CX
C                RESPECTIVELY-SEE CHAPT. ONE)
C         (5)    X11,X12:-LOWER & UPPER LIMITS OF LOCATION
C                X21,X22:-  "     "     "     "     "   THICKNESS
C                X31,X32:-  "     "     "     "     "   DEPTH
C         (6)    FX(K),FTOB(K)(IF FLAG .EQ. 0.0)
C                FX(K),FTOB(K),WHT(K)(IF FLAG .N.E. 0.0)
C                FX(K)=ARRAY OF X-CORD. OF FIELD POINTS
C                FTOB(K)=ARRAY OF OBSERVED ANOMALY
C                WHT(K)=ARRAY OF WEIGHTING OF FIELD POINTS
C         THE OUTPUT IS AS FOLLOWS:
C         (1)    TITLE:(AS IN INPUT)
C         (2)    F  :- OBJECTIVE FUNCTION VALUE ON EXIT
C         (3)    X(I):ARRAY OF VALUES OF NON-LINEAR
C                PARAMETERS(SCALED) ON EXIT
C         (4)    FXL,FXT,FD:
C                FXL =OPTIMUM VALUE OF LOCATION W.R.T ORIGIN
C                FXT =    "         "    OF THICKNESS
C                FD  =    "         "    OF DEPTH TO TOP
C         (5)    KTOT (AS IN INPUT)
C         (6)    RJ1,RJ2,F0T,FIT,F2T,BETA
C                RJ1,RJ2 :COMPONENTS OF MAGNETIZATION IN PLANE
C                OF PROFILE(CHAP. ONE)
C                F0T,FIT,F2T :REGIONAL FIELD LEVELS
C                BETA :ANGLE BETA(SEE CHAP. ONE)
C         (7)    FX(K),FTOB(K),FTOT(K),FRES(K)
C                FX(K) & FTOB(K) : (AS IN INPUT)
C                FTOT(K) : ARRAY OF COMPUTED ANOMALY
C                FRES(K) : ARRAY OF RESIDUALS(FTOB(K)-FTOT(K))
C         (8)    NCALL,FMIN :- NO. OF FUNCT CALLS AND CORRESPONDING
C                OBJECTIVE FUNCTION VALUE
C         (9)    SIM(I,J) :- ARRAY OF VERTICES OF SIMPLEX CORRESPON-
C                DING TO (8) ABOVE
C
C         WRITTEN BY OFOEGBU JAN. 1981
         IMPLICIT REAL*8(A-H,O-Z)
         REAL*4 FFOT2,FDT4,FXT1,FX12,FDT1,FDT2,FDT3,FTOB2,FX2
         DIMENSION W1(3),W2(3),W3(3),X(3),FX(300),FTOB(300)
```

```
     1,WHT(300),TITLE(10),FTOT(300),FRES(300,,04(,5)
    .;55(4),STM(4,3),FTOB2(300),FTOT2(200),FXX(300),
C
C       DECLARATION OF COMMON BLOCKS BEGIN
C
      COMMON/SC1/SC1
      COMMON/SC2/SC2
      COMMON/SC3/SC3
      COMMON/FX/FX
      COMMON/FTOB/FTOB
      COMMON/KTOT/KTOT
      COMMON/FTOT/FTOT
      COMMON/RJ1/RJ1
      COMMON/RJ2/RJ2
      COMMON/FOT/FOT
      COMMON/F1T/F1T
      COMMON/F2T/F2T
      COMMON/WHT/WHT
      COMMON/FLAG/FLAG
      EXTERNAL FUNCT,MONIT
C
C     READ IN INPUT PARAMETERS
C
      READ(5,11)TITLE
   11 FORMAT(10A4)
      WRITE(6,11)TITLE
      READ(5,*)NM,FLAG,MAXCAL,KTOT
      READ(5,*)AX,BX,CX
      READ(5,*)SC1,SC2,SC3
      IF(FLAG.NE.0.0)GO TO 710
      READ(5,*)(FX(K),FTOB(K),K=1,KTOT)
      GO TO 712
  710 READ(5,*)(FX(K),FTOB(K),WHT(K),K=1,KTOT)
  114 FORMAT(F10.2,F10.2)
  712 N=NM
C
C       SET UP AND SCALE INITIAL ESTIMATES OF PARAMETERS
C
      X(1)=AX/SC1
      X(2)=BX/SC2
      X(3)=CX/SC3
      IBOUND=0.0
C
C       SET UP AND SCALE BOUNDS ON PARAMETERS
C
      N1=N+1
      TOL=DSQRT(X02AAF(R))
      IFAIL=0
      CALL TIME(0)
      CALL E04CCF(N,X,F,TOL,N1,W1,W2,W3,W4,W5,STM,UNCT,
     $MONIT,MAXCAL,IFAIL)
      CALL TIME(1,1)
C
C       RESTORE RESULTANT VALUES OF PARAMETERS TO ACTUAL VALUES
C
      FXL=X(1)*SC1
      FXT=X(2)*SC2
      F0=X(3)*SC3
      FXT1=FXL-FXT/2
      FXT2=FXL+FXT/2
```

```
      FDT4=FD
      PIE=3.1415926
      IF(RJ2.EQ.0.0)GO TO 333
      BETA=DATAN2(RJ1,RJ2)
      GO TO 339
  333 BETA=PIE/2
C
C         COMPUTATION OF RESIDUALS BEGINS
C
  339 DO 25 K=1,KTOT
      FRES(K)=FTOT(K)-FTOB(K)
   25 CONTINUE
C
C         RESULTS OF COMPUTATIONS ARE NOW WRITTEN OUT
C
      WRITE(6,14)F
      WRITE(6,16)(X(J),J=1,N)
      WRITE(6,12)IFAIL
      WRITE(6,230)
      WRITE(6,160)FXL,FXT,FD
      WRITE(6,170)KTOT
      WRITE(6,190)RJ1,RJ2,FOT,FIT,F2T,BETA
      WRITE(6,210)
      WRITE(6,220)
      WRITE(6,200)(FX(K),FTOB(K),FTOT(K),FRES(K),K=1,KTOT)
  135 FORMAT(5F10.2)
      DO 117 K=1,KTOT
      FTOT2(K)=FTOT(K)
      FTOB2(K)=FTOB(K)
      FX2(K)=FX(K)
  117 CONTINUE
      YMA=FTOB2(1)
      YMI=FTOB2(1)
      XMI=FX2(1)
      XMA=FX2(1)
      DO 119 K=2,KTOT
      IF(FTOT2(K).GT.YMA)YMA=FTOT2(K)
      IF(FTOB2(K).GT.YMA)YMA=FTOB2(K)
      IF(FTOT2(K).LT.YMI)YMI=FTOT2(K)
      IF(FTOB2(K).LT.YMI)YMI=FTOB2(K)
      IF(FX2(K).GT.XMA)XMA=FX2(K)
      IF(FX2(K).LT.XMI)XMI=FX2(K)
  119 CONTINUE
      XMIN=0.0
      XMAX=XMA+2.0
      YMAX=YMA+20.0
      YMIN=YMI-10.0
      YMA4=(YMAX-YMIN)/3+YMI.
      XMA2=XMAX/13
      XMA3=XMAX/9
      XMA4=XMAX/8
      YMA5=XMAX/2
      FDT1=FDT4
      FDT2=FDT4+(XMAX-FDT4)/3
      FDT3=FDT2+(XMAX-FDT4)/3
      CALL PAPER(1)
      CALL PSPACE(0.20,0.60,0.55,0.95)
      CALL CTRMAG(7)
      CALL MAP(XMIN,XMAX,YMIN,YMA.)
      CALL BORDER
```

```
      CALL AXESSI(1.0,20.0)
      CALL CTRORI(1.0)
      CALL PLOTCS(-XMA4,YMA4,'MAGNETIC ANOMALY(GAMMA)',24)
      CALL CTRORI(0.0)
      CALL NSCURV(FX2,FTOB2,1,KTOT)
      CALL PTPLOT(FX2,FTOT2,1,KTOT,45)
      CALL FULL
      CALL BLKPEN
      CALL PSPACE(0.20,0.60,0.10,0.50)
      CALL MAP(XMIN,XMAX,XMAX,XMIN)
      CALL BORDER
      CALL AXESSI(50.0,1.0)
      CALL POSITN(FXT1,FDT1)
      CALL JOIN(FXT2,FDT1)
      CALL POSITN(FXT2,FDT1)
      CALL JOIN(FXT2,FDT2)
      CALL POSITN(FXT1,FDT1)
      CALL JOIN(FXT1,FDT2)
      CALL BROKEN(5,5,5,5)
      CALL POSITN(FXT1,FDT2)
      CALL JOIN(FXT1,FDT3)
      CALL POSITN(FXT2,FDT2)
      CALL JOIN(FXT2,FDT3)
      CALL PLOTCS(YMA5,-XMA7,'DISTANCE(KM)',12)
      CALL CTRORI(1.0)
      CALL PLOTCS(-XMA3,YMA5,'DEPTH(KM)',9)
      CALL CTRORI(0.0)
      CALL FULL
      CALL PSPACE(0.14,0.66,0.05,1.00)
      CALL BORDER
      CALL GREND
   20 STOP
   12 FORMAT(//'THIS HAS ERROR NUMBER',I3/)
   14 FORMAT(///27H FUNCTION VALUE ON EXIT IS,F13.4)
   16 FORMAT(13H AT THE POINT,7F9.4)
  110 FORMAT(I3)
  120 FORMAT(3F10.2)
  130 FORMAT(2F10.2)
  160 FORMAT(3F10.2)
  170 FORMAT(I3)
  190 FORMAT(2F10.4,F10.3,3F10.2)
  200 FORMAT(F10.2,2F13.4,F10.4)
  210 FORMAT(10X/'OBSERVED,COMPUTED,AND RESIDUALSIN GAMMA'/)
  220 FORMAT(10X/'  DIST      OBSERV      COMPUTED      RESIDUAL
  230 FORMAT(10X/'PARAMETER VALUES OBTAINED AFTER OPTIMIZATION'/)
      END
C
C     SUBROUTINE FUNCTION
C     ===================
C
C
C     THIS SUBROUTINE COMPUTES THE OBJECTIVE FUNCTION
C     TO BE MINIMIZED BY THE MAIN PROGRAM.
C
      SUBROUTINE FUNCT(N,XC,FC)
      IMPLICIT REAL*8(A-H,O-Z)
      DIMENSION XC(N),FTOC(300),FTOT(300),QSUM(300),FSUM(300)
     1,A(5,6),FTOB(300),FX(300)
     2,WHT(300),ALPHA(5,6),WKS1(5),WKS2(5),C(5,1)
C
C     DECLARATION OF COMMON BLOCKS BEGIN
```

```
C
      COMMON/SC1/SC1
      COMMON/SC2/SC2
      COMMON/SC3/SC3
      COMMON/FX/FX
      COMMON/FTOB/FTOB
      COMMON/KTOT/KTOT
      COMMON/FTOT/FTOT
      COMMON/RJ1/RJ1
      COMMON/RJ2/RJ2
      COMMON/FOT/FOT
      COMMON/FIT/FIT
      COMMON/F2T/F2T
      COMMON/WHT/WHT
      COMMON/FLAG/FLAG
      COM=1.E+2
C
C
C         DESCALING OF NON-LINEAR PARAMETERS BEGINS
C
      XL=XC(1)*SC1
      XT=XC(2)*SC2
      D=XC(3)*SC3
C
C         LEAST SQUARES COMPUTATION BEGINS
C
C
      SUMQ1=0.0
      SUMQ2=0.0
      SUMQT=0.0
      SUMQP=0.0
      SUMP1=0.0
      SUMP2=0.0
      SUMPT=0.0
      SUMT1=0.0
      SUMX1=0.0
      SUMX2=0.0
      SUMXT=0.0
      SUMXP=0.0
      SUMXQ=0.0
      SUMX2=0.0
      SUMX2T=0.0
      SUMX2P=0.0
      SUMX2Q=0.0
      SUMX3=0.0
      SUMX4=0.0
      DO 50 K=1,KTOT
      XX1=XL-XT/2-FX(K)
      XX2=XL+XT/2-FX(K)
      XX3=XX1*XX2
      RR1=DSQRT(D**2+XX1**2)
      RR2=DSQRT(D**2+XX2**2)
      IF(DABS(RR1).LT.0.0000001)RR1=0.0000001
      IF(DABS(RR2).LT.0.0000001)RR2=0.0000001
      TD=XT*D
      DXX=D**2+XX3
      PI=3.1415926/2
      ALG=2*COM*DLOG(RR2/RR1)
      IF(DXX.EQ.0.0)GO TO 510
      ATN=2*COM*DATAN2(TD,DXX)
      GO TO 512
  510 ATN=2*COM*PI
```

```
512  SUMQ1=SUMQ1+ALG
     SUMQ2=SUMQ2+ALG**2
     SUMQP=SUMQP+ALG*ATN
     SUMQT=SUMQT+ALG*FTOB(K)
     SUMP1=SUMP1+ATN
     SUMP2=SUMP2+ATN**2
     SUMPT=SUMPT+ATN*FTOB(K)
     SUMT1=SUMT1+FTOB(K)
     SUMX1=SUMX1+FX(K)
     SUMX2=SUMX2+(FX(K)**2)
     SUMX3=SUMX3+(FX(K)**3)
     SUMX4=SUMX4+(FX(K)**4)
     SUMXT=SUMXT+FTOB(K)*FX(K)
     SUMXP=SUMXP+ATN*FX(K)
     SUMXQ=SUMXQ+ALG*FX(K)
     SUMX2T=SUMX2T+FTOB(K)*FX(K)*FX(K)
     SUMX2P=SUMX2P+FX(K)*FX(K)*ATN
     SUMX2Q=SUMX2Q+FX(K)*FX(K)*ALG
  50 CONTINUE
     TOT=KTOT
     A(1,1)=SUMP2
     A(1,2)=SUMQP
     A(1,3)=SUMP1
     A(1,4)=SUMXP
     A(1,5)=SUMX2P
     A(2,1)=A(1,2)
     A(2,2)=SUMQ2
     A(2,3)=SUMQ1
     A(2,4)=SUMXQ
     A(2,5)=SUMX2Q
     A(3,1)=A(1,3)
     A(3,2)=A(2,3)
     A(3,3)=TOT
     A(3,4)=SUMX1
     A(3,5)=SUMX2
     A(4,1)=A(1,4)
     A(4,2)=A(2,4)
     A(4,3)=A(3,4)
     A(4,4)=SUMX2
     A(4,5)=SUMX3
     A(5,1)=A(1,5)
     A(5,2)=A(2,5)
     A(5,3)=A(3,5)
     A(5,4)=A(4,5)
     A(5,5)=SUMX4
     A(1,6)=SUMPT
     A(2,6)=SUMQT
     A(3,6)=SUMT1
     A(4,6)=SUMXT
     A(5,6)=SUMX2T
     N2=6
     M1=5
     NSYS=1
     DO 1 I=1,M1
   1 ALPHA(I,1)=A(I,1)
     DO 2 J=2,N2
   2 ALPHA(1,J)=A(1,J)/ALPHA(1,1)
     IF(M1.EQ.1)GO TO 9
     DO 6 K=2,M1
     KP=K+1
```

```
      KM=K-1
      DO 4 I=K,M1
      SUM=0.0
      DO 3 L=1,KM
    3 SUM=SUM+ALPHA(I,L)*ALPHA(L,K)
    4 ALPHA(I,K)=A(I,K)-SUM
      DO 6 J=KP,N2
      SUM=0.0
      DO 5 L=1,KM
    5 SUM=SUM+ALPHA(K,L)*ALPHA(L,J)
    6 ALPHA(K,J)=(A(K,J)-SUM)/ALPHA(K,K)
      DO 8 IT=1,NSYS
      J=M1+IT
      C(M1,IT)=ALPHA(M1,J)
      DO 8 I=2,M1
      K=M1+1-I
      KP=K+1
      SUM=0.0
      DO 7 L=KP,M1
    7 SUM=SUM+ALPHA(K,L)*C(L,IT)
    8 C(K,IT)=ALPHA(K,J)-SUM
      DO 11 J=1,NSYS
      RJ1=C(1,J)
      RJ2=C(2,J)
      FOT=C(3,J)
      FIT=C(4,J)
      F2T=C(5,J)
   11 CONTINUE
      GO TO 21
    9 DO 10 IT=1,NSYS
   10 C(1,IT)=ALPHA(1,IT+1)
      DO 17 J=1,NSYS
      RJ1=C(1,J)
      RJ2=C(2,J)
      FOT=C(3,J)
      FIT=C(4,J)
      F2T=C(5,J)
   17 CONTINUE
C
C        COMPUTATION OF OBJECTIVE FUNCTION NOW BEGINS
C
   21 FT=0.0
      DO 60 K=1,KTOT
      XX1=XL-XT/2-FX(K)
      XX2=XT/2+XL-FX(K)
      XX3=XX1*XX2
      RR1=DSQRT(D**2+XX1**2)
      RR2=DSQRT(D**2+XX2**2)
      IF(DABS(RR1).LT.0.0000001)RR1=0.0000001
      IF(DABS(RR2).LT.0.0000001)RR2=0.0000001
      TD=XT*D
      DXX=D**2+XX3
      ALOG=DLOG(RR2/RR1)
      IF(DXX.EQ.0.0)GO TO 514
      ATAN=DATAN2(TD,DXX)
      GO TO 516
  514 ATAN=PI
  516 QSUM(K)=2*COM*ATAN*RJ1
      PSUM(K)=2*COM*ALOG*RJ2
      FTOT(K)=QSUM(K)+PSUM(K)+FOT+FIT*FX(K)+F2T*FX(K)*FX(K)
```

```
      IF(FLAG.NE.0.0)GO TO 612
      FTOC(K)=(FTOB(K)-FTOT(K))**2
      GO TO 614
  612 FTOC(K)=((FTOB(K)-FTOT(K))*WHT(K))**2
  614 FT=FT+FTOC(K)
   60 CONTINUE
      FC=FT
      RETURN
      END
C
C
C     SUBROUTINE MONIT
C
      SUBROUTINE MONIT(FMIN,FMAX,SIM,N,N1,NCALL)
      IMPLICIT REAL*8(A-H,O-Z)
      DIMENSION SIM(N1,N)
      WRITE(6,11)NCALL,FMIN
      WRITE(6,12)((SIM(I,J),J=1,N),I=1,N1)
   11 FORMAT(6H AFTER, I5, 30H FUNCTION CALLS, THE VALUE IS,
     $ F10.4, 14H WITH SIMPLEX)
C  11 FORMAT(I5,14X,F10.4)
   12 FORMAT(4(3F12.4/))
      RETURN
      END
```

```
C                      PROGRAM OPDYE5
C                      ==============
C
C       THIS PROGRAM IS A TWO DIMENSIONAL DYKE INTERPRETATION
C       PROGRAM USING THE NON LINEAR OPTIMIZATION TECHNIQUES
C       THE PARAMETERS OPTIMIZED ARE: THE ZERO ORDER REGIONAL
C       FIELD,THE THICKNESS,DEPTH TO TOP,AND POSITION OF THE
C       CENTRE OF THE DYKE. ALSO OPTIMIZED ARE THE COMPONENTS
C       OF THE MAGNETIZATION IN THE PLANE OF THE PROFILE.
C       IT USES THE QUASI-NEWTON METHOD.
C       THE INPUT DATA IS AS FOLLOWS:
C       (1)     TITLE:(NOT MORE THAN 40 CHARACTERS)
C       (2)     NM,FLAG,KTOT:
C               NM=NO. OF NON-LINEAR PARAMETERS(USUALLY THREE)
C               FLAG:=0.0(NO WEIGHTING OF FIELD POINTS
C                     .N.E. 0.0(FIELD POINTS WEIGHTED)
C               KTOT=NO.OF FIELD POINTS-NOT MORE THAN 300
C       (3)     AX,BX,CX:
C               AX=INITIAL ESTIMATE OF LOCATION W.R.T ORIGIN
C               BX=   "        "        OF THICKNESS
C               CX=   "        "        OF DEPTH TO THE TOP
C       (4)     SC1,SC2,SC3 (SCALING FACTORS FOR AX,BX,CX
C               RESPECTIVELY-SEE CHAPT. ONE)
C       (5)     X11,X12:-LOWER & UPPER LIMITS OF LOCATION
C               X21,X22:-  "    "    "    "     "   THICKNESS
C               X31,X32:-  "    "    "    "     "   DEPTH
C       (6)     FX(K),FTOB(K)(IF FLAG .EQ. 0.0)
C               FX(K),FTOB(K),WHT(K)(IF FLAG .N.E. 0.0)
C               FX(K)=ARRAY OF X-CORD. OF FIELD POINTS
C               FTOB(K)=ARRAY OF OBSERVED ANOMALY
C               WHT(K)=ARRAY OF WEIGHTING OF FIELD POINTS
C       THE OUTPUT IS AS FOLLOWS:
C       (1)     TITLE:(AS IN INPUT)
C       (2)     F :- OBJECTIVE FUNCTION VALUE ON EXIT
C       (3)     X(I):ARRAY OF VALUES OF NON-LINEAR
C               PARAMETERS(SCALED) ON EXIT
C       (4)     FXL,FXT,FD:
C               FXL =OPTIMUM VALUE OF LOCATION W.R.T ORIGIN
C               FXT =    "        "     OF THICKNESS
C               FD  =    "        "     OF DEPTH TO TOP
C       (5)     KTOT (AS IN INPUT)
C       (6)     RJ1,RJ2,FOT,BETA
C               RJ1,RJ2 :COMPONENTS OF MAGNETIZATION IN PLANE
C               OF PROFILE(CHAP. ONE)
C               FOT :REGIONAL FIELD LEVEL
C               BETA :ANGLE BETA(SEE CHAP. ONE)
C       (7)     FX(K),FTOB(K),FTOT(K),FRES(K)
C               FX(K) & FTOB(K) : (AS IN INPUT)
C               FTOT(K) : ARRAY OF COMPUTED ANOMALY
C               FRES(K) : ARRAY OF RESIDUALS(FTOB(K)-FTOT(K))
C
C       WRITTEN BY OFOEGBU JAN. 1981
C
        IMPLICIT REAL*8(A-H,O-Z)
        REAL*4 FTOT2,FDT4,FXT1,FXT2,FDT1,FDT2,FDT3,FTOB2,FX2
        DIMENSION BL(3),BU(3),W(39),X(3),FX(300),FTOB(300)
      1,TITLE(10),FTOT(300),FRES(300),IW(9)
      2,WHT(300),FTOB2(300),FTOT2(300),FX2(300)
        COMMON/SC1/SC1
        COMMON/SC2/SC2
```

```
      COMMON/SC3/SC3
      COMMON/FX/FX
      COMMON/FTOB/FTOB
      COMMON/KTOT/KTOT
      COMMON/FTOT/FTOT
      COMMON/RJ1/RJ1
      COMMON/RJ2/RJ2
      COMMON/FOT/FOT
      COMMON/FLAG/FLAG
      COMMON/WHT/WHT
C     READ IN INPUT PARAMETERS
C
      READ(5,11)TITLE
   11 FORMAT(10A4)
      WRITE(6,11)TITLE
      READ(5,*)NM,FLAG,KTOT
      READ(5,*)AX,BX,CX
      READ(5,*)SC1,SC2,SC3
      READ(5,*)X11,X12
      READ(5,*)X21,X22
      READ(5,*)X31,X32
      IF(FLAG.NE.0.0)GO TO 121
      READ(5,*)(FX(K),FTOB(K),K=1,KTOT)
      GO TO 131
  121 READ(5,*)(FX(K),FTOB(K),WHT(K),K=1,KTOT)
  131 N=NM
C
C        SET UP AND SCALE INITIAL ESTIMATES OF PARAMETERS
C
      X(1)=AX/SC1
      X(2)=BX/SC2
      X(3)=CX/SC3
      IBOUND=0.0
C
C        SET UP AND SCALE BOUNDS ON PARAMETERS
C
      BL(1)=X11/SC1
      BU(1)=X12/SC1
      BL(2)=X21/SC2
      BU(2)=X22/SC2
      BL(3)=X31/SC3
      BU(3)=X32/SC3
      LIW=NM+2
      LW=39
      IFAIL=1
  114 FORMAT(F10.2,F10.2)
      CALL TIME(0)
      CALL E04JAF(N,IBOUND,BL,BU,X,F,IW,LIW,W,LW,IFAIL)
      IF(IFAIL.NE.0)WRITE(6,12)IFAIL
      IF(IFAIL.EQ.1)GO TO 20
      CALL TIME(1,1)
C
C        RESTORE RESULTANT VALUES OF PARAMETERS TO ACTUAL VALUES
C
      FXL=X(1)*SC1
      FXT=X(2)*SC2
      FD=X(3)*SC3
      FXT1=FXL-FXT/2
      FXT2=FXL+FXT/2
      FDT4=FD
```

```
      PI2=3.1415926
      IF(RJ2.EQ.0.0)GO TO 510
      BETA=DATAN2(RJ1,RJ2)
      GO TO 512
  510 BETA=PI2/2
C
C        COMPUTATION OF RESIDUALS BEGINS
C
C
  512 DO 25 K=1,KTOT
      FRES(K)=FTOT(K)-FTOB(K)
   25 CONTINUE
C
C        RESULTS OF COMPUTATIONS ARE NOW WRITTEN OUT
C
C
      WRITE(6,14)F
      WRITE(6,16)(X(J),J=1,N)
      WRITE(6,230)
      WRITE(6,160)FXL,FXT,FD
      WRITE(6,170)KTOT
      WRITE(6,190)RJ1,RJ2,FDT,BETA
      WRITE(6,210)
      WRITE(6,220)
      WRITE(6,200)(FX(K),FTOB(K),FTOT(K),FRES(K),K=1,KTOT)
  135 FORMAT(5F10.2)
      DO 117 K=1,KTOT
      FTOT2(K)=FTOT(K)
      FTOB2(K)=FTOB(K)
      FX2(K)=FX(K)
  117 CONTINUE
      YMA=FTOB2(1)
      YMI=FTOB2(1)
      XMI=FX2(1)
      XMA=FX2(1)
      DO 119 K=2,KTOT
      IF(FTOT2(K).GT.YMA)YMA=FTOT2(K)
      IF(FTOB2(K).GT.YMA)YMA=FTOB2(K)
      IF(FTOT2(K).LT.YMI)YMI=FTOT2(K)
      IF(FTOB2(K).LT.YMI)YMI=FTOB2(K)
      IF(FX2(K).GT.XMA)XMA=FX2(K)
      IF(FX2(K).LT.XMI)XMI=FX2(K)
  119 CONTINUE
      XMIN=0.0
      XMAX=XMA+2.0
      YMAX=YMA+20.0
      YMIN=YMI-10.0
      YMA4=(YMAX-YMIN)/3+YMIN
      XMA7=XMAX/13
      XMA3=XMAX/9
      XMA4=XMAX/8
      YMA5=XMAX/2
      FDT1=FDT4
      FDT2=FDT4+(XMAX-FDT4)/3
      FDT3=FDT2+(XMAX-FDT4)/3
      CALL PAPER(1)
      CALL PSPACE(0.20,0.60,0.55,0.95)
      CALL CTRMAG(7)
      CALL MAP(XMIN,XMAX,YMIN,YMAX)
      CALL BORDER
      CALL AXESSI(1.0,20.0)
      CALL CTRORI(1.0)
```

```
      CALL PLOTCS(-XMA4,YMA4,'MAGNETIC ANOMALY(GAMMA)',24)
      CALL CTRORI(0,0)
      CALL NSCURV(FX2,FTOB2,1,KTOT)
      CALL PTPLOT(FX2,FTOT2,1,KTOT,45)
      CALL FULL
      CALL BLKPEN
      CALL PSPACE(0.20,0.60,0.10,0.50)
      CALL MAP(XMIN,XMAX,XMAX,XMIN)
      CALL BORDER
      CALL AXESSI(50.0,1.0)
      CALL POSITN(FXT1,FDT1)
      CALL JOIN(FXT2,FDT1)
      CALL POSITN(FXT2,FDT1)
      CALL JOIN(FXT2,FDT2)
      CALL POSITN(FXT1,FDT1)
      CALL JOIN(FXT1,FDT2)
      CALL BROKEN(5,5,5,5)
      CALL POSITN(FXT1,FDT2)
      CALL JOIN(FXT1,FDT3)
      CALL POSITN(FXT2,FDT2)
      CALL JOIN(FXT2,FDT3)
      CALL PLOTCS(YMA5,-XMA7,'DISTANCE(KM)',12)
      CALL CTRORI(1,0)
      CALL PLOTCS(-XMA3,YMA5,'DEPTH(KM)',9)
      CALL CTRORI(0,0)
      CALL FULL
      CALL PSPACE(0.14,0.66,0.05,1.00)
      CALL BORDER
      CALL GREND
   20 STOP
   12 FORMAT(//'ERROR IN E04JAF 1H IFAIL=',I2/)
   14 FORMAT(///27H FUNCTION VALUE ON EXIT IS,F13.4)
   16 FORMAT(13H AT THE POINT,7F9.4)
  110 FORMAT(I3)
  120 FORMAT(3F10.2)
  130 FORMAT(2F10.2)
  160 FORMAT(3F10.2)
  170 FORMAT(I3)
  190 FORMAT(2F10.4,F10.3,F10.2)
  200 FORMAT(F10.2,2F13.4,F10.4)
  210 FORMAT(10X//'OBSERVED,COMPUTED,AND RESIDUALSIN GAMMA'/)
  220 FORMAT(10X//'    DIST       OBSERV       COMPUTED       RESIDUAL
  230 FORMAT(10X//'PARAMETER VALUES OBTAINED AFTER OPTIMIZATION'/)
      END
C
C     SUBROUTINE FUNCTION
C     =======================
C
C
C     THIS SUBROUTINE COMPUTES THE OBJECTIVE FUNCTION
C     TO BE MINIMIZED BY THE MAIN PROGRAM.
C
      SUBROUTINE FUNCT1(N,XC,FC)
      IMPLICIT REAL*8(A-H,O-Z)
      DIMENSION XC(N),FTOC(300),FTOT(300),QSUM(300),PSUM(300)
     1,WHT(300),FTOB(300),FX(300)
C
C     DECLARATION OF COMMON BLOCKS BEGINS
C
      COMMON/SC1/SC1
      COMMON/SC2/SC2
```

```
      COMMON/SC3/SC3
      COMMON/FX/FX
      COMMON/FTOB/FTOB
      COMMON/KTOT/KTOT
      COMMON/FTOT/FTOT
      COMMON/RJ1/RJ1
      COMMON/RJ2/RJ2
      COMMON/FOT/FOT
      COMMON/FLAG/FLAG
      COMMON/WHT/WHT
C
C        DESCALING OF NON-LINEAR PARAMETERS BEGINS
C
      XL=XC(1)*SC1
      XT=XC(2)*SC2
      D=XC(3)*SC3
C
C        LEAST SQUARES COMPUTATION NOW COMMENCES
C
C
      SUMQ1=0.0
      SUMQ2=0.0
      SUMQT=0.0
      SUMQP=0.0
      SUMP1=0.0
      SUMP2=0.0
      SUMPT=0.0
      SUMT1=0.0
      COM=1.E+2
      DO 50 K=1,KTOT
      XX1=XL-XT/2-FX(K)
      XX2=XL+XT/2-FX(K)
      XX3=XX1*XX2
      RR1=DSQRT(D**2+XX1**2)
      RR2=DSQRT(D**2+XX2**2)
      PI=3.1415926
      TD=XT*D
      DXX=D**2+XX3
      IF(DABS(RR1).LT.0.0000001)RR1=0.0000001
      IF(DABS(RR2).LT.0.0000001)RR2=0.0000001
      ALG=2*COM*DLOG(RR2/RR1)
      IF(DXX.EQ.0.0)GO TO 514
      ATN=2*COM*DATAN2(TD,DXX)
      GO TO 516
  514 ATN=2*COM*PI/2
  516 SUMQ1=SUMQ1+ALG
      SUMQ2=SUMQ2+ALG**2
      SUMQP=SUMQP+ALG*ATN
      SUMQT=SUMQT+ALG*FTOB(K)
      SUMP1=SUMP1+ATN
      SUMP2=SUMP2+ATN**2
      SUMPT=SUMPT+ATN*FTOB(K)
      SUMT1=SUMT1+FTOB(K)
   50 CONTINUE
      F1=KTOT*SUMP2-SUMP1*SUMP1
      F2=KTOT*SUMQP-SUMP1*SUMQ1
      F3=SUMP1*SUMT1-KTOT*SUMPT
      F4=KTOT*SUMQ2-SUMQ1*SUMQ1
      F5=SUMQ1*SUMT1-KTOT*SUMQT
      FJ1=F1*F4-F2*F2
      FJ2=F2*F2-F4*F1
```

```
      IF(DABS(FJ1).LT.0.0000001)FJ1=0.0000001
      IF(DABS(FJ2).LT.0.0000001)FJ2=0.0000001
      RJ1=(F5*F2-F3*F4)/FJ1
      RJ2=(F5*F1-F3*F2)/FJ2
      FOT=(SUMT1-RJ1*SUMP1-RJ2*SUMQ1)/KTOT
C
C        COMPUTATION OF OBJECTIVE FUNCTION NOW BEGINS
C
      FT=0.0
      DO 60 K=1,KTOT
      XX1=XL-XT/2-FX(K)
      XX2=XT/2+XL-FX(K)
      XX3=XX1*XX2
      RR1=DSQRT(D**2+XX1**2)
      RR2=DSQRT(D**2+XX2**2)
      TD=XT*D
      DXX=D**2+XX3
      IF(DABS(RR1).LT.0.0000001)RR1=0.0000001
      IF(DABS(RR2).LT.0.0000001)RR2=0.0000001
      ALOG=DLOG(RR2/RR1)
      IF(DXX.EQ.0.0)GO TO 518
      ATAN=DATAN2(TD,DXX)
      GO TO 520
  518 ATAN=PI/2
  520 QSUM(K)=2*COM*ATAN*RJ1
      PSUM(K)=2*COM*ALOG*RJ2
      FTOT(K)=QSUM(K)+PSUM(K)+FOT
      IF(FLAG.NE.0.0)GO TO 141
      FTOC(K)=(FTOB(K)-FTOT(K))**2
      GO TO 144
  141 FTOC(K)=(((FTOB(K)-FTOT(K)))*WHT(K))**2
  144 FT=FT+FTOC(K)
   60 CONTINUE
      FC=FT
      RETURN
      END
```

```
C                    PROGRAM OPDYE6
C                    ==================
C
C         THIS PROGRAM IS A TWO DIMENSIONAL DYKE INTERPRETATION
C         PROGRAM USING THE NON LINEAR OPTIMIZATION TECHNIQUES
C         THE PARAMETERS OPTIMIZED ARE: THE COMPONENTS OF THE
C         MAGNETIZATION OF THE DYKE IN THE PLANE OF THE PROFILE
C         ,THE THICKNESS,DEPTH TO TOP,AND POSITION OF THE -
C         CENTRE OF THE DYKE AS WELL AS THE ZEROTH ORDER
C         REGIONAL FIELD.THE SIMPLEX METHOD IS USED.
C         THE INPUT DATA IS AS FOLLOWS:
C         (1)    TITLE:(NOT MORE THAN 40 CHARACTERS)
C         (2)    NM,FLAG,MAXCAL,KTOT:
C                NM=NO. OF NON-LINEAR PARAMETERS(USUALLY THREE)
C                FLAG:=0.0(NO WEIGHTING OF FIELD POINTS
C                    .N.E. 0.0(FIELD POINTS WEIGHTED)
C                MAXCAL=MAXIMUM NO. OF ITERATIONS(TRY 500)
C                KTOT=NO.OF FIELD POINTS-NOT MORE THAN 300
C         (3)    AX,BX,CX:
C                AX=INITIAL ESTIMATE OF LOCATION W.R.T ORIGIN
C                BX=     "          "        OF THICKNESS
C                CX=     "          "        OF DEPTH TO THE TOP
C         (4)    SC1,SC2,SC3 (SCALING FACTORS FOR AX,BX,CX
C                RESPECTIVELY-SEE CHAPT. ONE)
C         (5)    X11,X12:-LOWER & UPPER LIMITS OF LOCATION
C                X21,X22:-   "     "     "      "      "   THICKNESS
C                X31,X32:-   "     "     "      "      "   DEPTH
C         (6)    FX(K),FTOB(K)(IF FLAG .EQ. 0.0)
C                FX(K),FTOB(K),WHT(K)(IF FLAG .N.E. 0.0)
C                FX(K)=ARRAY OF X-CORD. OF FIELD POINTS
C                FTOB(K)=ARRAY OF OBSERVED ANOMALY
C                WHT(K)=ARRAY OF WEIGHTING OF FIELD POINTS
C         THE OUTPUT IS AS FOLLOWS:
C         (1)    TITLE:(AS IN INPUT)
C         (2)    F :- OBJECTIVE FUNCTION VALUE ON EXIT
C         (3)    X(I):ARRAY OF VALUES OF NON-LINEAR
C                PARAMETERS(SCALED) ON EXIT
C         (4)    FXL,FXT,FD:
C                FXL =OPTIMUM VALUE OF LOCATION W.R.T ORIGIN
C                FXT =     "        "     OF THICKNESS
C                FD  =     "        "     OF DEPTH TO TOP
C         (5)    KTOT (AS IN INPUT)
C         (6)    RJ1,RJ2,FOT,BETA
C                RJ1,RJ2 :COMPONENTS OF MAGNETIZATION IN PLANE
C                OF PROFILE(CHAP. ONE)
C                FOT :REGIONAL FIELD LEVEL
C                BETA :ANGLE BETA(SEE CHAP. ONE)
C         (7)    FX(K),FTOB(K),FTOT(K),FRES(K)
C                FX(K) & FTOB(K) : (AS IN INPUT)
C                FTOT(K) : ARRAY OF COMPUTED ANOMALY
C                FRES(K) : ARRAY OF RESIDUALS(FTOB(K)-FTOT(K))
C         (8)    NCALL,FMIN :- NO. OF FUNCT CALLS AND CORRESPONDING
C                OBJECTIVE FUNCTION VALUE
C         (9)    SIM(I,J) :- ARRAY OF VERTICES OF SIMPLEX CORRESPON-
C                DING TO (8) ABOVE
C                    - BY OFOEGBU 1981
C
          IMPLICIT REAL*8(A-H,O-Z)
          REAL*4 FTOT2,FDT4,FXT1,FXT2,FDT1,FDT2,FDT3,FTOB2,FX2
          DIMENSION W2(3),W3(3),W1(3),X(3),FX(300),FTOB(300)
```

```
     1,W5(4),SIM(4,3),TITLE(10),FTOT(300),FRES(300),W4(3)
     2,WHT(300),FTOB2(300),FTOT2(300),FX2(300)
C
C          DECLARATION OF COMMON BLOCKS BEGINS
C
       COMMON/SC1/SC1
       COMMON/SC2/SC2
       COMMON/SC3/SC3
       COMMON/FX/FX
       COMMON/FTOB/FTOB
       COMMON/KTOT/KTOT
       COMMON/FTOT/FTOT
       COMMON/RJ1/RJ1
       COMMON/RJ2/RJ2
       COMMON/FOT/FOT
       COMMON/FLAG/FLAG
       COMMON/WHT/WHT
       EXTERNAL FUNCT,MONIT
C
C     READ IN INPUT PARAMETERS
C
       READ(5,11)TITLE
    11 FORMAT(10A4)
       WRITE(6,11)TITLE
       READ(5,*)NM,FLAG,MAXCAL,KTOT
       READ(5,*)AX,BX,CX
       READ(5,*)SC1,SC2,SC3
       N=NM
C
C         SET UP AND SCALE INITIAL ESTIMATES OF PARAMETERS
C
       X(1)=AX/SC1
       X(2)=BX/SC2
       X(3)=CX/SC3
       N1=N+1
       TOL=DSQRT(X02AAF(R))
C      MAXCAL=100
       IFAIL=0
       IF(FLAG.NE.0.0)GO TO 121
       READ(5,*)(FX(K),FTOB(K),K=1,KTOT)
       GO TO 131
   121 READ(5,*)(FX(K),FTOB(K),WHT(K),K=1,KTOT)
   114 FORMAT(F10.2,F10.2)
   131 CALL TIME(0)
       CALL E04CCF(N,X,F,TOL,N1,W1,W2,W3,W4,W5,SIM,FUNCT,
      $MONIT,MAXCAL,IFAIL)
C      CALL FUNCT(N,XC,FC)
    20 CALL TIME(1,1)
       WRITE(6,14)F
       WRITE(6,16)(X(I),I=1,N)
       WRITE(6,12)IFAIL
C
C         RESTORE RESULTANT VALUES OF PARAMETERS TO ACTUAL VALUES
C
       FXL=X(1)*SC1
       FXT=X(2)*SC2
       FD=X(3)*SC3
       FXT1=FXL-FXT/2
       FXT2=FXL+FXT/2
       FDT4=FD
```

```
      PI2=3.1415926
      IF(DABS(RJ2).LT.0.000001)GO TO 333
      BETA=DATAN2(RJ1,RJ2)
      GO TO 335
  333 BETA=PI2/2
  335 WRITE(6,230)
      WRITE(6,160)FXL,FXT,FD
      WRITE(6,170)KTOT
      WRITE(6,190)RJ1,RJ2,FOT,BETA
C
C        COMPUTATION OF RESIDUALS BEGINS
C
C
      DO 25 K=1,KTOT
      FRES(K)=FTOT(K)-FTOB(K)
   25 CONTINUE
      WRITE(6,210)
      WRITE(6,220)
      WRITE(6,200)(FX(K),FTOB(K),FTOT(K),FRES(K),K=1,KTOT)
  135 FORMAT(5F10.2)
      DO 117 K=1,KTOT
      FTOT2(K)=FTOT(K)
      FTOB2(K)=FTOB(K)
      FX2(K)=FX(K)
  117 CONTINUE
      YMA=FTOB2(1)
      YMI=FTOB2(1)
      XMI=FX2(1)
      XMA=FX2(1)
      DO 119 K=2,KTOT
      IF(FTOT2(K).GT.YMA)YMA=FTOT2(K)
      IF(FTOB2(K).GT.YMA)YMA=FTOB2(K)
      IF(FTOT2(K).LT.YMI)YMI=FTOT2(K)
      IF(FTOB2(K).LT.YMI)YMI=FTOB2(K)
      IF(FX2(K).GT.XMA)XMA=FX2(K)
      IF(FX2(K).LT.XMI)XMI=FX2(K)
  119 CONTINUE
      XMIN=0.0
      XMAX=XMA+2.0
      YMAX=YMA+20.0
      YMIN=YMI-10.0
      YMA4=(YMAX-YMIN)/34+YMIN
      XMA7=XMAX/13
      XMA3=XMAX/9
      XMA4=XMAX/8
      YMA5=XMAX/2
      FDT1=FDT4
      FDT2=FDT4+(XMAX-FDT4)/3
      FDT3=FDT2+(XMAX-FDT4)/3
      CALL PAPER(1)
      CALL PSPACE(0.20,0.60,0.55,0.95)
      CALL CTRMAG(7)
      CALL MAP(XMIN,XMAX,YMIN,YMAX)
      CALL BORDER
      CALL AXESSI(1.0,20.0)
      CALL CTRORI(1.0)
      CALL PLOTCS(-XMA4,YMA4,'MAGNETIC ANOMALY(GAMMA)',24)
      CALL CTRORI(0.0)
      CALL NSCURV(FX2,FTOB2,1,KTOT)
      CALL PTPLOT(FX2,FTOT2,1,KTOT,45)
      CALL FULL
```

```
      CALL  BLKPEN
      CALL  PSPACE(0.20,0.60,0.10,0.50)
      CALL  MAP(XMIN,XMAX,XMAX,XMIN)
      CALL  BORDER
      CALL  AXESSI(50.0,1.0)
      CALL  POSITN(FXT1,FDT1)
      CALL  JOIN(FXT2,FDT1)
      CALL  POSITN(FXT2,FDT1)
      CALL  JOIN(FXT2,FDT2)
      CALL  POSITN(FXT1,FDT1)
      CALL  JOIN(FXT1,FDT2)
      CALL  BROKEN(5,5,5,5)
      CALL  POSITN(FXT1,FDT2)
      CALL  JOIN(FXT1,FDT3)
      CALL  POSITN(FXT2,FDT2)
      CALL  JOIN(FXT2,FDT3)
      CALL  PLOTCS(YMA5,-XMA7,'DISTANCE(KM)',12)
      CALL  CTRORI(1.0)
      CALL  PLOTCS(-XMA3,YMA5,'DEPTH(KM)',9)
      CALL  CTRORI(0.0)
      CALL  FULL
      CALL  PSPACE(0.14,0.66,0.05,1.00)
      CALL  BORDER
      CALL  GREND
      STOP
   12 FORMAT(//'THIS HAS ERROR NUMBER',I3/)
   14 FORMAT(///27H FUNCTION VALUE ON EXIT IS,F13.4)
   16 FORMAT(13H AT THE POINT,7F9.4)
  110 FORMAT(I3)
  120 FORMAT(3F10.2)
  130 FORMAT(2F10.2)
  160 FORMAT(3F10.2)
  170 FORMAT(I3)
  190 FORMAT(2F10.4,F10.3,F10.2)
  200 FORMAT(F10.2,2F13.4,F10.4)
  210 FORMAT(10X/'OBSERVED,COMPUTED,AND RESIDUALSIN GAMMA'/)
  220 FORMAT(10X/'  DIST        OBSERV         COMPUTED         RESIDUAL
  230 FORMAT(10X/'PARAMETER VALUES OBTAINED AFTER OPTIMIZATION'/)
      END
C
C
C     SUBROUTINE FUNCTION
C     ===================
C
C
C     THIS SUBROUTINE COMPUTES THE OBJECTIVE FUNCTION
C     TO BE MINIMIZED BY THE MAIN PROGRAM.
C
      SUBROUTINE FUNCT(N,XC,FC)
      IMPLICIT REAL*8(A-H,O-Z)
      DIMENSION XC(N),FTOC(300),FTOT(300),QCUM(300),PSUM(300)
     1,WHT(300),FTOB(300),FX(300)
C
C     DECLARATION OF COMMON BLOCKS BEGINS
C
      COMMON/SC1/SC1
      COMMON/SC2/SC2
      COMMON/SC3/SC3
      COMMON/FX/FX
      COMMON/FTOB/FTOB
      COMMON/KTOT/KTOT
      COMMON/FTOT/FTOT
```

```
      COMMON/RJ1/RJ1
      COMMON/RJ2/RJ2
      COMMON/FOT/FOT
      COMMON/FLAG/FLAG
      COMMON/WHT/WHT
C
C     DESCALING OF NON-LINEAR PARAMETERS BEGINS
C
      XL=XC(1)*SC1
      XT=XC(2)*SC2
      D=XC(3)*SC3
C
C     LEAST SQUARES COMPUTATION NOW COMMENCES
C
      SUMQ1=0.0
      SUMQ2=0.0
      SUMQT=0.0
      SUMQP=0.0
      SUMP1=0.0
      SUMP2=0.0
      SUMPT=0.0
      SUMT1=0.0
      COM=1.E+2
      PI=3.1415926
      DO 50 K=1,KTOT
      XX1=XL-XT/2-FX(K)
      XX2=XL+XT/2-FX(K)
      XX3=XX1*XX2
      RR1=DSQRT(D**2+XX1**2)
      RR2=DSQRT(D**2+XX2**2)
      TD=XT*D
      DXX=D**2+XX3
      IF(DABS(RR1).LT.0.0000001)RR1=0.0000001
      IF(DABS(RR2).LT.0.0000001)RR2=0.0000001
      ALG=2*COM*DLOG(RR2/RR1)
      IF(DXX.EQ.0)GO TO 133
      ATN=2*COM*DATAN2(TD,DXX)
      GO TO 135
  133 ATN=2*COM*PI
  135 SUMQ1=SUMQ1+ALG
      SUMQ2=SUMQ2+ALG**2
      SUMQP=SUMQP+ALG*ATN
      SUMQT=SUMQT+ALG*FTOB(K)
      SUMP1=SUMP1+ATN
      SUMP2=SUMP2+ATN**2
      SUMPT=SUMPT+ATN*FTOB(K)
      SUMT1=SUMT1+FTOB(K)
   50 CONTINUE
      F1=KTOT*SUMP2-SUMP1*SUMP1
      F2=KTOT*SUMQP-SUMP1*SUMQ1
      F3=SUMP1*SUMT1-KTOT*SUMPT
      F4=KTOT*SUMQ2-SUMQ1*SUMQ1
      F5=SUMQ1*SUMT1-KTOT*SUMQT
      FJ1=(F1*F4-F2*F2)
      FJ2=(F2*F2-F4*F1)
      IF(DABS(FJ1).LT.0.0000001)FJ1=0.0000001
      IF(DABS(FJ2).LT.0.0000001)FJ2=0.0000001
      RJ1=(F5*F2-F3*F4)/FJ1
      RJ2=(F5*F1-F3*F2)/FJ2
      FOT=(SUMT1-RJ1*SUMP1-RJ2*SUMQ1)/KTOT
```

```fortran
C
C        COMPUTATION OF OBJECTIVE FUNCTION NOW BEGINS
C
         FT=0.0
         DO 60 K=1,KTOT
         XX1=XL-XT/2-FX(K)
         XX2=XT/2+XL-FX(K)
         XX3=XX1*XX2
         RR1=DSQRT(D**2+XX1**2)
         RR2=DSQRT(D**2+XX2**2)
         TD=XT*D
         DXX=D**2+XX3
         IF(DABS(RR1).LT.0.000001)RR1=0.000001
         IF(DABS(RR2).LT.0.000001)RR2=0.000001
         ALOG=DLOG(RR2/RR1)
         IF(DXX.EQ.0)GO TO 233
         ATAN=DATAN2(TD,DXX)
         GO TO 235
  233    ATAN=2*COM*PI
  235    QSUM(K)=2*COM*ATAN*RJ1
         PSUM(K)=2*COM*ALOG*RJ2
         FTOT(K)=QSUM(K)+PSUM(K)+FOT
         IF(FLAG.NE.0.0)GO TO 141
         FTOC(K)=(FTOB(K)-FTOT(K))**2
         GO TO 144
  141    FTOC(K)=(((FTOB(K)-FTOT(K)))*WHT(K))**2
  144    FT=FT+FTOC(K)
   60    CONTINUE
         FC=FT
         WRITE(7,171)XT,D,RJ1,RJ2,FOT,FT
  171    FORMAT(6F10.3)
         RETURN
         END
C
C
C        SUBROUTINE MONIT
C
         SUBROUTINE MONIT(FMIN,FMAX,SIM,N,N1,NCALL)
         IMPLICIT REAL*8(A-H,O-Z)
         DIMENSION SIM(N1,N)
         WRITE(6,11)NCALL,FMIN
         WRITE(6,12)((SIM(I,J),J=1,N),I=1,N1)
   11    FORMAT(6H AFTER, I5, 30H FUNCTION CALLS, THE VALUE IS,
        $ F10.4, 14H WITH SIMPLEX)
C  11    FORMAT(I5,14X,F10.4)
   12    FORMAT(4(3F12.4/))
         RETURN
         END
```

```
C                   PROGRAM OPDYE7
C                   ================
C
C
C       THIS PROGRAM IS A TWO DIMENSIONAL DYKE INTERPRETATION
C       PROGRAM USING THE NON LINEAR OPTIMIZATION TECHNIQUES
C       THE PARAMETERS OPTIMIZED ARE:THE MAGNETIZATION
C       IN THE PLANE OF THE PROFILE(J'),THE ANGLE BETA
C       ,THE THICKNESS,DEPTH TO TOP,AND POSITION OF THE -
C       CENTRE OF THE DYKE AS WELL AS THE ZEROTH AND FIRST
C       ORDER REGIONAL FIELDS.THE QUASI-NEWTON'S METHOD
C       IS USED.THE INPUT DATA IS AS FOLLOWS:
C       (1)     TITLE:(NOT MORE THAN 40 CHARACTERS)
C       (2)     NM,KTOT:
C               NM=NO. OF NON-LINEAR PARAMETERS(USUALLY FOUR)
C               KTOT=NO.OF FIELD POINTS-NOT MORE THAN 300
C       (3)     AX,BX,CX,DX:
C               AX=INITIAL ESTIMATE OF LOCATION W.R.T ORIGIN
C               BX=    "          "      OF THICKNESS
C               CX=    "          "      OF DEPTH TO THE TOP
C               DX=    "          "      OF ANGLE BETA
C       (4)     SC1,SC2,SC3,SC4 (SCALING FACTORS FOR AX,BX,CX,DX
C               RESPECTIVELY-SEE CHAPT. ONE)
C       (5)     X11,X12:-LOWER & UPPER LIMITS OF LOCATION
C               X21,X22:-   "     "    "     "     "  THICKNESS
C               X31,X32:-   "     "    "     "     "  DEPTH
C               X41,X42:-   "     "    "     "     "  BETA
C       (6)     FX(K),FTOB(K)
C               FX(K)=ARRAY OF X-CORD. OF FIELD POINTS
C               FTOB(K)=ARRAY OF OBSERVED ANOMALY
C       THE OUTPUT IS AS FOLLOWS:
C       (1)     TITLE:(AS IN INPUT)
C       (2)     F :- OBJECTIVE FUNCTION VALUE ON EXIT
C       (3)     X(I):ARRAY OF VALUES OF NON-LINEAR
C               PARAMETERS(SCALED) ON EXIT
C       (4)     FXL,FXT,FD,FBETA:
C               FXL =OPTIMUM VALUE OF LOCATION W.R.T ORIGIN
C               FXT =     "        "    OF THICKNESS
C               FD  =     "        "    OF DEPTH TO TOP
C          FBETA =      "         "    OF BETA
C       (5)     KTOT (AS IN INPUT)
C       (6)     RJ1,RJ2,FOT,FIT
C               RJ1,RJ2 :COMPONENTS OF MAGNETIZATION IN PLANE
C               OF PROFILE(CHAP. ONE)
C               FOT,FIT :REGIONAL FIELD LEVELS
C       (7)     FX(K),FTOB(K),FTOT(K),FRES(K)
C               FX(K) & FTOB(K) : (AS IN INPUT)
C               FTOT(K) : ARRAY OF COMPUTED ANOMALY
C               FRES(K) : ARRAY OF RESIDUALS(FTOB(K)-FTOT(K))
C
C       WRITTEN BY OFOEGBU JAN. 1981
        IMPLICIT REAL*8(A-H,O-Z)
        REAL*4 FTOT2,FDT4,FXT1,FXT2,FDT1,FOT2,FDT3,FTOB2,FX2
        DIMENSION BL(4),BU(4),W(54),X(4),FX(300),FTOB(300)
       1,TITLE(10),FTOT(300),FRES(300),IW(9)
       2,FTOB2(300),FTOT2(300),FX2(300)
        COMMON/SC1/SC1
        COMMON/SC2/SC2
        COMMON/SC3/SC3
        COMMON/SC4/SC4
        COMMON/FX/FX
```

```
      COMMON/FTOB/FTOB
      COMMON/KTOT/KTOT
      COMMON/FTOT/FTOT
      COMMON/RJ1/RJ1
      COMMON/FIT/FIT
      COMMON/FOT/FOT
C
C     READ IN INPUT PARAMETERS
C
      READ(5,11)TITLE
   11 FORMAT(10A4)
      WRITE(6,11)TITLE
      READ(5,*)NM,KTOT
      READ(5,*)AX,BX,CX,DX
      READ(5,*)SC1,SC2,SC3,SC4
      READ(5,*)X11,X12
      READ(5,*)X21,X22
      READ(5,*)X31,X32
      READ(5,*)X41,X42
      READ(5,*)(FX(K),FTOB(K),K=1,KTOT)
      N=NM
C
C        SET UP AND SCALE INITIAL ESTIMATES OF PARAMETERS
C
      X(1)=AX/SC1
      X(2)=BX/SC2
      X(3)=CX/SC3
      X(4)=DX/SC4
      IBOUND=0.0
C
C        SET UP AND SCALE BOUNDS ON PARAMETERS
C
      BL(1)=X11/SC1
      BU(1)=X12/SC1
      BL(2)=X21/SC2
      BU(2)=X22/SC2
      BL(3)=X31/SC3
      BU(3)=X32/SC3
      BL(4)=X41/SC4
      BU(4)=X42/SC4
      LIW=NM+2
      LW=54
      IFAIL=1
  114 FORMAT(F10.2,F10.2)
      CALL TIME(0)
      CALL E04JAF(N,IBOUND,BL,BU,X,F,IW,LIW,W,LW,IFAIL)
      CALL TIME(1,1)
      IF(IFAIL.NE.0)WRITE(6,12)IFAIL
      IF(IFAIL.EQ.1)GO TO 20
C
C        RESTORE RESULTANT VALUES OF PARAMETERS TO ACTUAL VALUES
C
      FXL=X(1)*SC1
      FXT=X(2)*SC2
      FD=X(3)*SC3
      FBETA=X(4)*SC4
      FXT1=FXL-FXT/2
      FXT2=FXL+FXT/2
      FDT4=FD
C
```

```
C          COMPUTATION OF RESIDUALS BEGINS
C
      DO 25 K=1,KTOT
      FRES(K)=FTOT(K)-FTOB(K)
   25 CONTINUE
C
C          RESULTS OF COMPUTATIONS ARE NOW WRITTEN OUT
C
      WRITE(6,14)F
      WRITE(6,16)(X(J),J=1,N)
      WRITE(6,230)
      WRITE(6,160)FXL,FXT,FD,FBETA
      WRITE(6,170)KTOT
      WRITE(6,190)RJ1,FIT,FOT
      WRITE(6,210)
      WRITE(6,220)
      WRITE(6,200)(FX(K),FTOB(K),FTOT(K),FRES(K),K=1,KTOT)
  135 FORMAT(5F10.2)
      DO 117 K=1,KTOT
      FTOT2(K)=FTOT(K)
      FTOB2(K)=FTOB(K)
      FX2(K)=FX(K)
  117 CONTINUE
      YMA=FTOB2(1)
      YMI=FTOB2(1)
      XMI=FX2(1)
      XMA=FX2(1)
      DO 119 K=2,KTOT
      IF(FTOT2(K).GT.YMA)YMA=FTOT2(K)
      IF(FTOB2(K).GT.YMA)YMA=FTOB2(K)
      IF(FTOT2(K).LT.YMI)YMI=FTOT2(K)
      IF(FTOB2(K).LT.YMI)YMI=FTOB2(K)
      IF(FX2(K).GT.XMA)XMA=FX2(K)
      IF(FX2(K).LT.XMI)XMI=FX2(K)
  119 CONTINUE
      XMIN=0.0
      XMAX=XMA+2.0
      YMAX=YMA+20.0
      YMIN=YMI-10.0
      YMA4=(YMAX-YMIN)/3+YMIN
      XMA7=XMAX/13
      XMA3=XMAX/9
      XMA4=XMAX/8
      YMA5=XMAX/2
      FDT1=FDT4
      FDT2=FDT4+(XMAX-FDT4)/3
      FDT3=FDT2+(XMAX-FDT4)/3
      WRITE(6,135)FXT1,FXT2,FDT1,FDT2,FDT3
      CALL PAPER(1)
      CALL PSPACE(0.20,0.60,0.55,0.95)
      CALL CTRMAG(7)
      CALL MAP(XMIN,XMAX,YMIN,YMAX)
      CALL BORDER
      CALL AXESSI(1.0,20.0)
      CALL CTRORI(1.0)
      CALL PLOTCS(-XMA4,YMA4,'MAGNETIC ANOMALY(GAMMA)',24)
      CALL CTRORI(0.0)
      CALL NSCURV(FX2,FTOB2,1,KTOT)
      CALL PTPLOT(FX2,FTOT2,1,KTOT,45)
      CALL FULL
```

```
      CALL  BLKPEN
      CALL  PSPACE(0.20,0.60,0.10,0.50)
      CALL  MAP(XMIN,XMAX,XMAX,XMIN)
      CALL  BORDER
      CALL  AXESSI(50.0,1.0)
      CALL  POSITN(FXT1,FDT1)
      CALL  JOIN(FXT2,FDT1)
      CALL  POSITN(FXT2,FDT1)
      CALL  JOIN(FXT2,FDT2)
      CALL  POSITN(FXT1,FDT1)
      CALL  JOIN(FXT1,FDT2)
      CALL  BROKEN(5,5,5,5)
      CALL  POSITN(FXT1,FDT2)
      CALL  JOIN(FXT1,FDT3)
      CALL  POSITN(FXT2,FDT2)
      CALL  JOIN(FXT2,FDT3)
      CALL  PLOTCS(YMA5,-XMA7,'DISTANCE(KM)',12)
      CALL  CTRORI(1.0)
      CALL  PLOTCS(-XMA3,YMA5,'DEPTH(KM)',9)
      CALL  CTRORI(0.0)
      CALL  FULL
      CALL  PSPACE(0.14,0.66,0.05,1.00)
      CALL  BORDER
      CALL  GREND
   20 STOP
   12 FORMAT(/'ERROR IN E04JAF 1H IFAIL=',I2/)
   14 FORMAT(///27H FUNCTION VALUE ON EXIT IS,F13.4)
   16 FORMAT(13H AT THE POINT,7F9.4)
  110 FORMAT(I3)
  120 FORMAT(3F10.2)
  130 FORMAT(2F10.2)
  160 FORMAT(4F10.2)
  170 FORMAT(I3)
  190 FORMAT(2F10.4,F10.3,F10.2)
  200 FORMAT(F10.2,2F13.4,F10.4)
  210 FORMAT(10X/'OBSERVED,COMPUTED,AND RESIDUALSIN GAMMA'/)
  220 FORMAT(10X/'  DIST        OBSERV         COMPUTED          RESIDUAL   '/)
  230 FORMAT(10X/'PARAMETER VALUES OBTAINED AFTER OPTIMIZATION'/)
      END
C
C
C     SUBROUTINE FUNCTION
C     =======================
C
C     THIS SUBROUTINE COMPUTES THE OBJECTIVE FUNCTION
C     TO BE MINIMIZED BY THE MAIN PROGRAM.
C
      SUBROUTINE FUNCT1(N,XC,FC)
      IMPLICIT REAL*8(A-H,O-Z)
      DIMENSION XC(N),FTOC(300),FTOT(300),QSUM(300),PSUM(300)
     1,FTOB(300),FX(300)
C
C     DECLARATION OF COMMON BLOCKS BEGINS
C
      COMMON/SC1/SC1
      COMMON/SC2/SC2
      COMMON/SC3/SC3
      COMMON/SC4/SC4
      COMMON/FX/FX
      COMMON/FTOB/FTOB
      COMMON/KTOT/KTOT
```

```
      COMMON/FTOT/FTOT
      COMMON/RJ1/RJ1
      COMMON/F1T/FIT
      COMMON/FOT/FOT
C
C     DESCALING OF NON-LINEAR PARAMETERS BEGINS
C
      XL=XC(1)*SC1
      XT=XC(2)*SC2
      D=XC(3)*SC3
      BETA=XC(4)*SC4
C
C     LEAST SQUARES COMPUTATION NOW COMMENCES
C
      SUMX1=0.0
      SUMX2=0.0
      SUMXT=0.0
      SUMXP=0.0
      SUMP1=0.0
      SUMP2=0.0
      SUMPT=0.0
      SUMT1=0.0
      COM=1.E+2
      DO 50 K=1,KTOT
      XX1=XL-XT/2-FX(K)
      XX2=XL+XT/2-FX(K)
      XX3=XX1*XX2
      RR1=DSQRT(D**2+XX1**2)
      RR2=DSQRT(D**2+XX2**2)
      CBET=DCOS(BETA)
      SBET=DSIN(BETA)
      TD=XT*D
      DXX=D**2+XX3
      ALG=2*COM*DLOG(RR2/RR1)*CBET
      ATN=2*COM*DATAN2(TD,DXX)*SBET
      ATN2=ATN+ALG
      SUMX1=SUMX1+FX(K)
      SUMX2=SUMX2+FX(K)**2
      SUMXP=SUMXP+FX(K)*ATN2
      SUMXT=SUMXT+FX(K)*FTOB(K)
      SUMP1=SUMP1+ATN2
      SUMP2=SUMP2+ATN2**2
      SUMPT=SUMPT+ATN2*FTOB(K)
      SUMT1=SUMT1+FTOB(K)
   50 CONTINUE
      F1=KTOT*SUMP2-SUMP1*SUMP1
      F2=KTOT*SUMXP-SUMP1*SUMX1
      F3=SUMP1*SUMT1-KTOT*SUMPT
      F4=KTOT*SUMX2-SUMX1*SUMX1
      F5=SUMX1*SUMT1-KTOT*SUMXT
      RJ1=(F5*F2-F3*F4)/(F1*F4-F2*F2)
      FIT=(F5*F1-F3*F2)/(F2*F2-F4*F1)
      FOT=(SUMT1-RJ1*SUMP1-FIT*SUMX1)/KTOT
C
C     COMPUTATION OF OBJECTIVE FUNCTION NOW BEGINS
C
      FT=0.0
      DO 60 K=1,KTOT
      XX1=XL-XT/2-FX(K)
      XX2=XT/2+XL-FX(K)
```

```
      XX3=XX1*XX2
      RR1=DSQRT(D**2+XX1**2)
      RR2=DSQRT(D**2+XX2**2)
      TD=XT*D
      DXX=D**2+XX3
      ALOG=DLOG(RR2/RR1)
      ATAN=DATAN2(TD,DXX)
      SBET2=DSIN(BETA)
      CBET2=DCOS(BETA)
      QSUM(K)=2*COM*ATAN*RJ1*SBET2
      PSUM(K)=2*COM*ALOG*RJ1*CBET2
      FTOT(K)=QSUM(K)+PSUM(K)+FOT+FX(K)*FIT
      FTOC(K)=(FTOB(K)-FTOT(K))**2
      FT=FT+FTOC(K)
   60 CONTINUE
      FC=FT
      RETURN
      END
```

```
C                    PROGRAM OPDYE8
C                    ==================
C
C      THIS PROGRAM IS A TWO DIMENSIONAL DYKE INTERPRETATION
C      PROGRAM USING THE NON LINEAR OPTIMIZATION TECHNIQUES
C      THE PARAMETERS OPTIMIZED IN THE PROGRAM OPDYE8
C      ARE:THE THICKNESS,DEPTH TO TOP,AND POSITION OF THE -
C      CENTRE OF THE DYKE. ALSO OPTIMIZED ARE THE COMPONENTS
C      OF THE MAGNETIZATION IN THE PLANE OF THE PROFILE. THE
C      PROGRAM ASSUMES THE REGIONAL LEVEL TO BE ALREADY REMOVED
C      THE INPUT DATA IS AS FOLLOWS:
C      (1)     TITLE:(NOT MORE THAN 40 CHARACTERS)
C      (2)     NM,FLAG,KTOT:
C              NM=NO. OF NON-LINEAR PARAMETERS(USUALLY THREE)
C              FLAG:=0.0(NO WEIGHTING OF FIELD POINTS
C                    .N.E. 0.0(FIELD POINTS WEIGHTED)
C              KTOT=NO.OF FIELD POINTS-MUST NOT EXCEED 300
C      (3)     AX,BX,CX:
C              AX=INITIAL ESTIMATE OF LOCATION W.R.T ORIGIN
C              BX=    "         "        OF THICKNESS
C              CX=    "         "        OF DEPTH TO THE TOP
C      (4)     SC1,SC2,SC3 (SCALING FACTORS FOR AX,BX,CX
C              RESPECTIVELY-SEE CHAPT. ONE)
C      (5)     X11,X12:-LOWER & UPPER LIMITS OF LOCATION
C              X21,X22:-   "    "    "     "    "  THICKNESS
C              X31,X32:-   "    "    "     "    "  DEPTH
C      (6)     FX(K),FTOB(K)(IF FLAG .EQ. 0.0)
C              FX(K),FTOB(K),WHT(K)(IF FLAG .N.E. 0.0)
C              FX(K)=ARRAY OF X-CORD. OF FIELD POINTS
C              FTOB(K)=ARRAY OF OBSERVED ANOMALY
C              WHT(K)=ARRAY OF WEIGHTING OF FIELD POINTS
C      THE OUTPUT IS AS FOLLOWS:
C      (1)     TITLE:(AS IN INPUT)
C      (2)     F :- OBJECTIVE FUNCTION VALUE ON EXIT
C      (3)     X(I):ARRAY OF VALUES OF NON-LINEAR
C              PARAMETERS(SCALED) ON EXIT
C      (4)     FXL,FXT,FD:
C              FXL =OPTIMUM VALUE OF LOCATION W.R.T ORIGIN
C              FXT =    "        "     OF THICKNESS
C              FD  =    "        "     OF DEPTH TO TOP
C      (5)     KTOT (AS IN INPUT)
C      (6)     RJ1,RJ2,BETA
C              RJ1,RJ2 :COMPONENTS OF MAGNETIZATION IN PLANE
C              OF PROFILE(CHAP. ONE)
C              BETA :ANGLE BETA(SEE CHAP. ONE)
C      (7)     FX(K),FTOB(K),FTOT(K),FRES(K)
C              FX(K) & FTOB(K) : (AS IN INPUT)
C              FTOT(K) : ARRAY OF COMPUTED ANOMALY
C              FRES(K) : ARRAY OF RESIDUALS(FTOB(K)-FTOT(K))
C
C      WRITTEN BY OFOEGBU JAN. 1981
C
      IMPLICIT REAL*8(A-H,O-Z)
      REAL*4 FTOT2,FDT4,FXT1,FXT2,FDT1,FDT2,FDT3,FTOB2,FX2
      DIMENSION BL(3),BU(3),W(39),X(3),FX(300),FTOB(300)
     1,TITLE(10),FTOT(300),FRES(300),IW(9)
     2,WHT(300),FTOB2(300),FTOT2(300),FX2(300)
      COMMON/SC1/SC1
      COMMON/SC2/SC2
      COMMON/SC3/SC3
```

```
      COMMON/FX/FX
      COMMON/FTOB/FTOB
      COMMON/KTOT/KTOT
      COMMON/FTOT/FTOT
      COMMON/RJ1/RJ1
      COMMON/RJ2/RJ2
      COMMON/FLAG/FLAG
      COMMON/WHT/WHT
C     READ IN INPUT PARAMETERS
C
      READ(5,11)TITLE
   11 FORMAT(10A4)
      WRITE(6,11)TITLE
      READ(5,*)NM,FLAG,KTOT
      READ(5,*)AX,BX,CX
      READ(5,*)SC1,SC2,SC3
      READ(5,*)X11,X12
      READ(5,*)X21,X22
      READ(5,*)X31,X32
      IF(FLAG.NE.0.0)GO TO 121
      READ(5,*)(FX(K),FTOB(K),K=1,KTOT)
      GO TO 131
  121 READ(5,*)(FX(K),FTOB(K),WHT(K),K=1,KTOT)
  131 N=NM
C
C       SET UP AND SCALE INITIAL ESTIMATES OF PARAMETERS
C
      X(1)=AX/SC1
      X(2)=BX/SC2
      X(3)=CX/SC3
      IBOUND=0.0
C
C       SET UP AND SCALE BOUNDS ON PARAMETERS
C
      BL(1)=X11/SC1
      BU(1)=X12/SC1
      BL(2)=X21/SC2
      BU(2)=X22/SC2
      BL(3)=X31/SC3
      BU(3)=X32/SC3
      LIW=NM+2
      LW=39
      IFAIL=1
  114 FORMAT(F10.2,F10.2)
      CALL TIME(0)
      CALL E04JAF(N,IBOUND,BL,BU,X,F,IW,LIW,W,LW,IFAIL)
      CALL TIME(1,1)
      IF(IFAIL.NE.0)WRITE(6,12)IFAIL
      IF(IFAIL.EQ.1)GO TO 20
C
C       RESTORE RESULTANT VALUES OF PARAMETERS TO ACTUAL VALUES
C
      FXL=X(1)*SC1
      FXT=X(2)*SC2
      FD=X(3)*SC3
      FXT1=FXL-FXT/2
      FXT2=FXL+FXT/2
      FDT4=FD
      BETA=DATAN2(RJ1,RJ2)
C
```

```
C          COMPUTATION OF RESIDUALS BEGINS
C
           DO 25 K=1,KTOT
           FRES(K)=FTOT(K)-FTOB(K)
    25 CONTINUE
C
C          RESULTS OF COMPUTATIONS ARE NOW WRITTEN OUT
C
C
           WRITE(6,14)F
           WRITE(6,16)(X(J),J=1,N)
           WRITE(6,230)
           WRITE(6,160)FXL,FXT,FD
           WRITE(6,170)KTOT
           WRITE(6,190)RJ1,RJ2,BETA
           WRITE(6,210)
           WRITE(6,220)
           WRITE(6,200)(FX(K),FTOB(K),FTOT(K),FRES(K),K=1,KTOT)
   135 FORMAT(5F10.2)
           DO 117 K=1,KTOT
           FTOT2(K)=FTOT(K)
           FTOB2(K)=FTOB(K)
           FX2(K)=FX(K)
   117 CONTINUE
           YMA=FTOB2(1)
           YMI=FTOB2(1)
           XMI=FX2(1)
           XMA=FX2(1)
           DO 119 K=2,KTOT
           IF(FTOT2(K).GT.YMA)YMA=FTOT2(K)
           IF(FTOB2(K).GT.YMA)YMA=FTOB2(K)
           IF(FTOT2(K).LT.YMI)YMI=FTOT2(K)
           IF(FTOB2(K).LT.YMI)YMI=FTOB2(K)
           IF(FX2(K).GT.XMA)XMA=FX2(K)
           IF(FX2(K).LT.XMI)XMI=FX2(K)
   119 CONTINUE
           XMIN=0.0
           XMAX=XMA+2.0
           YMAX=YMA+20.0
           YMIN=YMI-10.0
           YMA4=(YMAX+YMIN)/3
           XMA7=XMAX/13
           XMA3=XMAX/9
           XMA4=XMAX/8
           YMO5=XMAX/2.
           FDT1=FDT4
           FDT2=FDT4+(XMAX-FDT4)/3
           FDT3=FDT2+(XMAX-FDT4)/3
           CALL PAPER(1)
           CALL PSPACE(0.20,0.60,0.55,0.95)
           CALL CTRMAG(7)
           CALL MAP(XMIN,XMAX,YMIN,YMAX)
           CALL BORDER
           CALL AXESSI(1.0,20.0)
           CALL CTRORI(1.0)
           CALL PLOTCS(-XMA4,YMA4,'MAGNETIC ANOMALY(GAMMA)',24)
           CALL CTRORI(0.0)
           CALL NSCURV(FX2,FTOB2,1,KTOT)
           CALL PTPLOT(FX2,FTOT2,1,KTOT,45)
           CALL FULL
           CALL BLKPEN
```

```
      CALL  PSPACE(0.20,0.60,0.10,0.50)
      CALL  MAP(XMIN,XMAX,XMAX,XMIN)
      CALL  BORDER
      CALL  AXESSI(50.0,1.0)
      CALL  POSITN(FXT1,FDT1)
      CALL  JOIN(FXT2,FDT1)
      CALL  POSITN(FXT2,FDT1)
      CALL  JOIN(FXT2,FDT2)
      CALL  POSITN(FXT1,FDT1)
      CALL  JOIN(FXT1,FDT2)
      CALL  BROKEN(5,5,5,5)
      CALL  POSITN(FXT1,FDT2)
      CALL  JOIN(FXT1,FDT3)
      CALL  POSITN(FXT2,FDT2)
      CALL  JOIN(FXT2,FDT3)
      CALL  PLOTCS(YMA5,-XMA7,'DISTANCE(KM)',12)
      CALL  CTRORI(1.0)
      CALL  PLOTCS(-XMA3,YMA5,'DEPTH(KM)',9)
      CALL  CTRORI(0.0)
      CALL  FULL
      CALL  PSPACE(0.14,0.66,0.05,1.00)
      CALL  BORDER
      CALL  GREND
   20 STOP
   12 FORMAT(//'ERROR IN E04JAF IH IFAIL=',I2/)
   14 FORMAT(///27H FUNCTION VALUE ON EXIT IS,F13.4)
   16 FORMAT(13H AT THE POINT,7F9.4)
  110 FORMAT(I3)
  120 FORMAT(3F10.2)
  130 FORMAT(2F10.2)
  160 FORMAT(3F10.2)
  170 FORMAT(I3)
  190 FORMAT(2F10.4,F10.3,F10.2)
  200 FORMAT(F10.2,2F13.4,F10.4)
  210 FORMAT(10X//'OBSERVED,COMPUTED,AND RESIDUALSIN GAMMA'/)
  220 FORMAT(10X//' DIST      OBSERV      COMPUTED      RESIDUAL   '/)
  230 FORMAT(10X//'PARAMETER VALUES OBTAINED AFTER OPTIMIZATION'/)
      END
C
C     SUBROUTINE FUNCTION
C     ========================
C
C     THIS SUBROUTINE COMPUTES THE OBJECTIVE FUNCTION
C     TO BE MINIMIZED BY THE MAIN PROGRAM.
C
      SUBROUTINE FUNCT1(N,XC,FC)
      IMPLICIT REAL*8(A-H,O-Z)
      DIMENSION XC(N),FTOC(300),FTOT(300),QSUM(300),PSUM(300)
     1,WHT(300),FTOB(300),FX(300)
C
C     DECLARATION OF COMMON BLOCKS BEGINS
C
      COMMON/SC1/SC1
      COMMON/SC2/SC2
      COMMON/SC3/SC3
      COMMON/FX/FX
      COMMON/FTOB/FTOB
      COMMON/KTOT/KTOT
      COMMON/FTOT/FTOT
      COMMON/RJ1/RJ1
```

```
      COMMON/RJ2/RJ2
      COMMON/FLAG/FLAG
      COMMON/WHT/WHT
C
C     DESCALING OF NON-LINEAR PARAMETERS BEGINS
C
      XL=XC(1)*SC1
      XT=XC(2)*SC2
      D=XC(3)*SC3
C
C     LEAST SQUARES COMPUTATION NOW COMMENCES
C
      SUMQ2=0.0
      SUMQT=0.0
      SUMQP=0.0
      SUMP2=0.0
      SUMPT=0.0
      COM=1.E+2
      DO 50 K=1,KTOT
      XX1=XL-XT/2-FX(K)
      XX2=XL+XT/2-FX(K)
      XX3=XX1*XX2
      RR1=DSQRT(D**2+XX1**2)
      RR2=DSQRT(D**2+XX2**2)
      TD=XT*D
      DXX=D**2+XX3
      ALG=2*COM*DLOG(RR2/RR1)
      ATN=2*COM*DATAN2(TD,DXX)
      SUMQ2=SUMQ2+ALG**2
      SUMQP=SUMQP+ALG*ATN
      SUMQT=SUMQT+ALG*FTOB(K)
      SUMP2=SUMP2+ATN**2
      SUMPT=SUMPT+ATN*FTOB(K)
   50 CONTINUE
      F1=SUMQP*SUMQP-SUMP2*SUMQ2
      F2=SUMQT*SUMQP-SUMPT*SUMQ2
      RJ1=F1/F2
      RJ2=(SUMPT-RJ1*SUMP2)/SUMQP
C
C     COMPUTATION OF OBJECTIVE FUNCTION NOW BEGINS
C
      FT=0.0
      DO 60 K=1,KTOT
      XX1=XL-XT/2-FX(K)
      XX2=XT/2+XL-FX(K)
      XX3=XX1*XX2
      RR1=DSQRT(D**2+XX1**2)
      RR2=DSQRT(D**2+XX2**2)
      TD=XT*D
      DXX=D**2+XX3
      ALOG=DLOG(RR2/RR1)
      ATAN=DATAN2(TD,DXX)
      QSUM(K)=2*COM*ATAN*RJ1
      PSUM(K)=2*COM*ALOG*RJ2
      FTOT(K)=QSUM(K)+PSUM(K)
      IF(FLAG.NE.0.0)GO TO 141
      FTOC(K)=(FTOB(K)-FTOT(K))**2
      GO TO 144
  141 FTOC(K)=(((FTOB(K)-FTOT(K)))*WHT(K))**2
  144 FT=FT+FTOC(K)
```

```
C          PROGRAM DMAGN
C          ===============
C
C  THIS PROGRAM IS A FOTRAN PROGRAM WHICH COMPUTES
C  THE INNER AND EFFECTIVE MAGNETIZATIONS OF A
C  BODY DEVIDED INTO TWO DIMENSIONAL SQUARE BLOCKS
C  THE PROGRAM USES THE METHOD OF MATRIX INVERSION
C  THE MAGNETIZATION VALUES SO COMPUTED ARE USED TO
C  COMPUTE THE TOTAL FIELD ANOMALY FOR THE BODY
C  THE INPUT DATA CONSISTS OF THE FOLLOWING:
C          (1)     TITLE- NOT MORE THAN 40 CHARACTERS
C          (2)     N,SUC,FOT - N=NO. OF CELLS MAKING UP
C                  BODY ,SUC=SUSCEPTIBILITY & FOT=
C                  ORIGINAL INDUCING FIELD
C          (3)     X(I),Z(I) - X & Z CORDS. OF CELL CENTRES
C          (4)     XA(I),XB(I),ZC(I),ZD(I) - X & Z LIMITS OF
C                  CELL CORNERS(SEE CHAPT. TWO)
C          (5)     DP1,AX1,DP2,AX2 - DIP & AZIMUTH OF FIELD &
C                  MAGNETIZATION RESPECTIVELY
C          (6)     KTOT,ZCON,COX,DX -
C                  KTOT - NO FIELD POINTS
C                  ZCON - HEIGHT OF FIELD POINTS
C                  COX - INITIAL FIELD POINT
C                  DX - INTERVAL B/W FIELD POINTS
C     OUTPUT IS AS FOLLOWS:
C     (1)     TITLE - AS IN INPUT
C     (2)     N,SUC,FOT - AS IN INPUT
C     (3)     FX(K),FTOB(K),FTOT(K) -
C             FX(K) - ARRAY OF X-CORD. OF FIELD PTS.
C             FTOB(K) - ARRAY OF ORIGINAL ANOMALY
C             FTOT(K) - ARRAY OF EFFECTIVE ANOMALY
C     (4)     RJ(I) - ARRAY OF INNER MAGNETIZATION
C     (5)     C(I)  - ARRAY OF EFFECTIVE MAGNETIZATION
C     N/B - IT MAY BE NECESSARY TO MAKE THE DIMENSIONS OF
C           A,AA,C,B,WKS1 & WKS2 EXACTLY EQUAL TO N
C
      IMPLICIT REAL*8(A-H,O-Z)
      REAL*4 FTOB2,FTOT2,FX2
      DIMENSION A(80,80),FX2(80),FTOB(80),B(80),C(80),AA(80,80)
     1,FTOB2(80),WKS1(80),WKS2(80),FTOT(80),X(80),Z(80)
     2,FTOT2(140),FX(140),RJ(140),QSUM(100),PSUM(140),TITLE(10)
     3,QSUM2(140),PSUM2(140),XA(140),XB(140),ZC(140),ZD(140)
C READ IN INPUT PARAMETERS
      READ(5,11)TITLE
   11 FORMAT(10A4)
      READ(5,*)N,SUC,FOT
   10 FORMAT(I3,F10.4)
      READ(5,*)(X(I),Z(I),I=1,N)
   12 FORMAT(2F10.2)
      READ(5,*)(XA(J),XB(J),ZC(J),ZD(J),J=1,N)
  191 FORMAT(I5)
  192 FORMAT(4F10.2)
   64 FORMAT(4F10.2)
   63 FORMAT(F10.4)
      READ(5,*)DP1,AX1,DP2,AX2
   66 FORMAT(4F10.2)
      READ(5,*)KTOT,ZCON,COX,DX
   80 FORMAT(I3,F10.2)
   52 FORMAT(2F10.2)
      CDP1=DCOS(DP1*0.0174523)
```

```
            SDP1=DSIN(DP1*0.0174533)
            CAX1=DCOS(AX1*0.0174533)
            SAX1=DSIN(AX1*0.0174533)
            CDP2=DCOS(DP2*0.0174533)
            SDP2=DSIN(DP2*0.0174533)
            CAX2=DCOS(AX2*0.0174533)
            SAX2=DSIN(AX2*0.0174533)
            AT1=SDP1/CDP1
            AT2=SDP2/CDP2
            BT=DATAN2(AT1,CAX1)+DATAN2(AT2,CAX2)
            F1=DSQRT((SDP1**2)+(CDP1**2)*(CAX1**2))
            F2=DSQRT((SDP2**2)+(CDP2**2)*(CAX2**2))
            F3=F1*F2
            SBT=DSIN(BT)
            CBT=DCOS(BT)
            FT=SUC*FOT
C     SET UP COMPUTING DO LOOPS
            DO 40 I=1,N
            PI=3.1415926
            MUU=2.00
            DET=2.00
            COM=1.E+2
            GAM=1.00
            DO 40 J=1,N
C     CALCULATE THE PARAMETERS OF LENGHT TO BE USED
            X1=X(I)-XA(J)
            X2=X(I)-XB(J)
            Z1=Z(I)-ZC(J)
            Z2=Z(I)-ZD(J)
C     COMPUTE THE RADIAL AND ANGULAR TERMS R1,R2,R3,R4,Q1,Q2,Q3,Q4.
            R1=DSQRT((Z1**2)+(X1**2))
            R2=DSQRT((Z2**2)+(X1**2))
            R3=DSQRT((Z1**2)+(X2**2))
            R4=DSQRT((Z2**2)+(X2**2))
            P1=R2*R3
            P2=R1*R4
            ALG=DLOG(P1/P2)
            IF(X1.EQ.0)GO TO 13
            Q1=DATAN2(Z1,X1)
            Q2=DATAN2(Z2,X1)
            GO TO 15
   13       Q1=PI/2
            Q2=PI/2
   15       IF(X2.EQ.0)GO TO 17
            Q3=DATAN2(Z1,X2)
            Q4=DATAN2(Z2,X2)
            GO TO 19
   17       Q3=PI/2
            Q4=PI/2
   19       IF(I.EQ.J)GO TO 30
            A(I,J)=DET*F3*(SBT*ALG+CBT*(Q2-Q1+Q3-Q4))*SUC
            GO TO 50
   30       A(I,J)=1.0
   50       B(I)=FT
   40       CONTINUE
C     THE NEXT TEN STATEMENTS COMPUTES THE INNER AND EFFECTIVE
C     MAGNETIZATIONS WHICH NEED NOT BE IN THE EARTHS FIELD DIRECTION
            IA=N
            IAA=N
            IFAIL=1
```

```
          CALL FO4ATF(A,IA,B,N,C,AA,IAA,WKS1,WKS2,IFAIL)
          IF(IFAIL .EQ. 0)GO TO 20
          WRITE(6,18)IFAIL
          STOP
   20 DO 90 I=1,N
          RJ(I)=FT-C(I)
   90 CONTINUE
C
C THE VALUES OF MAGNETIZATION COMPUTED BY THE SUBROUTINE
C FO4ATF ARE NOW USED TO COMPUTE VALUES OF MAGNETIC
C ANOMALIES
C
C COMPUTATION OF THE CORDINATES OF FIELD POINTS BEGINS
          DO 25 K=1,KTOT
          RK=K
          FX(K)=(COX-DX)+DX*RK
          FZ=ZCON
   25 CONTINUE
C SET UP COMPUTING DO LOOPS
          DO 60 K=1,KTOT
          QSUM(K)=0.0
          PSUM(K)=0.0
          FTOT(K)=0.0
          FTOB(K)=0.0
          PSUM2(K)=0.0
          QSUM2(K)=0.0
          COM=1.E+2
          DO 55 J=1,N
C CALCULATE THE PARAMETERS OF LENGHT TO BE USED
          XX1=FX(K)-XA(J)
          XX2=FX(K)-XB(J)
          ZZ1=FZ-ZC(J)
          ZZ2=FZ-ZD(J)
C COMPUTE THE RADIAL AND ANGULAR TERMS R1,R2,R3,R4,Q1,Q2,Q3,Q4,
          RR1=DSQRT((ZZ1**2)+(XX1**2))
          RR2=DSQRT((ZZ2**2)+(XX1**2))
          RR3=DSQRT((ZZ1**2)+(XX2**2))
          RR4=DSQRT((ZZ2**2)+(XX2**2))
          PP1=RR2*RR3
          PP2=RR1*RR4
          DALG=DLOG(PP1/PP2)
          IF(XX1.EQ.0)GO TO 53
          T1=DATAN2(ZZ1,XX1)
          T2=DATAN2(ZZ2,XX1)
          GO TO 85
   53 T1=PI/2
          T2=PI/2
   85 IF(XX2.EQ.0)GO TO 87
          T3=DATAN2(ZZ1,XX2)
          T4=DATAN2(ZZ2,XX2)
          GO TO 89
   87 T3=PI/2
          T4=PI/2
C THE COMPUTATION OF ANOMALIES BEGINS
   89 GAL=SBT*DALG*C(J)
          QAL=CBT*(T2-T1+T3-T4)*C(J)
          GAL2=SBT*DALG*FT
          QAL2=CBT*(T2-T1+T3-T4)*FT
          PSUM2(K)=PSUM2(K)+GAL2
          QSUM2(K)=QSUM2(K)+QAL2
```

```
            PSUM(K)=PSUM(K)+GAL
            QSUM(K)=QSUM(K)+QAL
      55 CONTINUE
C    NOW COMPUTE ANOMALY VALUES
            FTOT(K)=2*F3*(PSUM(K)+QSUM(K))*COM
            FTOB(K)=2*F3*(PSUM2(K)+QSUM2(K))*COM
      60 CONTINUE
            DO 121 K=1,KTOT
            FTOT2(K)=FTOT(K)
            FTOB2(K)=FTOB(K)
            FX2(K)=FX(K)
     121 CONTINUE
C WRITE OUT OUTPUT
            WRITE(6,34)TITLE
      34 FORMAT(10A4)
            WRITE(6,999)N,SUC,FOT
     999 FORMAT(I5,F10.4,F10.4)
            WRITE(6,42)
      42 FORMAT(20X//'VALUES OF COMPUTED ANOMALIES IN UNITS OF GAMMA'
            WRITE(6,44)
      44 FORMAT(10X//'FX                FTOB            FTOT'/)
            WRITE(6,56)(FX(K),FTOT(K),FTOB(K),K=1,KTOT)
      56 FORMAT(F10.2,2F10.3)
            WRITE(6,31)
      31 FORMAT(20X//'VALUES OF COMPUTED INNER MAGNETIZATION'/)
            WRITE(6,74)
      74 FORMAT(20X//            JTOT                '/)
            DO 36 J=1,N
            WRITE(6,32)RJ(J)
      32 FORMAT(E16.7)
      36 CONTINUE
            WRITE(6,26)
      26 FORMAT(20X//'VALUES OF COMPUTED EFFECTIVE MAGNETIZATION'/)
            WRITE(6,29)
      29 FORMAT(20X//            JTOT                '/)
            DO 23 I=1,N
            WRITE(6,24)C(I)
      23 CONTINUE
      16 FORMAT(E16.7)
      14 FORMAT(41(8F14.6))
      18 FORMAT(//'ERROR IN F04ATF IFAIL=',I2)
      24 FORMAT(E16.7)
C
C THIS SECTION IS AN ADAPTATION OF THE DURHAM PLOTTER
C
            ZMAT=0.0
            DO 221 I=1,KTOT
            IF(FX2(I).GT.ZMAT)ZMAT=FX2(I)
     221 CONTINUE
            ZMAX=ZMAT+2.0
            CALL PSPACE(0.20,0.65,0.10,0.40)
            CALL CTRMAG(7)
            CALL MAP(0.00,ZMAX,20.00,0.00)
            CALL BORDER
            CALL AXESSI(300.0,2.0)
            DO 113 I=1,N
            XT1=XA(I)
            XT2=XB(I)
            ZT1=ZC(I)
            ZT2=ZD(I)
```

```
      CALL POSITN(XT1,ZT1)
      CALL JOIN(XT1,ZT2)
      CALL POSITN(XT1,ZT2)
      CALL JOIN(XT2,ZT2)
      CALL POSITN(XT2,ZT2)
      CALL JOIN(XT2,ZT1)
      CALL POSITN(XT2,ZT1)
      CALL JOIN(XT1,ZT1)
  113 CONTINUE
      CALL CTRMAG(7)
      CALL PLOTCS(10.00,-0.50,'DISTANCE(KM)',12)
      CALL CTRORI(1.0)
      CALL PLOTCS(-1.70,15.00,'DISTANCE(KM)',12)
      CALL CTRORI(0.0)
      YMI=0.0
      YMA=0.0
      DO 117 I=1,KTOT
      IF(FTOB2(I).GT.YMA)YMA=FTOB2(I)
      IF(FTOB2(I).LT.YMI)YMI=FTOB2(I)
      IF(FTOT2(I).LT.YMI)YMI=FTOT2(I)
      IF(FTOT2(I).GT.YMA)YMA=FTOT2(I)
  117 CONTINUE
      YMAT=YMA/20.0
      YMAX=YMA+YMAT
      YMA4=(YMAX-YMIN)/3
      YMIN=YMI-YMAT
      CALL PAPER(1)
      CALL PSPACE(0.20,0.65,0.45,0.90)
      CALL MAP(0.00,ZMAX,YMIN,YMAX)
      CALL BORDER
      CALL AXESSI(300.0,15.0)
      CALL CTRORI(1.0)
      CALL PLOTCS(-2.50,YMA4,'MAGNETIC ANOMALY(GAMMA)',23)
      CALL CTRORI(0.0)
      YMI3=YMIN+5.0
      YMI2=YMIN+10.0
      CALL NSCURV(FX2,FTOB2,1,KTOT)
      CALL BROKEN(4,4,4,4)
      CALL NSCURV(FX2,FTOT2,1,KTOT)
      CALL FULL
      CALL PSPACE(0.14,0.71,0.05,0.95)
      CALL BORDER
      YMA2=YMAX-YMIN
      YMA3=YMA2+20
      CALL PSPACE(0.20,0.65,0.45,0.90)
      CALL MAP(0.00,ZMAX,0.00,YMA2)
      CALL AXESSI(5.00,YMA3)
      CALL GREND
      STOP
      END
```

```
C          PROGRAM DMAGN2
C          =================
C
C THIS PROGRAM IS A MODIFIED FORM OF DMAGN WHICH
C COMPUTES THE EFFECTIVE AND MEAN EFFECTIVE
C MAGNETIZATIONS FOR A SYSTEM OF TWO DIMENSIONAL
C BLOCKS USING THE METHOD OF SUCCESSIVE IT-
C ERATIONS.THE MAGNETIZATION SO COMPUTED ARE
C USED TO COMPUTE THE TOTAL FIELD ANOMALY FOR
C THE BODY.THE PROGRAM IS BASED ON THE FORMULAE
C FOR TWO DIMENSIONAL RECTANGULAR BLOCKS.
C THE INPUT DATA CONSISTS OF THE THE FOLLOWING:
C          (1)     TITLE - NOT MORE THAN 40 CHARACTERS
C          (2)     N,SUC,FOT,MAXIT,FTS
C                  N=NO. OF BLOCKS OR CELLS
C                  SUC -SUSCEPTIBILITY
C                  FOT -ORIGINAL INDUCING FIELD
C                  MAXIT -NUMBER OF ITERATIONS(INCREASED IF
C                  CONVERGENCE DOES NOT TAKE PLACE)
C                  FTS -CONDITION FOR CONVERGENCE(SEE CHAPT. TWO)
C          (3)     X(I),Z(I) :- AS IN DMAGN
C          (4)     XA(I),XB(I),ZC(I),ZD(I) :- AS IN DMAGN
C          (5)     DP1,AX1,DP2,AX2 :- AS IN DMAGN
C          (6)     KTOT,ZCON,COX,DX :- AS IN DMAGN(KTOT<500)
C          OUTPUT IS AS FOLLOWS:
C          (1)     TITLE - AS IN INPUT
C          (2)     N,SUC,FOT,MAXIT :- AS IN INPUT
C          (3)     DP1,AX1,DP2,AX2 :- AS IN INPUT
C          (4)     FX(K),FTOB(K),FTOT(K) :- AS IN DMAGN
C          (5)     RJ(I) - ARRAY OF EFFECTIVE MAGNETIZATION
C          (6)     RJKM - MEAN OF EFFECTIVE MAGNETIZATION
C
       IMPLICIT REAL*8(A-H,O-Z)
       REAL*4 FTOT2,FG1,FG2,FG3,FTOB2,FX2
       DIMENSION TITLE(10),B(500),C(500),FVT(500)
      1,FTOT2(500),FTOB2(500),SUM(500),FTOT(500),X(500),Z(500)
      2,FTOB(500),FX2(500),FX(500),RJ(500),QSUM(500),PSUM(500)
      3,QSUM2(500),PSUM2(500),XA(500),XB(500),ZC(500),ZD(500)
      4,FG1(40),FG2(40),FG3(40)
C READ IN INPUT PARAMETERS
       READ(5,11)TITLE
   11 FORMAT(10A4)
       READ(5,*)N,SUC,FOT,MAXIT,FTS
   10 FORMAT(2I5,F10.2)
       READ(5,*)(X(I),Z(I),I=1,N)
   12 FORMAT(2F10.2)
       READ(5,*)(XA(J),XB(J),ZC(J),ZD(J),J=1,N)
   64 FORMAT(4F10.2)
   63 FORMAT(2F10.4)
       READ(5,*)DP1,AX1,DP2,AX2
       READ(5,*)KTOT,ZCON,COX,DX
   66 FORMAT(4F10.2)
       CDP1=DCOS(DP1*0.0174533)
       SDP1=DSIN(DP1*0.0174533)
       CAX1=DCOS(AX1*0.0174533)
       SAX1=DSIN(AX1*0.0174533)
       CDP2=DCOS(DP2*0.0174533)
       SDP2=DSIN(DP2*0.0174533)
       CAX2=DCOS(AX2*0.0174533)
       SAX2=DSIN(AX2*0.0174533)
```

```
      AT1=SDP1/CDP1
      AT2=SDP2/CDP2
      BT=DATAN2(AT1,CAX1)+DATAN2(AT2,CAX2)
      F1=DSQRT((SDP1**2)+(CDP1**2)*(CAX1**2))
      F2=DSQRT((SDP2**2)+(CDP2**2)*(CAX2**2))
      F3=F1*F2
      SBT=DSIN(BT)
      CBT=DCOS(BT)
      FT=SUC*FOT
      EPS=FT*FTS
C SET UP COMPUTING DO LOOPS
      RJK=0.0
      DO 60 I=1,N
      RJ(I)=FT
      PI=3.1415926
      DET=2.00
      COM=1.E+2
      DO 50 J=1,N
C CALCULATE THE PARAMETERS OF LENGHT TO BE USED
      IF(I.EQ.J)GO TO 55
      X1=X(I)-XA(J)
      X2=X(I)-XB(J)
      Z1=Z(I)-ZC(J)
      Z2=Z(I)-ZD(J)
C COMPUTE THE RADIAL AND ANGULAR TERMS R1,R2,R3,R4,Q1,Q2,Q3,Q4,
      R1=DSQRT((Z1**2)+(X1**2))
      R2=DSQRT((Z2**2)+(X1**2))
      R3=DSQRT((Z1**2)+(X2**2))
      R4=DSQRT((Z2**2)+(X2**2))
      P1=R2*R3
      P2=R1*R4
      ALG=DLOG(P1/P2)
      IF(X1.EQ.0)GO TO 13
      Q1=DATAN2(Z1,X1)
      Q2=DATAN2(Z2,X1)
      GO TO 15
   13 Q1=PI/2
      Q2=PI/2
   15 IF(X2.EQ.0)GO TO 17
      Q3=DATAN2(Z1,X2)
      Q4=DATAN2(Z2,X2)
      GO TO 19
   17 Q3=PI/2
      Q4=PI/2
   19 A=DET*F3*(SBT*ALG+CBT*(Q2-Q1+Q3-Q4))
C    ITERATION PROCEDURE BEGINS
      SUM(J)=0.0
      IBEG=1
      IFIN=MAXIT
      ICNT=1
   65 DO 30 K=IBEG,IFIN
      IF(K.GT.1)GO TO 40
      FVT(K)=FT*A*SUC
      GO TO 25
   40 FVT(K)=FTX*A*SUC
   25 FTX=FVT(K)
      SUM(J)=SUM(J)+FTX
C    TEST FOR CONVERGENCE IS NOW CARRIED OUT
      IF(FTX.LT.EPS)GO TO 35
   30 CONTINUE
```

```
        ICNT=ICNT+1
        IBEG=IFIN+1
        IFIN=IFIN+MAXIT
        IF(FTX.GT.EPS)GO TO 65
        GO TO 35
    55  SUM(J)=0.0
    35  RJ(I)=RJ(I)-SUM(J)
    50  CONTINUE
    22  FORMAT(E16.7)
        RJK=RJK+RJ(I)
    60  CONTINUE
        RJKM=RJK/N
C   THE  MAGNETIZATION  VALUES  COMPUTED  ABOVE
C   ARE  USED  TO  CALCULATE  THE  MAGNETIC  ANOMALY.
    80  FORMAT(I5,F10.2)
    52  FORMAT(2F10.2)
C   COMPUTATION  OF  THE  CORDINATES  OF  FIELD  POINTS  BEGINS
        DO 70 K=1,KTOT
        RK=K
        FX(K)=(COX-DX)+DX*RK
        FZ=ZCON
    70  CONTINUE
C   SET  UP  COMPUTING  DO  LOOPS
        DO 74 K=1,KTOT
        QSUM(K)=0.0
        PSUM(K)=0.0
        FTOT(K)=0.0
        QSUM2(K)=0.0
        PSUM2(K)=0.0
        FTOB(K)=0.0
        COM=1.E+2
        DO 75 J=1,N
C   CALCULATE  THE  PARAMETERS  OF  LENGHT  TO  BE  USED
        XX1=FX(K)-XA(J)
        XX2=FX(K)-XB(J)
        ZZ1=FZ-ZC(J)
        ZZ2=FZ-ZD(J)
C   COMPUTE  THE  RADIAL  AND  ANGULAR  TERMS  R1,R2,R3,R4,Q1,Q2,Q3,Q4.
        RR1=DSQRT((ZZ1**2)+(XX1**2))
        RR2=DSQRT((ZZ2**2)+(XX1**2))
        RR3=DSQRT((ZZ1**2)+(XX2**2))
        RR4=DSQRT((ZZ2**2)+(XX2**2))
        PP1=RR2*RR3
        PP2=RR1*RR4
        DALG=DLOG(PP1/PP2)
        IF(XX1.EQ.0)GO TO 53
        T1=DATAN2(ZZ1,XX1)
        T2=DATAN2(ZZ2,XX1)
        GO TO 85
    53  T1=PI/2
        T2=PI/2
    85  IF(XX2.EQ.0)GO TO 87
        T3=DATAN2(ZZ1,XX2)
        T4=DATAN2(ZZ2,XX2)
        GO TO 89
    87  T3=PI/2
        T4=PI/2
C   THE  COMPUTATION  OF  ANOMALIES  BEGINS
    89  GAL=SBT*DALG*RJ(J)
        QAL=CBT*(T2-T1+T3-T4)*RJ(J)
```

```
      GAL2=SBT*DALG*FT
      QAL2=CBT*(T2-T1+T3-T4)*FT
      PSUM2(K)=PSUM2(K)+GAL2
      QSUM2(K)=QSUM2(K)+QAL2
      PSUM(K)=PSUM(K)+GAL
      QSUM(K)=QSUM(K)+QAL
   75 CONTINUE
      FTOT(K)=2*F3*(PSUM(K)+QSUM(K))*COM
      FTOB(K)=2*F3*(PSUM2(K)+QSUM2(K))*COM
   74 CONTINUE
      DO 107 K=1,KTOT
      FTOT2(K)=FTOT(K)
      FTOB2(K)=FTOB(K)
      FX2(K)=FX(K)
  107 CONTINUE
C WRITE OUT RESULTS OF COMPUTATION
      WRITE(6,34)TITLE
   34 FORMAT(10A4)
      WRITE(6,45)
   45 FORMAT(20X/'INPUT PARAMETERS USED'/)
      WRITE(6,47)N,SUC,FOT,MAXIT
   47 FORMAT(I5,2F10.4,I5)
      WRITE(6,49)DP1,AX1,DP2,AX2
   49 FORMAT(4F10.2)
      WRITE(6,42)
   42 FORMAT(20X/'VALUES OF COMPUTED ANOMALIES IN UNITS OF GAMMA'/)
      WRITE(6,44)
   44 FORMAT(10X/'FX            FTOB            FTOT'/)
      WRITE(6,56)(FX(K),FTOB(K),FTOT(K),K=1,KTOT)
   56 FORMAT(F10.2,2F10.3)
      WRITE(6,26)
   26 FORMAT(20X/'VALUES OF COMPUTED EFFECTIVE MAGNETIZATION'/)
      WRITE(6,29)
   29 FORMAT(20X/'              JTOT              '/)
      DO 23 I=1,N
      WRITE(6,24)RJ(I)
   23 CONTINUE
      WRITE(6,48)
   48 FORMAT(20X/'COMPUTED VALUE OF MEAN MAGNETIZATION'/)
      WRITE(6,22)RJKM
   24 FORMAT(E16.7)
C
C THIS SECTION IS AN ADAPTATION OF THE DURHAM PLOTTER
C
      ZMAX=KTOT+2
      CALL PSPACE(0.20,0.65,0.10,0.40)
      CALL CTRMAG(7)
      CALL MAP(0.00,ZMAX,20.00,0.00)
      CALL BORDER
      CALL AXESSI(300.0,2.0)
      DO 113 I=1,N
      XT1=XA(I)
      XT2=XB(I)
      ZT1=ZC(I)
      ZT2=ZD(I)
      CALL POSITN(XT1,ZT1)
      CALL JOIN(XT1,ZT2)
      CALL POSITN(XT1,ZT2)
      CALL JOIN(XT2,ZT2)
      CALL POSITN(XT2,ZT2)
```

```
      CALL  JOIN(XT2,ZT1)
      CALL  POSITN(XT2,ZT1)
      CALL  JOIN(XT1,ZT1)
113 CONTINUE
      CALL  CTRMAG(7)
      CALL  PLOTCS(10.00,-0.50,'DISTANCE(KM)',12)
      CALL  CTRORI(1.0)
      CALL  PLOTCS(-1.70,15.00,'DISTANCE(KM)',12)
      CALL  CTRORI(0.0)
      YMI=0.0
      YMA=0.0
      DO 117 I=1,KTOT
      IF(FTOB2(I).GT.YMA)YMA=FTOB2(I)
      IF(FTOB2(I).LT.YMI)YMI=FTOB2(I)
117 CONTINUE
      YMAT=YMA/20.0
      YMAX=YMA+YMAT
      YMA4=(YMAX-YMIN)/3
      YMIN=YMI-YMAT
      CALL  PAPER(1)
      CALL  PSPACE(0.20,0.65,0.45,0.90)
      CALL  MAP(0.00,ZMAX,YMIN,YMAX)
      CALL  BORDER
      CALL  AXESSI(300.0,15.0)
      CALL  CTRORI(1.0)
      CALL  PLOTCS(-2.50,YMA4,'MAGNETIC  ANOMALY(GAMMA)',23)
      CALL  CTRORI(0.0)
      YMI3=YMIN+5.0
      YMI2=YMIN+10.0
      CALL  NSCURV(FX2,FTOB2,1,KTOT)
      CALL  BROKEN(4,4,4,4)
      CALL  NSCURV(FX2,FTOT2,1,KTOT)
      CALL  FULL
      CALL  PSPACE(0.14,0.71,0.05,0.95)
      CALL  BORDER
      YMA2=YMAX-YMIN
      YMA3=YMA2+20
      CALL  PSPACE(0.20,0.65,0.45,0.90)
      CALL  MAP(0.00,ZMAX,0.00,YMA2)
      CALL  AXESSI(5.00,YMA3)
      CALL  GREND
      STOP
      END
```

```
C
C
C                    PROGRAM UPCON
C                    ================
C
C
C         THIS PROGRAM COMPUTES THE UPWARD OR DOWNWARD CONTINUED
C         VALUE OF A GIVEN MAGNETIC OR GRAVITY ANOMALY.
C         THE INPUT DATA FOR UPCON IS AS FOLLOWS:
C         (1)     TITLE - NOT MORE THAN 40 CHARACTERS
C         (2)     FLAG -IF L.T. 0.0(GRAVITY)
C         (3)     LX,Z,FRQO :
C                 LX - NO. OF FIELD POINTS (POWERS OF TWO)
C                 Z - HEIGHT OF CONTINUATION
C                 FRQO - FREQUENCY OF DATA
C         (4)     DIST(I),A(I) :
C                 DIST(I)- ARRAY OF X-CORD OF FIELD PTS.
C                 A(I) - ARRAY OF ANOMALY VALUES
C         OUTPUT IS AS FOLLOWS:
C         (1)     TITLE - AS IN INPUT
C         (2)     LX,Z,FRQO - AS IN INPUT
C         (3)     DIST(I),A(I) :
C                 DIST(I) - AS IN INPUT
C                 A(I) - ARRAY OF CONTINUED ANOMALY
C         (4)     X(I),Y(I) (REAL AND IMAGINARY PARTS OF
C                 FOURIER TRANSFORM)
C
C                         OFOEGBU MAY 1981
C
      DIMENSION TITLE(10),A(900),DIST(900),S(900),FH(900)
     1,AI(900),FAR(900),FAI(900)
      READ(5,10)TITLE
      READ(5,*)FLAG
      READ(5,*)LX,Z,FRQO
      READ(5,*)(DIST(I),A(I),I=1,LX)
      DO 111 I=1,LX
      IF(I.EQ.1)XMIN=DIST(I)
      IF(I.EQ.LX)XMAX=DIST(I)
  111 CONTINUE
      CALL SCAN(LX,A,TMIN,TMAX)
      CALL PLOT(LX,DIST,A,XMIN,XMAX,TMIN,TMAX)
C
C     THE EXPONENTIAL COFFICIENTS FOR UPWARD CONTINUATION
C     ARE NOW COMPUTED
C
      NN1=LX/2+1
      IF(FLAG .LT. 0.0)GO TO 17
      FACT=-6.28319*FRQO*Z/LX
      GO TO 18
   17 FACT=6.28319*FREQO*Z/LX
   18 DO 30 I=2,NN1
      FH(I)=EXP(FACT*(I-1))
      LI2=LX-I+2
      FH(LI2)=FH(I)
   30 CONTINUE
      FH(1)=1.0
      CALL SINTAB(LX,S)
      CALL SAVE(LX,FAR,A)
      CALL CONST(LX,FAI,0.0)
      CALL FURRY(LX,FAR,FAI,1.0,S)
      CALL MULT(LX,FAR,FAR,FH)
      CALL MULT(LX,FAI,FAI,FH)
```

```
      CALL SAVE(LX,A,FAR)
      CALL SAVE(LX,AI,FAI)
      CALL FURRY(LX,A,AI,-1.0,S)
      CALL SCAN(LX,A,ZMIN,ZMAX)
      CALL PLOT(LX,DIST,A,XMIN,XMAX,ZMIN,ZMAX)
      WRITE(6,10)TITLE
      WRITE(6,12)LX,Z,FRQO
      WRITE(6,16)(DIST(I),A(I),I=1,LX)
   10 FORMAT(10A4)
   11 FORMAT(F10.2)
   12 FORMAT(I5,2F10.2)
   14 FORMAT(2F10.2)
   16 FORMAT(2F10.2)
      STOP
      END
C*********************************************************************
      SUBROUTINE FURRY(LX,X,Y,SIGNI,S)
C     DESCRIPTION - THIS SUBROUTINE COMPUTES THE FAST FOURIER TRANSFORM
C                   THE COOLEY-TUKEY ALGORITHM.
C     PARAMETERS - LX=NUMBER OF DATA POINTS
C                  X=ARRAY CONTAINING REAL PART OF TRANSFORM
C                  Y=ARRAY CONTAINING IMAGINARY PART OF TRANSFORM
C                  SIGNI=+1. FOR FORWARD TRANSFORM
C                       =-1. FOR REVERSE TRANSFORM
C                  S=ARRAY OF SINE VALUES GENERATED BY SUBROUTINE SINTAB
C
C     SOURCE - CLAREBOUT, MODIFIED BY ALAN NUNNS
      DIMENSION X(LX),Y(LX),S(LX)
      SC=1.0
      IF(SIGNI.LT.0.0) SC=1.0/LX
      NN=LX/2
      N=LX/4
C   REORDER DATA POINTS BY REVERSING ORDER OF THE BINARY
C   DIGITS OF THEIR INDICES(INDEX OF X(J) IS (J-1)) AND
C   MULTIPLY BY SCALE CONSTANT SC
C
      J=1
      DO 30 I=1,LX
      IF(I.GT.J) GO TO 10
      TEMPX=X(J)*SC
      TEMPY=Y(J)*SC
      X(J)=X(I)*SC
      Y(J)=Y(I)*SC
      X(I)=TEMPX
      Y(I)=TEMPY
   10 M=NN
   20 IF(J.LE.M) GO TO 30
      J=J-M
      M=M/2
      IF(M.GE.1) GO TO 20
   30 J=J+M
      L=1
      NL=NN
   40 ISTEP=2*L
      IND=1
      DO 55 M=1,L
      INDN=IND-N-1
      IF(INDN) 41,42,43
   41 WX=S(1-INDN)
      WY=S(IND)*SIGNI
```

```
      GO TO 45
   42 WX=0.
      WY=SIGNI
      GO TO 45
   43 WX=-S(INDN+1)
      WY=S(N+1-INDN)*SIGNI
   45 DO 50 I=M,LX,ISTEP
      TEMPX=WX*X(I+L)-WY*Y(I+L)
      TEMPY=WX*Y(I+L)+WY*X(I+L)
      X(I+L)=X(I)-TEMPX
      Y(I+L)=Y(I)-TEMPY
      X(I)=X(I)+TEMPX
   50 Y(I)=Y(I)+TEMPY
   55 IND=IND+NL
      L=ISTEP
      NL=NL/2
      IF(L.LT.LX) GO TO 40
      WRITE(7,65)(X(I),Y(I),I=1,LX)
   65 FORMAT(2F10.2)
      RETURN
      END
C***************************************************************
      SUBROUTINE SINTAB(LX,S)
C     DESCRIPTION - THIS SUBROUTINE CALCULATES A SIN TABLE USED IN FURRY
C
C     PARAMETERS - S=SIN VALUES OF DIMENSION LX WHERE:
C                     S(I)=SIN(2*PI*(I-1)/LX)  I=1,2,.........,(LX/4)+1
C                              LX=NO. OF PTS. IN FFTA
C         *****************************************************
      DIMENSION S(LX)
      N1=LX/4+1
      ARG=0.0
      DELARG=6.2831853/FLOAT(LX)
      DO 10 I=1,N1
      S(I)=SIN(ARG)
      ARG=ARG+DELARG
   10 CONTINUE
      RETURN
      END
C***************************************************************
      SUBROUTINE CONST(LX,X,VAL)
C   THIS SUBROUTINE ASSIGNS THE VALUE VAL TO EACH ELEMENT
C   X(I),I=1,2,.....,LX OF X
C
      DIMENSION X(LX)
      DO 10 I=1,LX
      X(I)=VAL
   10 CONTINUE
      RETURN
      END
C***************************************************************
      SUBROUTINE SAVE(LX,X,Y)
C
C   THIS SUBROUTINE SAVES THE ARRAY Y(I) AS ARRAY X(I),I=1,LX
C
      DIMENSION X(LX),Y(LX)
      DO 10 I=1,LX
      X(I)=Y(I)
   10 CONTINUE
      RETURN
```

```
      END
C***********************************************************
      SUBROUTINE MULT(LX,Z,X,Y)
C
C     THIS SUBROUTINE MULTIPLIES X(I) BY Y(I) AND PUT THE RESULT
C     IN THE ARRAY Z(I),I=1,2,.....LX
C
      DIMENSION X(LX),Y(LX),Z(LX)
      DO 10 I=1,LX
      Z(I)=X(I)*Y(I)
   10 CONTINUE
      RETURN
      END
C*********************************************
      SUBROUTINE SCAN(LX,X,Y,Z)
      DIMENSION X(LX)
      Y=X(1)
      Z=X(1)
      DO 55 I=2,LX
      IF(X(I) .GT. Z)Z=X(I)+10.0
      IF(X(I) .LT. Y)Y=X(I)-10.0
   55 CONTINUE
      RETURN
      END
C***********************************************
      SUBROUTINE PLOT(LX,X,Y,XMN,XMA,YMN,YMA)
      DIMENSION X(LX),Y(LX)
      CALL PAPER(1)
      CALL PSPACE(0.20,0.90,0.20,0.90)
      CALL CSPACE(0.0,1.0,0.0,1.0)
      CALL MAP(XMN,XMA,YMN,YMA)
      CALL BORDER
      CALL CTRMAG(8)
      CALL AXES
      N=LX
      CALL PTPLOT(X,Y,1,N,43)
      CALL NSCURV(X,Y,1,N)
      CALL GREND
      RETURN
      END
```

```
C           PROGRAM MGRAV
C           ================
C
C           THIS PROGRAM COMPUTES THE PSEUDOGRAVITY ANOMALY
C           CORRESPONDING TO A GIVEN MAGNETIC ANOMALY USING
C           THE EQUIVALENT LAYER THEORY.A DETAILED ACCOUNT OF
C           THE THEORY OF THE METHOD CAN BE FOUND IN CHAP.
C           ONE OR IN INGLES(1971).
C           INPUT DATA IS AS FOLLOWS:
C           (1)    TITLE:-NOT MORE THAN 40 CHARACTERS
C           (2)    N,CONST:
C                  N=NO. OF BLOCKS MAKING UP EQUIVALENT LAYER/
C                  NO. OF AVAILABLE POINTS OF MAGNETIC OBSERVATIONS
C                  CONST=CONSTANT OF PROPORTIONALITY BETWEEN DENSITY
C                  AND MAGNETIZATION
C           (3)    ST,AIN,ZT1,ZT2:
C                  ST=FIRST X-CORD OF FIRST BLOCK
C                  AIN=WIDTH OF BLOCKS MAKING UP EQUIVALENT LAYER
C                  ZT1,ZT2:-DEPTH TO TOP AND BOTTOM SURFACES OF
C                  BLOCKS MAKING UP EQUIVALENT LAYER
C           (4)    DP1,AX1,DP2,AX2:
C                  DP1,AX1:-DIP AND AXIMUTH OF EARTH'S FIELD
C                  DP2,AX2:-DIP AND AXIMUTH OF MAGNETIZATION
C           (5)    KTOT,ZCON,COX,DX:
C                  KTOT=NO. OF FIELD POINTS
C                  ZCON=Z-CORD OF FIELD POINTS
C                  COX=X-CORD OF FIRST FIELD POINT
C                  DX=SPACING OF FIELD POINTS
C           (6)    X(I),Z(I),FT(I): ARRAYS CONTAINING THE X AND
C                  Z-CORDS. OF THE GIVEN MAGNETIC ANOMALY AND THE
C                  VALUES OF THE MAGNETIC ANOMALY AT THE POINTS
C                  DEFINED BY X AND Z
C           THE OUTPUT IS AS FOLLOWS:
C           (1)    TITLE: AS IN INPUT
C           (2)    XA(I),XB(I),ZC(I),ZD(I):-THE EXTENSION OF THE
C                  BLOCKS FORMING LAYER ALONG X AND Z DIRECTIONS
C           (3)    X(I),Z(I),FT(I),FTOT(I):
C                  X(I),Z(I),FT(I):-AS IN INPUT
C                  FTOT(I):-ARRAY OF COMPUTED PSEUDOGRAVITY ANOMALY
C           (4)    RJ(I),PJ(I):-ARRAYS OF COMPUTED MAGNETIZATION AND
C                  DENSITY DISTRIBUTION OF THE BLOCKS MAKING UP THE
C                  EQUIVALENT LAYER.
C           IT MAY BE NECESSARY FOR A,AA,B,C,WKS1 & WKS2 TO
C           HAVE DIMENSIONS EQUAL TO N
C
C
           IMPLICIT REAL*8(A-H,O-Z)
           DIMENSION A(300,300),XT(300),FTOT(300),X(300),Z(300)
          2,FT(300),FX(300),RJ(300),SUM(300),WORK(300),TITLE(10)
          3,B(300),PJ(300),FZ(300),XA(300),XB(300),ZC(300),ZD(300)
          4,C(300),AA(300,300),WKS1(300),WKS2(300)
           COMMON /A/A
           COMMON /AA/AA
           COMMON /B/B
           COMMON/XA/XA
           COMMON/XB/XB
           COMMON/ZC/ZC
           COMMON/ZD/ZD
           COMMON/X/X
           COMMON/Z/Z
```

```
      COMMON/FT/FT
      COMMON/KTOT/KTOT
      COMMON/CONST/CONST
      COMMON/TITLE/TITLE
      COMMON/N/N
C READ IN INPUT PARAMETERS
      READ(5,11)TITLE
   11 FORMAT(10A4)
      READ(5,*)N,CONST
   10 FORMAT(I3,F10.4)
      READ(5,*)ST,AIN,ZT1,ZT2
      READ(5,*)DP1,AX1,DP2,AX2
   66 FORMAT(4F10.2)
      READ(5,*)KTOT,ZCON,COX,DX
      READ(5,*)(X(I),Z(I),FT(I),I=1,N)
      NB=N+1
      DO 1 J=1,NB
    1 XT(J)=(ST-AIN)+AIN*J
      DO 2 J=1,N
      XA(J)=XT(J)
      XB(J)=XT(J+1)
      ZC(J)=ZT1
      ZD(J)=ZT2
    2 CONTINUE
      CDP1=DCOS(DP1*0.0174533)
      SDP1=DSIN(DP1*0.0174533)
      CAX1=DCOS(AX1*0.0174533)
      SAX1=DSIN(AX1*0.0174533)
      CDP2=DCOS(DP2*0.0174533)
      SDP2=DSIN(DP2*0.0174533)
      CAX2=DCOS(AX2*0.0174533)
      SAX2=DSIN(AX2*0.0174533)
      AT1=SDP1/CDP1
      AT2=SDP2/CDP2
      BT=DATAN2(AT1,CAX1)+DATAN2(AT2,CAX2)
      F1=DSQRT((SDP1**2)+(CDP1**2)*(CAX1**2))
      F2=DSQRT((SDP2**2)+(CDP2**2)*(CAX2**2))
      F3=F1*F2
      SBT=DSIN(BT)
      CBT=DCOS(BT)
C SET UP COMPUTING DO LOOPS
      DO 40 I=1,N
      PI=3.1415926
      MUU=2.00
      DET=-2.00
      COM=1.E+2
      GAM=6.67
      DO 40 J=1,N
C CALCULATE THE PARAMETERS OF LENGHT TO BE USED
      X1=X(I)-XA(J)
      X2=X(I)-XB(J)
      Z1=Z(I)-ZC(J)
      Z2=Z(I)-ZD(J)
C COMPUTE THE RADIAL AND ANGULAR TERMS R1,R2,R3,R4,Q1,Q2,Q3,Q4.
      R1=DSQRT((Z1**2)+(X1**2))
      R2=DSQRT((Z2**2)+(X1**2))
      R3=DSQRT((Z1**2)+(X2**2))
      R4=DSQRT((Z2**2)+(X2**2))
      P1=R2*R3
      P2=R1*R4
```

```
      ALG=DLOG(P1/P2)
      IF(X1.EQ.0)GO TO 13
      Q1=DATAN2(Z1,X1)
      Q2=DATAN2(Z2,X1)
      GO TO 15
   13 Q1=PI/2
      Q2=PI/2
   15 IF(X2.EQ.0)GO TO 17
      Q3=DATAN2(Z1,X2)
      Q4=DATAN2(Z2,X2)
      GO TO 19
   17 Q3=PI/2
      Q4=PI/2
   19 A(I,J)=2*F3*(SBT*ALG+CBT*(Q2-Q1+Q3-Q4))*COM
      B(I)=FT(I)
   40 CONTINUE
      CALL INVT
      STOP
      END
C
C
C
      SUBROUTINE INVT
C
C       THE SUBROUTINE INVT INVERTS THE MATRIX FORMED FROM
C       THE GIVEN MAGNETIC ANOMALIES TO GIVE THE DISTRIBUTION
C       OF MAGNETIZATION WHICH IS THEN USED TO FIND THE
C       CORRESPONDING DISTRIBUTION OF DENSITY AND CONSEQUENTLY
C       THE PSEUDOGRAVIMETRIC ANOMALY CORRESPONDING TO THE GIVEN
C       MAGNETIC ANOMALY AND EQUIVALENT LAYER.
C
      IMPLICIT REAL*8(A-H,O-Z)
      DIMENSION A(300,300),B(300),AA(300,300),C(300),FT(300),X(300)
     1,SUM(300),Z(300),XA(300),XB(300),ZC(300),ZD(300),PJ(300),RJ(300)
     2,FX(300),FTOT(300),FZ(300),WKS1(300),WKS2(300),TITLE(10)
      INTEGER I,N,J,IA,IAA,IFAIL
      COMMON/A/A
      COMMON/B/B
      COMMON/XA/XA
      COMMON/XB/XB
      COMMON/ZC/ZC
      COMMON/ZD/ZD
      COMMON/X/X
      COMMON/Z/Z
      COMMON/FT/FT
      COMMON/KTOT/KTOT
      COMMON/CONST/CONST
      COMMON/TITLE/TITLE
      COMMON/N/N
      IA=N
      IAA=N
      IFAIL=1
      CALL F04ATF(A,IA,B,N,C,AA,IAA,WKS1,WKS2,IFAIL)
      IF(IFAIL .EQ. 0)GO TO 200
      WRITE(6,18)IFAIL
      STOP
  200 DO 33 I=1,N
      RJ(I)=C(I)
      PJ(I)=RJ(I)*CONST
   33 CONTINUE
   18 FORMAT(/'ERROR IN F04ATF IFAIL=',I2)
```

```
      DO 51 K=1,KTOT
      FX(K)=X(K)
      FZ(K)=Z(K)
   51 CONTINUE
      DO 60 K=1,KTOT
      GAM=6.67
      PI=3.1415926
      SUM(K)=0.0
      FTOT(K)=0.0
      COM=1.E+5
      DO 55 J=1,N
C CALCULATE THE PARAMETERS OF LENGHT TO BE USED
      XX1=-(FX(K)-XA(J))
      XX2=-(FX(K)-XB(J))
      ZZ1=-(FZ(K)-ZC(J))
      ZZ2=-(FZ(K)-ZD(J))
C COMPUTE THE RADIAL AND ANGULAR TERMS R1,R2,R3,R4,Q1,Q2,Q3,Q4,
      RR1=DSQRT((ZZ1**2)+(XX1**2))
      RR2=DSQRT((ZZ2**2)+(XX1**2))
      RR3=DSQRT((ZZ1**2)+(XX2**2))
      RR4=DSQRT((ZZ2**2)+(XX2**2))
      ALG1=DLOG(RR4/RR3)
      ALG2=DLOG(RR2/RR1)
      PP1=XX2*ALG1
      PP2=XX1*ALG2
      IF(XX1.EQ.0)GO TO 53
      T1=DATAN2(ZZ1,XX1)
      T2=DATAN2(ZZ2,XX1)
      GO TO 85
   53 T1=PI/2
      T2=PI/2
   85 IF(XX2.EQ.0)GO TO 87
      T3=DATAN2(ZZ1,XX2)
      T4=DATAN2(ZZ2,XX2)
      GO TO 89
   87 T3=PI/2
      T4=PI/2
C THE COMPUTATION OF PSEUDOGRAVITY  ANOMALY BEGINS
   89 QAL=(PP1-PP2-ZZ1*(T1-T3)+ZZ2*(T2-T4))*PJ(J)
      SUM(K)=SUM(K)+QAL
   55 CONTINUE
      FTOT(K)=2*GAM*SUM(K)
   60 CONTINUE
C WRITE OUT RESULTS OF COMPUTATIONS
      WRITE(6,34)TITLE
   34 FORMAT(10A4)
      WRITE(6,3)(XA(J),XB(J),ZC(J),ZD(J),J=1,N)
    3 FORMAT(4F10.2)
      WRITE(6,42)
   42 FORMAT(20X/'VALUES OF PSEUDOGRAV.AND MAGNETIC ANOMALIES '/)
      WRITE(6,44)
   44 FORMAT(10X/'FX            FT              FTOT'/)
      WRITE(6,56)(FX(K),FZ(K),FT(K),FTOT(K),K=1,KTOT)
   56 FORMAT(4F10.3)
      WRITE(6,31)
   31 FORMAT(20X/'VALUES OF COMPUTED  MAGNETIZATION'/)
      WRITE(6,74)
   74 FORMAT(20X/'              JTOT            DEN            '/)
      DO 36 J=1,N
      WRITE(6,32)RJ(J),PJ(J)
```

```
 32 FORMAT(2F10.3)
 36 CONTINUE
 16 FORMAT(F10.3)
 14 FORMAT(41(8F14.6))
    RETURN
    END
```

```
C                   PROGRAM MANOM
C                   ====================
C
C
C       THIS PROGRAM COMPUTES THE TOTAL FIELD MAGNETIC
C       ANOMALY DUE TO AN ARBITRARILY SHAPED TWO -
C       DIMENSIONAL BODY OF ARBITRARY DIRECTION OF
C       MAGNETIZATION. INPUT DATA IS AS FOLLOWS:
C       (1)     TITLE(NOT MORE THAN 40 CHARACTERS)
C       (2)     NB,NS:NO OF BODY AND FIELD POINTS RESPECTIVELY
C       (3)     ST,AIN,ZS:X-CORD. OF FIRST FIELD POINT,SPACING
C               OF FIELD PTS. AND Z-CORD. OF FIELD POINTS
C       (4)     AJ,A,CB,EI,ED:MAGNETIZATION OF BODY(A/M),
C               DIP & DECLINATION OF MAG. & EARTH'S FIELD
C       (5)     XB(I),ZB(I):X & Z CORDS. OF BODY POINTS
C       THE OUTPUT FROM MANOM IS AS FOLLOWS:
C       (1)     TITLE:(AS IN INPUT)
C       (2)     XB(I),ZB(I):(AS IN INPUT)
C       (3)     AJ,A,CB,EI,ED (AS IN INPUT)
C       (4)     XS(I),FT(I):X-CORD. & COMPUTED ANOMALY(GAMMAS)
C
C
        IMPLICIT REAL*8(A-H,O-Z)
        DIMENSION XB(40),X(40),TITLE(10),ZB(40),T(40),XS(500),FT(500)
       1,XX(50)
        READ(5,11)TITLE
   11   FORMAT(10A4)
        WRITE(6,11)TITLE
        READ(5,*)NB,NS
        READ(5,*)ST,AIN,ZS
        READ(5,*)AJ,A,CB,EI,ED
        READ(5,*)(XB(I),ZB(I),I=1,NB)
        WRITE(6,62)(XB(J),ZB(J),J=1,NB)
        WRITE(6,60)AJ,A,CB,EI,ED
        PI=4.0*ATAN(1.0)
        DR=PI/180.0
        PI2=PI/2.0
        A=DR*A
        EI=DR*EI
        ED=DR*ED
        CB=CB*DR
        DO 1 I=1,NB
    1   ZB(I)=ZB(I)-ZS
        DO 13 I=1,NS
   13   XS(I)=ST+(I-1)*AIN
        XJ=AJ*DCOS(A)*DCOS(CB)
        ZJ=AJ*DSIN(A)
        DO 10 I=1,NS
        DO 20 J=1,NB
        XX(J)=XB(J)-XS(I)
        XSS=DABS(XX(J))
        IF(XSS.LT.0.000001) GOTO 30
        T(J)=DATAN2(ZB(J),XX(J))
        GOTO 20
   30   T(J)=PI2
   20   CONTINUE
        SUM=0.0
        DO 50 J=1,NB
        K=J+1
        IF(J.EQ.NB) K=1
        X1=XX(J)
```

```
      Z1=ZB(J)
      T1=T(J)
      X2=XX(K)
      Z2=ZB(K)
      T2=T(K)
      ZA=Z1-Z2
      ZA=DABS(ZA)
      IF(ZA.LT.0.00000001) GOTO 50
      R1=DSQRT(X1*X1+Z1*Z1)
      R2=DSQRT(X2*X2+Z2*Z2)
      X12=X1-X2
      Z21=Z2-Z1
      T12=T1-T2
      RRX=R2/R1
      RR=DLOG(RRX)
      ZZ=Z21*Z21
      XZ=Z21*X12
      DE=ZZ+X12*X12
      P=(ZZ*T12+XZ*RR)/DE
      Q=(XZ*T12-ZZ*RR)/DE
      V=2.0*(XJ*Q-ZJ*P)
      H=2.0*(XJ*P+ZJ*Q)
      TF=V*DSIN(EI)+H*DCOS(EI)*DCOS(ED)
      SUM=SUM+TF
   50 CONTINUE
      FT(I)=100.0*SUM
   10 CONTINUE
   60 FORMAT(5F10.2)
      WRITE(7,62)(XS(I),FT(I),I=1,NS)
   62 FORMAT(2F10.2)
      STOP
      END
```

```
C                 PROGRAM   FACT1
C                 ====================
C         THIS PROGRAM EVALUATES BOTH THE BALLISTIC AND MAGNETOMETRIC
C         DEMAGNETIZATION FACTORS FOR A CYLINDER. IT USES THE RATHER
C         SIMPLE FORMULAR DERIVABLE FROM FIRST PRINCIPLES(CHAPT. TWO).
C         THE INPUT DATA CONSISTS ONLY OF THE EXTENSIONS OF THE CYLINDER
C         IN THE X AND Z DIRECTIONS.THE PROGRAM THEN CALCULATES THE
C         DIMENSIONAL RATIOS AS WELL AS THE DEMAGNETIZATION FACTORS.
C                         OFOEGBU    1980
C
        DIMENSION AL(200),R(200),P(200),DNB(200),DNM(200)
C         READ IN ELEMENTS OF DIMENSIONS OF CYLINDER
        READ(5,11)TITLE
11      FORMAT(10A4)
        READ(5,*)N
        READ(5,*)(AL(I),R(I),I=1,N)
C         CALCULATION OF DIMENSIONAL RATIOS NOW BEGINS
        DO 20 I=1,N
        P(I)=AL(I)/R(I)
20      CONTINUE
C         COMPUTATION OF DEMAGNETIZATION FACTORS BEGINS
        DO 30 I=1,N
        PI=3.1415926
        ALG=ALOG(8/P(I))
        Q1=ALOG(4/P(I))
        Q2=P(I)**2
        IF(P(I).GT.1)GO TO 40
        DNB(I)=1-((2*P(I)/PI)*(ALG-1))
        DNM(I)=1-((2*P(I)/PI)*(Q1-0.5))
        GO TO 30
40      DNB(I)=(0.5/Q2)*(1-(1.5/Q2)+(25/(8*(P(I)**4))))
        DNM(I)=(4/(3*PI*P(I)))-(1/(8*Q2))
30      CONTINUE
        WRITE(6,14)
14      FORMAT(10X/'VALUES OF COMPUTED DEMAGNETIZATION FACTORS'/)
        WRITE(6,16)
16      FORMAT(10X/'  RATIO     BALLISTIC    MAGNETOMETRIC  '/)
        WRITE(6,18)(P(I),DNB(I),DNM(I),I=1,N)
18      FORMAT(F10.2,2F13.6)
        STOP
        END
```

Figure 5.5 Aeromagnetic map of lower and middle Benue Trough of Nigeria showing the position of profiles interpreted (Compiled from 1:100,000 sheets of aeromagnetic map of Nigeria. Published by the Geological Survey of Nigeria)

Scale

0 10 20   40   70 km